MOLECULAR INSIGHTS INTO THE NICHE OF HARMFUL BROWN TIDES

By

Louie L. Wurch

B.S., Humboldt State University, 2005

Submitted in partial fulfillment of the requirements for the degree of

Doctor of Philosophy

at the

MASSACHUSETTS INSTITUTE OF TECHNOLOGY

and the

WOODS HOLE OCEANOGRAPHIC INSTITUTION

September 2011

Signature of Author

_____

Joint Program in Oceanography/Applied Ocean Science and Engineering
Massachusetts Institute of Technology
and Woods Hole Oceanographic Institution
September 6, 2011

Certified by

_____

Dr. Sonya T. Dyhrman
Thesis Supervisor

Accepted by

_____

Dr. Simon Thorrold
Chair, Joint Committee for Biological Oceanography
Woods Hole Oceanographic Institution

Molecular Insights into the Niche of Harmful Brown Tides

By Louie Wurch

Submitted in partial fulfillment of the requirement
for the degree of Doctor of Philosophy in
Biological Oceanography

Recurrent brown tide blooms caused by the harmful alga *Aureococcus anophagefferens* have decimated coastal ecosystems and shellfisheries along the Eastern U.S and South Africa. The exact mechanisms controlling bloom formation, sustenance, and decline are unclear, however bottom-up factors such as nutrient type and supply are thought to be critical. Traditional assays for studying algal nutrient physiology require bulk community measurements or *in situ* nutrient perturbations. Although useful, these techniques lack the ability to target individual species in complex, mixed microbial assemblages. The motivation for this thesis is to examine the metabolic strategies utilized by *A. anophagefferens* for meeting its nitrogen (N) and phosphorus (P) demand at the cellular level using molecular tools that, even in the presence of complex microbial assemblages, can be used to track how nutrients influence the bloom dynamics of *A. anophagefferens* in the environment. Chapter two examines the global transcriptional responses of *A. anophagefferens* to N and P deficiency. Results demonstrate that *A. anophagefferens* has the capacity to utilize multiple forms of organic N and P when inorganic forms become unavailable. Chapter three analyzed the global protein changes in response to P deficiency and P re-supply. Consistent with transcript patterns, *A. anophagefferens* increases protein abundance for a number of genes involved in inorganic and organic P metabolism when inorganic P is deficient. Furthermore, increases in a sulfolipid biosynthesis protein combined with lipid data suggest *A. anophagefferens* can adjust its P requirement by switching from phospholipids to sulfolipids when inorganic P is unavailable. Analysis of protein abundances from P-deficient cells that were re-fed inorganic P demonstrates variations in the timing of turnover among various proteins upon release from phosphate deficiency. Chapter four tests the expression patterns of candidate gene markers of nutrient physiology under controlled culture experiments. Results show that expression patterns of a phosphate transporter and xanthine/uracil/vitamin C permease are indicators of P and N deficiency, respectively. Taken together, these findings provide insight into the fundamental and ecological niche space of this harmful algal species with respect to N and P and provide a platform for assaying nutrient controls on natural brown tide blooms.

Thesis Supervisor:
Dr. Sonya T. Dyhrman
Title: Associate Scientist, Biology Department, Woods Hole Oceanographic Institution

Acknowledgments

Throughout my career as a graduate student I have was supported by the Woods Hole Oceanographic Institution Academic Programs Office, an EPA STAR graduate fellowship (#FP916901). I also utilized funds from a student research grant from the Woods Hole Coastal Ocean Institute, a National Oceanic and Atmospheric Administration ECOHAB grant (#NA09NOS4780206), and National Science Foundation grant (#OCE-0723667).

A Ph.D. thesis represents an incredible amount of work over a long period of time. There were countless people that have contributed either directly to my thesis by assisting me in research, discussions, etc., or indirectly by providing support and much needed distractions. First and foremost, I have to thank my advisor and mentor Sonya Dyhrman. She has put a tremendous amount of effort into training me to be a scientist and a colleague and has provided invaluable feedback and guidance in my thesis research. I would also like to thank my thesis committee: Prof. Christopher Gobler, Dr. Donald Anderson, Dr. Scott Doney, and Prof. Edward DeLong. It is a substantial amount of work to serve on a thesis committee and requires a great deal of time. I am very thankful for all of your guidance through this process. It is an amazing experience to have such successful scientists guide me and help me critically think about my research. Finally, I would like to thank my family and friends for your support. I could not hope to possibly name and thank everyone properly, but please know I appreciate all of you and your support.

Table of Contents

CHAPTER ONE

Introduction

Phytoplankton in the world's oceans account for roughly half of all primary production on Earth (Field et al 1998). Through the uptake and fixation of CO_2 into organic carbon, phytoplankton form the base of the marine food web, are essential in exporting CO_2 from the atmosphere to the deep ocean (thus critical in regulating climate), and drive the biogeochemical cycling of nitrogen (N), phosphorus (P), and other important nutrients. Therefore understanding the controls on phytoplankton growth remains a key area of oceanographic research.

Nutrient availability is a principal factor governing phytoplankton growth in the ocean and different phytoplankton species all require the same basic nutrients to grow (e.g. N, P, iron, etc.). G.E. Hutchinson initially proposed a paradox in 1961 termed the "paradox of the plankton". According to the law of competitive exclusion, if multiple species compete for the same resource, eventually one species alone should outcompete all the others so that in a final state of equilibrium, only one species would exist (Gause 1932). There are many species of phytoplankton present in the ocean, and understanding how individual species partition themselves into the distinct niches that must allow them to co-occur in the ocean remains a fundamental challenge. Conversely, occasionally a given set of environmental variables will lead to temporary competitive exclusion, whereby one phytoplankton species will dominate the system leading to monospecific algal blooms (e.g. brown tide blooms, Gobler et al. 2005, Sunda et al. 2006). If the build-

up of biomass from one phytoplankton species has negative consequences to the ecosystem it is referred to a harmful algal bloom (HAB). Note, however, that not all HABs are the result of one species dominating the system. For example, some phytoplankton produce toxins that can be harmful even at very low cell concentrations (Burkholder and Glasgow 1997, Smayda 1997). Nonetheless, numerous HABs form due to the ability of certain phytoplankton species to outcompete other phytoplankton species under certain conditions, leading to monospecific, or nearly monospecific, blooms.

Due to the impacts of HABs on the environment, fisheries, and human health, a substantial amount of effort has been poured into the mechanisms by which HAB-forming species can exploit a given geochemical environment (e.g. see reviews by Smayda et al. 2006 and Anderson et al. 2008). Traditional methods for studying how HAB species interact and compete with co-ocurring species under variable geochemical conditions rely on cultured isolates or community level assays for determining factors such as nutrient preference, uptake rates, and elemental composition (Dyhrman 2008). Molecular methods offer a means in which the nutrition of individual species living in complex mixed assemblages can be examined at the cellular level. This, in turn, allows a way by which the realized niche space of an individual speices can be resolved.

The entire physiological potential of an organism is encoded in its genome. For instance, the genome sequencing of the diatom *Thalassiosira pseudonana* identified novel genes for silica transport, a complete urea cycle, and a variety of genes for utilizing exogenous nutrient compounds (Armbrust et al. 2004). A genomic comparison between two species of the picoeukaryote *Ostreococcus* provided insight into how these two

organisms diverged and adapted to unique ecological niches (Palenik et al. 2007). The reader is also directed to Scanlan et al. 2009 for a review on how niche adaptation and ecological success are reflected in the genomes of two genera of cyanobacteria. The recent genome sequencing of the HAB species *Aureococcus anophagefferens* has demonstrated that this species is well adapted to anthropogenically-influenced estuaries (Gobler et al. 2011).

The genome of an organism reveals the physiological capacity of that organism, but it is the ordered expression of that genome that ultimately dictates how an organism is adjusting to its current environment. For example, under N and P deficiency, some phytoplankton will induce genes for efficiently scavenging nutrients from a variety of sources and this induction can be seen at the transcriptional level (Grossman 2000, Dyhrman 2008). Global transcriptome profiling studies have also examined nutrient deficiency responses in coccolithophores, dinoflagellates, diatoms, and the pelagophyte *A. anophagefferens* (Dyhrman et al. 2006, Erdner and Anderson 2006, Mock et al. 2008, Wurch et al. 2011). A targeted study of N metabolism genes in *A. anophagefferens* demonstrated the up-regulation of transporters for nitrate, formate/nitrite, urea, ammonium, and amino acids among others during general N deficiency (Berg et al. 2008). Proteomic studies are complementary to genomic and transcriptomic studies because protein represents the end product of gene expression. Recently, mass spectrometry-based proteomic approaches have been used to analyze biosynthetic and metabolic pathways in the diatom *T. pseudonana*, the picoeukaryote *Ostreococcus tauri*, and the cyanobacterium *Crocosphaera watsonii* (Nunn et al. 2009, Saito et al. 2011, Le

Bihan et al. 2011). Transcriptome and proteome studies reveal how phytoplankton can tailor the expression of their genomes to adjust to variations in their geochemical environment, providing key insight into competition, nutrient scavenging/metabolism, and nutrient conservation strategies. These parameters can be used to outline the realized niche space for individual phytoplankton species.

A. anophagefferens as a model species

As mentioned above, it is particularly critical to understand the strategies and niche space of those species that cause negative consequences to the ecosystem, as is the case for HABs. Occasionally, one phytoplankton species can exploit a given environment to the complete exclusion of all other competitors. An example of this is the brown tide events that have caused extensive damage to coastal ecosystems in the eastern United States and South Africa (Gobler et al. 2005). Brown tides are caused by *A. anophagefferens*, a relatively small (~2 μm diameter) eukaryotic phytoplankton species within the algal class Pelagophyceae (DeYoe et al. 1997). A related alga, *Aureoumbra lagunensis*, is responsible for brown tides in Texas (DeYoe et al. 1995, 1997). Brown tide events caused by *A. anophagefferens* occur almost annually in waters around Long Island (Gobler et al. 2005).

A. anophagefferens has emerged as a model phytoplankton species for studying high biomass HABs due to its severe impact upon the coastal ecosystem and much attention has been paid to understanding what causes brown tides to form (Gobler et al. 2005, Sunda et al. 2006). Culture work has demonstrated that *A. anophagefferens* can

access N from a variety of sources. This includes dissolved inorganic N (DIN) compounds such as nitrate and ammonium, and dissolved organic N (DON) compounds such as urea, formamide, amino acids, chitobiose, and acetamide (Berg et al. 2002, Mulholland et al. 2002, MacIntyre et al. 2004, Pustizzi et al. 2004, Berg et al. 2008). In field studies, natural assemblages of phytoplankton during brown tide events can utilize DON compounds (e.g. urea and amino acids) and *A. anophagefferens* has a relatively higher affinity for reduced N (e.g. ammonia) and DON relative to nitrate (Lomas et al. 1996, Berg et al. 1997; 2003, Mulholland et al. 2002; 2004). Low nitrate inputs resulting from variability in groundwater flow have been positively correlated to brown tides around Long Island (LaRoche et al. 1997). Mesocosm experiments during a natural bloom pointed to an inverse correlation between DIN enrichment and *A. anophagefferens* cell densities (Keller and Rice, 1989). Further evidence showed that DIN enrichment led to a decrease in the relative abundance of *A. anophagefferens* within the phytoplankton community (Gobler and Sañudo-Wilhelmy 2001b, Gobler et al. 2002; 2004, Kana et al. 2004).

The data from these studies suggest that *A. anophagefferens* prefers reduced and organic forms of N to nitrate. However, in culture, *A. anophagefferens* has similar growth rates whether the sole N source is nitrate or urea (MacIntyre et al. 2004, Pustizzil et al. 2004). Using growth rates in cultures of competing phytoplankton species grown on various N sources, model simulations predicted that of the species tested, diatoms and cyanobacteria would dominate phytoplankton communities supplied primarily with nitrate, while *A. anophagefferens* will dominate phytoplankton communities primarily

supplied with ammonia and DON (Taylor et al. 2006). These model simulations are consistent with field observations showing significant reductions in DON as *A. anophagefferens* cell densities increase (Gobler et al. 2004).

Far less is known about the role of P in brown tide events. As with DIN, brown tides tend to correlate with relatively low DIP concentrations (Gobler et al. 2005) and there is a significant drawdown of DOP during peak *A. anophagefferens* cell densities (Gobler et al. 2004). Culture work demonstrated that both non-axenic and axenic strains of *A. anophagefferens* could utilize DOP (e.g. glycerol-phosphate, adenosine monophosphate) as a sole P source (Dzurica et al. 1989, Wurch et al. 2011). Therefore, DOP may be important in fueling blooms when DIP is unavailable.

Taken together, these past studies have demonstrated that (1) *A. anophagefferens* can utilize DON and DOP in culture; (2) brown tides generally correlate with low levels of DIN and DIP; and (3) there is a reduction in DON and DOP during peak bloom periods. This suggests that *A. anophagefferens* gains competitive advantages when inorganic nutrients become depleted while organic nutrients are still available. The goal of this thesis is to determine the molecular mechanisms by which *A. anophagefferens* takes advantage of this scenario allowing it to outcompete co-occurring phytoplankton species and to use these data to confirm additional details of the realized niche space that would not be possible with community level assays. The specific data chapters are outlined below:

Chapter 2: Nutrient-regulated transcriptional responses in the brown tide-forming alga *Aureococcus anophagefferens*.

Global transcriptional responses were analyzed under N- and P-deficient conditions to identify the metabolic strategies employed by *A. anophagefferens* to cope with N and P deficiency (Wurch et al. 2011).

Chapter 3: Proteome changes driven by phosphorus deficiency and recovery in the brown tide-forming alga, *Aureococcus anophagefferens*.

The global protein abundances of *A. anophagefferens* were profiled to determine which proteins were differentially abundant under P-deficient conditions and whether changes in the P-deficient transcriptome were manifested at the protein level. Global protein abundances were also assayed for P-deficient cells that had been re-fed phosphate and allowed 24 hours to respond, providing insight into the timing of protein turnover.

Chapter 4: Targeted gene expression in culture and field populations of *Aureococcus anophagefferens*: Patterns in nitrogen and phosphorus metabolism.

Expression patterns of target genes involved in N and P metabolism were analyzed under a variety of culture conditions. Those genes whose expression patterns are indicative of N or P deficiency were examined in natural field samples of *A. anophagefferens* during a bloom in Quantuck Bay, 2007.

References:

Anderson, D.M., Burkholder, J.M., Cochlan, W.P., Glibert, P.M., Gobler, C.J., Heil, C.A., et al. (2008) Harmful algal blooms and eutrophication: Examining linkages from selected coastal regions of the United States. *Harmful Algae* **8:** 39-53.

Armbrust, E.V., Berges, J.A., Bowler, C., Green, B.R., Martinez D., et al. (2004) The genome of the diatom Thalassiosira pseudonana: Ecology, evolution, and metabolism. *Science* **306:** 79-86.

Berg, G. M., Glibert, P.M., Lomas, M.W., and Burford, M.A. (1997) Organic nitrogen uptake and growth by the chrysophyte *Aureococcus anophagefferens* during a brown tide event. *Mar. Biol.* **129**: 377-387.

Berg, G.M., Repeta, D.J., and LaRoche, J. (2002) Dissolved organic nitrogen hydrolysis rates in axenic cultures of *Aureococcus anophagefferens* (Pelagophyceae): comparison with heterotrophic bacteria. *Appl. Environ. Microbiol.* **68**: 401-404.

Berg, G.M., Repeta, D.J., and LaRoche, J. (2003) The role of the picoeukaryote *Aureococcus anophagefferens i*n cycling of marine high-molecular weight dissolved organic nitrogen. *Limnol. Oceanogr.* **48**: 1825-1830.

Berg, G.M., Shrager, J., Glockner, G., Arrigo, K.R., and Grossman, A.R. (2008) Understanding nitrogen limitation in *Aureococcus anophagefferens* (Pelagophyceae) through cDNA and qRT-PCR analysis. *J. Phycol.* **44**: 1235-1249.

Burkholder, J.M., and Glasgow, H.B. (1997) *Pfiesteria piscicida* and other *Pfiesteria*-like dinoflagellates: Behavior, impacts, and environmental controls. *Limnol. Oceanogr.* **42:** 1052-1075.

DeYoe, H.R., Chan, A.M., and Suttle C.A. (1995) Phylogeny of *Aureococcus anophagefferens* and a morphologically similar bloom-forming alga from Texas as determined by 18S ribosomal RNA sequence analysis. *J. Phycol.* **31**: 413-418.

DeYoe, H.R., Stockwell, D., Bidigare, R., Latasa, M., Johnson, P., Hargraves, P., and Suttle, C. (1997) Description and characterization of the algal species *Aureoumbra lagunensis* gen. et sp. Nov. and referral of *Aureoumbra* and *Aureococcus* to the Pelagophyceae. *J. Phycol.* **33**: 1042-1048.

Dyhrman, S.T., Haley, S.T., Birkeland, S.R., Wurch, L.L., Cipriano, M.J., and McArthur, A.G. (2006) Long Serial Analysis of Gene Expression for gene discovery and transcriptome profiling in the widespread marine coccolithophore *Emiliania huxleyi*. *Appl. Environ. Microbiol.***72**: 252-260.

Dyhrman, S.T. (2008) Molecular approaches to diagnosing nutritional physiology in harmful algae: Implications for studying the effects of eutrophication. *Harmful Algae* **8**: 167-174.

Dzurica, S., Lee, C., Cosper, E.M., and Carpenter, E.J. (1989) Role of environmental variables, specifically organic compounds and nutrients, in the growth of the chrysophyte *Aureococcus anophagefferens*. p. 229-252. *In* E.M. Cosper, V.M. Bricelj, and E.J. Carpenter (eds.), Novel Phytoplankton Blooms: Causes and Impacts of Recurrent Brown Tides and Other Unusual Blooms, Volume 35. Springer, New York.

Erdner, D.L., and Anderson, D.M. (2006) Global transcriptional profiling in the toxic dinoflagellate *Alexandrium fundyense* using massively parallel signature sequencing. *BMC Genomics* **7**: 88.

Field, C.B., Behrenfeld, M.J., Randerson J.T., and Falkowski, P. (1998) Primary production of the biosphere: Integrating terrestrial and oceanic components. *Science* **281:** 237-240.

Gause, G.F. (1932) Experimental studies on the struggle for existence: 1. Mixed population of two species of yeast. *J. Exp. Biol.* **9:** 389-402.

Gobler, C.J., and Sañudo-Wilhelmy, S.A. (2001a) Temporal variablility of groundwater seepage and brown tide blooms in a Long island embayment. *Mar. Ecol. Prog. Ser.* **217**: 299-309.

Gobler, C.J., and Sañudo-Wilhelmy, S.A. (2001b) Effects of organic carbon, organic nitrogen, inorganic nutrients, and iron additions on the growth of phytoplankton and bacteria during a brown tide bloom. *Mar. Ecol. Prog. Ser.* **209**: 19-34.

Gobler, C.J., Renaghan, M.J., and Buck, N.J. (2002) Impacts of nutrients and grazing mortality on the abundance of *Aureococcus anophagefferens* during a New York brown tide bloom. *Limnol. Oceanogr.* **47**: 129-141.

Gobler, C.J., Boneillo, G.E., Debenham, C., and Caron, D.A. (2004) Nutrient limitation, organic matter cycling, and plankton dynamics during an *Aureococcus anophagefferens* bloom in Great South Bay, N.Y. *Aquat. Microb. Ecol.* **35**: 31-43.

Gobler, C.J., Lonsdale, D.J., and Boyer, G.L. (2005) A review of the causes, effects, and potential management of harmful brown tide blooms caused by *Aureococcus anophagefferens* (Hargraves et Sieburth). *Estuaries* **28**: 726-749.

Gobler, C.J., Berry, D.L., Dyhrman, S.T., Wilhelm, S.W., Salamov, A. et al. (2011) Niche of harmful algal *Aureococcus anophagefferens* revealed through ecogenomics. **108:** 4352-4357.

Grossman, A. (2000) Acclimation of *Chlamydomonas reinhardtii* to its nutrient environment. *Protist* **151**: 201-224.

Hutchinson, G. E. (1961) The paradox of the plankton. *American Naturalist* **95:** 137-145.

Kana, T.M., Lomas, M.W., MacIntyre H.L., Cornwell, J.C., and Gobler, C.J. (2004) Stimulation of the brwon tide organism, *Aureococcus anophagefferens*, by selective nutrient additions to *in situ* mesocosms. *Harmful Algae* **3**: 377-388.

Keller, A.A., and Rice, R.L. (1989) Effects of nutrient enrichment on natural populations of the brown tide phytoplankton *Aureococcus anophagefferens* (Chrysophyceae). *J. Phycol.* **25**: 636-646.

LaRoche, J., Nuzzi, R., Waters, R., Wyman, K., Falkowski, P.G., and Wallace, D.W.R. (1997) Brown tide blooms in Long Island's coastal waters linked to variability in groundwater flow. *Glob. Change Biol.* **3**: 397–410.

Le Bihan, T., Martin, S.F., Chirnside, E.S., van Ooijen, G, Barrios-LLenera, M.E., et al. (2011) Shotgun proteomic analysis of the unicellular alga Ostreococcus tauri, *J. Prot.* doi:10.1016/j.jprot.2011.05.028

Lomas, M. W., Glibert, P.M., and Berg, G.M. (1996) Characterization of nitrogen uptake by natural populations of *Aureococcus anophagefferens* (Chrysophyceae) as a function of incubation duration, substrate concentration, light, and temperature. *J. Phycol.* **32**: 907-916.

Mock T., Samanta M.P., Iverson V., Berthiaume C., Robison M., Holtermann K., et al. (2008) Whole genome expression profiling of the marine diatom *Thalassiosira pseudonana* identifies genes involved in silicon bioprocesses. *Proc. Nat. Acad. Sci. U.S.A.* **105**:1579–1584.

Mulholland, M.R., Gobler, C.J., and Lee, C. (2002) Peptide hydrolysis, amino acid oxidation and N uptake in communities seasonally dominated by *Aureococcus anophagefferens*. *Limnol. Oceanogr.* **47**: 1094-1108.

Mulholland, M.R., Boneillo, G., and Minor E.C. (2004) A comparison of N and C uptake during brown tide (*Aureococcus anophagefferens*) blooms from two coastal bays on the east coast of the USA. *Harmful Algae.* **3**: 361-376.

Nunn, B.L., Aker, J.R., Shaffer, S.A., Tsai, Y., Strzepek R.F., et al. (2009) Deciphering diatom biochemical pathways via whole-cell proteomics. *Aquat. Microb. Ecol.* **55**: 241-253.

Palenik, B., Grimwood, J., Aerts, A., Rouze, P., Salamov, A, et al. (2007) The tiny eukaryote Ostreococcus provides genomic insights into the paradox of plankton speciation. *PNAS* **104:** 7705-7710.

Pustizzi, F., MacIntyre, H.L., Warner, M.E., and Hutchins, D.A. (2004) Interaction of nitrogen source and light intensity on the growth and photosynthesis of the brown tide alga *Aureococcus anophagefferens*. *Harmful Algae* **3**: 343-360.

Saito, M.A., Bertrand, E.M., Dutkiewicz, S., Bulygin, V.V., Moran, D.M. et al. (2011) Iron conservation by reduction of metalloenzyme inventories in the marine diazotroph Crocosphaera watsonii. *PNAS* **108:** 2184-2189.

Scanlan, D.J., Ostrowski, M., Mazard, S., Dufresne, A., Garczarek, L. et al. (2009) Ecological Genomics of Marine Picocyanobacteria. *Microbiol. Mol. Biol. R.* **73:** 249-299.

Smayda, T.J. (1997) Harmful algal blooms: Their ecophysiology and general relevance to phytoplankton blooms in the sea. *Limnol. Oceanogr.* **42**: 1137-1153.

Sunda, W.G., Graneli, E., and Gobler, C.J. (2006) Positive feedback and the development and persistence of ecosystem disruptive algal blooms. *J. Phycol.* **42**: 963-974.

Taylor, G.T., Gober, C.J., and Sañudo-Wilhelmy, S.J. (2006) Speciation and concentrations of dissolved nitrogen as determinants of brown tide *Aureococcus anophagefferens* bloom initiation. *Mar. Ecol. Prog. Ser.* **312:** 67-83.

Wurch L.L., Haley S.T., Orchard E.D., Gobler C.J., and Dyhrman S.T. (2011) Nutrient-regulated transcriptional responses in the brown tide forming algal *Aureococcus anophagefferens*. *Environ. Microbiol.* **13**: 468-481.

CHAPTER TWO

Nutrient-regulated transcriptional responses in the brown tide-forming alga *Aureococcus anophagefferens*

Louie L. Wurch[a]

Sheean T. Haley[b]

Elizabeth D. Orchard[a]

Christopher J. Gobler[c]

Sonya T. Dyhrman[b,d]

[a]MIT-WHOI Joint Program in Oceanography/Applied Ocean Science and Engineering,

Cambridge, MA 02139

[b]Woods Hole Oceanographic Institution Biology Department

Woods Hole, MA 02543

[c]Stony Brook University, School of Marine and Atmospheric Sciences

Stony Brook, NY 11794

[d]Corresponding author: sdyhrman@whoi.edu Fax: (508) 457-2134

Wurch, L.L., Haley, S.T., Orchard, E.D., Gobler, C.J., and Dyhrman S.T. (2011) Nutrient-regulated transcriptional responses in the brown tide-forming alga *Aureococcus anophagefferens*. *Environ. Micobiol.* **13:** 468-481.

environmental microbiology

Environmental Microbiology (2011) **13**(2), 468–481 doi:10.1111/j.1462-2920.2010.02351.x

Nutrient-regulated transcriptional responses in the brown tide-forming alga *Aureococcus anophagefferens*

Louie L. Wurch,[1] Sheean T. Haley,[2] Elizabeth D. Orchard,[1] Christopher J. Gobler[3] and Sonya T. Dyhrman[2]*

[1]*MIT-WHOI Joint Program in Oceanography/Applied Ocean Science and Engineering, Cambridge, MA 02139, USA.*

[2]*Woods Hole Oceanographic Institution, Biology Department, Woods Hole, MA 02543, USA.*

[3]*Stony Brook University, School of Marine and Atmospheric Sciences, Stony Brook, NY 11794, USA.*

Summary

Long-SAGE (serial analysis of gene expression) was used to profile the transcriptome of the brown tide-forming alga, *Aureococcus anophagefferens*, under nutrient replete (control), and nitrogen (N) and phosphorus (P) deficiency to understand how this organism responds at the transcriptional level to varying nutrient conditions. This approach has aided *A. anophagefferens* genome annotation efforts and identified a suite of genes upregulated by N and P deficiency, some of which have known roles in nutrient metabolism. Genes upregulated under N deficiency include an ammonium transporter, an acetamidase/formamidase and two peptidases. This suggests an ability to utilize reduced N compounds and dissolved organic nitrogen, supporting the hypothesized importance of these N sources in *A. anophagefferens* bloom formation. There are also a broad suite of P-regulated genes, including an alkaline phosphatase, and two 5′-nucleotidases, suggesting *A. anophagefferens* may use dissolved organic phosphorus under low phosphate conditions. These N- and P-regulated genes may be important targets for exploring nutrient controls on bloom formation in field populations.

Introduction

Aureococcus anophagefferens is a small (~2 μm) eukaryotic phytoplankton responsible for the brown tide events that have plagued many coastal ecosystems in the Eastern United States, most notably Long Island waters. Shortly after its discovery in 1985, it became evident that brown tide events were decimating the Long Island scallop industry and causing substantial losses to eelgrass habitat (Dennison *et al*., 1989; Greenfield and Lonsdale, 2002; Greenfield *et al*., 2004). This, combined with the regularity of blooms occurring in the Eastern United States, has led to *A. anophagefferens* becoming a widely studied harmful algal bloom (HAB) species (see reviews by Gobler *et al*., 2005 and Sunda *et al*., 2006).

Occurrences of HABs in coastal ecosystems have been commonly attributed to nutrient loading, whereby increased levels of nitrogen (N) and phosphorus (P) relieve algae from nutrient limitation (see review by Anderson *et al*., 2008). In contrast, *A. anophagefferens* often blooms in periods when concentrations of dissolved inorganic nitrogen (DIN) and dissolved inorganic phosphorus (DIP) are low. For example, blooms have been linked to low nitrate inputs resulting from variability in ground water flow (LaRoche *et al*., 1997). Mesocosm experiments during a natural bloom also showed enrichment with DIN and DIP inversely correlated with *A. anophagefferens* cell densities (Keller and Rice, 1989). Further experimental evidence shows a reduction of the relative abundance of *A. anophagefferens* within the phytoplankton community during DIN enrichment (Gobler and Sañudo-Wilhelmy 2001, Gobler *et al*., 2002; 2004; Kana *et al*., 2004).

Culture work has shown that *A. anophagefferens* can utilize N from a variety of organic compounds, including proteins, chitobiose and acetamide (Berg *et al*., 2002; Mulholland *et al*., 2002). These observations are supported by field studies indicating that natural assemblages of phytoplankton during brown tide events have the ability to use N from dissolved organic nitrogen (DON) such as amino acids and urea (Berg *et al*., 1997; 2003; Mulholland *et al*., 2002), and that *A. anophagefferens* has a higher affinity for reduced N (e.g. ammonium) and DON (e.g. urea and amino acids) than nitrate (Lomas *et al*., 1996; Mulholland *et al*., 2002; 2004). To date, there is only one study that has examined N-regulated gene expression in *A. anophagefferens*. Using a quantitative RT-PCR approach on targeted genes involved in N transport and metabolism, it was demonstrated that *A. anophagefferens* upregulates a variety of genes, in response to acute N deficiency and

Received 26 April, 2010; accepted 16 August, 2010. *For correspondence. E-mail sdyhrman@whoi.edu; Tel. (+1) (508) 289 3608; Fax (+1) (508) 457 2134.

growth on different N sources including transporters for nitrate, formate/nitrite, urea, ammonium and amino acids among others (Berg *et al*., 2008). Studies of P physiology are more limited. *A. anophagefferens* is capable of growing on dissolved organic phosphorus (DOP, e.g. glycerol-phosphate) as its sole P source (Dzurica *et al*., 1989), but DOP metabolism in this group has not been comprehensively examined, either in culture studies or in the field. Further, there are no studies of functional genes related to P physiology in this species.

When taken together, these studies indicate that *A. anophagefferens* may have the capacity to utilize reduced nitrogen, or organic nutrients when the concentration of inorganic nutrients becomes low. Phytoplankton have evolved mechanisms for efficiently scavenging N and P from a variety of sources and these mechanisms can be induced at the transcriptional level when a nutrient becomes limiting (Grossman, 2000; Dyhrman *et al*., 2006; 2008). Global transcriptome profiling studies have shown broad transcriptional regulation to nutrient deficiency in coccolithophores and diatoms (Dyhrman *et al*., 2006; Mock *et al*., 2008). This has also been seen in the HAB-forming species *Alexandrium fundyense* (Erdner and Anderson, 2006), and transcriptional studies are an increasingly popular tool for studies of HAB nutritional physiology (Dyhrman, 2008). There are a number of approaches for examining transcription in a non-targeted manner, ranging from microarrays (e.g. Mock *et al*., 2008) to next generation sequencing of cDNA (e.g. Erdner and Anderson, 2006). The Long-SAGE method used in this study is a sequencing-based approach, which avoids some of the challenges involved with microarrays, that infer abundance based upon hybridization, suffer from background noise, cross-hybridization problems and only measure relative abundance (Irizarry *et al*., 2005). An adaptation of the original SAGE method (Velculescu *et al*., 1995), Long-SAGE generates tag libraries without *a priori* knowledge of gene sequences via the detection of 21 bp nucleotide sequence tags making it possible to evaluate the simultaneous expression patterns of many genes quantitatively (Saha *et al*., 2002). In this regard, Long-SAGE is similar to newer sequencing methods (digital gene expression and mRNA seq), but without the depth of coverage provided by advances in next generation sequencing capabilities (see review by Morozova *et al*., 2009). Long-SAGE tags are generated by the most 3′ Nla III restriction site on the transcript, and as a consequence, errors can be reduced by only considering tags mapping to the most 3′ Nla III site of a gene. Long-SAGE has been useful for identifying transcriptome profiles for other algae, including the coccolithophore *Emiliania huxleyi* (Dyhrman *et al*., 2006) and the dinoflagellate *Pfiesteria shumwayae* (Coyne *et al*., 2004).

In this study, transcriptional responses of *A. anophagefferens* to N and P deficiency (–N and –P) relative to a nutrient replete control were assayed to identify genes that *A. anophagefferens* may upregulate when inorganic nutrients are depleted. These transcriptional responses were detected by mapping Long-SAGE tags to the 11 510 gene models identified by *in silico* modelling of the *A. anophagefferens* whole genome sequence (http://genome.jgi-psf.org/Auran1/Auran1.home.html). To our knowledge this is the first non-targeted transcriptional study in a Pelagophyte.

Results

Tag sampling and annotation

A total of 112 000 tags were sampled, representing 31 862 unique tags, from *A. anophagefferens* grown under P-deficient (–P), N-deficient (–N) and nutrient replete (control) conditions (Fig. 1). At this sampling depth, there is still a high rate of unique tag discovery (Fig. 2). All 31 862 unique Long-SAGE tags were annotated by mapping to available *A. anophagefferens* expressed sequence tag (EST) or genomic sequences. Of these 31 862 unique tags, 11 847 (37.2%) aligned to the genome with a 100% identical match to all 21 bp. A number of tags mapped to genes with annotations suggesting a role in N or P metabolism (Tables S1–S4).

Differential regulation

Aureococcus anophagefferens exhibited a broad transcriptional response to N and P deficiency, with 131 tags upregulated twofold or greater in –P, 56 tags upregulated twofold or greater in –N, 34 tags upregulated

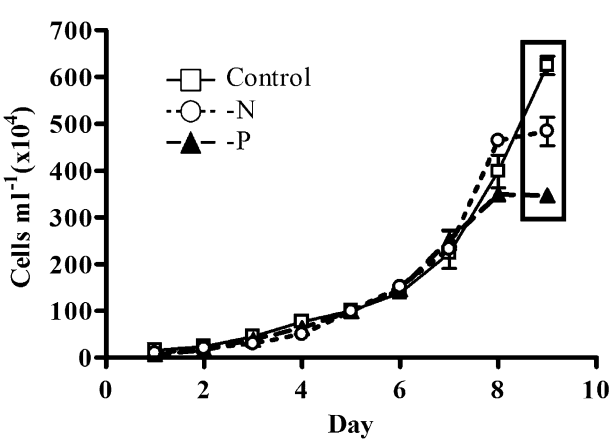

Fig. 1. Growth of *A. anophagefferens* under nutrient replete (control), phosphorus-deficient (–P) and nitrogen-deficient (–N) conditions. The treatments were harvested on day 9 (box). Error bars represent standard deviation of the mean for the control ($n = 3$), –N and –P ($n = 2$).

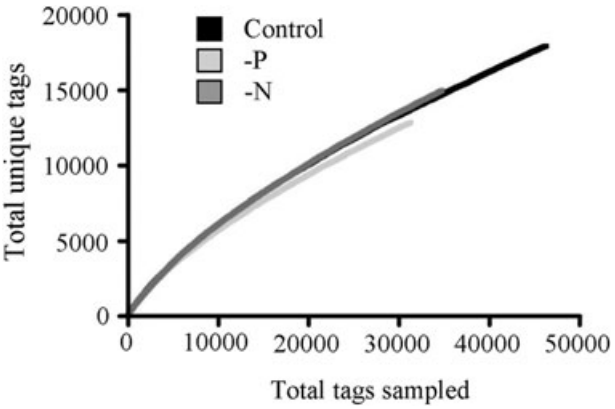

Fig. 2. Long-SAGE tag data plotted showing the relationship between total tags sampled in each library and the number of unique tags found. A predicted asymptote (~50 000) was calculated by plotting the inverse of total tags sampled versus the inverse of unique tags and calculating the y-intercept.

twofold or greater in both –P and –N, and 73 tags downregulated twofold or greater in both –N and –P. A tag in a given treatment is considered upregulated (or downregulated) if it shows twofold or greater expression relative to both of the other libraries with an *R*-value ≥ 2. In some cases, a tag was absent from one or more libraries, and is considered differentially regulated if the *R*-value ≥ 2. The *R*-value is a log likelihood ratio statistic that scores tags by their deviation from the null hypothesis of equal frequencies given the tag sampling depth for each Long-SAGE library (Stekel *et al*., 2000). A complete list of these 294 differentially expressed tags is available in the *Supporting Information* (Tables S1–S4). Approximately 80% of differentially expressed tags could be mapped to available sequence data whereas 20% could not be aligned (Fig. 3). Of tags that mapped to the genome, 43% were aligned with gene models (Fig. 3). Roughly 49% of tags mapping to sequence data could not be assigned a function either because they aligned to: (i) ESTs or genome sequence representing hypothetical or predicted proteins, (ii) ESTs showing no database homology or (iii) genome sequence where no model is predicted (Tables S1–S4). Thus, approximately 31% of differentially expressed tags could be assigned a putative function (Tables 1–4).

Of 131 tags upregulated twofold or greater in the –P treatment, many mapped to genes with putative functions in DIP and DOP acquisition (Tables 1 and S1). Tag 1819 mapped to a putative inorganic phosphate transporter, and showed an increase of almost sixfold in the –P library relative to the control library (Table 1). Two tags (6248 and 1817) mapped to two unique 5′-nucleotidases. Tag 6248 was upregulated 4.7-fold in the –P library relative to the control library, and was upregulated 13.9-fold relative to the –N library (Table 1). Similarly, tag 1817 was upregulated 6.6-fold in the –P library relative to the control library, and was absent in the –N library (Table 1). Consistent with the upregulation of the putative 5′-nucleotidases, *A. anophagefferens* is able to grow on the nucleotide, adenosine monophosphate (AMP), as a sole P source (Fig. 4). Tag 4828 mapped to an alkaline phosphatase and showed almost threefold upregulation relative to the control library and 6.4-fold upregulation relative to the –N library (Table 1). Other tags upregulated in the –P library mapped to a putative oxidoreductase, a nuclease, a transcription initiation factor, a variety of kinases and a phosphatase (Table 1).

Of 56 tags upregulated twofold or greater in the –N treatment, some mapped to genes involved in both DIN and DON metabolism (Tables 2 and S2). For example, tag 4223 mapped to an ammonium transporter and was upregulated 10-fold in the –N library relative to the –P library and was absent from the control library (Table 2). Tag 3830 mapped to an acetamidase/formamidase that was upregulated 11-fold in the –N library relative to the –P library and was upregulated roughly twofold in the –N library relative to the control. Tag 17565 mapped to a xanthine/uracil/vitamin C permease and was only present in the –N library (Table 2). There were also tags that mapped to genes involved in protein metabolism, including two peptidases (tags 5832 and 3352), and an N-acetylglucoasmine transferase (Tag 17579) (Table 2). Finally, a variety of tags showed upregulation in –N with less clear roles in N metabolism, including an arylsulfatase, phosphoglycerate dehydrogenase, a dynein heavy chain, and DNA-directed RNA polymerase.

There are 34 tags that can be considered to be related to a general stress response because they are

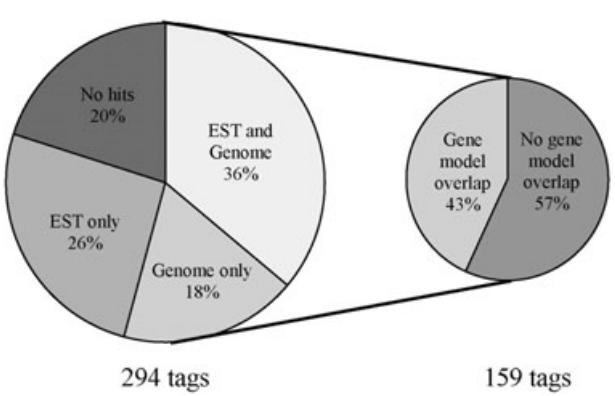

Fig. 3. The percentage of tags showing differential regulation (294 total tags) that map to available sequence data, and the percentage of tags that overlap with gene models from the subset of those tags that map to the *A. anophagefferens* genome (159 tags). See text for a description of the criteria a tag must meet to be considered differentially regulated.

Table 1. Successfully annotated tags showing upregulation in the –P library. Only tags that show greater than twofold change in the –P library relative to the control and –N libraries with an *R*-value > 2 are included. ESTs are given for tags annotated by mapping to an EST. A protein ID is given for: (i) tags that map directly to the genome where a gene model exists or (ii) tags that map to an EST that overlaps with a gene model on the genome.

			Fold change versus:				
Tag ID	Tag sequence	*R*-value	Control	–N	Putative annotation	EST	Protein ID
1817	CATGCCGGGCGCCTTCGACGC	22.53	6.6	Absent[a]	5′-nucleotidase (manually curated)[b]	–	21301
1819	CATGGGCGTCAAGCTCACGGC	20.38	5.7	Absent	Inorganic phosphate transporter (manually curated)	–	22152
157	CATGGTGAAGTTGCAAAAGGC	16.19	2.5	6.8	NADP-dependent oxidoreductase [*Hahella chejuensis* KCTC 2396]	–	67152
1831	CATGGCGCCCCTCGCCCGCGT	10.09	4.8	4.4	Endonuclease/exonuclease protein-like protein [*Leishmania major*]	–	72478
2957	CATGGTCTCCGTCTTCCACCC	9.116	4.8	4.9	ABC1-like [*Oryza sativa* Japonica Group]	–	70922
1922	CATGGTCTGGGCCGGCGAGGG	7.792	4.949	7.3	Nucleoside diphosphate kinase Nm23-SD1 [*Suberites domuncula*]	–	22626
1833	CATGGAGAACATCCACCGCGC	7.194	3.4	27.9	Mitochondrial substrate carrier family protein [*Arabidopsis thaliana*]	–	22191
1921	CATGTCCCAGTTCATCCTCGC	6.070	Absent	13.9	PREDICTED: similar to CG8472-PA, isoform A [*Strongylocentrotus purpuratus*]	–	72105
1883	CATGCGGGAGTCGCTAAGCTG	5.601	4.4	3.0	Beta transducin-like protein HET-E2C [*Podospora anserina*]	4211177:40	–
1972	CATGACGACGACCACCACCAC	4.928	Absent	Absent	Peptidase [*Salinibacter ruber* DSM 13855]	4205112:1	–
2802	CATGGACGCCGTCGACGCCGC	4.928	Absent	Absent	Pulvinus outward-rectifying channel for potassium SPOCK1 [*Samanea saman*]	4205553:1	–
1556	CATGTAGACACCCCCCCCTCC	4.593	3.1	2.1	Dimethylaniline monooxygenase (N-oxide forming).	–	29808
1506	CATGGACTACTGGCTCCTCGG	4.451	2.9	4.6	Cathepsin L [*Theromyzon tessulatum*]	4209574:1	–
2385	CATGATCGCCGCGCTGCGGCC	4.402	2.6	19.3	Fucokinase, isoform CRA_d [Homo sapiens]	4217517:1	–
4828	CATGGACGCGGCCGTCAAGCG	4.224	2.9	6.4	Alkaline phosphatase-like protein [*Teredinibacter turnerae* T7901]	4205689:1	–
136	CATGTACATACATCGCACATT	4.017	5.3	Absent	BRF1 homolog, subunit of RNA polymerase III transcription initiation factor IIIB [*Danio rerio*]	71825	–
1879	CATGCCCTCGACGCCGCAGCG	3.689	9.5	7.0	Chain A, 4ank: A Designed Ankyrin Repeat Protein With Four Identical Consensus Repeats	4209777:1	–
1595	CATGGACTCCGTCAAGCGCGG	3.579	4.9	Absent	Glycosyl transferase, group 1	–	60545
6248	CATGGGCGCGCTCCGCGCCGT	3.467	4.7	13.9	5′-nucleotidase (manually curated)	–	28588
1917	CATGCGCGCGCAGATCTGCGA	3.125	3.7	4.8	Protein kinase-like [*Medicago truncatula*]	4211177:384	–
14815	CATGGCAAGATTGTGGTTCCT	2.962	13.1	9.7	Glycoside hydrolase (manually curated)	–	64125
2371	CATGTCCACGCCGCAGCTCCG	2.939	5.3	11.8	ABC transporter (manually curated)	–	62521
2034	CATGATCATCTCGCCGTCGTC	2.738	Absent	Absent	PHD-finger family protein [*Trichomonas vaginalis* G3]	EH117526	–
3008	CATGGCCTGCTACCGGGGCCA	2.738	Absent	Absent	PREDICTED: similar to ankyrin 2,3/unc44, partial [*Strongylocentrotus purpuratus*]	EH117401	–
1904	CATGGCGTCGGGCTACGGCCC	2.531	5.1	Absent	Twin-arginine translocation pathway signal sequence domain protein, putative [*Phaeobacter gallaeciensis* 2.10]	4205643:1	–
1957	CATGGAGTAGATCCACCCGTC	2.504	3.5	3.6	Serine/threonine-protein kinase ripk4, putative [*Penicillium marneffei* ATCC 18224]	4206124:1	
1929	CATGCTCATCGCCTGCGTCGT	2.463	3.3	4.3	Synaptobrevin domain-containing protein [*Dictyostelium discoideum* AX4]	–	36201
2817	CATGGCAAATCCTGCCAAGGT	2.454	6.6	9.7	Mitogen-activated protein kinase 2 [*Toxoplasma gondii*]	–	55052
3045	CATGAAGGCGCCGTAGCTGCC	2.433	5.3	5.9	Flagellar associated protein [*Chlamydomonas reinhardtii*]	EH117555	–
1869	CATGTCCAACCGCAAGTAGCT	2.366	Absent	3.2	Type I fatty acid synthase, putative [*Toxoplasma gondii* RH]	–	72815
14836	CATGCGCCTCTCGTACTACGG	2.190	Absent	Absent	OTU-like cysteine protease family protein [*Tetrahymena thermophila*]	4208711:1	
14902	CATGGACGCGTACGATTTGGT	2.190	Absent	Absent	Trehalose-phosphatase (manually curated)	–	53568
14850	CATGTACGTCGGCGAGGGCGG	2.081	Absent	5.4	Cellulase, endoglucanase (manually curated)	–	12783
279	CATGCCGCCGACGACGCGGTC	2.019	2.5	2.3	PREDICTED: similar to coiled-coil domain containing 93 [*Ciona intestinalis*]	4206222:1	–

a. Fold change cannot be calculated on tags absent from a given library, but are included in the table with *R*-value > 2.
b. Manually curated notes the gene model was manually assigned a function and reviewed by a curator.

Table 2. Successfully annotated tags showing upregulation in the –N library. Only tags that show greater than twofold change in the –N library relative to the control and –P libraries with an *R*-value > 2 are included. A protein ID is given for: (i) tags that map directly to the genome where a gene model exists or (ii) tags that map to an EST that overlaps with a gene model on the genome. ESTs are given for tags annotated by mapping to an EST.

			Fold change versus:				
Tag ID	Tag sequence	*R*-value	Control	–P	Putative annotation	EST	Protein ID
4223	CATGGACGACTCGAAGCACGG	4.742	Absent[a]	10.3	Ammonium transporter (manually curated)[b]	–	52202
11372	CATGTATCCCCTGAGAACTGG	3.159	6.1	Absent	Dynein-1-beta heavy chain, flagellar inner arm I1 complex [*Chlamydomonas reinhardtii*]	–	72661
3447	CATGGCCGACGCGGGCGAGGT	2.892	5.9	6.1	DEAD (Asp-Glu-Ala-Asp) box polypeptide 46 [*G. gallus*]	–	65005
5832	CATGACGAAGTAGTACTTGCC	2.772	5.4	3.0	Peptidase [*Salinibacter ruber* DSM 13855]	EH117491	–
2091	CATGGGCCCCCACGAGCGCGA	2.643	3.6	5.0	D-3-phosphoglycerate dehydrogenase [*Thalassiosira pseudonana* CCMP1335]	4211036:1	–
17565	CATGCTCTTCCACCTCGGCCT	2.586	Absent	Absent	Xanthine/uracil/vitamin C permease [*Micromonas* sp. RCC299]	–	52593
17581	CATGGAGCTCTGGCTCGCCGC	2.586	Absent	Absent	Arylsulfatase (manually curated)	–	64446[c]
3890	CATGGTCGGCTACGGTGGCGG	2.426	3.2	6.5	Pherophorin-dz1 protein [Volvox carteri f. nagariensis]	4210976:3	–
6403	CATGCATCACTTTGGACTAAT	2.358	2.7	Absent	DNA-directed RNA polymerase II 135 kDa polypeptide, putative, expressed [*Oryza sativa* (japonica cultivar-group)]	–	38738
3830	CATGTCGATAGAATCCAATGG	2.291	2.3	11.2	Acetamidase/formamidase (manually curated)	–	37987
3345	CATGCAGGCCGTCGGTCTCTG	2.238	2.0	11.2	NADPH protochlorophyllide reductase [*Bigelowiella natans*]	4207500:1	–
3352	CATGGGCCCCGGCCGCCGCCG	2.121	3.1	Absent	Peptidase M16A, coenzyme PQQ biosynthesis protein PqqF [*Medicago truncatula*]	–	22177
17579	CATGTTCTCCGCGTCGTGGCT	2.069	Absent	Absent	O-linked N-acetylglucosamine (GlcNAc) transferase [*Danio rerio*]	–	32337
5046	CATGAAGGTGGCCGAGGCCCT	2.003	2.1	10.3	Poly A binding protein, cytoplasmic 1 a [*Danio rerio*]	–	70409

a. Fold change cannot be calculated on tags absent from a given library, but are included in the table with *R*-value > 2.
b. Manually curated notes the gene model was manually assigned a function and reviewed by a curator.
c. Tag maps 3′ of gene model, but does not overlap.

Table 3. Successfully annotated tags showing greater than twofold upregulation in both the –N and –P libraries relative to the control library (*R*-value > 2). A protein ID is given for: (i) tags that map directly to the genome where a gene model exists or (ii) tags that map to an EST that overlaps with a gene model on the genome. ESTs are given for tags annotated by mapping to an EST.

			Fold change for:				
Tag ID	Sequence	*R*-value	–P	–N	Putative annotation	EST	Protein ID
1814	CATGATGGGCGTCACGGGCGC	15.58	4.8	3.2	Chloroplast light harvesting protein isoform 3 [*Isochrysis galbana*]	–	59955
10695	CATGGAGGAGGTCAACCTCCT	3.940	14.6	17.6	Contains oxidoreductase domain	–	72519
2687	CATGTTCGGCGAGGGCCAGAC	3.834	4.4	2.7	Plastid light harvesting protein isoform 39 (manually curated)[a]	–	77828
922	CATGCCGGCGGCCGTGCCGGG	3.401	3.6	3.9	Fucoxanthin chlorophyll a/c protein, deviant [*Phaeodactylum tricornutum* CCAP 1055/1]	4208996:1	–
1894	CATGCTCGGGCTCGCGCACGC	3.327	7.8	3.6	Glycosyl transferase group 1 [*Herpetosiphon aurantiacus* ATCC 23779]	4211177:45	–
1481	CATGGCCCGCAGCGACCTCCA	3.276	2.3	5.4	Sensory transduction histidine kinase [*Psychroflexus torquis* ATCC 700755]	–	71871
1839	CATGCCCGACTACACCAAGTC	3.041	3.4	2.0	Oxidoreductase, acting on the aldehyde or oxo group of donors, disulfide as acceptor/pyruvate dehydrogenase (acetyl-transferring) [*Arabidopsis thaliana*]	–	53060
1951	CATGTTCCTGTCGCTCGACGT	3.026	16.0	6.8	Cation efflux system protein [*Oceanicola batsensis* HTCC2597]	4211177:393	–
6839	CATGGTCGGCGGCATCGACGA	3.026	16.0	6.8	RecName: Full = ATP synthase subunit beta, mitochondrial; Flags: Precursor	4206114:1	–
3296	CATGCCGACGCCGCGCGCGCT	2.610	Absent[b]	Absent	PREDICTED: similar to dishevelled associated activator of morphogenesis 1 isoform 1 [*Danio rerio*]	–	70943
1941	CATGTGGATGCAAGCGGCTGC	2.580	3.3	3.7	Glutaminyl-tRNA synthetase, putative [*Perkinsus marinus* ATCC 50983]	4211177:152	–
2546	CATGGCGCGGTACCAGATCGG	2.057	7.3	2.7	O-methyltransferase, putative [*Streptomyces ghanaensis* ATCC 14672]	4211177:220	–

a. Manually curated notes the gene model was manually assigned a function and reviewed by a curator.
b. Fold change cannot be calculated on tags absent from a given library, but are included in the table with *R*-value > 2.

Table 4. Successfully annotated tags showing greater than twofold downregulation in –N and –P libraries relative to the control (*R*-value > 2). A protein ID is given for: (i) tags that map directly to the genome where a gene model exists or (ii) tags that map to an EST that overlaps with a gene model on the genome. ESTs are given for tags annotated by mapping to an EST.

			Fold change in:				
Tag ID	Tag sequence	*R*-value	–P	–N	Putative annotation	EST	Protein ID
2	CATGGTCCTCCGCCTCCGCGG	11.54	–2.5	–2.4	Polyubiquitin [*Trichomonas vaginalis*]	–	17856
184	CATGTAGGACGGACACGTAAG	10.06	–5.4	–3.7	Phosphoribosylaminoimidazole carboxylase, *Candida glabrata*	4213887:1	–
257	CATGAGCTCCCGGCTGCGGGC	3.971	–3.8	–5.2	ATP-dependent Clp protease proteolytic subunit [*Cyanidioschyzon merolae*]	4206479:1	–
216	CATGGGCGACGCCGTCGCCGC	3.932	–12.4	–6.6	3-isopropylmalate dehydrogenase [*Synechococcus elongatus* PCC 6301]	EH412414	–
187	CATGTAGGCGCGCCCGCGCGT	3.846	–6.2	–3.3	Methionine sulfoxide reductase A [*Synechococcus* sp. WH 5701]	–	59179
1516	CATGTCCTGCAAGAAGGACAC	3.604	–5.7	–3.7	Eukaryotic translation initiation factor 5A [*Micromonas pusilla* CCMP1545]	–	59757
80	CATGGTGAAGATCCCCCAGGC	3.600	Absent[a]	–8.8	Lipocalin [*Pelobacter propionicus* DSM 2379]	4212868:1	–
53	CATGGCCTAAAAAAAAAATAA	3.251	Absent	–8.1	RS1, ribosomal protein 1 [*Thalassiosira pseudonana*]	4211021:1	–
3728	CATGGGGCTCTACGTCTACGG	3.213	Absent	–2.0	Anthranilate phosphoribosyltransferase, chloroplast precursor putative, expressed [*Oryza sativa* (japonica cultivar-group)]	4206546:1	–
4679	CATGCTTAAAGAACTAATATA	2.927	–11.0	–3.9	PREDICTED: similar to ferredoxin-NADP reductase [*Ornithorhynchus anatinus*]	4211085:1	–
4690	CATGGAGGGCGAGAAGATCGC	2.900	–3.8	Absent	Eukaryotic translation initiation factor 2 subunit 3, X-linked [*Mus musculus*]	–	22992
240	CATGTACTCCTAGAGGGTGCA	2.896	–2.1	Absent	RAD23 [*Phaeodactylum tricornutum* CCAP 1055/1]	4216537:1	
144	CATGGCGCCGTATCAATAGCG	2.857	–2.5	–2.1	Protein kinase NPK2 [*Nicotiana tabacum*]	–	72184
367	CATGACGACGCCGGGCAGCCC	2.730	–5.5	–5.9	Proteophosphoglycan 5 [*Leishmania major* strain Friedlin]	4206526:2	–
122	CATGGACCTCAACCAGGTCAA	2.691	Absent	Absent	Replication factor A [*Capsicum chinense*]	4216955:1	–
468	CATGCGCGACGAGTTCCACGT	2.642	–10.3	–3.7	Aspartate aminotransferase [*Phaeodactylum tricornutum* CCAP 1055/1]	4214969:2	–
4707	CATGGCGCCGGACTACGTCGA	2.520	Absent	–2.0	1 origin recognition complex subunit 2 [*Oryza sativa*]	4212823:1	–
3028	CATGCACGGCTGATGAGCCCC	2.437	–2.3	Absent	ABC transporter [*Thalassiosira pseudonana* CCMP1335]	4210715:1	–
707	CATGGGCTACAACGGCGGCAC	2.331	–5.5	–3.9	Light-inducible protein atls1, putative [*Ricinus communis*]	4215630:1	–
996	CATGGAGGACGAGGGGCGATG	2.307	Absent	Absent	Lipase/esterase [*Synechococcus* sp. CC9311]	–	70850
4919	CATGCGGCGCGGCGCGGCGGC	2.307	Absent	Absent	Centrin, putative [*Plasmodium falciparum* 3D7]	4211177:12	–
4890	CATGTGCAAGAAGCCCGGCTG	2.260	–5.5	Absent	Putative GTP-binding protein typA [*Oryza sativa*]	–	52055
375	CATGACGGACCTCCGCGACAA	2.229	Absent	–5.9	Malate/L-lactate dehydrogenase (manually curated)[b]	4211088:1	
4684	CATGATGATCGAATGATCCAC	2.156	–9.6	–2.6	Nitrite reductase (manually curated)	–	37238
4697	CATGCGTGTCTACCCGGCCGC	2.106	–8.2	–4.4	Nitrate transporter (manually curated)	–	60332
4807	CATGTACCTCAAGCAGGACTC	2.081	Absent	–2.2	DNA ligase I [*Coprinopsis cinerea*]	–	36790
110	CATGGACTAAAATTGATCACA	2.058	–5.5	–2.9	Elongation factor 1B-gamma, putative/eEF-1B gamma, putative [*Arabidopsis thaliana*]	4210815:1	–
131	CATGGCCGCGGCCATCGGCGT	2.015	–3.8	–2.3	F-ATPase family transporter: protons (mitochondrial) [*Ostreococcus lucimarinus* CCE9901]	4206441:1	–

a. Fold change cannot be calculated on tags absent from a given library, but are included in the table with *R*-value > 2.
b. Manually curated notes the gene model was manually assigned a function and reviewed by a curator.

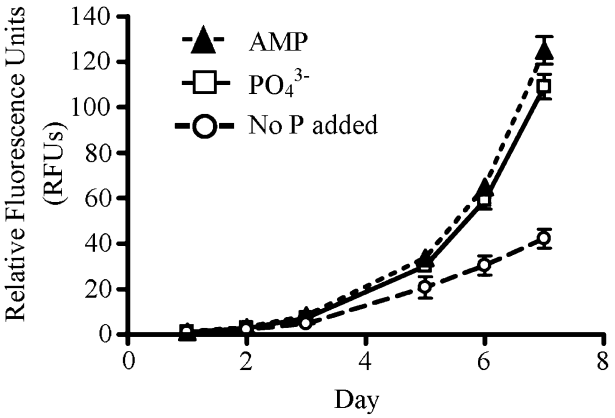

Fig. 4. Growth of *A. anophagefferens* on different P sources: 50 μM phosphate (PO_4^{3-}), 50 μM AMP and a no P added control. RFUs (Relative Fluorescence Units) serve as a proxy for biomass. Error bars represent standard errors of the mean ($n = 3$).

upregulated in both –P and –N relative to the control (Table S3). Two tags (10695 and 1839) mapped to two different oxidoreductases (Table 3). Tag 10695 showed strong upregulation in both –P (14.6-fold) and –N (17.7-fold) relative to the control (Table 3). Tag 1839 also showed upregulation in both –P and –N, with a threefold increase in –P and twofold increase in –N relative to the control (Table 3). Additionally, three tags (1814, 2687 and 922) mapped to three different proteins involved in light harvesting, with all three tags showing similar magnitudes of upregulation (Table 3).

The final category contains tags that were downregulated in both –N and –P, which consists of 73 tags (Table S4). This may also be the result of a general stress response. Tags in this category were downregulated twofold or greater in the –P and –N libraries relative to the control with an *R*-value ≥ 2. Two tags mapped to genes with known roles in DIN metabolism. Tag 4684 mapped to a nitrite reductase while tag 4697 mapped to a nitrate transporter (Table 4). Also in this category is tag 2, a highly expressed tag that mapped to polyubiquitin, and other tags that mapped to genes related to general metabolism (Table 4).

Some tags mapped to genes with known roles in N and P metabolism, but did not meet the criteria for differential regulation. For example, tag 113 mapped to a putative urea transporter and shows similar expression in the –N and control, compared with a depressed signal under –P (data not shown). Other tags that mapped to genes with known roles in nutrient metabolism included, but are not limited to, a variety of N substrate transporters, nitrate reductase, and urease (Fig. 5).

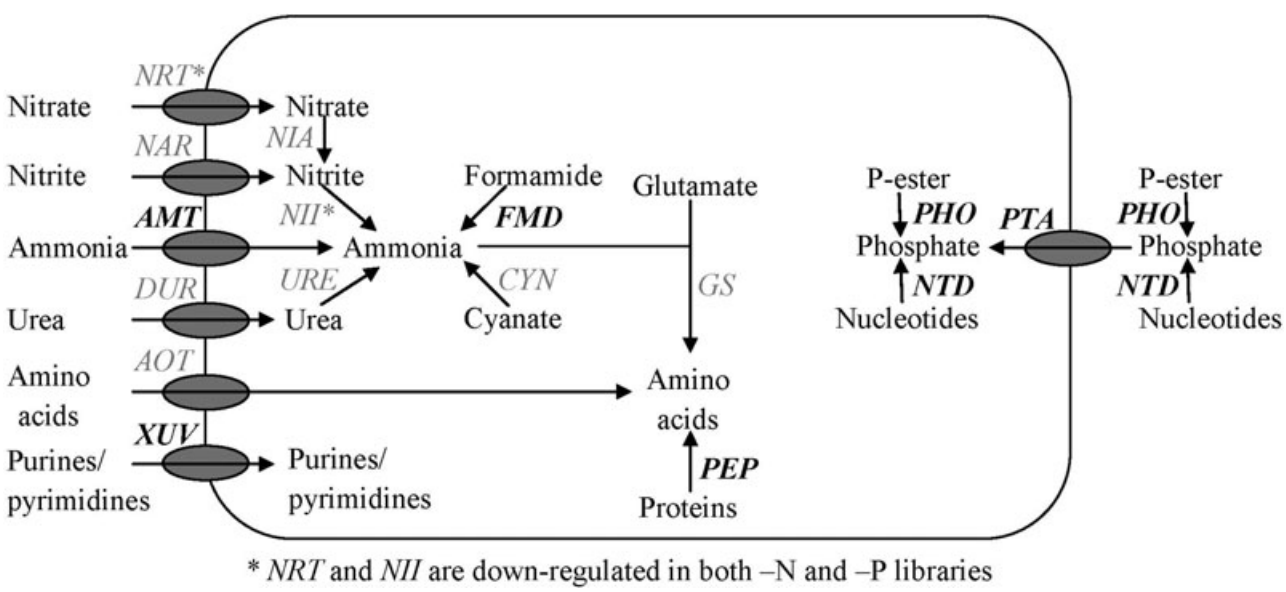

Fig. 5. Schematic of N and P acquisition/metabolism genes identified in *A. anophagefferens* with Long-SAGE data. Putative N-related transporter localizations are based upon a previous study (Berg *et al*., 2008). Localizations of P-related genes are for clarity of the figure only. Genes are in italics, with bold indicating the presence of a tag that is upregulated in either the nitrogen-deficient (–N) or phosphorus-deficient (–P) library. *AMT*, *FMD*, *XUV* and *PEP* are upregulated in the –N library while *PHO*, *NTD* and *PTA* are upregulated in the –P library. *NRT* and *NII* are downregulated in both –N and –P libraries. Other expressed genes include *NAR* (tag 381: CATGGTCCTCAACGACGCGAC), *NIA* (tag 11818*:* CATGTAATTCACGAAGGTCGG), *DUR* (tag 113: CATGCTAACTTGTATAATAAT), *URE* (tag 2023: CATGGTCCTCAACGACGCGAC), *AOT* (tag 31113: CATGTCGCTGACGGGCAACGT), *CYN* (tag 2141: CATGCGCCGCCAGTAGCGGGT) and *GS* (tag 18182: CATGTCCTGCAACCCCTACCT). Gene names are as follows: *NRT*, nitrate transporter; *NAR*, formate/nitrite transporter; *AMT*, ammonium transporter; *DUR*, urea transporter; *AOT*, amino acid transporter; *XUV*, xanthine/uracil/vitamin C transporter; *NIA*, nitrate reductase; *NII*, nitrite reductase; *URE*, urease; *FMD*, acetamidase/formamidase; *CYN*, cyanase; *GS*, glutamine synthetase; *PEP*, peptidase; *PHO*, phosphatase/alkaline phosphatase; *NTD*, 5′-nucleotidase; *PTA*, phosphate transporter.

Discussion

As a consequence of its devastating effects to the coastal ecosystem and commercial shellfishing industries, *A. anophagefferens* has become a widely studied HAB species (as reviewed in Gobler *et al*., 2005; Sunda *et al*., 2006). Nutrient supply is considered an important factor that may drive brown tide dynamics, and it is hypothesized that *A. anophagefferens* will use reduced N and DON under nitrate-deficient conditions. *A. anophagefferens* may also switch to growth on DOP under phosphate-deficient conditions. In this study, Long-SAGE was used to profile the *A. anophagefferens* transcriptome under N- and P-deficient and nutrient replete (control) conditions with the goal of gaining a better understanding of the molecular mechanisms underlying N and P metabolism in *A. anophagefferens* and to examine molecular level evidence of switching from growth on inorganic nutrients to growth on organic matter at the onset of nutrient deficiency.

Long-SAGE and genome annotation

Here, 31 862 unique Long-SAGE tags have been identified and 11 847 (37.2%) of these tags mapped to the genome. As previously reviewed, these results are consistent with other Long-SAGE studies where on average, 36.5% of Long-SAGE tags can be mapped to the genome if it is available (Wang, 2007). This may be explained by the fact that an exact match between the tag and genomic sequence is required, and there is most likely variation in the genomes of individual organisms, even of the same strain. Furthermore, if a tag is located at an intron/exon boundary, it will not map back to the genome. An individual tag may also map to multiple sites if two different genes have the same most 3′ Nla III restriction site and downstream sequence. A total of 1045 (or 8.8%) of tags hit multiple sites, and were excluded from further analysis.

Despite these limitations and the fact that this study only covered a fraction of the transcriptome, these expression data have enhanced the *A. anophagefferens* genome annotation effort by assigning expression data to many genes, supporting *in silico* gene calls, and locating regions where genes may exist, but were not otherwise identified. For example, tag 1819 mapped to the genome in a location where both an EST and a gene model exist. In this example, expression data have been successfully assigned to this gene model, and the tag was successfully annotated as an inorganic phosphate transporter. Alternatively, Tag 1817 mapped to the genome in a location where a gene has been predicted (putative 5′-nucleotidase), but no EST support is available. In this case, the Long-SAGE tag has provided support for the *in silico* gene model prediction, and an annotation has been assigned to the tag. As a final example, tag 14 821 mapped to the genome where no gene model exists, and is located too far from the nearest gene model to be part of the 3′ untranslated region. This tag is found eight times exclusively in the –P library. This is a case where tag data have provided evidence for the existence of a gene that was not otherwise identified.

The Long-SAGE resulted in roughly 30 000 unique tags, and predicts the unique tag yield to be about 50 000 based on the frequency of unique tag recovery. If only one unique tag was sampled from every transcript, this would result in a transcriptome size of 50 000 genes, higher than the 11 510 gene models identified with *in silico* modelling with the genome sequence (http://genome.jgi-psf.org/Auran1/Auran1.home.html). However, transcriptome size estimates are often substantially elevated with Long-SAGE data because multiple unique tags can be generated for the same transcript at non-primary Nla III sites with incomplete restriction digests during library construction. This is likely the primary reason for the inflated gene number estimated here. However, this discrepancy is not entirely due to incomplete digestion, as tags (e.g. tag 14 821) mapped to the genome in regions where there was no gene model prediction. In *Thalassiosira pseudonana*, a tiling array (that is not restricted to the assumptions about gene content that is the case for traditional microarrays) identified 1132 transcripts that were not present in the 11 390 modelled gene set (Mock *et al*., 2008). Here, Long-SAGE is similar in the ability to identify putative genes that were not detected with *in silico* gene modelling for the genome sequence, which highlights the value of these data types in supporting genome annotation efforts. Even with the relatively low depth of sampling in this study, it is apparent that highly expressed genes detectable in a low resolution dataset are missing from the gene models predicted in the *A. anophagefferens* genome. With advances in sequencing technology, it is becoming possible to perform large-scale short-read sequencing of the transcriptome with exceptionally high coverage, and decreasing cost. The application of these techniques will be valuable for helping to support future genome annotation efforts as well as discovering novel genes (Morozova *et al*., 2009).

Responses to P deficiency

A strong transcriptional response was observed in the –P library. A number of these –P tags mapped to genes with known roles in both inorganic and organic P metabolism. One of the most highly P-regulated tags (R-value > 20) mapped to a putative inorganic phosphate transporter. This would suggest that one strategy employed by *A. anophagefferens* during P deficiency is to produce more phosphate transporters, or switch to a more efficient one.

This strategy has been observed in other eukaryotic algae (Chung *et al*., 2003; Dyhrman *et al*., 2006).

Two tags (6248 and 1817) upregulated in the –P library mapped to two different 5′-nucleotidases. This enzyme cleaves phosphorus from nucleotides and has been suggested to be involved in P-scavenging from exogenous nucleotides in other eukaryotic algae (Flynn *et al*., 1986; Dyhrman and Palenik, 2003). In the ocean, nucleotides can be released from cells by grazing or lysis and may represent a major source of P, with concentrations reaching 10–20 nM (Ammerman and Azam, 1985). *A. anophagefferens* can grow well on AMP as its sole P source, indicating that nucleotides may be an important P source for field populations. Although both of the tags mapping to the 5′-nucleotidase are generally upregulated in the –P library, the intensity and pattern of their regulation is distinct and they could be serving different functions within the cell.

Tag 4828 is significantly upregulated in the –P library and mapped to an EST that aligns with a gene model for alkaline phosphatase in the *A. anophagefferens* genome. This enzyme is known to cleave phosphorus from a variety of DOP compounds and has been shown to be induced under P limitation in other algae (Dyhrman and Palenik, 1999; 2003; Landry *et al*., 2006; Xu *et al*., 2006). Algal alkaline phosphatases can be difficult to identify, for example the *E. huxleyi* alkaline phosphatase (Landry *et al*., 2006; Xu *et al*., 2006) has no database homology. The putative *A. anophagefferens* alkaline phosphatase is similar to the alkaline phosphatase identified in the *T. pseudonana* genome.

The presence and upregulation of tags mapping to genes related to DOP hydrolysis suggests that *A. anophagefferens* has the ability to utilize P-ester (especially 5′-nucleotides) and perhaps other DOP compounds when DIP is low. This hypothesis is consistent with field observations of significant reductions in DOP concentration during the peak of brown tides, when *A. anophagefferens* cell densities exceed 10^6 cells ml^{-1} in New York estuaries (Gobler *et al*., 2004). Given the lack of studies on *A. anophagefferens* P physiology, these observations warrant further investigation using a semi-continuous or continuous culture study to differentiate short-term responses to P deficiency, examined herein, from the long-term acclimation strategies that may be more indicative of natural populations.

Responses to N deficiency

Under N-deficient conditions, *A. anophagefferens* upregulates a number of genes putatively involved in N acquisition. Tag 4223 is upregulated 15-fold in the –N library and mapped to an EST that shows sequence homology to characterized ammonium transporters in the diatom *Cylindrotheca fusiformis*. The ammonium transporters in *C. fusiformis* are transcriptionally regulated, with highest mRNA copies in N-deficient cells (Hildebrand, 2005), consistent with the pattern observed herein. *A. anophagefferens* has several ammonium transporters, and this ammonium transporter is different than the one previously shown to be upregulated under N-deficient conditions in *A. anophagefferens* (Berg *et al*., 2008). Clearly, *A. anophagefferens* upregulates a variety of ammonium transporters in response to N deficiency, which is consistent with the preference for reduced N observed in low nitrate field populations (Gobler *et al*., 2005).

Past studies have shown that *A. anophagefferens* can hydrolyse proteins, and grow well on DON, such as aminosugars, urea and amino acids, as a sole N source (Berg *et al*., 2002; 2003; Mulholland *et al*., 2002). It has also been reported to grow on small amides as a sole N source, including acetamide and, to a lesser extent, formamide (Berg *et al*., 2008). This is consistent with other studies that identified that dinoflagellates, coccolithophores and diatoms grow on acetamide, and that coccolithophores grow well on formamide (Palenik and Henson, 1997). Tag 3830, which mapped to an acetamidase/formamidase, is upregulated in the –N library, which suggests that *A. anophagefferens* can break down these small amides, and that this process is regulated by N deficiency. Increased activities of acetamidase and formamidase were detected in N-deficient *E. huxleyi* (Palenik and Henson, 1997), which is consistent with the transcript regulation observed herein. The sources and concentrations of amides in marine systems are poorly understood, but they may serve as N sources for field populations, especially those experiencing N deficiency. *A. anophagefferens* also upregulates a putative xanthine/uracil/vitamin C permease. In a tiling array experiment with *T. pseudonana*, a putative xanthine/uracil/vitamin C permease was also shown to be upregulated under N-deficient conditions (Mock *et al*., 2008). As a result of the broad annotation it is difficult to determine the function of this gene in *A. anophagefferens*. Uric acid permeases have been shown to promote the uptake of uric acid into cells of *Bacillus subtilis* in N-deficient conditions (Schultz *et al*., 2001). This gene may be serving a similar role in *A. anophagefferens*. Two tags mapping to putative peptidases were identified in the Long-SAGE libraries, with higher expression in the –N library relative to the –P library. Given their regulation pattern, these peptidases may serve to scavenge N from peptides, although peptidases serve many roles in a cell besides N scavenging from proteins. Further, there is a tag upregulated in the –N library that mapped to an N-acetylglucosamine transferase. *O*-GlcNAcylation (mediated by N-acetylglucosamine transferase) has been shown to affect protein activity, stability and localization and this,

taken together with the upregulation of the peptidases, suggests an increased protein metabolism and protein processing during N deficiency. Whether this is related to recycling of N inside the cell, or the acquisition of N from proteins or peptides from seawater, deserves further study.

It should be noted that both control and –N treatments consisted of nitrate as the primary N source. In the diatom *C. fusiformis*, ammonia transporters are transcriptionally regulated with highest mRNA copies in N-starved cells, followed by cells grown on NO_3^- only, and lowest mRNA copies in ammonium-grown cells (Hildebrand, 2005), suggesting negative regulation by ammonium. In *A. anophagefferens*, it has been shown that certain genes involved in N-metabolism can be transcriptionally regulated by N source (Berg *et al*., 2008). It may be possible that a stronger global transcriptional response would be seen if *A. anophagefferens* had been grown on ammonia, rather than nitrate, as the primary N source in the control library. Regardless, these data support the observation that *A. anophagefferens* can utilize a wide variety of N sources and switches to these N sources (including reduced and organic forms) at the onset of N deficiency. As discussed with P-regulated genes, additional culture studies could be used to identify if these responses are related to acclimation to N deficiency.

General stress response

A number of tags were upregulated in response to both P and N deficiency, possibly as part of a general stress response. Interestingly, three tags (1814, 2687 and 922) mapped to proteins involved in light harvesting. Regulation of these gene families in other algae is variable. In the coccolithophore *E. huxleyi*, a Long-SAGE study showed downregulation of a fucoxanthin chlorophyll a/c binding (Fcp) protein under N starvation (Dyhrman *et al*., 2006), and in diatoms genes encoding Fcp and LHC-like proteins were significantly upregulated in Fe-limited conditions (Allen *et al*., 2008). In the case of *A. anophagefferens*, it may be that there is broad downregulation of many genes under stress, and that this downregulation is not as strong, or not as rapid for light harvesting related machinery. In fact, a number of tags were downregulated in both –N and –P libraries, and have highest copy numbers in the control library. Owing to the fact that it requires resources to actively express genes, this downregulation may be driven by a global stress response to conserve resources. A more detailed time-course study that quantifies RNA levels, and includes an Fe-deficient condition would examine the consistency of the regulation on genes encoding proteins related to light harvesting.

Tag 2 mapped to a ubiquitin gene and is expressed at a high copy number in the control library, but is downregulated in both –N and –P libraries. Ubiquitin is a protein involved in post-translational modification of proteins, usually targeting them for proteosomal destruction (Hershko and Heller, 1985). A high expression of this protein in nutrient replete, exponentially growing, *A. anophagefferens* cultures suggests changes in protein turnover relative to the other treatments, and that this pathway is responsive to general stress. In the group of tags elevated in the control library, one tag (4684) mapped to a nitrite reductase while tag 4697 mapped to a nitrate transporter. Another targeted gene expression study of this species showed upregulation of this same nitrate transporter under acute N deficiency (25 days in low N medium) compared with *A. anophagefferens* grown on acetamide as the sole N source (Berg *et al*., 2008). Berg and colleagues (2008) also demonstrated that the nitrate transporter gene was induced by nitrate. In the Long-SAGE study presented here, nitrate was used as the N source for all treatments, and nitrate replete expression patterns (control) were compared with cells grown roughly 8 days in low nitrate medium (–N), which may explain some of the differences. Nevertheless, these data indicate that the nitrate transporter expression is sensitive to both total N concentration as well as nitrate concentration. Therefore, the regulation patterns observed in the Long-SAGE libraries may be controlled by a combination of growth on nitrate and total N availability.

This is the first transcriptional data to examine general stress responses in a Pelagophyte. These transcriptional data suggest that under stress conditions, such as N and P deficiency, *A. anophagefferens* may broadly downregulate many genes involved in general metabolism, while maintaining light harvesting capability. However, the lack of tags mapping to genes encoding heat shock proteins, chaperons and other markers of a cellular stress response, indicates that higher resolution sampling is required to detect a comprehensive stress response transcriptome.

Non-differentially expressed genes

In addition to transcripts discussed above, a number of tags mapped to genes with known roles in N and P metabolism. These remaining tags of interest are all at too low a copy number to resolve differential expression patterns. This includes tags that mapped to transporters for compounds known to be utilized as an N source by *A. anophagefferens*, including nitrate, ammonium, urea and amino acids (Fig. 5). There was also a tag that mapped to a formate/nitrite transporter, although it is unclear whether *A. anophagefferens* can utilize nitrite as a sole N source (Fig. 5). Finally, tags that mapped to the enzymes nitrite reductase, nitrate reductase, glutamine

synthetase, urease and cyanase were found (Fig. 5). The expression data of these N-related genes are consistent with data from *A. anophagefferens* EST libraries (Berg *et al*., 2008), and given that the Long-SAGE data comprise the most highly expressed genes, it also indicates that these genes are highly expressed in the cells. The cyanase is included as related to N metabolism because cyanase hydrolyses cyanate into ammonium and carbon dioxide, and has been shown to play an important role in scavenging N from cyanate in cyanobacteria (Kamennaya *et al*., 2008). The Long-SAGE results suggest that cyanase is expressed, but not regulated by N in *A. anophagefferens*; however, a targeted study would address this with more sensitivity than afforded by the current analysis.

In this set of N metabolism transcripts, tag 113 mapped to an EST with sequence homology to a high affinity urea transporter from the picoeukaryote *Ostreococcus tauri* (Derelle *et al*., 2006). This tag is expressed under nutrient replete and –N conditions, but downregulated under P deficiency. The same urea transporter has been shown to be upregulated under acute N deficiency (Berg *et al*., 2008). This difference may be explained by the fact that Long-SAGE is not as sensitive as quantitative RT-PCR at the depth of sequencing in this study, or that cells in the Berg and colleagues' 2008 study were grown on acetamide, not nitrate. Regardless, both evidence from quantitative RT-PCR and Long-SAGE support the hypothesis that *A. anophagefferens* is able to scavenge urea from the environment. Consistent with this finding, several culture studies have demonstrated that *A. anophagefferens* can grow equally well on both urea and nitrate as an N source (MacIntyre *et al*., 2004; Pustizzi *et al*., 2004) and that urea enrichments can stimulate *A. anophagefferens* blooms *in situ* (Kana *et al*., 2004).

Conclusions

The goal of this study was to examine the transcriptome of *A. anophagefferens* under varying environmental conditions (such as –N or –P), to elucidate the broad-scale responses of this organism to nutrient deficiency, and to gain a better understanding of the metabolic pathways involved in nutrient acquisition. Many of the tags that are most highly upregulated in the –N and –P library mapped to predicted or hypothetical genes, or areas of the genome where no gene model exists (Tables S1–S3). This underscores how little is known about the genes and pathways of nutrient metabolism in this Pelagophyte and the importance of further studies focused on characterizing these genes and their function. However, this study supports the hypothesis that *A. anophagefferens* can metabolize reduced or organic forms of N and P when inorganic nutrients are not available. *A. anophagefferens* expresses and regulates a suite of genes related to N acquisition/metabolism, including the genes necessary for growth on a variety of N compounds (Fig. 5). This is consistent with observations from both culture and field data (Lomas *et al*., 1996; Berg *et al*., 1997; 2002; 2003; Mulholland *et al*., 2002; Kana *et al*., 2004; MacIntyre *et al*., 2004; Pustizzi *et al*., 2004). *A. anophagefferens* also expresses genes involved in both DIP and DOP uptake and metabolism, and these appear to be highly upregulated under P deficiency (Fig. 5). Very little is known about how P influences *A. anophagefferens* blooms, but the results indicate that DOP could be important to the P nutrition of this species adding further evidence for the importance of organic nutrients in fuelling the growth of this harmful species in sensitive coastal regions.

These data have identified gene targets with expression patterns that are indicative of a switch to growth on organic nutrients. As such, monitoring the quantitative expression of these gene targets may serve as a tool for examining N and P deficiency in natural populations over the course of a bloom cycle, ultimately providing a much needed link between nutrient supply and *A. anophagefferens* bloom dynamics.

Experimental procedures

Culture conditions

Aureococcus anophagefferens CCMP 1984 was obtained from the Provasoli-Guillard Center for the Culture of Marine Phytoplankton (CCMP). The cultures were grown in batch to examine the instantaneous transcriptome response of *A. anophagefferens* to nutrient deficiency at 18°C on a 14:10 h light : dark cycle (140 μmol quanta m^{-2} s^{-1}). Nitrogen- and phosphate-replete (883 μM NO_3^- and 36.3 μM PO_4^{3-}) cells, –N (40 μM NO_3^-) cells and –P (1 μM PO_4^{3-}) cells were grown in autoclaved L1 media with no Si (Guillard and Hargraves, 1993), prepared using 0.2 μm filtered Vineyard Sound seawater. Vitamins (thiamine, biotin and B_{12}) were sterile filtered and added to the media after autoclaving. The growth of the cultures was monitored daily by cell counts on a haemacytometer. Replete cells were harvested during mid log phase of growth, while –N and –P cells were harvested at the onset of stationary phase when N or P was depleted (Fig. 1). With additions of N (883 μM NO_3^-) or P (36.3 μM PO_4^{3-}) to the nutrient-depleted treatments, the cells resumed exponential growth (data not shown). To test whether *A. anophagefferens* can grow on AMP, an additional culture experiment was performed. *A. anophagefferens* was grown in L1 media with no Si as described above with the following changes: In the PO_4^{3-} treatment, cells were grown in media containing (36.3 μM PO_4^{3-}). For the AMP treatment, cells were grown in media containing no added PO_4^{3-}, but instead contained AMP at a concentration of 36.3 μM. Media with no added P were used as a control and growth was monitored with a Turner Designs fluorometer.

Total RNA extraction

Approximately 2×10^7 cells were harvested (8000 *g* for 10 min) from each treatment and immediately stored in liquid nitrogen until extraction. Total RNA was extracted using TRI reagent (Sigma) according to the manufacturer's instructions. RNA concentrations were quantified with a UV spectrophotometer. Integrity of the total RNA was assessed by 1% (wt/vol) agarose gel electrophoresis.

Long-SAGE library construction

Long-SAGE libraries were constructed using approximately 30 μg RNA isolated from extractions of replete (control), –P, and –N *A. anophagefferens* cells following the I-SAGE Long kit protocol (Invitrogen). Recombinant pZEro1 clones produced by Long-SAGE were purified using GeneMachines RevPrep Orbit (Genomic Solutions) and were sequenced on an ABI 3730xl DNA sequencer (Applied Biosystems). The sequences collected were analysed with software created at the Marine Biological Laboratory specifically for SAGE analysis and used in the context of previous work (Dyhrman *et al*., 2006). The SAGE software extracts ditag sequences from the ABI 3730xl results according to the Long-SAGE sequence grammar, parses out individual Long-SAGE tags, excludes tags with sequence ambiguities, and reduces all Long-SAGE tags to a look-up table of unique Long-SAGE tag sequences and their observed frequencies among all of the *A. anophagefferens* Long-SAGE libraries. All Long-SAGE tags were mapped to sequence data (see below) for annotation, but those tags found only once (singletons) were excluded from differential expression analysis.

Tags were annotated by mapping to *A. anophagefferens* ESTs on GenBank (http://www.ncbi.nlm.nih.gov), or the unpublished *A. anophagefferens* genome data sequenced by the DOE Joint Genome Institute (JGI) and located on their portal page (http://www.jgi.doe.gov/Aureococcus). Because Long-SAGE tags are short (21 bp), an exact match was required. Tags mapping to the genome were annotated based on their overlap or proximity to gene models. ESTs specific to *A. anophagefferens* were used to help annotate tags in which a gene model could not be assigned, or for tags that did not map to the genome sequence, but did map to ESTs. These ESTs were assembled into clusters and blasted against GenBank using blastX to assign a putative function using an expect value cut-off of 1e-5.

Long-SAGE tags were scored for differential expression among the three libraries by using the *R* statistic (Stekel *et al*., 2000), a log likelihood ratio statistic that scores tags by their deviation from the null hypothesis of equal frequencies given the tag sampling depth for each Long-SAGE library. Higher scores represent a greater deviation from the null hypothesis, while scores close to zero represent near constitutive expression. To reduce the effects of sampling error in highlighting differential expression, only tags with an *R*-value of 2 or greater are presented. Additionally, if more than one tag mapped to the same sequence, only the most 3′ tag was included here. The tag data discussed in this publication have been deposited in NCBI's Gene Expression Omnibus (Edgar *et al*., 2002) and are accessible through GEO Series accession number GSE21465 (http://www.ncbi.nlm.nih.gov/geo/query/acc.cgi?acc=GSE21465).

Acknowledgements

This paper is a result of research funded by the National Oceanic and Atmospheric Administration Center for Sponsored Coastal Ocean Research under award NA09NOS4780206 to WHOI. ECOHAB publication number 614. Further support came from funds from the Woods Hole Oceanographic Institution, the Woods Hole Center for Oceans and Human Health and the Woods Hole Coastal Ocean Institute, a STAR Research Assistance Agreement No. R-83041501-0 awarded by the U.S. Environmental Protection Agency, as well as an EPA STAR fellowship (STAR Fellowship assistance agreement number FP916901). We would like to thank the JGI and the *Aureococcus* genome consortium. The *Aurecoccus* genome sequencing and analysis were performed under the auspices of the US Department of Energy's Office of Science, Biological and Environmental Research Program, and by the University of California, Lawrence Berkeley National Laboratory under contract No. DE-AC02-05CH11231, Lawrence Livermore National Laboratory under Contract No. DE-AC52-07NA27344, and Los Alamos National Laboratory under contract No. DE-AC02-06NA25396. We would also like to thank the Marine Biological Laboratory's Josephine Bay Paul Center for sequencing and informatics assistance, particularly Shanda Birkeland and Andrew McArthur. Finally, we thank Alan Kuo, Astrid Terry, and Igor Grigoriev from the JGI for their efforts on the *Aureococcus anophagefferens* genome annotation as well as informatics supporting this study.

References

Allen, A.E., LaRoche, J., Maheswari, U., Lommer, M., Schauer, N., Lopez, P.J., *et al*. (2008) Whole-cell response of the pennate diatom *Phaeodactylum tricornutum* to iron starvation. *Proc Natl Acad Sci USA* **105:** 10438–10443.

Ammerman, J.W., and Azam, F. (1985) Bacterial 5′-nucleotidase in aquatic ecosystems – a novel mechanism of phosphorus regeneration. *Science* **227:** 1338–1340.

Anderson, D.M., Burkholder, J.M., Cochlan, W.P., Glibert, P.M., Gobler, C.J., Heil, C.A., *et al*. (2008) Harmful algal blooms and eutrophication: examining linkages from selected coastal regions of the United States. *Harmful Algae* **8:** 39–53.

Berg, G.M., Glibert, P.M., Lomas, M.W., and Burford, M.A. (1997) Organic nitrogen uptake and growth by the chrysophyte *Aureococcus anophagefferens* during a brown tide event. *Mar Biol* **129:** 377–387.

Berg, G.M., Repeta, D.J., and LaRoche, J. (2002) Dissolved organic nitrogen hydrolysis rates in axenic cultures of *Aureococcus anophagefferens* (Pelagophyceae): comparison with heterotrophic bacteria. *Appl Environ Microbiol* **68:** 401–404.

Berg, G.M., Repeta, D.J., and LaRoche, J. (2003) The role of the picoeukaryote *Aureococcus anophagefferens* in cycling of marine high-molecular weight dissolved organic nitrogen. *Limnol Oceanogr* **48:** 1825–1830.

Berg, G.M., Shrager, J., Glockner, G., Arrigo, K.R., and Grossman, A.R. (2008) Understanding nitrogen limitation in *Aureococcus anophagefferens* (Pelagophyceae)

through cDNA and qRT-PCR analysis. *J Phycol* **44:** 1235–1249.

Chung, C.C., Hwang, S.P.L., and Chang, J. (2003) Identification of a high affinity phosphate transporter gene in a prasinophyte alga, *Tetraselmis chui*, and its expression under nutrient limitation. *Appl Environ Microbiol* **69:** 754–759.

Coyne, K.J., Burkholder, J.M., Feldman, R.A., Hutchins, D.A., and Cary, S.C. (2004) Modified serial analysis of gene expression method for construction of gene expression profiles of microbial eukaryotic species. *Appl Environ Microbiol* **70:** 5298–5304.

Dennison, W.C., Marshall, G.J., and Wigand, C. (1989) Effects of 'brown tide' shading on eelgrass (*Zostera marina*) distributions. In *Novel Phytoplankton Blooms: Causes and Impacts of Recurrent Brown Tides and Other Unusual Blooms, Volume 35*. Cosper, E.M., Bricelj, V.M., and Carpenter, E.J. (eds). New York, NY, USA: Springer, pp. 675–692.

Derelle, E., Ferraz, C., Rombauts, S., Rouze, P., Worden, A.Z., Robbens, S., *et al*. (2006) Genome analysis of the smallest free-living eukaryote, *Ostreococcus tauri* unveils many unique features. *Proc Natl Acad Sci USA*: **103:** 11647–11652.

Dyhrman, S.T. (2008) Molecular approaches to diagnosing nutritional physiology in harmful algae: implications for studying the effects of eutrophication. *Harmful Algae* **8:** 167–174.

Dyhrman, S.T., and Palenik, B. (1999) Phosphate stress in cultures and field populations of the dinoflagellate *Prorocentrum minimum* detected by a single-cell alkaline phosphatase assay. *Appl Environ Microbiol* **65:** 3205–3212.

Dyhrman, S.T., and Palenik, B. (2003) Characterization of ectoenzyme activity and phosphate-regulated proteins in the coccolithophorid *Emiliania huxleyi*. *J Plankton Res* **205:** 230–231.

Dyhrman, S.T., Haley, S.T., Birkeland, S.R., Wurch, L.L., Cipriano, M.J., and McArthur, A.G. (2006) Long Serial Analysis of Gene Expression for gene discovery and transcriptome profiling in the widespread marine coccolithophore *Emiliania huxleyi*. *Appl Environ Microbiol* **72:** 252–260.

Dzurica, S., Lee, C., Cosper, E.M., and Carpenter, E.J. (1989) Role of environmental variables, specifically organic compounds and nutrients, in the growth of the chrysophyte *Aureococcus anophagefferens*. In *Novel Phytoplankton Blooms: Causes and Impacts of Recurrent Brown Tides and Other Unusual Blooms, Volume 35*. Cosper, E.M., Bricelj, V.M., and Carpenter, E.J. (eds). New York, NY, USA: Springer, pp. 229–252.

Edgar, R., Domrachev, M., and Lash, A.E. (2002) Gene Expression Omnibus: NCBI gene expression and hybridization array data repository. *Nucleic Acids Res* **30:** 207–210.

Erdner, D.L., and Anderson, D.M. (2006) Global transcriptional profiling in the toxic dinoflagellate *Alexandrium fundyense* using massively parallel signature sequencing. *BMC Genomics* **7:** 88.

Flynn, K.J., Öpik, H., and Syrett, P.J. (1986) Localization of the alkaline phosphatase and 5′-nucleotidase activities of the diatom *Phaeodactylum tricornutum*. *J Gen Microbiol* **132:** 289–298.

Gobler, C.J., and Sañudo-Wilhelmy, S.A. (2001) Effects of organic carbon, organic nitrogen, inorganic nutrients, and iron additions on the growth of phytoplankton and bacteria during a brown tide bloom. *Mar Ecol Prog Ser* **209:** 19–34.

Gobler, C.J., Renaghan, M.J., and Buck, N.J. (2002) Impacts of nutrients and grazing mortality on the abundance of *Aureococcus anophagefferens* during a New York brown tide bloom. *Limnol Oceanogr* **47:** 129–141.

Gobler, C.J., Boneillo, G.E., Debenham, C., and Caron, D.A. (2004) Nutrient limitation, organic matter cycling, and plankton dynamics during an *Aureococcus anophagefferens* bloom in Great South Bay, N.Y. *Aquat Microb Ecol* **35:** 31–43.

Gobler, C.J., Lonsdale, D.J., and Boyer, G.L. (2005) A review of the causes, effects, and potential management of harmful brown tide blooms caused by *Aureococcus anophagefferens* (Hargraves et Sieburth). *Estuaries* **28:** 726–749.

Greenfield, D.I., and Lonsdale, D.J. (2002) Mortality and growth of juvenile hard clam *Mercenaria mercenaria* during brown tide. *Mar Biol* **141:** 1045–1050.

Greenfield, D.I., Lonsdale, D.J., Cerrato, R.M., and Lopez, G.R. (2004) Effects of background concentrations of *Aureococcus anophagefferens* (brown tide) on growth and feeding in the bivalve *Mercenaria mercenaria*. *Mar Ecol Prog Ser* **274:** 171–181.

Grossman, A. (2000) Acclimation of *Chlamydomonas reinhardtii* to its nutrient environment. *Protist* **151:** 201–224.

Guillard, R.R.L., and Hargraves, P.E. (1993) *Stichochrysis immobilis* is a diatom, not a chrysophyte. *Phycologia* **32:** 234–236.

Hershko, A., and Heller, H. (1985) Occurrence of a polyubiquitin structure in ubiquitin-protein conjugates. *Biochem Biophys Res Commun* **128:** 1079–1086.

Hildebrand, M. (2005) Cloning and functional characterization of ammonium transporters from the marine diatom *Cylindrotheca* fusiformis. *J Phycol* **41:** 105–113.

Irizarry, R.A., Warren, D., Spencer, F., Kim, I.F., Biswal, S., Frank, B.C., *et al*. (2005) Multiple-laboratory comparison of microarray platforms. *Nat Methods* **2:** 477–477.

Kamennaya, N.A., Chernihovsky, M., and Post, A.F. (2008) The cyanate utilization capacity of marine unicellular Cyanobacteria. *Limnol Oceanogr* **53:** 2485–2494.

Kana, T.M., Lomas, M.W., MacIntyre, H.L., Cornwell, J.C., and Gobler, C.J. (2004) Stimulation of the brwon tide organism, *Aureococcus anophagefferens*, by selective nutrient additions to *in situ* mesocosms. *Harmful Algae* **3:** 377–388.

Keller, A.A., and Rice, R.L. (1989) Effects of nutrient enrichment on natural populations of the brown tide phytoplankton *Aureococcus anophagefferens* (Chrysophyceae). *J Phycol* **25:** 636–646.

Landry, D.M., Gaasterland, T., and Palenik, B.P. (2006) Molecular characterization of a phosphate-regulated cell-surface protein from the coccolithophorid, *Emiliania huxleyi* (Prymnesiophyceae). *J Phycol* **42:** 814–821.

LaRoche, J., Nuzzi, R., Waters, R., Wyman, K., Falkowski, P.G., and Wallace, D.W.R. (1997) Brown tide blooms in

Long Island's coastal waters linked to variability in groundwater flow. *Glob Change Biol* **3:** 397–410.
Lomas, M.W., Glibert, P.M., and Berg, G.M. (1996) Characterization of nitrogen uptake by natural populations of *Aureococcus anophagefferens* (Chrysophyceae) as a function of incubation duration, substrate concentration, light, and temperature. *J Phycol* **32:** 907–916.
MacIntyre, H.L., Lomas, M.W., Cornwell, J.C., Suggett, D., Gobler, C.J., Koch, E., and Kana, T.M. (2004) Mediation of benthic-pelagic coupling by microphytobenthos: an energy and nutrient based model for initiation of blooms of *Aureococcus anophagefferens*. *Harmful Algae* **3:** 403–437.
Mock, T., Samanta, M.P., Iverson, V., Berthiaume, C., Robison, M., Holtermann, K., *et al*. (2008) Whole genome expression profiling of the marine diatom *Thalassiosira pseudonana* identifies genes involved in silicon bioprocesses. *Proc Natl Acad Sci USA* **105:** 1579–1584.
Morozova, O., Hirst, M., and Marra, M.A. (2009) Applications of new sequencing technologies for transcriptome analysis. *Annu Rev Genomics Hum Genet* **10:** 135–151.
Mulholland, M.R., Gobler, C.J., and Lee, C. (2002) Peptide hydrolysis, amino acid oxidation and N uptake in communities seasonally dominated by *Aureococcus anophagefferens*. *Limnol Oceanogr* **47:** 1094–1108.
Mulholland, M.R., Boneillo, G., and Minor, E.C. (2004) A comparison of N and C uptake during brown tide (*Aureococcus anophagefferens*) blooms from two coastal bays on the east coast of the USA. *Harmful Algae* **3:** 361–376.
Palenik, B., and Henson, S.E. (1997) The use of amides and other nitrogen sources by the phytoplankton *Emiliania huxleyi*. *Limnol Oceanogr* **42:** 1544–1551.
Pustizzi, F., MacIntyre, H.L., Warner, M.E., and Hutchins, D.A. (2004) Interaction of nitrogen source and light intensity on the growth and photosynthesis of the brown tide alga *Aureococcus anophagefferens*. *Harmful Algae* **3:** 343–360.
Saha, S., Sparks, A.B., Rago, C., and Akmaev, V. (2002) Using the transcriptome to annotate the genome. *Nat Biotechnol* **19:** 508–512.
Schultz, A.C., Nygaard, P., and Saxild, H.H. (2001) Functional analysis of 14 genes that constitute the purine catabolic pathway in *Bacillus subtilis* and evidence for a novel regulon controlled by the PucR transcription activator. *J Bacteriol* **183:** 3293–3302.
Stekel, D.J., Git, Y., and Falciani, F. (2000) The comparison of gene expression from multiple cDNA libraries. *Genome Res* **10:** 2055–2061.
Sunda, W.G., Graneli, E., and Gobler, C.J. (2006) Positive feedback and the development and persistence of ecosystem disruptive algal blooms. *J Phycol* **42:** 963–974.
Velculescu, V.E., Zhang, L., Vogelstein, B., and Kinzler, K.W. (1995) Serial analysis of gene expression. *Science* **270:** 484–487.
Wang, S.M. (2007) Understanding SAGE data. *Trends Genet* **23:** 42–50.
Xu, Y., Wahlund, T.M., Feng, L., Shaked, Y., and Morel, F.M.M. (2006) A novel alkaline phosphatase in the coccolithophore *Emiliania huxleyi* (Prymnesiophyceae) and its regulation by phosphorus. *J Phycol* **42:** 835–844.

Supporting information

Additional Supporting Information may be found in the online version of this article:

Table S1. Complete list of tags showing greater than twofold upregulation in the –P library relative to both the control and –N libraries ($R \geq 2$).
Table S2. Complete list of tags showing greater than twofold upregulation in the –N library relative to both the control and –P libraries ($R \geq 2$).
Table S3. Complete list of tags showing greater than twofold upregulation in both the –P and –N libraries relative to the control library ($R \geq 2$).
Table S4. Complete list of tags showing greater than twofold upregulation in the control library relative to both the –P and –N libraries ($R \geq 2$).

Please note: Wiley-Blackwell are not responsible for the content or functionality of any supporting materials supplied by the authors. Any queries (other than missing material) should be directed to the corresponding author for the article.

CHAPTER THREE

Proteome changes driven by phosphorus deficiency and recovery in the brown tide-forming alga, *Aureococcus anophagefferens*

Louie L. Wurch[a]

Erin M. Bertrand[b]

Mak A. Saito[b]

Benjamin A.S. Van Mooy[b]

Sonya T. Dyhrman[a,c]

[a]Biology Department, Woods Hole Oceanographic Institution, Woods Hole, MA 02543 USA

[b]Department of Marine Chemistry & Geochemistry, Woods Hole Oceanographic Institution, Woods Hole, MA 02543 USA

[c]Corresponding author: sdyhrman@whoi.edu

In prep: PLoS ONE

Abstract

Shotgun mass spectrometry was used to detect proteins in *Aureococcus anophagefferens* and monitor their relative abundance across nutrient replete (control), phosphate-deficient (–P) and –P refed with phosphate (P-refed) conditions. Spectral counting techniques identified differentially abundant proteins and demonstrated that under phosphate deficiency, *A. anophagefferens* increases proteins involved in both inorganic and organic phosphorus (P) scavenging, including a phosphate transporter, 5'-nucleotidase, and alkaline phosphatase. Additionally, an increase in abundance of a sulfolipid biosynthesis protein was detected in –P and P-refed conditions. Analysis of the polar membrane lipids showed that cellular concentrations of the sulfolipid sulphoquinovosyldiacylglycerol (SQDG) was nearly two-fold greater in the –P condition versus the control condition, while cellular phospholipids were approximately 8-fold less. Transcript and protein abundance generally appeared to be more tightly coupled for gene products involved in P metabolism compared to those involved in a range of other metabolic functions. Comparison of protein abundances between the –P and P-refed conditions identified differences in the timing of protein degradation and turnover. This suggests that culture studies examining nutrient starvation responses will be valuable in interpreting protein abundance patterns for cellular nutritional status and history in metaproteomic datasets.

Introduction

Aureococcus anophagefferens is the phytoplankton species responsible for harmful brown tides that have caused extensive damage to a number of coastal

ecosystems in the Eastern United States (Gobler et al. 2005). Brown tides have led to a collapse of the Long Island scallop industry and caused substantial losses to eelgrass habitats (Dennison et al. 1989, Greenfield and Lonsdale 2002, Greenfield et al. 2004). Furthermore, brown tides are becoming more frequent and widespread, as evidenced by brown tides now occurring in South Africa (Gobler et al. 2005). Due to its negative impacts and the regular and widespread occurrence of blooms, *A. anophagefferens* has become a broadly studied harmful algal bloom (HAB) species (see reviews Gobler et al. 2005, Sunda et al. 2006) and is the first HAB species to have its genome sequenced (Gobler et al. 2011).

Past studies have suggested that brown tides are driven by periods of low dissolved inorganic nitrogen (DIN) and low dissolved inorganic phosphorus (DIP) availability (LaRoche et al. 1997, Keller and Rice 1989, Gobler and Sañudo-Wilhelmy 2001, Gobler et al. 2002, Gobler et al. 2004, Kana et al. 2004). Although studies of phosphorus (P) effects on bloom dynamics are more limited than those of nitrogen (N), field observations from brown tides have shown significant reductions in dissolved organic phosphorus (DOP) concentrations during peak *A. anophagefferens* cell densities (Gobler et al. 2004). Analysis of the genome suggests that *A. anophagefferens* has the capacity to utilize P from a variety of organic sources, including esters, diesters, and nucleotides (Gobler et al. 2011). In culture, *A. anophagefferens* can utilize nucleotide DOP such as adenosine monophosphate (AMP) as a sole P source, which is consistent with genome observations (Gobler et al. 2011, Wurch et al. 2011). When DIP becomes deficient, *A. anophagefferens* exhibits a broad transcriptional response, up-regulating a

variety of these P-scavenging genes such as a phosphate transporter, 5'-nucleotidase, and alkaline phosphatase, where the latter two are important enzymes used by phytoplankton to access P from the DOP pool (Wurch et al. 2011). These data, combined with field observations, suggest that DOP could be important in controlling bloom persistence and decline.

Genome and transcriptome sequencing efforts have provided key insights into the metabolic potential of harmful phytoplankton species (Parker et al. 2008, Dyhrman 2008). Despite the value of these sequencing efforts, studies in humans have demonstrated that much of the transcribed genome is never translated (Birney et al. 2007), suggesting that transcriptome analyses may overestimate actual cellular processes and physiological responses to nutritional status. Mass spectrometry-based proteomics allow direct measurements of changes in an organism's protein pool, thus more accurately assessing the arsenal of chemical responses these organisms employ for growth under different physiological conditions. Proteomics is also a valuable compliment to nucleic acid sequencing approaches as a tool for examining whether physiological responses can be linked to upstream transcriptional patterns. Recently, mass spectrometry-based proteomic approaches have successfully been employed to analyze primary metabolic and biosynthetic pathways in the diatom *Thalassiosira pseudonana* (Nunn et al. 2007) as well as the diazotrophic unicellular marine cyanobacteria *Crocosphaera watsonii* (Saito et al. 2011). Similar proteomic techniques are currently being applied to *in situ* ocean communities and have allowed for the direct observation of expressed proteins from mixed microbial consortia (Sowell et al. 2009,

Morris et al. 2010). These metaproteomic approaches revealed that transporters dominate the pool of identifiable proteins in low nutrient environments on ocean-wide scales (Sowell et al. 2009, Morris et al. 2010). However, without detailed information on protein regulation, it is difficult to link the abundance of particular proteins, like these transporters, to cellular physiology or a cell's geochemical environment.

Herein, shotgun mass spectrometry was used to identify protein abundances in *A. anophagefferens* in nutrient replete (control) and phosphate-deficient (–P) treatments. In order to examine the timing of these responses, proteins were also assayed in a phosphate-refed (P-refed) treatment, where replete levels of phosphate were added to –P cells over a 24-hour period. Protein abundances were compared between two treatments using spectral counting and compared to transcript expression patterns from a previous study (Wurch et al. 2011).

Materials and Methods

Culture conditions

An axenic culture of *A. anophagefferens* strain CCMP 1984 was obtained from the Provasoli-Guillard Center for the Culture of Marine Phytoplankton (CCMP). Culture treatments were grown in triplicate Fernbach flasks in 2L of media per replicate at 18°C on a 14 hour:10 hour light:dark cycle at 150 µmol quanta m^{-2} s^{-1}. Locally collected Vineyard Sound seawater was filtered (0.2 µm) and used to make modified L1 media with no added silica (Guillard and Hargraves 1993). P concentrations were modified as follows: 36 µM phosphate for the control treatment and 1 µM phosphate for the P-

deficient (–P) treatment. Vitamins (thiamine, biotin, and B_{12}) were sterile filtered and added after autoclaving. Each flask was then inoculated with *A. anophagefferens* stock culture to a starting concentration of 10^5 cells mL^{-1}. Growth was monitored daily by cell counts on a hemacytometer and relative fluorescence using a Turner Designs fluorometer. Cells were harvested by centrifugation to form pellets and immediately stored in liquid nitrogen. Control treatment cells were harvested on day 6 during exponential phase of growth and –P treatment cells were harvested on day 8, at onset of stationary phase (Figure S1). Phosphate was then added back to the remaining –P cells to a final concentration of 36 μM. These P-refed cells were harvested 24 hours later.

Protein extraction and digestion

Cell pellets (single biological replicate from each treatment) were resuspended in 700 μL B-PER reagent (Thermo Scientific, Rockford, IL) supplemented with 5 mM EDTA and 1 mM phenylmethanesulfonylfluoride (a serine protease inhibitor). Samples were incubated at room temperature for 40 minutes with occasional gentle vortexing and then incubated on ice for 10 minutes. The cells were then sonicated with a microtip (Branson digital sonifier) on ice for 1 minute at constant duty cycle. Samples were centrifuged for 40 minutes at 14,100 RCF and 4°C, and protein was precipitated out of the supernatants overnight in 50% acetone 50% methanol 0.5 mM HCl at -20 °C. Precipitated protein was collected by centrifugation at 14,100 RCF for 30 minutes at 4 °C and dried by speed vacuum at room temperature. Protein was resuspended in 100 uL of the extraction buffer. Aliquots were taken for protein determination by DC assay using

bovine serum albumin as a protein standard (BioRad Inc., Hercules CA). Proteins were stored at -80 °C until digestion.

Protein samples were digested following the tube gel digestion procedure (Lu and Zhu 2005) with minor modifications. Briefly, samples were immobilized in 15% acrylamide in pH 7.5 Tris buffer, fixed with 10% acetic acid and 50% ethanol, washed successively with 10% acetic acid and 50% methanol, then acetonitrile and 25 mM ammonium bicarbonate to remove detergents and protease inhibitors and then cut into 1 mm^3 pieces. Samples were reduced with 10 mM dithiothreitol (DTT) at 56 °C for 1 hour, alkyated with 30 mM iodoacetamide for 1 hour, and then washed in 25 mM ammonium bicarbonate and digested with trypsin in 25 mM ammonium bicarbonate for 16 hours at 37 °C (1:20 ratio trypsin to total protein, Promega Gold Mass Spectrometry Grade, Promega Inc., Madison WI). The peptides were extracted by three successive additions of 50% acetonitrile (Fisher Optima) with 5% formic acid (Michrom Ultra Pure). The extracted peptides were combined and concentrated by speed vacuum for about three hours to less than 20 µL, diluted with 2% acetonitrile and 0.1% formic acid in water (Fisher Optima) and stored at -80 °C.

Shotgun mass spectrometry

The protein digestions were analyzed (4 ug total protein per analysis) using a peptide Cap Trap in-line with a reversed phase Magic C18 AQ column (0.2 x 150 mm, 3 µm particle size, 200 Å pore size, Michrom Bioresources Inc. Auburn CA) on a Paradigm MS4 HPLC system (Michrom Bioresources Inc.) at a flow rate of 2 µl $minute^{-1}$, similar to

previously described methods [24]. A LTQ linear ion trap mass spectrometer (Thermo Scientific Inc. San Jose CA) was used with an ADVANCE nanocapillary captive electrospray source (Michrom Bioresources Inc.). The chromatography consisted of a hyperbolic gradient from 5% buffer A to 95% buffer B for 300 minutes, where A was 0.1% formic acid (Michrom Ultra Pure) in water (Fisher Optima) and B was 0.1% formic acid in acetonitrile (Fisher Optima). The mass spectrometer was set to perform MS/MS on the top 7 most abundant ions using data-dependent settings with a dynamic exclusion window of 30 seconds. Ions were monitored over the range of 400-2000 m/z. Technical triplicate measurements were conducted for each biological sample.

Mass spectrometry data processing and proteome profiling

The mass spectra collected in this study were searched using SEQUEST (Bioworks version 3.3, Thermo Inc., San Jose CA). An amino acid database for *A. anophagefferens* was constructed by combining all "project data" from the *A. anophagefferens* genome sequencing (11520 sequences from NCBI: http://www.ncbi.nlm.nih.gov/genomeprj/13500) and adding plastid proteins (105 sequences from NCBI: http://www.ncbi.nlm.nih.gov/genomeprj/36625), along with common contaminants as well as a reversed 'decoy' version of these databases for false discovery rate analysis (data downloaded on March 8th, 2011). Searches were conducted with a static modification for cysteine of +57 for alkylation by iodoacetamide and allowing for variable modifications expected if methionine was oxidized (+16), if cysteine or methionine were present as seleno-residues (+47) or if selenocysteine was

modified to dehydroalanine (-91) (Ma et al. 2003). Database search results were further processed using the PeptideProphet statistical model (Keller et al. 2002) within Scaffold 3.0 (Proteome Software Inc., Portland OR). Relative protein abundance was determined using spectral counting in Scaffold 3.0. Spectral counts are normalized across samples in each experiment, including technical replicates, to allow comparison of relative protein abundance and result in a quantitative value abundance score, as previously described (Saito et al. 2011). Proteins discussed as 'differentially abundant' were determined by the Fisher exact test as previously described (Zhang et al. 2006) with p-values < 0.05. False discovery identification rate was estimated using a reversed decoy database as previously described (Kall et al. 2008).

The proteins that met the criteria for being differentially abundant were compared by a hierarchical cluster analysis using Cluster 3.0 (Eisen et al. 1998). Average abundance scores for each sample were log transformed, centered about the mean and normalized by multiplying all values by a scale factor S so that the sum of the squares of the values for each protein is 1.0. The treatments were not centered or normalized. The data were then clustered by both protein and treatment using a centered correlation as metric and complete linkage as clustering method. The data were displayed using Java Tree View (Saldanha 2004).

Proteome comparison to transcriptome

A previous study (Wurch et al. 2011) generated transcriptome expression data under conditions identical to those examined in this study, excluding the P-refed cells,

using Long Serial Analysis of Gene Expression (Long-SAGE). Tag data from Long-SAGE were compared to the protein data obtained from this study. Only the –P and control treatments, and only genes with products identified in this study as well as the Long-SAGE study with at least two tags mapping to a given protein ID, were included in this analysis. Abundance scores from the proteome and tag counts from the transcriptome were compared using fold change in the –P treatment relative to the control. If the fold change resulted in a fraction due to a higher abundance in the control versus the –P, then the negative inverse was taken (e.g. a fold change of 0.5 would be converted to -2). To quantify the percentages of genes that were correlated at the transcript and protein level fold changes were compared between the transcript and protein data. If the transcript and protein data both showed a fold change ≥ 1.5 or ≤ -1.5, that gene was considered correlated. If the transcript showed a fold change ≥ 1.5 and the protein showed a fold change ≤ -1.5, or vice versa, that gene was considered not correlated. If either the protein or transcript showed a fold change between -1.5 and 1.5, that gene was considered neutral.

Targeted gene expression

A follow-up experiment was conducted to examine targeted gene expression of an inorganic phosphate transporter (NCBI #: 323454760). Control, –P, and P-refed conditions were generated as discussed above. Cells were collected on a 0.2 μm polycarbonate filter by vacuum filtration and immediately placed in CTAB extraction

solution (Teknova, Hollister CA) amended by the addition of 1% mass/volume polyvinylpyrrolidone. Samples were stored at -80°C until further processing.

Total RNA was isolated from each sample using the UltraClean® Plant RNA Isolation Kit (MO BIO Laboratories, Inc., Carlsbad CA) using modified manufacturer's instructions. First, samples were centrifuged at 10,000 x g to separate cell lysate from the filter and 650 uL of sample was transferred to a fresh 1.5 mL tube. Secondly, 300 μL of PMR1 was added to each sample and mixed by vortexing followed by the addition of 800 μL of PMR4 to each sample and again mixed by vortexing. Finally, samples were loaded onto the columns and RNA extraction continued according to manufacturer's instructions. Isolated RNA was then treated with TURBO™ DNase (Ambion, Austin TX) to remove potential genomic DNA contamination and RNA was then quantified spectrophotometrically. A total of 100 ng of RNA was primed with oligo dT primers and reverse transcribed into cDNA using the iScript Select cDNA Synthesis kit (Bio-Rad, Hercules CA). For each sample, a second reaction was performed in which no reverse transcriptase was added to serve as a control for genomic DNA contamination in subsequent analysis. These controls were all negative suggesting no contamination.

Species-specific primers were designed from genomic sequences using MacVector (MacVector, Inc., Cary NC). Amplicons were screened for secondary structure using Mfold software (Zuker 2003) to confirm the primers were qPCR compatible. A qRT-PCR assay was designed to optimize primer efficiency and examine relative abundance of cDNA transcripts across treatments using the comparative C_T method (Livak and Schmittgen 2001). The ΔC_T (C_T target – C_T reference) was examined

over a range of cDNA concentrations to ensure equal amplification efficiencies between target and reference amplicons. A plot of the $\log_{10}$ cDNA dilution versus ΔC_T was constructed to ensure the value of the slope did not differ significantly from zero. In this case, a constitutively expressed gene encoding an *A. anophagefferens* ubiquitin-conjugating enzyme (UbE2) was used as a reference gene (Berg et al. 2008). For UbE2, primer sequences are 5': GCGAGCTCCAGGACTTTATG and 3': CGGGGTCGAGGAAGTAGAC with an amplification efficiency of 102.7% and amplicon size of 192 nucleotides. For the phosphate transporter, primer sequences are 5': CATCCTCTACGGCATCACCAAG and 3': ATCCAGAAGACGGAGTTGACGC with an amplification efficiency of 104.9% and 141 nucleotide amplicon size. Here, the reference condition was P-replete grown cells, the reference gene was UbE2, and the experimental treatments were –P grown cells and P-refed cells. Fold-change was determined using the Relative Expression Software Tool (REST) located at http://www.gene-quantification.de/download.html. REST accounts for differences in efficiency between primer sets when calculating fold changes. The *p*-values were determined by a pair-wise fixed reallocation randomization analysis (Pfaffl et al. 2002).

Polar membrane lipid analysis

The polar membrane lipid compositions of *A. anophagefferens* were examined using previously described approaches (Martin et al. 2011, Poppendorf et al. 2011). Briefly, batch cultures of *A. anophagefferens* strain CCMP 1984 were grown in either control or –P media as described above. Cells were harvested in log phase by filtration

on GF/F filters, and immediately frozen in liquid nitrogen. Polar lipids were later extracted into dichloromethane (Martin et al. 2011) and analyzed by HPLC/MS/MS using normal phase chromatographic conditions on an Agilent 1200 HPLC coupled via an electrospray ionization source to a Thermo Vantage TSQ triple quadrupole mass spectrometer (Poppendorf et al. 2011).

Results and Discussion

Shotgun mass spectrometry was used to identify proteome responses to P deficiency. A total of 3,431 unique peptide identifications were made from 214,913 total spectra, with a false discovery rate of 0.6%. From these data, 641 unique proteins (Table S1) were detected representing about 5.5% of the current 11,596 predicted gene models in the *A. anophagefferens* genome (see methods for description of statistical analyses). Although most of these proteins could be assigned a putative function, 37 could not and are listed as either hypothetical or predicted proteins (Table S1). A large percentage of the 641 proteins were annotated as ribosomal (13.3% or 85 proteins, Table S1).

There were 46 different light harvesting complex (LHC) proteins detected out of the 62 encoded in the genome (Gobler et al. 2011) (Table S1). This is far more than detected in the proteome of the diatom *T. pseudonana* under optimal growth conditions, where a total of 14 different LHC homologues were identified [Nunn et al. 2009). *A. anophagefferens* is well adapted to low light conditions, reaching maximum growth rates at lower irradiances than its algal competitors, including the diatoms *T. pseudonana*, *Phaeodactylum tricornutum* and picoeukaryotes *Ostreococcus tauri* and *O. lucimarinus*

(Gobler et al. 2011). This is consistent with the observation that *A. anophagefferens* has more unique LHC genes encoded in its genome than its algal competitors (Gobler et al. 2011).

Differential protein abundance

The abundance of the 641 proteins detected in this study were compared among treatments using spectral counting techniques. Out of the 641 proteins detected in this study, 49.6% (318 proteins) were differentially abundant in at least one treatment (control, –P, P-refed) relative to the other two based upon abundance score (see methods for description of statistical tests used to determine differentially abundant proteins) (Figure 1, Table S2). These 318 proteins were hierarchically clustered in order to group proteins with similar abundance patterns (Figure 2). The –P and P-refed treatments clustered together meaning the proteome of the P-refed treatment more closely resembled the proteome from the –P treatment than it did the control. Therefore, starting from a P-deficient state, 24 hours was not enough time for *A. anophagefferens* to return to a replete nutrient proteome composition. The proteins grouped together into eight distinct regulation patterns across the three treatments (A-H; Figure 2).

Highest abundance in control

There were 75 proteins that were more abundant in the control condition relative to the –P and P-refed treatments (cluster A-B, Figure 2) and so are repressed during P deficiency. It appears that once phosphate is added to the –P cells, either these proteins

remain repressed or there is a delay in their synthesis. The most abundant protein detected in this study, the large subunit of ribulose-1,5-bisphosphate carboxylase/oxygenase (RuBisCO), fell into this category (NCBI #: 242620086) and was about 3.6-fold less abundant under –P conditions (Table S2). Also abundant in this study was a small chain RuBisCO protein (NCBI #: 242620087). This protein was down-regulated 4.2 fold under –P (Table S2). In the diatom *T. pseudonana*, a RuBisCO large subunit was among the most abundant proteins detected under optimal growth conditions as well (Nunn et al. 2009). Although carbon fixation was not specifically examined in this study, these protein abundance results suggest that carbon fixation is likely reduced when P is deficient in *A. anophagefferens*. In the P-refed treatment, both the RuBisCO large and small subunit proteins were more abundant than the –P treatment, but still low relative to the control. Thus carbon fixation likely increases after P deficiency is alleviated, but 24 hours was not enough time for carbon fixation in cells to fully recover.

A number of proteins with known roles in N metabolism were most abundant in the replete control (Figure 3, Table S2). A urease enzyme (NCBI #: 323449776) was slightly less abundant in the –P treatment versus the control, although this result was not statistically significant. However, in the P-refed treatment, it was significantly 7-fold less abundant. Ureases are enzymes that break down urea into carbon dioxide and ammonia and are necessary for using urea as a potential N source. Urea, along with other organic N sources, is thought to play an important role in forming and sustaining *A. anophagefferens* blooms (Berg et al. 1997, Mulholland et al. 2002, Fan et al. 2003, Gobler et al. 2005). Also found in this cluster is a cyanase enzyme (NCBI #:

323447336). This cyanase was significantly less abundant under both –P and P-refed conditions. Cyanases hydrolyze cyanate, a byproduct of urea breakdown, into ammonia and carbon dioxide and have been shown to be important for obtaining N from cyanate in cyanobacteria (Kamennaya et al. 2008, Kammennaya and Post 2011). Additionally, an ammonium transporter (NCBI #: 323457240) was found in this cluster and was over 4-fold less abundant in –P and almost 2-fold less abundant in P-refed conditions. This ammonium transporter shows similarity to characterized ammonium transporters in *Cylindrotheca fusiformis*, where they are induced in N-deficient cells (Hildebrand 2005). Ammonium transporters in *A. anophagefferens* have also been shown to be transcriptionally up-regulated under N-deficient conditions (Berg et al. 2008, Wurch et al. 2011). Finally, an acetamidase/formamidase (NCBI #: 323450867) is found in this cluster and is down-regulated 2.8-fold and 1.4-fold in the –P and P-refed treatments, respectively. In the coccolithophore *Emiliania huxleyi*, it was demonstrated that activities of acetamidase and formamidase increased under N deficiency (Palenik and Henson 1997). Transcriptome data showed an increase in an acetamidase/formamidase in *A. anophagefferens* under N-deficient conditions (Wurch et al. 2011). The lower abundance of these N-metabolism proteins in the –P treatment suggests that *A. anophagefferens* may reduce its N-scavenging machinery during P deficiency. The fact that these N-metabolism proteins are also low in the P-refed treatments suggests that once P deficiency is alleviated, the N-scavenging machinery takes longer than 24 hours to respond. These results could have implications for utilizing N metabolism/scavenging

proteins as markers of N deficiency in field populations, given that their expression may also be indirectly controlled by P availability.

Finally, a selenoprotein was also relatively more abundant in the control treatment. The *A. anophagefferens* genome appears to be enriched in genes encoding possible selenoproteins compared to other phytoplankton (Gobler et al. 2011). In this analysis, two putative selenoproteins were detected (NCBI #: 323452479 and 323451867), although the specific peptides containing selenoresidues were not identified in these proteins (Table S2). However, this is not evidence that putative selenoproteins are not important or do not contain selenium in this organism because, typically, methods that detect selenoproteins require the use of LC-ICP-MS verification and sample processing techniques designed to avoid Se residue destruction (Ma et al. 2003, Ballihaut et al. 2007). Selenoprotein 323451867 was significantly more abundant in the control compared to the –P treatment while 323451979 was not abundant and did not show differential expression between these treatments. However, without knowledge of the function of these two selenoproteins, it is difficult to interpret these results.

Highest abundance in P-refed

The 33 proteins in clusters C and E are most abundant in the P-refed treatment and of lower abundance in the –P and/or control treatments (Figure 2). These proteins are induced after phosphate is re-supplied to P-deficient cells. Many of these proteins were slightly more abundant in the –P condition relative to the control (Cluster E, Figure 2). It could be that these proteins are induced when phosphate is unavailable and

continue to be produced even after phosphate is re-supplied. One of these proteins is a putative sulfolipid biosynthesis protein (SQD1) that is 2.1-fold more abundant under –P conditions (Figure 3, Table S2). In *Arabidopsis thaliana*, reduced phosphate availability increases SQD1 mRNA expression and protein product and leads to an increase in sulfolipid content (Essigmann et al. 1998). In the ocean, it has been demonstrated that some phytoplankton are able to reduce their P requirement by substituting P lipids with sulfolipids (Van Mooy et al. 2009). The differential abundance of this sulfolipid biosynthesis protein (NCBI #: 323449174) suggests that *A. anophagefferens* employs a similar strategy of switching phospholipids for sulfolipids to adjust P quota. Analysis of the polar membrane lipids showed that cellular concentrations of the sulfolipid sulphoquinovosyldiacylglycerol (SQDG) was nearly 1.5-fold greater in the –P condition versus the control condition (2,864±29 versus 2,001±29 amol cell^{-1}), while cellular phospholipids were approximately 8-fold less (133±11 versus 1,104±41 amol cell^{-1}). In the P-refed condition, the putative sulfolipid biosynthesis protein was even more abundant (3.6 fold higher versus the control), than under the –P condition mentioned above (2.1- fold) meaning induction continues even after 24 hours of experiencing excess levels of phosphate. This result is unexpected because in the diatom *T. pseudonana*, P-deficient cells reduced their non-P lipids from ~43% to ~7% of their total lipid content over a period of 24 hours once phosphate became available (Martin et al. 2010), suggesting that 24 hours would be enough time to observe a change in abundance of proteins involved in this lipid-switching response. An alternative explanation is that the P-lipids are scavenged immediately for their P, while the activity

of the biosynthesis protein is post-translationally controlled. A delay in lipid switching response after P-addition could aid *A. anophagefferens* in maintaining lower P-quotas for longer time periods after nutrient pulses, perhaps conferring some advantage in their dynamic coastal environment where fluctuations between states of nutrient limitation could potentially be more rapid than in other areas.

Similar to *T. pseudonana*, we observed that *A. anophagefferens* also synthesizes the betaine lipid diacylglycerylcarboxyhydroxymethylcholine (DGCC) in response to P stress; concentrations of DGCC were 3,225±39 amol cell^{-1} under –P conditions but were undetectable under control conditions (<10 amol cell^{-1}). The protein responsible for synthesis of the betaine lipid diacylglyceryltrimethylhomoserine (DGTS) has been identified in the green alga *Chlamydomonas reinhardtii* (BTA1Cr) (Riekhof et al. 2005), but both DGTS and homologs of BTA1Cr are absent in *A. anophagefferens*. Very little is currently known of the synthesis of DGCC, although there is some evidence to suggest that, similar to DGTS, S-adenosyl methionine is a key intermediate in its synthesis (Kato et al. 2006). A time-course experiment that traced lipid composition in concert with SQD1 and putative DGCC synthases would help elucidate these aspects of *A. anophagefferens* P physiology.

Lowest abundance in control

There were 104 proteins generally more abundant in the –P and P-refed treatments relative to the control, falling into cluster F (Figure 2, Table S2). These proteins are more abundant when phosphate becomes deficient and continue to be present

when P is resupplied. As such, proteins in this group are not actively degraded when phosphate is re-supplied to the –P cells and may continue to be produced. Within this cluster, 14 proteins are manually curated LHCs. LHC proteins are known to have variable regulation patterns in other algae. For example diatom genes encoding LHC-like proteins were significantly up-regulated in iron starved conditions (Allen et al. 2008). Additionally, a transcriptome profiling analysis in the coccolithophore *E. huxleyi* demonstrated down-regulation of an LHC-like protein during N starvation (Dyhrman et al. 2006). The 14 LHC-like proteins in this study were significantly more abundant in both the –P and P-refed treatments versus the control (Figure 3, Table S2). One of these 14 LHC-like proteins (NCBI# 323457207) mapped to a gene that was previously shown to be up-regulated at the transcriptional level under general N and P stress (Wurch et al. 2011). It is difficult to predict whether these LHC proteins are involved in light harvesting, photoprotection, or some other physiological role and a more detailed study that quantifies RNA levels and protein levels in a variety of stress conditions would be needed to discern the variables governing LHC expression patterns.

Also in this cluster were 9 proteins involved in glycolysis, including a phosphoglucomutase (NCBI#: 323452848), phosphoglucose isomerase (NCBI#: 323455682), a triose phosphate isomerase (NCBI#: 323447110), a glyceraldehyde-3-phosphate dehydrogenase (NCBI#: 323449032), an enolase (NCBI#: 323453907), a pyruvate kinase (NCBI#: 323450876), a UTP--glucose-1-phosphate uridylyltransferase (NCBI#: 323452847), a nucleoside diphosphate kinase (NCBI#: 323454769), and a phosphoenolpyruvate carboxylase (PEPC) (NCBI#: 323453325) (Figure 2, Table S2).

Glycolysis is the conversion of one molecule of glucose into two molecules of pyruvate, and requires 2 molecules of inorganic phosphate. Due to this P requirement, glycolysis enzyme activities in higher plants are affected by P supply in order to bypass those reactions that demand phosphate (see review: Paxton 1996). Based on the abundance patterns of these nine enzymes under –P and P-refed conditions, *A. anophagefferens* also appears to modulate or switch its glycolytic pathway in response to P supply. For example, PEPC can serve as a glycolytic bypass enzyme by diverting phosphoenolpyruvate (PEP) to oxaloacetate (OAA) and releasing inorganic phosphate. This bypass has been suggested in higher plants (Nagano et al. 1994) and the green alga *Selenastrum minutum* (Theodorou et al. 1991). OAA can then be converted to malate through the activity of malate dehydrogenase and eventually to pyruvate through a malic enzyme, thus completing the bypass of the ADP-requiring step of converting PEP directly to pyruvate catalyzed by pyruvate kinase (Paxton 1996). However, considering that two PKs (see below) were more abundant during –P conditions and no malic enzyme was detected in this study, it is difficult to interpret whether *A. anophagefferens* is using PEPC to bypass the ADP-requiring PK step of glycolysis, or simply liberating inorganic phosphate from PEP and replenishing tricarboxylic acid cycle intermediates.

Other proteins in the glycolysis pathway did not show differences in abundance among the three treatments (Table S1) while some showed differences, but did not fall into this particular cluster. For example, another pyruvate kinase (NCBI#: 323453799) was 20-fold more abundant under –P relative to the control, but only 5-fold more abundant in P-refed conditions (Figure 2, Table S2), suggesting a stronger response to P

re-supply relative to other glycolysis enzymes. Another glyceraldehyde-3-phosphate dehydrogenase (NCBI#: 323455041) showed lowest abundance under –P and P-refed conditions, but highest abundances in the control treatment (Figure 2, Table S2). These results reflect the complexity of how *A. anophagefferens* is tailoring its glycolysis pathway to conserve P, while still trying to meet its respiration demands.

A number of proteins with known roles in P metabolism are found in cluster F, with lowest abundance in the control. Two inorganic phosphate transporters are significantly more abundant in both the –P and P-refed treatments (Figure 3, Table S2). One of the phosphate transporters (NCBI #: 323454760) is 59-fold more abundant in the –P treatment and 50-fold more abundant in the P-refed treatment compared to the control, while the other phosphate transporter (NCBI #: 323456737) is 7-fold more abundant in the –P treatment and 4-fold in the P-refed treatment) (Figure 3, Table S2). This suggests that *A. anophagefferens* makes more phosphate transporters when they are experiencing P starvation. Other eukaryotic algae have also been observed to employ this same strategy (Dyhrman et al. 2006, Chung et al. 2003). In the P-refed condition, these phosphate transporters are lower than –P, but are still elevated relative to the control (Figure 3, Table S2). This is evidence of a lag between environmental changes and protein response and demonstrates that 24 hours is not enough time to observe a significant decrease in these phosphate transporters, possibly because these membrane proteins are not actively degraded.

To further explore this phenomenon, an additional experiment was performed to re-create control, –P, and P-refed conditions and test whether or not expression of the

more abundant phosphate transporter (NCBI #: 323454760) changed at the transcriptional level over this 24 hour period (Figure 4). Results from this experiment demonstrate that the phosphate transporter transcript is up-regulated over 400-fold under –P conditions relative to the control (Figure 4). After 24 hours of being re-fed phosphate, the transcript expression levels of the phosphate transporter were not detected (Figure 4). A biological replicate was examined for each condition and the results were similar with the phosphate transporter being up-regulated over 500-fold under –P and not detectable under P-refed conditions. In both P-refed biological replicates, the reference gene amplified in an efficient C_T range, but the phosphate transporter did not amplify, indicating that the phosphate transporter transcript abundance was too low to detect, but the RNA and subsequent cDNA were of good quality. In the specific case of this phosphate transporter, the expression of mRNA is tightly linked to exogenous P concentrations, while the protein abundance appears to decay more slowly. Consequently, the interpretation of transcript and protein abundance measurements for this transporter should consider these timing differences, where the transcript could detect short-term P supply, and the protein would reflect the cell's physiological history as well as its current environment. While the slower decay of the phosphate transporter protein relative to its transcript may be due to the slower degradation of proteins associated with membranes (Hare and Taylor 1991), it is also possible that there has been little selection pressure to actively degrade this transporter versus allowing it to dilute away with growth and cell division. The observed persistence of the phosphate transporter for more than 24 hours after re-exposure to P would allow the cell to replenish its depleted phosphate cellular

quota. Under this scenario, it seems likely that the transcriptome and proteome could have co-evolved their regulation to have an optimal response to environmental stimuli. It is interesting to note that this discrepancy between timing of transcripts and protein signals in this phosphate transporter is likely unidirectional: a short-term change to phosphate depleted conditions (instead of replete) would likely be detectable much more quickly on a protein level because there would not be a need to wait for the existing transporter protein to be diluted away by cellular division.

A 5'-nucleotidase (NCBI #: 323455642) was also significantly more abundant in both –P (18-fold) and P-refed (23-fold) conditions versus the control. 5'-nucleotidase enzymes cleave the phosphate group from the 5' end of the sugar moiety in nucleotides and may be used by algae to scavenge phosphate from exogenous nucleotides in the environment (Flynn et al. 1986, Dyhrman et al. 2003). Consistent with an extracellular function, SignalP (version 3.0) was used to determine that this 5'-nucleotidase contains a signal peptide suggesting this protein is secreted (Bendtsen et al. 2004, Nielsen et al. 1997). Nucleotides released from grazing or cell lysis could potentially be a reservoir for P in the ocean with concentrations reaching 10-20 nM (Ammerman and Azam 1985). *A. anophagefferens* can utilize adenosine monophosphate (AMP) as a sole P source in culture (Wurch et al. 2011). These data, combined with the 5'-nucleotidase protein data in this study, suggests that nucleotides may be an important source of P for *A. anophagefferens* when DIP is scarce. As with the phosphate transporter proteins, the abundance of 5'-nucleotidase did not decline when cells were re-fed with P suggesting that the 5'-nucleotidase protein is not actively degraded upon P addition.

Finally, a clathrin protein (NCBI #: 323455486) was found in this cluster and was over 16-fold more abundant in –P and 21-fold more abundant in the P-refed conditions versus the control. Recently, clathrin was shown to be one of the most abundant proteins in the diatom *T. pseudonana* (Nunn et al. 2009) and was also detected in a proteomic analysis of the coccolithophore *E. huxleyi* (Jones et al. 2010). Here, clathrin in *A. anophagefferens* was not only abundant, but was variable with higher abundances in the –P and P-refed treatments relative to the control. Clathrin is the major coat protein of clathrin-coated vesicles (CCVs) (Pearse 1975). CCVs selectively sort and transport proteins and lipids from the outer membrane of cells to endosomes (see Kirchhausen 2000, Brodsky et al. 2001 for reviews of CCV formation and function). Clathrin-mediated endocytosis (CME) is also a mechanism by which eukaryotic cells can internalize nutrients and other macromolecules (Conner and Schmid 2003). Given that CME can be a mechanism for internalizing nutrients, this protein could play a direct role in P scavenging from the environment. Alternatively, perhaps clathrin is involved in reconfiguring the lipid composition of cellular membranes since *A. anophagefferens* decreases phospholipids and increases non-phospholipids under –P conditions. The fact that clathrin has been shown to be abundant in diatoms, coccolithophores, and now the pelagophyte *A. anophagefferens* is intriguing and warrants further investigation (Nunn et al. 2009, Jones et al. 2010).

Highest abundance in -P

There were 26 unique proteins that were most abundant under –P conditions and fall into clusters G and H (Figure 2, Table S2). These proteins are most abundant under P deficiency, but are rapidly turned over 24 hours after being refed phosphate. Four of these proteins are LHCs and their presence is consistent with the observation that LHC proteins in *A. anophagefferens* are induced during nutrient stress (Figure 3, Table S2). Proteins with known roles in P metabolism found in this cluster include an alkaline phosphatase (NCBI #: 323455998) which increased 4.3-fold in –P versus control, and was not significantly different in the P-refed versus control (Figure 3, Table S2). Alkaline phosphatases cleave phosphate from a variety of organic molecules and are induced in other algae during P deficiency (Dyhrman and Palenic 1999, 2003, Fan et al. 2003). The induction of this alkaline phosphatase during P-deficient conditions suggests *A. anophagefferens* has the ability to utilize DOP compounds to meet its P demand when DIP is unavailable. After 24 hours of being re-fed P, the abundance of the alkaline phosphatase is similar to the control, suggesting rapid turnover or degradation of this protein upon release from P deficiency. This result is similar to findings from the coccolithophore, *E. huxleyi*, where alkaline phosphatase activity was induced under P-deficient conditions, and this activity rapidly decreased 24 hours after cells were refed P (Dyhrman and Palenik 2003). This is in contrast to the P scavenging proteins that remain abundant in P-refed conditions (e.g. inorganic phosphate transporter and 5'-nucleotidase).

Alkaline phosphatase has been observed to be prone to loss from *E. coli* and a marine cyanobacterium (Malamy and Horecker 1961), and thus may be rapidly lost from

the cell rather than being targeted specifically for degradation. Regardless, the disparities in duration among different P-deficient induced proteins after release from P deficiency are intriguing, and should be considered for interpreting protein presence and abundance in natural populations under conditions of non-steady state phosphate and DOP concentrations. In this case, the phosphate transporter and alkaline phosphatase would be indicative of P deficiency at different timescales. Furthermore, the induction of alkaline phosphatase under –P conditions, combined with the results from the 5'-nucleotidase discussed above, is consistent with the observation that at peak cell densities during *A. anophagefferens* blooms there is a significant drawdown of DOP (Gobler et al. 2004).

Lowest abundance in -P

The 80 proteins in cluster D are most abundant in the control and P-refed treatments and low abundance in the –P treatment (Figure 2). There are a few N-related proteins in this cluster, including a nitrate transporter (NCBI #: 323448256), a nitrate and nitrite reductase (NCBI #: 323453433 and 323453434) and a urea transporter (NCBI #: 323451781) (Figure 3, Table S2). The down-regulation of these proteins under –P conditions is consistent with the N proteins discussed above. However, these proteins appear to be more responsive as they are relatively abundant again under P-refed conditions.

The majority of the proteins in this category are ribosomal (Figure 3, Table S2). Ribosomes are formed from ribosomal proteins along with ribosomal RNA, and are the macromolecular machines responsible for translation and protein syntheisis. Protein

synthesis requires a large energy input. For example, up to 40% of *E. coli's* total cell energy turnover goes toward protein synthesis (Wilson and Nierhaus 2007). Therefore, protein synthesis must be tightly controlled to meet the biosynthetic demands of the cell and not waste resources on unnecessary protein synthesis. In *A. anophagefferens* there is a global down-regulation of ribosomal proteins during P deficiency. It is unclear whether this is a strategy to conserve resources, or a by-product of stationary growth. Once phosphate is available, these ribosomal proteins are immediately abundant again, suggesting that they are tightly coupled to the cell's growth environment and are indicative of nutrient availability to *A. anophagefferens*.

Insights gained from P resupply

Some P-responsive proteins decreased in abundance upon P resupply while others did not. This is likely a function of how quickly these proteins are degraded upon sensing a P supply increase. The variability in this turnover may be a function of the position of the protein within the cell, for example integral membrane proteins may be degraded slower since they are more difficult to access. Another explanation is that this time could also be a function of the protein's continued utility to the cell upon P resupply. Perhaps upon P addition it is advantageous to keep phosphate transporters in abundance for some time to take full advantage of the sudden increase. In contrast, alkaline phosphatase is no longer of utility once there is plenty of inorganic P available, and so this protein is quickly degraded.

One of the primary aims of these types of studies is identifying genes and proteins that can be used as biomarkers of nutritional physiology in field populations. This study highlights the importance of including a refed treatment in such analyses. A simple +P/-P only gives a snapshot of protein abundances. For example, both the phosphate transporter and alkaline phosphatase proteins were more abundant under –P conditions relative to the control. Without a P-refed treatment, both proteins would be considered equally good biomarkers for P deficiency. However, this study revealed that due to differences in protein turnover, these two proteins could provide information about different stages of P deficiency under non-steady state nutrient conditions such as during a bloom situation.

Proteome/transcriptome comparison

A previous study examined the transcriptome of *A. anophagefferens* under nutrient replete (control) and –P conditions using Long Serial Analysis of Gene Expression (Long-SAGE) (Wurch et al. 2011). The transcriptome and proteome data were compared to examine choreography between the two datasets. Of the 641 unique proteins in this study, 257 were also present in the transcriptome (Table S3). An examination of the –P relative to control fold-change for both the transcript data (SAGE tag counts) and protein data (average abundance score) indicate that for some targets, the transcriptome and proteome responses are coordinated (Figure 5, Table S1). The inorganic phosphate transporter (NCBI #: 323454760) and alkaline phosphatase (NCBI #: 323455998) display significant up-regulation at both the transcript and protein levels

(Figure 5). Less tightly linked, but still up-regulated in the –P treatment at both the transcript and protein levels are a 5'-nucleotidase (NCBI #: 323455642) and clathrin (NCBI #: 323455486) (Figure 5). No transcript data could be found for the sulfolipid biosynthesis protein from the Long-SAGE study (Wurch et al. 2011). Long-SAGE tags are generated at the most 3' *NLAIII* site of an mRNA and are often found in the untranslated region (UTR) of an mRNA. The genome was searched in the 3' direction of the sulfolipid biosynthesis gene and no tag was found. A higher resolution (deeper sequencing) analysis or targeted gene expression assay would be needed to determine how the transcript is for this sulfolipid biosynthesis gene is regulated.

N-metabolism and LHC genes show little correlation in expression patterns between transcript and protein levels. Ribosomal proteins tend to be ubiquitously down-regulated under –P at the protein level, and for the most part, at the transcript level as well (Figure 5). Genes involved in protein degradation also appear to be somewhat choreographed with expression patterns at both the transcript and protein level indicating down-regulation under –P conditions (Figure 5, Table S3). This suggests that certain proteins are rapidly being turned over under nutrient replete conditions where growth rates are high. With the data available here, it is unclear as to which specific proteins are being targeted, and therefore difficult to put the expression patterns in context of adapting to P deficiency. Nonetheless, in order for an organism to change its proteome to adapt to variations in its environment, new proteins have to be made and proteins which are no longer needed must be recycled, and given the extensive proteome rearrangement

observed here in response to P supply, it is not surprising that genes involved in protein degradation are also sensitive to P supply.

Although the actual fold changes are quite different between the transcripts and proteins for a given gene, 27.2 percent of the genes showed a "correlated" pattern (see methods). Approximately 58.4 percent of genes were considered "neutral", meaning the fold changes for either the transcript, protein, or both were less than 1.5 fold different from the control (Figure 5, Table S1). The patterns displayed by these "neutral" genes could partly be explained if there is a lag between the induction of transcripts and subsequent translation of proteins (e.g. high transcript, neutral protein) or the repression of transcripts and turnover of proteins (e.g. neutral transcript and high protein). In yeast it has recently been shown that transcriptional patterns 1-2 hours after treatment were best correlated with protein abundances 4-6 hours after treatment with the antibiotic rapamycin, supporting the idea of a lag between induction of transcripts and translation of proteins (Fournier et al. 2010). Furthermore, in yeast it was recently reported that an induction of mRNA due to osmotic stress is well correlated with an induction of proteins, but transcript reduction produced almost no change in the corresponding proteins (Lee et al. 2011). Clearly, a snap shot view of the transcriptome and proteome at the same time point would not give the most correlated pattern because the transcripts and proteins are being induced and degraded at different time scales. Only 14.4 percent of genes showed a "not correlated" pattern, where the transcript and protein fold changes were opposite. This result could be due to the transcript and protein data being generated from different

biological samples, where slight variations in growth rate and point of harvest within the diel cycle could make a large difference in the expression patterns of certain genes.

The relative timing of the transcriptional and protein responses is biologically interesting and could be practically useful in interpreting expression patterns of both transcripts and proteins from environmental datasets. From culture studies, the expression patterns of certain genes can be linked to a cell's physiological condition. For example, the phosphate transporter discussed in this study is significantly up-regulated at both the transcript and protein level when *A. anophagefferens* experiences P deficiency. This gene could thus be used as a marker for examining P deficiency in natural populations. However, the abundance of the protein may have a different interpretation than the abundance of the transcript. In this example, the phosphate transporter protein was still abundant after the cells were exposed to replete P, and its presence may indicate P deficiency in the recent past and not necessarily the cell's current environment. The transcript for this phosphate transporter appeared to give finer resolution for assaying P deficiency, and its abundance may be more indicative of the cell's current geochemical environment. Conversely, since some genes are not being correlated, the abundance of a transcript may not equate to the protein being abundant and it would be difficult to infer activity, in a strictly temporal sense, based upon transcript abundance alone. These issues should be kept in mind when working with microbial community, metatranscriptomic, or metaproteomic datasets.

Conclusion

This study examined the timing of global protein responses in algal cells subjected to, and then alleviated from, P deficiency. Throughout this study, a number of proteins were identified as being differentially regulated by P availability. *A. anophagefferens* increases its ability to scavenge or conserve P by: (1) up-regulating proteins involved in DOP acquisition, such as a 5'-nucleotidase and alkaline phosphatase; (2) increasing its ability to transport phosphate by up-regulating more phosphate transporters or switching to a more efficient phosphate transporter; (3) lower its P demand by switching sulfolipids for phospholipids; (4) and adjusting its glycolysis pathway. Insight into the timing of these responses was gained by examining protein abundances in a P-refed condition. In this case, many proteins were more abundant under P deficiency, but were not repressed 24 hours after being refed phosphate. This lag in response provides insight into the biological response to P deficiency, as well as the evolved coordination between transcript and protein expression. In addition, this lag has practical importance in the use of transcript and protein abundances as indicators of physiological state (e.g. P stress) *in situ*. If P acquisition proteins, like the phosphate transporter that is not quickly degraded, are abundant in a field sample, it may not be entirely reflective of the immediate P abundances in the environment in dynamic non-steady state bloom conditions. Instead, it may be reflecting a previous environmental condition, or multiple different conditions integrated over time. These considerations are important for interpreting transcriptomic and proteomic profiles in metadatasets, particularly in relation to nutrient abundances. A comparison with the transcriptome

shows that P-responsive proteins related to P metabolism/scavenging appear to be correlated. A time lag between the transcriptional responses versus the protein responses may account for those genes that are "neutral" or "not correlated". Finally, the breadth of response at both the transcriptome and proteome level of *A. anophagefferens* to P deficiency, combined with field observations of significant DOP drawdown during peak cell densities, suggest that P may play a more important role in brown tide formation, persistence and decline than previously thought.

Acknowledgments

Research for this work was supported by a National Oceanic and Atmospheric Administration ECOHAB grant (#NA09NOS4780206) and National Science Foundation grant (#OCE-0723667). Further support came from the Woods Hole Coastal Ocean Institute. LLW was supported by a Environmental Protection Agency STAR Fellowship (#FP916901). EMB was supported by a National Science Foundation (NSF) Graduate Research Fellowship (#2007037200) and an Environmental Protection Agency STAR Fellowship (#F6E20324). We would like to thank Patrick Martin for assistance in harvesting samples for lipid analysis and Helen Fredricks for assistance with HPLC/MS/MS analysis of polar membrane lipids. We would also like to thank Sheean Haley for assistance with culturing and data interpretation. Finally, we would like to acknowledge Christopher Gobler for useful comments and feedback on the manuscript as well as his work on the genome of *A. anophagefferens*.

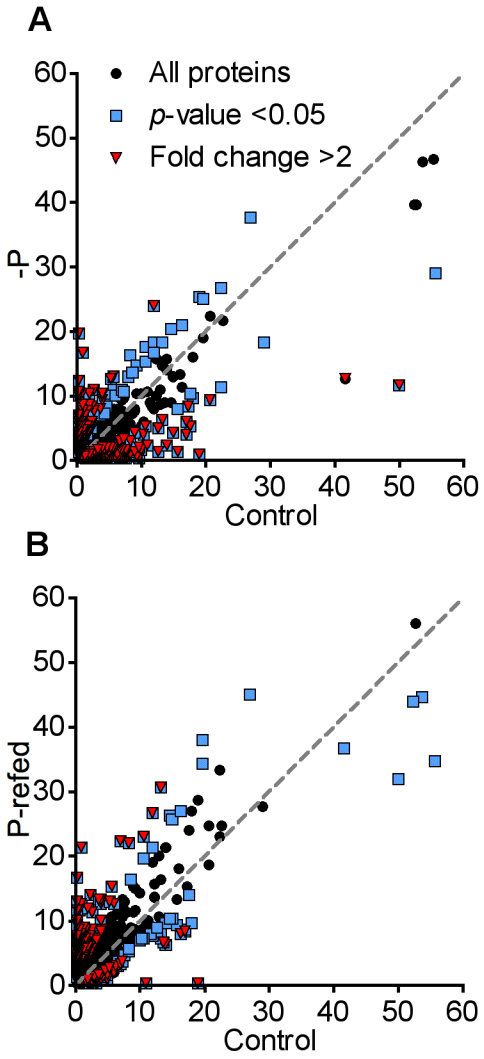

Figure 1. Scatter plot with the abundance of each protein in the (A) –P and control conditions and (B) P-refed and control conditions. Blue squares indicate proteins that are significantly different (p-value < 0.05) between the conditions based upon the Fisher exact test. Red triangles specify proteins that are greater than 2-fold different between conditions. The gray dashed line indicates equal abundances between the conditions.

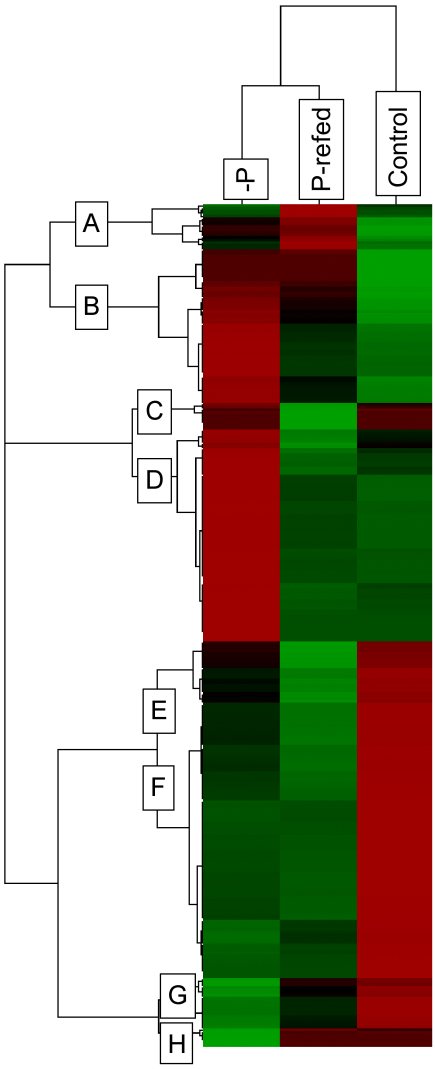

Figure 2. Hierarchical cluster analysis of the 318 proteins classified as differentially abundant. This analysis groups proteins by similarity of patterns. The spectral counts for each protein were averaged across treatments (-P, P-refed, control). Green indicates higher abundance than the mean while red indicates reduced abundance relative to the mean. Black indicates no difference from the mean. The intensity of the color is indicative of the degree of difference from the mean, with brighter colors displaying stronger differences. Letters indicate clusters of similar pattern.

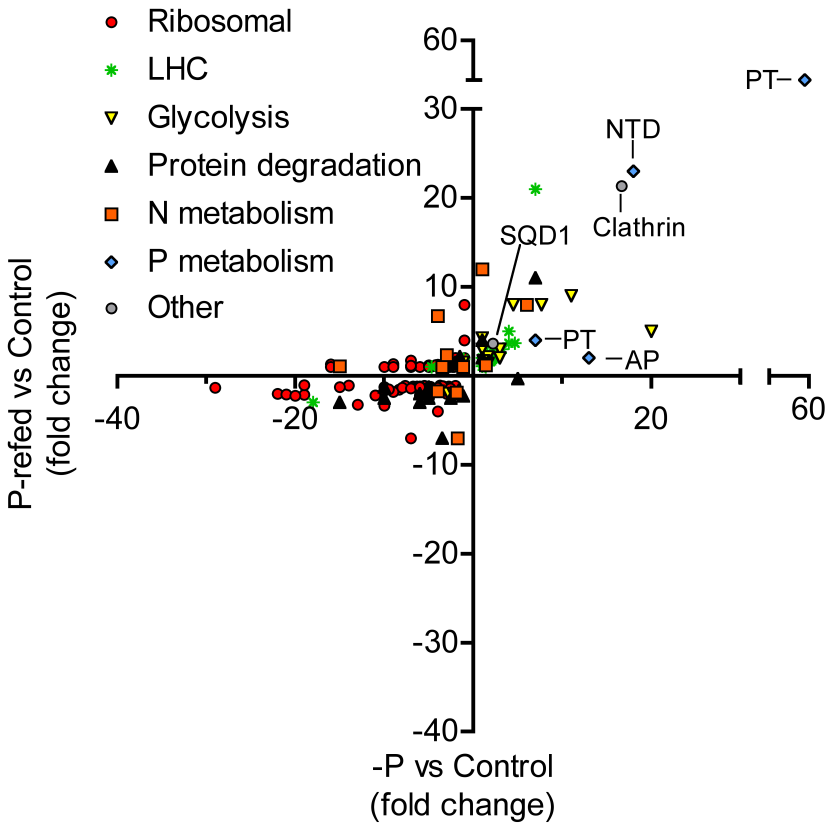

Figure 3. Scatter plot highlighting those proteins that fell into the categories of being putatively related to ribosomal, light harvesting complex-like (LHC), glycolysis, protein degradation, N-metabolism, P-metabolism, or other (e.g. clathrin). For those proteins involved in putative P-metabolism, specific proteins are highlighted and include: PT: Inorganic phosphate transporter, SQD1: Sulfolipid biosynthesis gene, NTD: 5'-nucleotidase, AP: Alkaline phosphatase. Clathrin is also noted. Fold-changes were calculated relative to the control treatment.

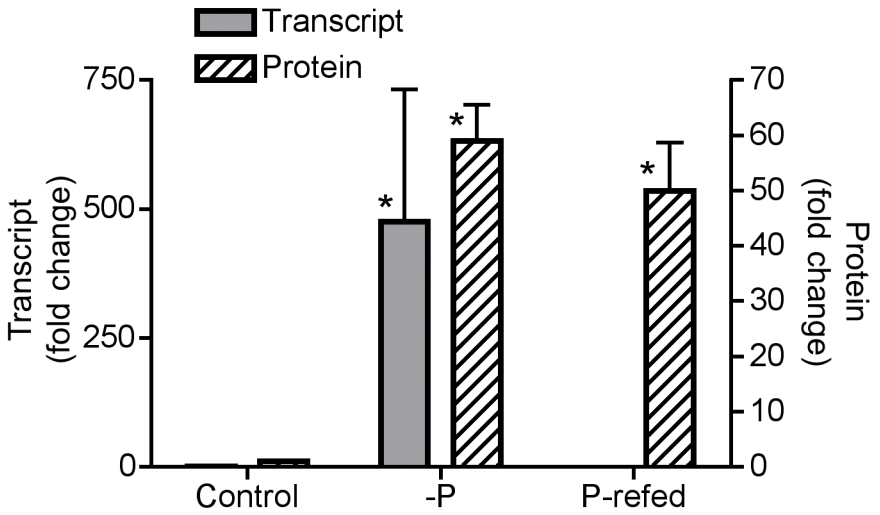

Figure 4. Bar graph comparing the expression of one inorganic phosphate transporter (NCBI #: 323454760) at the transcriptional level and abundance at the protein level under control, -P and P-refed conditions. Transcript data are plotted as fold change relative to the control condition using the comparative C_T method for qRT-PCR with a reference gene that encodes a ubiquitin-conjugating enzyme. Error bars for transcript data specify standard error of the average fold change of triplicate measurements on a single biological replicate between the sample condition (control, -P, P-refed) and the reference condition (control). Protein data are plotted as fold change relative to the control condition based upon spectral counts. Error bars for protein data specify standard error of the fold change among triplicate technical measurements of spectral counts for each condition. An asterisk (*) indicates that the fold change was significantly higher than the reference condition (*p*-value of less than 0.05) based upon a pair-wise fixed reallocation randomization analysis for the transcript data and a Fisher exact test for the protein data.

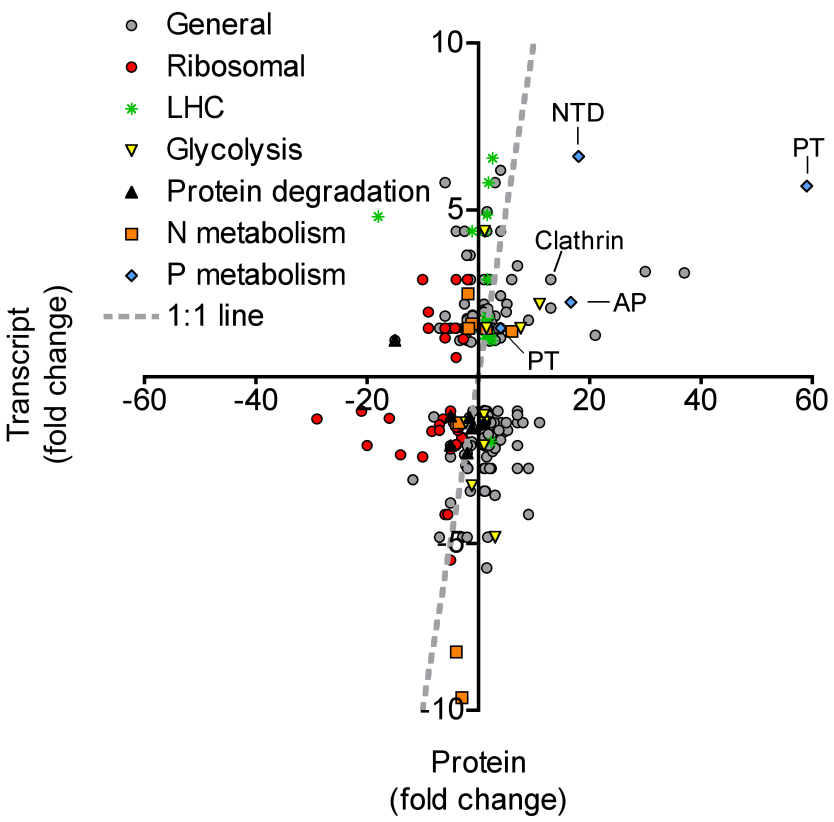

Figure 5. Scatter plot comparing the proteome data and transcriptome data in the –P treatment. All fold-changes are calculated relative to a control. The gray dashed line represents the 1:1 line. Data points falling on or near that line have similar regulation patterns at both the transcript and protein level. Specific protein IDs pointed out include: Clathrin, PT: Inorganic phosphate transporter, NTD: 5'-nucleotidase, and AP: Alkaline phosphatase. The sulfolipid biosynthesis protein (SQD1) was not represented in the transcriptome data.

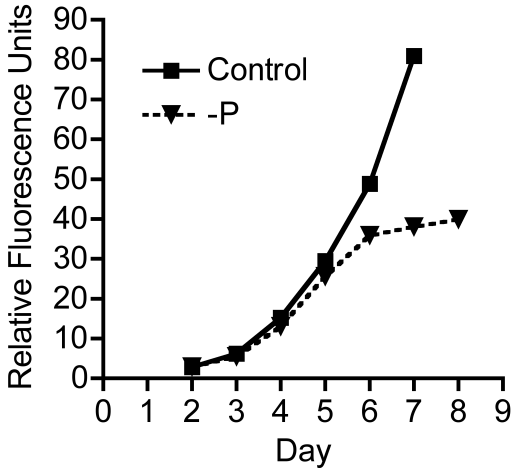

Figure S1. Growth of *A. anophagefferens* under nutrient replete (control) and P-deficient (-P) conditions plotted as Relative Fluorescence Units. The control treatment was harvested on day 6. On day 8, –P cells were harvested to generate the –P treatment. Remaining –P cells were re-fed phosphate and harvested 24 hours later to generate the P-refed treatment.

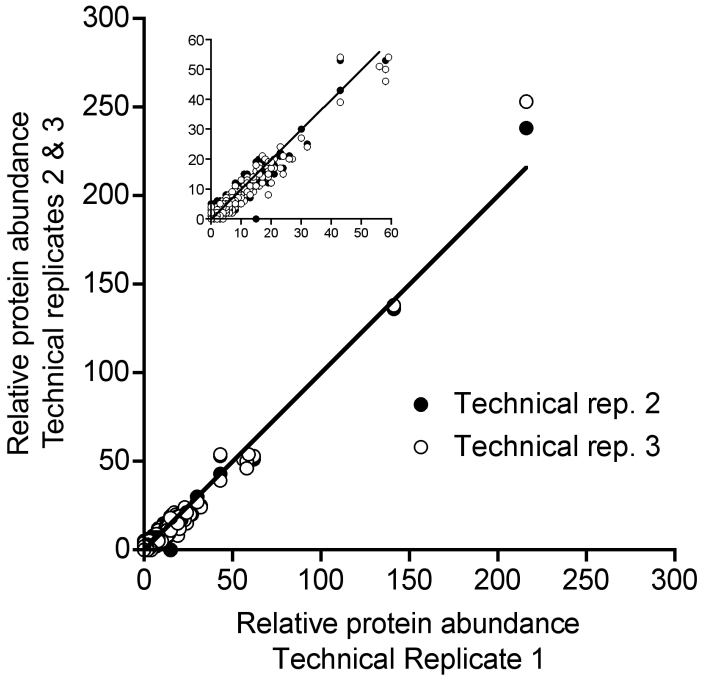

Figure S2. Scatter plot showing accuracy of method for spectral counting. Technical replicates of spectral count data from control conditions are plotted against each other. A 1:1 line is shown for comparison.

References

Allen AE, LaRoche J, Maheswari U, Lommer M, Schauer N et al. (2008) Whole-cell response of the pinnate diatom *Phaeodactylum tricornutum* to iron starvation. Proceedings of the National Academy of Sciences of the United States of America 105: 10438-10443.

Ammerman JW, Azam F (1985) Bacterial 5'-nucleotidase in aquatic ecosystems – a novel mechanism of phosphorus regeneration. Science 227: 1338-1340.

Ballihaut G, Mounicou S, Lobinski R (2007) Multitechnique mass-spectrometric approach for the detection of bovine glutathione peroxidase selenoprotein: focus on the selenopeptide. Analytical and Bioanalytical Chemistry 388: 585-591.

Bendtsen JD, Nielsen H, von Heijne G, Brunak S (2004) Improved prediction of signal peptides: SignalP 3.0. Journal of Molecular Biology 340:783-795.

Berg GM, Glibert PM, Lomas MW, Burford MA (1997) Organic nitrogen uptake and growth by the chrysophyte *Aureococcus anophagefferens* during a brown tide event. Marine Biology 129: 377-387.

Berg, GM, Shrager J, Glockner G, Arrigo KR, Grossman AR (2008) Understanding nitrogen limitation in *Aureococcus anophagefferens* (Pelagophyceae) through cDNA and qRT-PCR analysis. Journal of Phycology 44: 1235-1249.

Birney E, Stamatoyannopoulos JA, Dutta A, Guigo R, Gingeras TR, et al. (2007) Identification and analysis of functional elements in 1% of the human genome by the ENCODE pilot project. Nature 447:799–816.

Brodsky FM, Chen CY, Knuehl C, Towler MC, Wakeham DE (2001) Biological basket weaving: formation and function of clathrin-coated vesicles. Annual Review of Cell and Developmental Biology 17: 517-568.

Chung CC, Hwang SPL, Chang J (2003) Identification of a high affinity phosphate transporter gene in a prasinophyte alga, *Tetraselmis chui*, and its expression under nutrient limitation. Applied and Environmental Microbiology 69: 754-759.

Conner SD, Schmid SL (2003) Regulated portals of entry into the cell. Nature 422: 37-44.

Dennison WC, Marshall GJ, Wigand C (1989) Effects of "brown tide" shading on eelgrass (*Zostera marina*) distributions, p. 675-692. In E.M. Cosper, V.M. Bricelj, and E.J. Carpenter (eds.), Novel Phytoplankton Blooms: Causes and Impacts of Recurrent Brown Tides and Other Unusual Blooms, Volume 35. Springer, New York.

Dyhrman ST, Palenik B (1999) Phosphate stress in cultures and field populations of the dinoflagellate *Prorocentrum minimum* detected by a single-cell alkaline phosphatase assay. Applied and Environmental Microbiology 65: 3205-3212.

Dyhrman ST, Palenik B (2003) Characterization of the ecoenzyme activity and phosphate-regulated proteins in the coccolithophorid *Emiliania huxleyi*. Journal of Plankton Research 25: 1215-1225.

Dyhrman ST, Haley ST, Birkeland SR, Wurch LL, Cipriano MJ et al. (2006) Long Serial Analysis of Gene Expression for gene discovery and transcriptome profiling in the widespread marine coccolithophore *Emiliania huxleyi*. Applied and Environmental Microbiology 72: 252-260.

Dyhrman ST (2008) Molecular approaches to diagnosing nutritional physiology in harmful algae: Implications for studying the effects of eutrophication. Harmful Algae 8: 167-174.

Eisen MB, Spellman PT, Brown PO, Botstein D (1998) Cluster analysis and display of genome-wide expression patterns. Proceedings of the National Academy of Sciences of the United States of America 95: 14863-14868.

Essigmann B, Güler S, Narang RA, Linke D, Benning C (1998) Phosphate availability affects the thylakoid lipid composition and the expression of SQD1, a gene required for sulfolipid biosynthesis in *Arabidopsis thaliana*. Proceedings of the National Academy of Sciences of the United States of America. 95: 1950-1955.

Fan C, Glibert PM, Alexander J, Lomas MW (2003) Characterization of urease activity in three marine phytoplankton species, *Aureococcus anophagefferens*, *Prorocentrum minimum*, and *Thalassiosira weissflogii*. Marine Biology 142: 949-958.

Fournier ML, Paulson A, Pavelka N, Mosley AL, Gaudenz K et al. (2010) Delayed correlation of mRNA and protein expression in rapamycin-treated cells and a role for Ggc1 in cellular sensitivity to rapamycin. Molecular and Cellular Proteomics 9: 271-284.
Gobler CJ, Sañudo-Wilhelmy SA (2001) Effects of organic carbon, organic nitrogen, inorganic nutrients, and iron additions on the growth of phytoplankton and bacteria during a brown tide bloom. Marine Ecology Progress Series 209: 19-34.

Flynn KJ, Opik H, Syrett PJ (1986) Localization of the alkaline phosphatase and 5'-nucleotidase activities of the diatom *Phaeodactylum tricornutum*. Journal of General Microbiology. 132: 289-298.

Gobler C J, Renaghan MJ, Buck NJ (2002) Impacts of nutrients and grazing mortality on the abundance of *Aureococcus anophagefferens* during a New York brown tide bloom. Limnology and Oceanography 47: 129-141.

Gobler CJ, Boneillo GE, Debenham C, Caron DA (2004) Nutrient limitation, organic matter cycling, and plankton dynamics during an *Aureococcus anophagefferens* bloom in Great South Bay, N.Y. Aquatic Microbial Ecology 35: 31-43.

Gobler CJ, Lonsdale DJ, Boyer GL (2005) A review of the causes, effects, and potential management of harmful brown tide blooms caused by *Aureococcus anophagefferens* (Hargraves et Sieburth). Estuaries: 28: 726-749.

Gobler C, Berry D, Dyhrman S, Wilhelm S, Salamov A et al. (2011) Niche of harmful alga *Aureococcus anophagefferens* revealed through ecogenomics. Proceedings of the National Academy of Sciences of the United States of America. 108: 4352-4357.

Greenfield DI, Lonsdale DJ (2002) Mortality and growth of juvenile hard clam *Mercenaria mercenaria* during brown tide. Marine Biology 141: 1045-1050.

Greenfield DI, Lonsdale DJ, Cerrato RM, Lopez GR (2004) Effects of background concentrations of *Aureococcus anophagefferens* (brown tide) on growth and feeding in the bivalve *Mercenaria mercenaria*. Marine Ecology Progress Series 274: 171-181.

Guillard RRL, Hargraves PE (1993) *Stichochrysis immobilis* is a diatom, not a chrysophyte. Phycologia 32: 234-236.

Hare, J.F. and K. Taylor, 1991. Mechanisms of plasma membrane protein degradation: Recycling proteins are degraded more rapidly than those onfined to the cell surface. Proc. Nail. Acad. Sci. 88:5902-5906.

Hildebrand M (2005) Cloning and functional characterization of ammonium transporters from the marine diatom *Cylindrotheca fusiformis*. Journal of Phycology 41: 105-113.

Jones BM, Edwards RJ, Skipp PJ, O'Connor CD, Iglesias-Rodriguez MD (2010) Shotgun proteomic analysis of *Emiliania huxleyi*, a marine phytoplankton species of major biogeochemical importance. Marine Biotechnology doi: 10.1007/s10126-010-9320-0.

Kall L, Storey JD, Noble WS (2008) Non-parametric estimation of posterior error probabilities associated with peptides identified by tandem mass spectrometry. Bioinformatics 24: 42-46.

Kana TM, Lomas MW, MacIntyre HL, Cornwell JC, Gobler CJ (2004) Stimulation of the brwon tide organism, *Aureococcus anophagefferens*, by selective nutrient additions to in situ mesocosms. Harmful Algae 3: 377-388.

Kamennaya NA, Chernihovsky M, Post AF (2008) The cyanate utilization capacity of marine unicellular Cyanobacteria. Limnology and Oceanography 53: 2485-2494.

Kamennaya NA, Post AF (2011) Characterization of cyanate metabolism in marine *Synechococcus* and *Prochlorococcus spp*. Applied and Environmental Microbiology 77: 291-301.

Kato M, Kobayashi Y, Torii A, Yamada M (2006) Betaine lipids in marine algae. in Advanced research on plant lipids: proceedings of the 15th International Symposium on Plant Lipids., edited by N. Murata, pp. 19-22, Kluwer, Dordrecht.

Keller AA, Rice RL (1989) Effects of nutrient enrichment on natural populations of the brown tide phytoplankton *Aureococcus anophagefferens* (Chrysophyceae). Journal of Phycology 25: 636-646.

Keller A, Nesvizhskii AL, Kolker E, Aebersold R (2002) Empiracle statistical model to estimate the accuracy of peptide identifications made by MS/MS and database search. Analytical Chemistry 74: 5383-5392.

Kirchhausen T (2000) Clathrin. Annual Review of Biochemistry 69: 699-727.

LaRoche J, Nuzzi R, Waters R, Wyman, K, Falkowski PG, and Wallace DWR (1997) Brown tide blooms in Long Island's coastal waters linked to variability in groundwater flow. Global Change Biology 3: 397–410.

Lee MV, Topper SE, Hubler SL, Hose J, Wenger CD et al. (2011) A dynamic model of proteome changes reveals new roles for transcript alteration in yeast. Molecular Systems Biology 7: 514.

Livak KJ, Schmittgen TD (2001) Analysis of relative gene expression data using real-time quantitative PCR and the $2^{-\Delta\Delta CT}$) method. Methods 25:402-408.

Lu XN, Zhu HM (2005) Tube-gel digestion – A novel proteomic approach for high throughput analysis of membrane proteins. Molecular and Cellular Proteomics 4: 1948-1958.

Ma S, Caprioli RM, Hill KE, Burk RF (2003) Loss of selenium from selenoproteins: conversion of selenocysteine to dehydroalanine in vitro. Journal of the American Society for Mass Spectrometry 14: 593-600.

Malamy, M., and Horecker, B.L. (1961). The localization of alkaline phosphatase in E. coli, K12. Biochemical and Biophysical Research Communications 5: 104-108.

Martin P, Van Mooy BAS, Heithoff A, Dyhrman ST (2011) Phosphorus supply drives rapid turnover of membrane phospholipids in the diatom *Thalassiosira pseudonanna*. The ISME Journal 5: 1057-1060.

Morris RM, Nunn BL, Frazar C, Goodlett DR, Ting YS, Rocap G (2010) Comparative metaproteomics reveals ocean-scale shifts in microbial nutrient utilization and energy transduction. The ISME Journal 4: 673-685.

Mulholland MR, Gobler CJ, Lee C (2002) Peptide hydrolysis, amino acid oxidation and N uptake in communities seasonally dominated by *Aureococcus anophagefferens*. Limnology and Oceanography 47: 1094-1108.

Nagano M, Hachiya A, Ashihara H (1994) Phosphate starvation and a glycolytic bypass catalyzed by phosphoenolpyruvate carboxylase in suspension cultured *Catharanthus roseus* cells. Zeitschrift für Naturforschung C-A Journal of Biosciences 49: 742–750.

Nielsen H, Engelbrecht J, Brunak S, von Heijne G (1997) Identification of prokaryotic and eukaryotic signal peptides and prediction of their cleavage sites. Protein Engineering 10:1-6.

Nunn BL, Aker JR, Shaffer SA, Tsai Y, Strzepek RF et al. (2009) Deciphering diatom biochemical pathways via whole-cell proteomics. Aquatic Microbial Ecology 55: 241-253.

Palenik B, Henson SE (1997) The use of amides and other nitrogen sources by the phytoplankton *Emiliania huxleyi*. Limnology and Oceanography 42: 1544-1551.

Parker MS, Mock T, Armbrust EV (2008) Genomic insights into marine microalgae. Annual Review of Genetics 42: 619-645.

Paxton WC (1996) The organization and regulation of plant glycolysis. Annual Review of Plant Physiology and Plant Molecular Biology 47: 185-214.

Pearse BMF (1975) Coated vesicles from pig brain: purification and biochemical characterization. Journal of Molecular Biology 97:93–98.

Pfaffl MW, Horgan GW, Dempfle L (2002) Relative expression software tool (REST©) for group-wise comparison and statistical analysis of relative expression results in real-time PCR. Nucleic Acids Research 30: e36 doi:10.1093/nar/30.9.e36.

Popendorf KJ, Lomas MW, Van Mooy BAS (2011), Microbial sources of intact polar diacylglycerolipids in the western North Atlantic Ocean. Organic Geochemistry. doi:10.1016/j.orggeochem.2011.05.003

Riekhof WR, Sears BB, Benning C (2005), Annotation of genes involved in glycerolipid biosynthesis in *Chlamydomonas renhardtii*: discovery of the betaine lipids synthase BTA1Cr. Eukaryotic Cell 4: 242-252.

Saito MA, Bertrand EM, Dutkiewicz S, Bulygin VV, Moran DM et al. (2011) Iron conservation by reduction of metalloenzyme inventories in the marine diazotroph *Crocosphaera watsonii*. Proceedings of the National Academy of Sciences of the United States of America 108: 2184-2189.
Saldanha AJ (2004) Java Treeview - extensible visualization of microarray data. Bioinformatics 20: 3246-3248.

Sowell SM, Wilhelm LJ, Norbeck AD, Lipton MS, Nicora CD et al. (2009) Transport functions dominate the SAR11 metaproteome at low-nutrient extremes in the Sargasso Sea. The ISME Journal 3: 93-105.

Sunda WG, Graneli E, Gobler CJ (2006) Positive feedback and the development and persistence of ecosystem disruptive algal blooms. Journal of Phycology 42: 963-974.

Theodorou ME, Elrifi IR, Turpin DH, Plaxton WC (1991) Effects of phosphorus limitation on respiratory metabolism in the green alga *Selenastrum minutum*. Plant Physiology 95:1089–1095.

Van Mooy BAS, Fredricks HF, Pedler BE, Dyhrman ST, Karl DM et al. (2009) Phytoplankton in the ocean use non-phosphorus lipids in response to phosphorus scarcity. Nature 458: 69-72.

Wilson DN, Nierhaus KH (2007) The weird and wonderful world of bacterial ribosome regulation. Critical Reviews in Biochemistry and Molecular Biology 42: 187-219.

Wurch LL, Haley ST, Orchard ED, Gobler CJ, Dyhrman ST (2011) Nutrient-regulated transcriptional responses in the brown tide forming algal *Aureococcus anophagefferens*. Environmental Microbiology 13: 468-481.

Zhang B, VerBerkmoes NC, Langston MA, Uberbacher E, Hettich RL, et al. (2006) Detecting differential and correlated protein expression in label-free shotgun proteomics. Journal of Proteome Research 5: 2909-2918.

Zuker M (2003) Mfold web server for nucleic acid folding and hybridization prediction. Nucleic Acids Research 31: 3406-3415.

Table S1) Annotated proteins identified in this study.

NCBI number	JGI protein ID	General call	Mean of spectral counts			Fisher Exact Test (*P*-value)			Fold Changes	
			-P	P-refed	Control	Cont vs -P	Cont vs Refeed	Refeed vs -P	(-P / Control	(Refeed/ Control)
242620086		Ribulose-1,5-bisphosphate carboxylase/oxygenase large subunit [Aureococcus anophagefferens]	64.000	105.333	235.667	0.000	0.000	-0.020	0.272	0.447
323455041	36610	Glyceraldehyde-3-phosphate dehydrogenase	61.667	68.333	138.333	0.000	0.000	-0.023	0.446	0.494
323453252	58968	Transketolase	46.667	73.667	55.333	-0.370	-0.170	-0.092	0.843	1.331
323447300	60370	Histone	39.667	56.000	52.667	-0.100	-0.140	-0.410	0.753	1.063
323447299	60369	Histone	46.333	44.667	53.667	-0.450	-0.001	-0.003	0.863	0.832
242620112		ATP synthase CF1 beta chain	39.667	44.000	52.333	-0.110	-0.001	-0.058	0.758	0.841
242620069		photosystem II p680 chlorophyll A apoprotein (CP-47)	29.000	34.667	55.667	0.000	0.000	-0.200	0.521	0.623
323453579	71305	Phosphoglycerate kinase	37.667	45.000	27.000	-0.001	-0.011	-0.170	1.395	1.667
242620087		Ribulose bisphosphate carboxlyase small chain	11.667	32.000	50.000	0.000	0.000	0.000	0.233	0.640
323456332	36205	Heat shock protein (Hsp 70)	25.000	38.000	19.667	-0.021	-0.002	-0.250	1.271	1.932
242620034		ATP synthase CF1 alpha chain	18.333	27.667	29.000	-0.030	-0.076	-0.310	0.632	0.954
323456125	77959	Chloroplast light harvesting protein	25.333	28.667	19.000	-0.011	-0.100	-0.130	1.333	1.509
323450237	59236	ATP synthase	26.667	33.333	22.333	-0.040	-0.096	-0.310	1.194	1.493
323454637	59935	Chaperonin ATPase	19.000	34.333	19.667	-0.350	-0.012	-0.049	0.966	1.746
323448984	31888	Ferredoxin NADP reductase	21.667	24.667	22.667	-0.350	-0.300	-0.170	0.956	1.088
323457021	10068	Hypothetical	21.000	27.000	16.333	-0.029	-0.045	-0.400	1.286	1.653
323456170	69644	Adenosylhomocysteinase	20.333	26.333	14.667	-0.014	-0.019	-0.410	1.386	1.795
323456989	59795	Fructose bisphosphate aldolase	16.000	27.000	18.000	-0.520	-0.120	-0.140	0.889	1.500
323451553	71821	Glutamine synthetase	14.667	30.667	13.333	-0.180	0.000	-0.011	1.100	2.300
323455001	22269	Fructose bisphosphate aldolase	18.333	26.667	12.000	-0.006	-0.001	-0.390	1.528	2.222
323448136	72618	Elongation factor	11.333	23.000	22.333	-0.005	-0.210	-0.033	0.507	1.030
323449461	69930	Chloroplast light harvesting protein	24.000	21.333	12.000	0.000	-0.036	-0.008	2.000	1.778
323450901	70239	Actin	17.667	23.000	10.667	-0.003	-0.003	-0.440	1.656	2.156
242620067		elongation factor Tu	13.000	25.667	15.000	-0.510	-0.035	-0.034	0.867	1.711
323455179	59911	Peptidyl-prolyl cis-trans isomerase	15.667	21.333	14.000	-0.150	-0.130	-0.540	1.119	1.524
323456525	52245	ATP synthase	9.333	18.667	20.667	-0.002	-0.072	-0.058	0.452	0.903
323448027	60343	Chloroplast light harvesting protein	16.667	19.000	12.000	-0.023	-0.120	-0.200	1.389	1.583
323455979	69630	ATPase	5.333	24.000	17.667	0.000	-0.280	0.000	0.302	1.358
242620040		photosystem II 44 kDa apoprotein (P6)	18.333	16.333	13.333	-0.020	-0.510	-0.019	1.375	1.225
323448510	55209	S-adenosylmethionine synthetase	16.333	22.000	8.333	-0.001	0.000	-0.510	1.960	2.640
323450741	65524	Carbamoyl-phosphate synthase, Carboxyl transferase, Biotin carboxylase, Biotin binding site	11.000	20.000	13.000	-0.480	-0.130	-0.110	0.846	1.538
242620037		Hsp70-type chaperone	15.333	19.667	10.667	-0.021	-0.030	-0.420	1.438	1.844
242620082		photosystem I P700 chlorophyll A apoprotein A1	10.333	14.000	17.667	-0.041	-0.027	-0.540	0.585	0.792
242620041		photosystem II D2 protein	15.667	15.667	12.333	-0.059	-0.440	-0.081	1.270	1.270
323449102	59430	ATP synthase	13.333	18.000	16.000	-0.440	-0.410	-0.520	0.833	1.125
323455486	52498	Clathrin vesicle coat	16.667	21.333	1.000	0.000	0.000	-0.410	16.667	21.333

323452189	64431	PT-repeat	8.333	15.333	17.333	-0.007	-0.078	-0.140	0.481	0.885
323455687	70922	HMG1/2 (high mobility group) box, Amino acid/polyamine transporter II, Transcription elongation factor S-II, N-terminal	11.000	22.333	7.000	-0.025	0.000	-0.035	1.571	3.190
323447336	60366	Cyanase	9.667	9.667	18.000	-0.018	0.000	-0.150	0.537	0.537
323454769	22626	Nucleoside diphosphate kinase	13.667	16.333	8.667	-0.013	-0.038	-0.300	1.577	1.885
323454760	22152	Inorganic phosphate transporter	19.667	16.667	0.000	0.000	0.000	-0.009	N/A[1]	N/A
323449723	30727	Photosystem 1 reaction center subunit	14.000	9.667	14.000	-0.320	-0.014	-0.003	1.000	0.690
323448531	72519	Oxidoreductase	15.333	8.000	13.333	-0.130	-0.004	0.000	1.150	0.600
323451585	69835	14-3-3 protein	10.333	15.000	9.333	-0.230	-0.140	-0.440	1.107	1.607
323454939	71070	Chloroplast light harvesting protein	14.667	11.667	9.333	-0.011	-0.490	-0.011	1.571	1.250
323447968	67669	Zn-finger, RING	8.000	9.333	15.667	-0.017	-0.002	-0.340	0.511	0.596
323447788	77845	Chloroplast light harvesting protein	10.333	14.333	10.000	-0.310	-0.270	-0.520	1.033	1.433
242620083		photosystem I P700 chlorophyll A apoprotein A2	9.000	10.333	14.667	-0.084	-0.014	-0.300	0.614	0.705
323448543	72529	Enolase (phosphopyruvate dehydratase)	6.000	8.667	17.000	0.000	0.000	-0.490	0.353	0.510
323448051	77848	Chloroplast light harvesting protein	13.000	11.333	8.000	-0.012	-0.310	-0.036	1.625	1.417
242620115		Cytochrome f	10.667	9.333	11.000	-0.400	-0.110	-0.056	0.970	0.848
323453090	63510	Aconitate hydratase	12.667	13.000	5.333	0.000	-0.010	-0.130	2.375	2.438
323451606	77816	Chloroplast light harvesting protein	8.000	15.333	9.000	-0.540	-0.091	-0.110	0.889	1.704
323446473	68712	Expressed protein	8.667	10.667	13.000	-0.160	-0.068	-0.400	0.667	0.821
323447782	33635	Histone	4.333	8.333	9.000	-0.047	-0.210	-0.200	0.481	0.926
323451957	37568	Rieske protein (Iron sulfur protein), Chloroplast light harvesting protein	7.333	13.000	7.667	-0.450	-0.120	-0.190	0.957	1.696
323447684	33813	Cytochrome c6	4.000	8.333	17.000	0.000	0.000	-0.150	0.235	0.490
242620091		Magnesium chelatase subunit	9.667	13.333	7.333	-0.098	-0.073	-0.530	1.318	1.818
323447679	67892	Hypothetical	8.333	8.000	11.667	-0.250	-0.022	-0.140	0.714	0.686
323451317	37768	G-protein beta WD-40 repeat (Guanine nucleotide-binding protein)	1.333	13.333	15.667	0.000	-0.066	0.000	0.085	0.851
323453907	24196	Enolase (phosphopyruvate dehydratase)	10.667	11.333	7.333	-0.046	-0.220	-0.190	1.455	1.545
323451650	27306	Chloroplast hydroxymethylbilane synthase	4.333	10.333	15.000	0.000	-0.011	-0.057	0.289	0.689
242620031		ATP synthase CF0 B'chain subunit II	9.000	10.000	11.333	-0.390	-0.130	-0.260	0.794	0.882
323453726	37153	Chaperonin ATPase	8.000	15.333	5.667	-0.090	-0.002	-0.110	1.412	2.706
323455658	69678	Oxygen-evolving enhancer 1	9.333	11.000	7.000	-0.097	-0.200	-0.330	1.333	1.571
323449032	70352	Glyceraldehyde-3-phosphate dehydrogenase	10.000	12.667	6.000	-0.021	-0.030	-0.430	1.667	2.111
323452387	53694	Ketol-acid reductoisomerase	9.667	11.667	6.667	-0.056	-0.110	-0.360	1.450	1.750
242620075		Cytochrome c550	8.000	7.667	12.000	-0.170	-0.011	-0.140	0.667	0.639
323453500	69741	ADP-ribosylation factor	7.667	11.333	9.000	-0.510	-0.480	-0.440	0.852	1.259
323448862	38836	Carbamoyl-phosphate synthase, Carboxyl transferase, Biotin carboxylase, Biotin/lipoyl attachment	10.667	13.000	0.333	0.000	0.000	-0.360	32.000	39.000
242620119		ATP-dependent clp protease ATP-binding subunit	7.333	12.000	7.000	-0.340	-0.120	-0.290	1.048	1.714
323450172	72073	Peptidase	6.000	11.667	7.667	-0.410	-0.230	-0.140	0.783	1.522
323453642	24591	O-acetylhomoserine/O-acetylserine sulfhydrylase	5.000	9.000	12.667	-0.004	-0.023	-0.240	0.395	0.711

323450799	71916	Kringle, PT-repeat, Serine/threonine dehydratase	6.000	8.667	10.333	-0.100	-0.110	-0.490	0.581	0.839
323452158	27009	Chloroplast light harvesting protein	9.333	12.667	4.000	-0.003	-0.002	-0.540	2.333	3.167
323445392	72895	Mucin-2 precursor	6.333	7.333	13.333	-0.016	-0.002	-0.360	0.475	0.550
242620120		photosystem II Q(b) protein (D1)	7.333	9.000	8.667	-0.500	-0.350	-0.410	0.846	1.038
323456329	70752	Glutamate-1-semialdehyde aminotransferase	9.333	13.333	4.000	-0.003	-0.001	-0.470	2.333	3.333
323454246	69716	UDP-glucose 6-dehydrogenase	8.333	14.000	2.333	0.000	0.000	-0.240	3.571	6.000
323447374	34246	Ribulose-5-phosphate 3-epimerase	5.667	7.667	8.333	-0.250	-0.220	-0.550	0.680	0.920
323456872	60769	FAD linked oxidase, N-terminal	10.333	12.000	2.000	0.000	0.000	-0.300	5.167	6.000
323445193	35642	Histone	5.333	7.333	10.667	-0.040	-0.028	-0.560	0.500	0.688
323454481	71195	Sulfate adenylyltransferase	13.000	6.000	5.667	0.000	-0.420	0.000	2.294	1.059
323457207	77828	Chloroplast light harvesting protein	10.000	10.000	5.333	-0.009	-0.096	-0.140	1.875	1.875
323449174	31507	Sulfolipid biosynthesis protein	8.000	13.333	3.667	-0.008	0.000	-0.260	2.182	3.636
323452005	77832	Chloroplast light harvesting protein	10.333	10.000	4.000	-0.001	-0.019	-0.110	2.583	2.500
323452847	25732	UTP--glucose-1-phosphate uridylyltransferase	8.667	12.667	1.000	0.000	0.000	-0.440	8.667	12.667
323456453	20700	Glutamine synthetase	6.667	11.000	6.333	-0.350	-0.130	-0.300	1.053	1.737
323451419	37826	Citrate synthase	3.333	10.667	7.333	-0.054	-0.290	-0.010	0.455	1.455
323456364	59843	Histone	5.333	7.000	10.000	-0.066	-0.037	-0.520	0.533	0.700
323446545	77850	Chloroplast light harvesting protein	10.000	13.667	12.333	-0.410	-0.400	-0.540	0.811	1.108
323452848	25705	Phosphoglucomutase	10.000	11.667	0.667	0.000	0.000	-0.310	15.000	17.500
323450439	72012	Chaperonin	6.000	9.333	7.000	-0.530	-0.420	-0.390	0.857	1.333
323447358	77844	Chloroplast light harvesting protein	5.333	8.333	7.667	-0.280	-0.420	-0.400	0.696	1.087
323454334	77810	Chloroplast light harvesting protein	7.667	9.000	6.000	-0.150	-0.280	-0.350	1.278	1.500
323447744	55489	Chloroplast light harvesting protein	7.667	7.333	6.333	-0.190	-0.510	-0.150	1.211	1.158
323450268	29808	Flavin-containing monooxygenase-like	12.333	10.000	0.000	0.000	0.000	-0.023	N/A	N/A
323455568	77960	Chloroplast light harvesting protein	8.000	9.000	6.333	-0.150	-0.340	-0.290	1.263	1.421
323455382	61597	Dynein heavy chain, AAA ATPase	7.333	8.667	4.333	-0.042	-0.087	-0.360	1.692	2.000
323454019	77822	Chloroplast light harvesting protein	6.333	7.333	5.333	-0.240	-0.400	-0.360	1.188	1.375
323453856	6122	Ribosomal protein L6E	1.667	8.000	10.000	0.000	-0.087	-0.004	0.167	0.800
323456180	52316	Ribosomal protein L5	2.333	6.333	14.000	0.000	0.000	-0.080	0.167	0.452
323452815	60076	Ribosomal protein L4/L1e	1.333	8.333	12.667	0.000	-0.012	-0.001	0.105	0.658
323453541	24359	Pyruvate kinase	6.333	9.667	5.667	-0.290	-0.160	-0.410	1.118	1.706
323452454	71657	Xanthine dehydrogenase	11.000	4.667	5.667	-0.005	-0.190	0.000	1.941	0.824
242620038		Photosystem I reaction center subunit II	7.667	7.333	7.000	-0.280	-0.380	-0.150	1.095	1.048
323450616	65502	Pyruvate carboxylase	7.667	11.333	2.667	-0.002	0.000	-0.440	2.875	4.250
323450905	71945	Endonuclease/exonuclease/phosphatase	11.000	8.667	2.667	0.000	-0.007	-0.024	4.125	3.250
323452472	60091	Chloroplast light harvesting protein	10.333	8.333	4.000	-0.001	-0.076	-0.034	2.583	2.083
323454267	77759	Inositol phosphatase	7.333	7.000	5.333	-0.120	-0.460	-0.150	1.375	1.313
323456600	52193	Ribosomal protein L30, L7, Peptidase	4.000	7.333	10.333	-0.009	-0.038	-0.260	0.387	0.710
323457284	60527	Mucin-associated surface protein	8.667	8.000	4.667	-0.016	-0.180	-0.110	1.857	1.714
323456271	77805	Chloroplast light harvesting protein	10.000	7.667	4.000	-0.001	-0.120	-0.025	2.500	1.917
323449755	30726	Amino transferase class-III	10.000	11.667	0.000	0.000	0.000	-0.310	N/A	N/A

323454635	23580	Chloroplast 3-oxoacyl-[acyl-carrier protein] reductase orecursor	4.667	8.333	7.333	-0.210	-0.480	-0.260	0.636	1.136
323449750	38422	Chloroplast light harvesting protein	8.333	7.333	4.667	-0.023	-0.270	-0.088	1.786	1.571
323447058	68367	Hypothetical protein	1.000	0.333	19.000	0.000	0.000	-0.210	0.053	0.018
323448850	31983	Ribosomal protein	2.000	8.000	9.667	0.000	-0.110	-0.009	0.207	0.828
323454622	23768	Ubiquitin	4.333	8.000	8.333	-0.079	-0.260	-0.240	0.520	0.960
323452479	78109	Selenoprotein	5.333	5.667	8.333	-0.200	-0.046	-0.290	0.640	0.680
323453956	77824	Chloroplast light harvesting protein	6.000	7.333	4.667	-0.190	-0.270	-0.430	1.286	1.571
323451749	64743	Calcium-binding EF-hand, Pleckstrin-like, LMBR1-like conserved region	6.333	7.667	6.000	-0.350	-0.490	-0.410	1.056	1.278
323450447	77838	Chloroplast light harvesting protein	6.333	8.333	5.333	-0.240	-0.250	-0.510	1.188	1.563
323451960	77831	Chloroplast light harvesting protein	7.000	8.000	4.667	-0.083	-0.180	-0.330	1.500	1.714
323455169	5527	Ribosomal protein	0.667	8.667	9.333	0.000	-0.210	0.000	0.071	0.929
323450465	60205	Ribosomal protein L18	1.667	8.667	7.000	-0.003	-0.520	-0.002	0.238	1.238
323453622	24147	Phosphoserine aminotransferase	3.000	8.667	6.667	-0.062	-0.460	-0.032	0.450	1.300
323455964	20379	Ribosomal protein	1.667	8.333	7.667	-0.001	-0.420	-0.003	0.217	1.087
242620081		cytochrome b559 alpha chain	3.333	3.667	5.667	-0.200	-0.076	-0.390	0.588	0.647
323449769	30589	Ribosomal protein	3.000	7.000	8.333	-0.012	-0.140	-0.120	0.360	0.840
323448873	38843	Ribosomal protein	1.333	7.667	9.000	0.000	-0.140	-0.002	0.148	0.852
323456798	70540	Chloroplast light harvesting protein	7.000	6.000	5.333	-0.150	-0.490	-0.098	1.313	1.125
323445949	70003	Ribosomal protein	1.000	7.000	7.667	0.000	-0.220	-0.002	0.130	0.913
323451525	69840	Chloroplast light harvesting protein	5.333	8.000	4.333	-0.240	-0.140	-0.450	1.231	1.846
323457181	69604	Ribosomal protein	0.000	7.333	9.667	0.000	-0.067	0.000	0.000	0.759
323454031	23855	Chloroplast light harvesting protein	7.000	7.333	3.667	-0.025	-0.110	-0.240	1.909	2.000
323455981	59810	Chloroplast light harvesting protein	6.667	7.000	4.333	-0.080	-0.250	-0.250	1.538	1.615
323450876	28850	Pyruvate kinase	7.667	8.000	1.000	0.000	0.000	-0.220	7.667	8.000
323451948	4875	Ribosomal protein	3.000	8.667	5.667	-0.150	-0.270	-0.032	0.529	1.529
323454655	77806	Chloroplast light harvesting protein	6.000	6.000	4.000	-0.100	-0.340	-0.220	1.500	1.500
323453816	77825	Chloroplast light harvesting protein	7.667	6.333	4.000	-0.019	-0.290	-0.071	1.917	1.583
323457186	18502	3-isopropylmalate dehydrogenase	5.000	5.667	6.000	-0.510	-0.290	-0.360	0.833	0.944
323454039	36932	Translation elongation factor	2.667	6.667	6.667	-0.038	-0.330	-0.098	0.400	1.000
323450925	60177	Ribosomal protein	1.000	5.333	8.333	0.000	-0.033	-0.014	0.120	0.640
323451995	59038	Triosephosphate isomerase	6.667	5.667	4.000	-0.055	-0.400	-0.100	1.667	1.417
323450518	59217	Rieske protein (Iron sulfur protein)	6.000	7.667	2.333	-0.010	-0.011	-0.480	2.571	3.286
323457115	19513	Chloroplast precursor CbxX/CfqX	7.667	6.667	1.667	0.000	-0.008	-0.093	4.600	4.000
323445826	69058	Hypothetical protein	5.667	5.333	5.000	-0.300	-0.440	-0.190	1.133	1.067
323449647	66270	Oxidoreductase	5.000	6.667	4.000	-0.240	-0.240	-0.540	1.250	1.667
323455325	61510	Hypothetical protein	5.667	4.667	4.000	-0.140	-0.550	-0.110	1.417	1.167
323451117	28296	Ribosomal protein	2.000	7.667	6.000	-0.024	-0.490	-0.013	0.333	1.278
323448922	77815	Chloroplast light harvesting protein	4.667	5.667	2.667	-0.086	-0.130	-0.440	1.750	2.125
323455846	70817	Sodium/Calcium exchanger	3.333	5.333	5.667	-0.200	-0.300	-0.420	0.588	0.941
323447987	59574	Pyridoxal-5'-phosphate-dependent enzyme, beta subunit	4.667	3.667	6.667	-0.310	-0.025	-0.120	0.700	0.550
323454183	36703	Amino transferase class-I and II	5.333	8.667	1.667	-0.006	-0.001	-0.350	3.200	5.200
323456156	36157	Translation elongation factor	4.333	5.000	5.000	-0.560	-0.370	-0.400	0.867	1.000
323451429	77817	Chloroplast light harvesting protein	5.000	5.333	5.000	-0.440	-0.440	-0.310	1.000	1.067

323452321	71636	ATP-dependent Clp protease	3.667	6.667	3.333	-0.390	-0.130	-0.280	1.100	2.000
323453146	77879	Chloroplast light harvesting protein	5.333	10.667	5.667	-0.490	-0.085	-0.130	0.941	1.882
323448060	55398	Ribosomal protein	1.333	5.333	7.667	0.000	-0.062	-0.033	0.174	0.696
323456741	35830	Mitochondrial substrate carrier	6.000	8.667	0.667	0.000	0.000	-0.490	9.000	13.000
323455317	20736	Inorganic pyrophosphatase	5.333	5.000	4.333	-0.240	-0.530	-0.190	1.231	1.154
323449640	30567	Ribosomal protein	1.000	5.333	6.333	-0.001	-0.190	-0.014	0.158	0.842
242620018		photosystem I reaction center subunit XI	5.667	5.000	3.667	-0.100	-0.450	-0.150	1.545	1.364
323456110	20291	Pyruvate carboxylase	4.333	6.333	1.667	-0.027	-0.011	-0.500	2.600	3.800
323450214	60208	Ribosomal protein	2.000	6.667	5.333	-0.050	-0.520	-0.034	0.375	1.250
323450445	65714	Co or Mg Chelatase	4.000	7.333	1.667	-0.042	-0.003	-0.260	2.400	4.400
323455642	21301	5'-nucleotidase	6.000	7.667	0.000	0.000	0.000	-0.480	N/A	N/A
323453007	70153	Initiation factor	2.333	7.000	3.333	-0.410	-0.097	-0.045	0.700	2.100
323448492	32656	Chloroplast photosystem II 12 kDa extrinsic protein	8.667	3.000	2.000	0.000	-0.440	0.000	4.333	1.500
323453325	71481	Phosphoenolpyruvate carboxylase	5.333	6.667	0.667	0.000	0.000	-0.460	8.000	10.000
323450330	72047	ABC transporter	7.000	6.333	0.000	0.000	0.000	-0.130	N/A	N/A
323453338	53446	Acetyl-coenzyme A synthetase	4.667	5.667	2.000	-0.032	-0.047	-0.440	2.333	2.833
323450260	29608	Inorganic pyrophosphatase	4.667	6.000	2.000	-0.032	-0.033	-0.500	2.333	3.000
242620036		60 kDa chaperonin	3.000	5.333	3.667	-0.520	-0.390	-0.330	0.818	1.455
323452746	60075	Ribosomal protein	1.000	5.000	6.333	-0.001	-0.150	-0.021	0.158	0.789
323456545	70049	Ribosomal protein	0.333	6.000	6.333	0.000	-0.290	0.000	0.053	0.947
323456061	20268	Calcium transporting ATpase	2.667	8.333	1.667	-0.220	-0.001	-0.024	1.600	5.000
323452301	37496	Ribosomal protein	1.667	5.000	5.667	-0.018	-0.240	-0.087	0.294	0.882
323451867	77983	Selenoprotein	2.000	4.667	6.667	-0.011	-0.081	-0.190	0.300	0.700
323455294	22099	ABC transporter	4.000	7.333	1.000	-0.009	0.000	-0.260	4.000	7.333
323448025	60342	Tubulin alpha-2 chain	3.667	7.667	1.000	-0.016	0.000	-0.160	3.667	7.667
323456379	20552	Carbamoyl-phosphate synthase	3.333	6.667	0.333	-0.003	0.000	-0.210	10.000	20.000
323452318	53660	Myosin head, motor region	3.000	9.333	0.000	-0.001	0.000	-0.018	N/A	N/A
323455059	58776	Dihydrolipoamide S-acetyltransferase	4.333	4.667	3.333	-0.240	-0.440	-0.340	1.300	1.400
323451115	6356	Manganese and iron superoxide dismutase	3.000	4.333	4.667	-0.300	-0.310	-0.540	0.643	0.929
323454557	23003	Heat shock protein (Hsp 70)	4.667	5.333	3.000	-0.130	-0.230	-0.380	1.556	1.778
242620088		Rubisco expression protein	4.333	5.000	2.333	-0.080	-0.140	-0.400	1.857	2.143
323447119	34507	Ribosomal protein	0.333	7.000	5.333	0.000	-0.460	0.000	0.063	1.313
323452337	71644	Phosphate ABC transporter	0.000	4.667	7.667	0.000	-0.030	0.000	0.000	0.609
323453613	58899	Chloroplast Ribose 5-phosphate isomerase	4.000	2.667	5.333	-0.410	-0.030	-0.086	0.750	0.500
323447711	72700	Heat shock protein Hsp90	4.000	5.000	3.333	-0.310	-0.370	-0.490	1.200	1.500
323454985	36612	Histidinol dehydrogenase	2.333	4.667	4.333	-0.200	-0.460	-0.270	0.538	1.077
323450867	37987	Acetamidase/Formamidase	2.000	4.000	5.667	-0.035	-0.110	-0.300	0.353	0.706
242620099		Cytochrome b6	5.000	3.667	2.333	-0.036	-0.380	-0.083	2.143	1.571
242620033		ATP synthase CF1 delta chain	3.333	5.000	2.333	-0.230	-0.140	-0.490	1.429	2.143
323457045	52124	Cobalmin synthesis protein/P47K like	4.667	4.333	1.333	-0.008	-0.056	-0.210	3.500	3.250
323450976	28757	Ribosomal protein	1.000	5.000	4.667	-0.013	-0.450	-0.021	0.214	1.071
323451977	69812	GDP-mannose 3,5-epimerase	4.333	7.333	0.000	0.000	0.000	-0.330	N/A	N/A
242620108		Photosystem I iron-sulfur center subunit VII	5.000	2.333	4.667	-0.370	-0.041	-0.013	1.071	0.500
323448756	55048	RNA binding protein	2.667	6.667	1.667	-0.220	-0.008	-0.098	1.600	4.000
323452597	37371	AMP-dependent synthetase and ligase	3.000	6.000	2.000	-0.220	-0.033	-0.230	1.500	3.000
323450333	59240	Isocitrate dehydrogenase NADP-dependent	7.000	3.000	1.333	0.000	-0.220	-0.002	5.250	2.250
323452437	26536	Dihydrolipoamide dehydrogenase	3.000	4.333	3.667	-0.520	-0.560	-0.540	0.818	1.182
323455535	70921	ABC transporter	3.000	3.667	5.000	-0.240	-0.140	-0.490	0.600	0.733
323449224	31415	Geranylgeranyl reductase	2.000	5.000	2.667	-0.490	-0.210	-0.150	0.750	1.875
323446107	60394	Ribosomal Protein	2.000	4.667	4.667	-0.098	-0.380	-0.190	0.429	1.000
323452672	71555	Hypothetical protein	9.000	6.667	13.667	-0.140	0.000	-0.026	0.659	0.488

323450747	7898	Ribosomal Protein	0.333	5.333	5.333	0.000	-0.360	-0.001	0.063	1.000
323448256	60332	Nitrate transporter	0.333	9.000	1.333	-0.230	0.000	0.000	0.250	6.750
242620095		30S ribosomal protein S4	0.000	3.667	7.333	0.000	-0.011	-0.002	0.000	0.500
323446616	68630	S-adenosylmethionine synthetase	2.333	4.667	3.667	-0.330	-0.530	-0.270	0.636	1.273
323448900	32040	Transketolase	3.667	3.000	3.000	-0.310	-0.440	-0.180	1.222	1.000
323455645	70952	Hypothetical protein, no significant BLAST	5.667	3.000	2.333	-0.015	-0.550	-0.015	2.429	1.286
323452673	63886	Hypothetical protein	11.333	8.000	16.333	-0.170	0.000	-0.009	0.694	0.490
323454364	53011	Serine hydroxymethyltransferase	3.000	5.000	1.667	-0.150	-0.051	-0.400	1.800	3.000
323454110	8613	Ribosomal protein	1.333	4.667	5.000	-0.019	-0.310	-0.065	0.267	0.933
323453341	25486	Tryptophan synthase	3.000	3.667	2.333	-0.310	-0.380	-0.490	1.286	1.571
323454315	77808	Chloroplast light harvesting protein	4.333	4.000	1.333	-0.013	-0.080	-0.220	3.250	3.000
323448626	70385	Elongation factor	2.667	6.000	2.333	-0.400	-0.059	-0.160	1.143	2.571
323455519	52520	Helicase	3.667	6.000	0.667	-0.006	-0.001	-0.390	5.500	9.000
323449333	59391	Ribosomal protein	0.333	4.000	5.000	-0.001	-0.190	-0.008	0.067	0.800
323451781	71789	Urea transporter	0.000	5.333	5.000	0.000	-0.440	0.000	0.000	1.067
323456516	19845	Enoyl-acyl carrier	3.333	4.000	2.000	-0.160	-0.220	-0.460	1.667	2.000
323449254	38679	Carbamoyl-phosphate synthase	2.000	4.667	1.667	-0.420	-0.072	-0.190	1.200	2.800
323449672	77821	Chloroplast light harvesting protein	4.667	3.667	1.000	-0.003	-0.059	-0.120	4.667	3.667
323454820	59906	Chloroplast light harvesting protein	1.000	4.667	4.667	-0.013	-0.380	-0.031	0.214	1.000
323447110	70459	Triosephosphate isomerase	3.000	5.333	0.667	-0.020	-0.002	-0.330	4.500	8.000
323456607	19548	Aminotransferase	3.333	7.333	0.000	-0.001	0.000	-0.140	N/A	N/A
323448815	38929	Ribosomal Protein	0.000	3.333	7.000	0.000	-0.010	-0.004	0.000	0.476
323452938	63826	Chloroplast inner membrane protein	2.667	4.000	2.667	-0.500	-0.400	-0.510	1.000	1.500
323448307	77917	Chloroplast light harvesting protein	2.667	4.333	3.000	-0.590	-0.420	-0.440	0.889	1.444
323451227	77837	Chloroplast light harvesting protein	2.333	4.333	3.333	-0.410	-0.510	-0.330	0.700	1.300
323456836	60700	Hypothetical protein	5.333	4.333	0.333	0.000	-0.003	-0.110	16.000	13.000
323446872	34777	Ribosomal Protein	1.667	3.667	3.667	-0.160	-0.410	-0.260	0.455	1.000
323451587	28033	Ribosomal Protein	0.333	3.000	6.667	0.000	-0.009	-0.034	0.050	0.450
323449278	38591	Ribosomal Protein	1.667	3.333	4.333	-0.081	-0.190	-0.330	0.385	0.769
323454417	71232	Beta-ketoacyl ACP synthase	4.000	4.000	1.000	-0.009	-0.040	-0.290	4.000	4.000
242620043		50S ribosomal protein L3	0.000	3.000	6.333	0.000	-0.014	-0.007	0.000	0.474
323450235	29718	Ttubulin beta chain	3.000	5.333	0.000	-0.001	0.000	-0.330	N/A	N/A
323447579	39329	Ribosomal protein	1.000	2.667	4.667	-0.013	-0.067	-0.240	0.214	0.571
323449835	54518	Chloroplast light harvesting protein	2.667	4.333	1.667	-0.220	-0.100	-0.440	1.600	2.600
323454677	71112	IspG protein, diphosphate synthetase	4.333	3.667	1.000	-0.005	-0.059	-0.170	4.333	3.667
323448097	55396	Chloroplast light harvesting protein	2.333	7.000	0.000	-0.005	0.000	-0.045	N/A	N/A
323451404	64968	Tyrosinase, Phytanoyl-CoA dioxygenase	4.667	2.000	2.000	-0.032	-0.480	-0.012	2.333	1.000
323446694	34909	Ribosomal protein	1.000	3.333	3.667	-0.048	-0.330	-0.130	0.273	0.909
323455547	59886	Calreticulin precursor, calnexin	1.000	4.000	4.000	-0.031	-0.400	-0.064	0.250	1.000
323453645	24362	Phosphoribosylaminoimidazole carboxylase	3.000	3.667	1.667	-0.150	-0.190	-0.490	1.800	2.200
323450079	59252	Cysteine synthase	1.667	2.333	4.667	-0.057	-0.041	-0.600	0.357	0.500
323447664	39321	Protein kinase	1.000	3.667	3.667	-0.048	-0.410	-0.092	0.273	1.000
323455675	77882	Chloroplast light harvesting protein	4.000	3.667	1.000	-0.009	-0.059	-0.230	4.000	3.667
323454033	58885	Triosephosphate isomerase	1.333	5.667	1.333	-0.570	-0.011	-0.023	1.000	4.250
323451116	28333	Aliphatic amidase	2.333	2.333	3.667	-0.330	-0.140	-0.370	0.636	0.636
323453409	24874	Diaminopimelate epimerase	4.667	1.667	1.000	-0.003	-0.470	-0.006	4.667	1.667
323450958	59175	Peptidase	2.333	3.667	0.333	-0.023	-0.008	-0.480	7.000	11.000
323453799	24373	Pyruvate kinase	6.667	1.667	0.333	0.000	-0.160	0.000	20.000	5.000
323453165	70159	Ras GTPase	3.000	3.000	1.333	-0.090	-0.220	-0.330	2.250	2.250

323451373	27934	Ribosomal protein	0.667	3.333	3.667	-0.020	-0.330	-0.061	0.182	0.909
323453682	71358	Hypothetical protein	0.333	1.000	4.000	-0.003	-0.007	-0.440	0.083	0.250
242620032		ATP synthase CF0 B chain subunit I	3.000	2.333	2.667	-0.400	-0.360	-0.190	1.125	0.875
323454382	71247	20S proteasome	1.667	1.667	2.667	-0.370	-0.190	-0.430	0.625	0.625
323448356	69968	Ribosomal protein	1.667	3.000	3.333	-0.220	-0.340	-0.410	0.500	0.900
323451802	64802	Hypothetical protein	2.667	3.333	2.000	-0.310	-0.350	-0.520	1.333	1.667
323450585	59202	Phosphoglycerate/bisphospho glycerate mutase	2.667	2.667	2.333	-0.400	-0.560	-0.350	1.143	1.143
323454249	23507	GDP-mannose 4,6-dehydratase	1.333	4.000	2.667	-0.260	-0.400	-0.120	0.500	1.500
323449374	66454	Hypotheical protein	1.667	3.000	2.333	-0.470	-0.550	-0.410	0.714	1.286
323456684	69589	3-hydroxyacyl-CoA dehydrogenase	3.000	3.667	0.333	-0.006	-0.008	-0.490	9.000	11.000
323455682	69676	Phosphoglucose isomerase	3.667	3.000	0.333	-0.002	-0.022	-0.180	11.000	9.000
323455903	36266	Ribosomal protein	0.333	4.000	3.000	-0.018	-0.500	-0.008	0.111	1.333
323454360	58864	Ribosomal protein	0.333	2.667	3.333	-0.010	-0.260	-0.054	0.100	0.800
323453694	37118	Glutamate synthase	1.000	6.000	0.000	-0.100	0.000	-0.006	N/A	N/A
323450314	65882	Dimethymetaquinone methyltransferase	2.000	2.000	3.333	-0.310	-0.130	-0.400	0.600	0.600
323446737	34869	Acyl carrier protein	2.000	1.667	4.000	-0.180	-0.033	-0.300	0.500	0.417
323457240	18463	Ammonium transporter	1.000	2.333	4.000	-0.031	-0.093	-0.330	0.250	0.583
323454160	71132	Peptidase	1.333	4.333	2.000	-0.460	-0.160	-0.090	0.667	2.167
323446671	17075	Beta-hydroxyacyl-(acyl-carrier-protein) dehydratase FabZ	1.000	3.000	3.000	-0.110	-0.440	-0.180	0.333	1.000
323454408	23206	Ferredoxin--NADP(+) reductase	22.333	24.667	20.667	-0.140	-0.520	-0.120	1.081	1.194
323452383	37542	Ribose-phosphate pyrophosphokinase	3.667	3.667	0.333	-0.002	-0.008	-0.300	11.000	11.000
323456630	60414	Heparan Sulfate 2-0-sulfotranserase	0.333	2.333	4.667	-0.001	-0.041	-0.084	0.071	0.500
323448438	72539	RNA binding protein	1.333	2.667	3.000	-0.190	-0.350	-0.370	0.444	0.889
323454510	71184	Proteasome	2.667	1.333	3.000	-0.590	-0.074	-0.079	0.889	0.444
323455949	52186	Proteasome	1.000	3.333	3.000	-0.110	-0.520	-0.130	0.333	1.111
323451767	27224	Hydroxyisobutyrate dehydrogenase	0.667	3.667	2.333	-0.120	-0.380	-0.041	0.286	1.571
323454706	23304	Ribonucleoprotein complex subunit	0.667	2.667	3.333	-0.032	-0.260	-0.130	0.200	0.800
323452898	25785	Glutamate dehydrogenase	3.000	3.333	0.333	-0.006	-0.013	-0.410	9.000	10.000
323455708	10538	Cell division protein FtsH	3.000	4.667	0.000	-0.001	0.000	-0.460	N/A	N/A
323451167	60165	Ribosomal porotein	0.000	1.333	4.333	0.000	-0.009	-0.110	0.000	0.308
323457264	51957	Nicotinamide nucleotide transhydrogenase	3.667	3.333	0.000	0.000	-0.002	-0.240	N/A	N/A
323454696	59930	Tetrahydrofolate dehydrogenase/cyclohydrolase	1.000	5.667	0.333	-0.270	0.000	-0.009	3.000	17.000
323456719	60533	Hypothetical protein	3.000	2.333	1.333	-0.090	-0.390	-0.190	2.250	1.750
323449474	31056	Semialdehyde dehydrogenase	3.333	1.667	1.000	-0.028	-0.470	-0.051	3.333	1.667
323451071	71877	Ribosomal protein	0.333	3.333	3.333	-0.010	-0.420	-0.021	0.100	1.000
323450177	38219	Ras small GTPase	2.667	3.333	0.333	-0.012	-0.013	-0.520	8.000	10.000
323449160	69937	Proteasome	0.000	1.667	5.000	0.000	-0.007	-0.064	0.000	0.333
323454354	53005	Ormate nitrite transporter	2.000	2.333	2.333	-0.590	-0.470	-0.490	0.857	1.000
323450131	30014	Xanthine/uracil/vitamin C permease	2.333	2.000	1.667	-0.310	-0.610	-0.290	1.400	1.200
323452963	25646	Light inducinble protein	2.333	2.333	1.333	-0.210	-0.390	-0.370	1.750	1.750
323446228	35224	Ribosomal protein	1.000	3.000	2.333	-0.230	-0.550	-0.180	0.429	1.286
323449422	72267	Luteovirus ORF6 protein	1.333	1.333	3.333	-0.130	-0.046	-0.460	0.400	0.400
323455449	59875	Ribosomal protein	1.000	2.667	2.667	-0.160	-0.450	-0.240	0.375	1.000
323451852	77830	Chloroplast light harvesting protein	1.333	3.000	2.000	-0.460	-0.440	-0.290	0.667	1.500
323451675	71753	Hypothetical protein	2.000	2.333	1.667	-0.420	-0.520	-0.490	1.200	1.400
323452748	25684	TB2/DP1/HVA22 related protein	3.000	2.000	1.000	-0.047	-0.350	-0.130	3.000	2.000
323452124	16956	Cytochrome	1.000	1.667	4.000	-0.031	-0.033	-0.540	0.250	0.417
323449261	66559	Ribosomal protein	0.000	4.000	2.333	-0.012	-0.300	-0.001	0.000	1.714

323453524	69744	Glutathion transferase	2.333	3.667	0.000	-0.005	-0.001	-0.480	N/A	N/A
323454682	71109	GDP dissociation protein	2.333	3.000	0.000	-0.005	-0.004	-0.550	N/A	N/A
323453260	4272	Phosphoadenosine phosphosulfate reductase	1.667	2.000	2.000	-0.580	-0.480	-0.530	0.833	1.000
323455961	59805	Chloroplast light harvesting protein	2.333	2.333	1.667	-0.310	-0.520	-0.370	1.400	1.400
323450829	71930	Ras small GTPase	1.000	2.667	1.333	-0.570	-0.290	-0.240	0.750	2.000
323457083	58588	Magnesium chelatase	2.667	2.000	1.667	-0.220	-0.610	-0.200	1.600	1.200
323453963	77823	Chloroplast light harvesting protein	2.000	2.333	1.667	-0.420	-0.520	-0.490	1.200	1.400
323452943	60062	Ribosomal protein	0.667	3.000	2.667	-0.080	-0.540	-0.091	0.250	1.125
323455143	22183	Ribosomal protein	0.667	2.000	3.000	-0.051	-0.190	-0.270	0.222	0.667
323449038	38757	Peptidase	0.333	2.667	3.333	-0.010	-0.260	-0.054	0.100	0.800
242620045		50S ribosomal protein L2	0.000	3.333	3.000	-0.003	-0.520	-0.004	0.000	1.111
242620089		Conserved hypothetical plastid protein Ycf39	2.000	3.667	0.333	-0.044	-0.008	-0.370	6.000	11.000
323452812	25795	Dihydrolipoamide dehydrogenase	0.000	1.000	5.000	0.000	-0.001	-0.190	0.000	0.200
323452243	64345	Glycinamide ribonucleotide synthetase-aminoimidazole ribonucleotide synthetase-glycinamide ribonucleotide transformylase	1.000	2.000	2.333	-0.230	-0.370	-0.420	0.429	0.857
323448587	38989	Adenylosuccinate synthetase	1.000	2.333	2.667	-0.160	-0.360	-0.330	0.375	0.875
323456068	52275	Heat shock protein	1.000	2.333	1.667	-0.430	-0.520	-0.330	0.600	1.400
323451686	59069	Chloroplast light harvesting protein	2.333	1.667	1.667	-0.310	-0.510	-0.200	1.400	1.000
323451892	53834	H+-transporting ATPase	0.667	2.000	2.667	-0.080	-0.270	-0.270	0.250	0.750
323448447	32730	Endopeptidase Clp activity	2.000	2.000	2.000	-0.530	-0.480	-0.400	1.000	1.000
323454156	23622	Myo-inositol 2-dehdrogenase	0.667	3.000	1.333	-0.400	-0.220	-0.091	0.500	2.250
323452393	64290	OmpA/MotB domain-containing protein	3.333	1.667	0.333	-0.003	-0.160	-0.051	10.000	5.000
323447335	77912	Formate/nitrite transporter	2.000	2.667	0.000	-0.011	-0.008	-0.590	N/A	N/A
323450320	60213	Ribosomal protein	0.000	3.000	3.000	-0.003	-0.440	-0.007	0.000	1.000
242620044		50S ribosomal protein L23	0.000	1.667	3.667	-0.001	-0.052	-0.064	0.000	0.455
323449109	69941	Low molecular weight phosphotyrosine protein phosphatase	2.000	3.667	0.000	-0.011	-0.001	-0.370	N/A	N/A
323452273	64100	Hypotheical protein	3.000	3.000	0.000	-0.001	-0.004	-0.330	N/A	N/A
323450582	65618	Transketolase	2.333	3.000	0.000	-0.005	-0.004	-0.550	N/A	N/A
323451061	71871	Histidine kinase	1.667	3.000	0.000	-0.023	-0.004	-0.410	N/A	N/A
323450099	54387	Proteasome	1.000	2.667	2.000	-0.320	-0.530	-0.240	0.500	1.333
323453003	37193	Vesicle coat complex	1.667	2.333	1.667	-0.540	-0.520	-0.600	1.000	1.400
323454002	15386	Peptidyl-prolyl cis-trans isomerase	1.667	3.000	0.667	-0.180	-0.062	-0.410	2.500	4.500
323453823	71380	Brix domain	2.333	2.000	1.000	-0.130	-0.350	-0.290	2.333	2.000
323453684	37110	H+-transporting two-sector ATPase	1.667	3.333	0.667	-0.180	-0.040	-0.330	2.500	5.000
323455795	70840	Hypotheical protein	1.333	1.000	3.000	-0.190	-0.038	-0.340	0.444	0.333
323449806	30491	Phytoene dehydrogenase-related protein	1.000	2.667	0.667	-0.440	-0.095	-0.240	1.500	4.000
323448789	55095	GUN4 like domain	2.333	2.667	0.333	-0.023	-0.036	-0.460	7.000	8.000
323453085	71458	Calcium-binding EF-hand	1.000	3.667	1.000	-0.600	-0.059	-0.092	1.000	3.667
323455637	58713	RAN function family member - supported with BLASTp	1.333	3.000	0.333	-0.150	-0.022	-0.290	4.000	9.000
323454406	59975	Armet super family domain	0.333	1.667	2.667	-0.030	-0.190	-0.200	0.125	0.625
242620051		50S ribosomal protein L14	0.333	2.000	3.333	-0.010	-0.130	-0.130	0.100	0.600
323448823	72468	Adenylylsulfate kinase	1.667	2.667	0.000	-0.023	-0.008	-0.510	N/A	N/A
323454381	23365	Cystathione gamma lyase	0.000	3.000	2.000	-0.022	-0.440	-0.007	0.000	1.500
323451378	59110	Sterol methyltransferase	2.333	2.667	0.000	-0.005	-0.008	-0.460	N/A	N/A
323453289	71496	BLASTp putative protein with GPS domain	0.667	3.333	1.333	-0.400	-0.160	-0.061	0.500	2.500
323450531	29439	Calcium ATPase	1.333	2.000	1.333	-0.570	-0.490	-0.570	1.000	1.500
323449845	72180	Hypothetical protein	1.667	2.000	0.667	-0.180	-0.210	-0.530	2.500	3.000
323450569	54227	Ribosomal protein	0.000	1.667	3.000	-0.003	-0.130	-0.064	0.000	0.556
323452077	17528	Ribosomal protein	0.333	2.667	2.333	-0.051	-0.560	-0.054	0.143	1.143

323453164	53460	N-ethylmaleimide sensitive fusion protein	1.667	3.333	0.000	-0.023	-0.002	-0.330	N/A	N/A
323452089	53803	IMP dehydrogenase/GMP reductase	0.000	1.667	3.000	-0.003	-0.130	-0.064	0.000	0.556
323454388	23619	Splicing factor	0.333	3.333	1.000	-0.360	-0.088	-0.021	0.333	3.333
323452833	37435	CAP protein	2.333	2.667	0.000	-0.005	-0.008	-0.460	N/A	N/A
323447982	33371	Peptidyl-prolyl cis-trans isomerase	0.667	4.333	0.333	-0.450	-0.003	-0.018	2.000	13.000
323456174	61355	Translational activator	0.667	3.000	0.333	-0.450	-0.022	-0.091	2.000	9.000
323454181	12877	Zinc-containing alcohol dehydrogenase superfamily	1.333	3.000	0.000	-0.048	-0.004	-0.290	N/A	N/A
323456017	59818	CTP synthase	1.000	1.667	1.000	-0.600	-0.470	-0.540	1.000	1.667
323452600	77873	Inorganic phosphate transporter	1.333	1.667	0.333	-0.150	-0.160	-0.580	4.000	5.000
323446721	39490	Coproporphyrinogen III oxidase	0.667	2.000	1.667	-0.280	-0.610	-0.270	0.400	1.200
323447291	34298	Phosphoglycerate mutase	2.000	1.333	0.667	-0.110	-0.430	-0.210	3.000	2.000
323447671	72706	Ribosomal protein	0.667	2.000	2.333	-0.120	-0.370	-0.270	0.286	0.857
323450970	28783	Ribosomal protein	0.333	2.000	2.667	-0.030	-0.270	-0.130	0.125	0.750
323455165	21835	Inorganic pyrophosphatase	1.667	1.667	0.333	-0.083	-0.160	-0.430	5.000	5.000
323452927	71545	Asparagine synthase	0.667	3.000	1.000	-0.560	-0.130	-0.091	0.667	3.000
323449776	77854	Urease	1.333	0.333	2.333	-0.350	-0.019	-0.110	0.571	0.143
323451387	28095	20S proteasome, A and B subunits	0.333	1.333	3.333	-0.010	-0.046	-0.300	0.100	0.400
323452801	64057	Hypothetical protein	1.000	1.000	0.333	-0.270	-0.380	-0.500	3.000	3.000
323453239	70163	Proliferating cell nuclear antigen, PCNA	0.000	2.000	2.333	-0.012	-0.370	-0.037	0.000	0.857
242620066		30S ribosomal protein S7	0.000	2.333	2.333	-0.012	-0.470	-0.021	0.000	1.000
323452338	37524	Helicase and restriction enzyme domain	0.000	2.333	1.667	-0.042	-0.520	-0.021	0.000	1.400
323455998	70668	Alkaline phosphatase	4.333	0.667	0.000	0.000	-0.300	-0.001	N/A	N/A
323447466	72743	Acting binding FH2	1.667	1.333	1.667	-0.540	-0.390	-0.320	1.000	0.800
323452857	25558	Glutathione reductase	0.667	2.000	1.667	-0.280	-0.610	-0.270	0.400	1.200
323452157	59049	Ribosomal protein	0.667	1.000	2.000	-0.190	-0.170	-0.640	0.333	0.500
323452499	26373	Homoserine dehydrogenase	1.000	1.667	2.000	-0.320	-0.380	-0.540	0.500	0.833
323448899	31937	Dehydrogenase	1.000	2.333	0.667	-0.440	-0.140	-0.330	1.500	3.500
323455705	20758	Serine hydroxymethyltransferase	1.000	2.333	0.667	-0.440	-0.140	-0.330	1.500	3.500
323457101	59786	Chaperonin	1.000	2.000	0.667	-0.440	-0.210	-0.420	1.500	3.000
323456188	19929	Heat shock protein	0.667	2.333	0.667	-0.640	-0.140	-0.190	1.000	3.500
323454770	1561	Calreticulin/calnexin	2.000	2.667	0.333	-0.044	-0.036	-0.590	6.000	8.000
323456208	36201	Synaptobrevin	2.333	2.000	0.000	-0.005	-0.026	-0.290	N/A	N/A
323452787	17219	Ribosomal protein	0.000	1.667	2.333	-0.012	-0.270	-0.064	0.000	0.714
323449760	59319	Glycine cleavage system	1.000	3.000	0.333	-0.270	-0.022	-0.180	3.000	9.000
323452846	26092	Argininosuccinate synthase	1.333	2.333	0.667	-0.290	-0.140	-0.470	2.000	3.500
323453590	63073	ATPase	1.667	3.000	0.000	-0.023	-0.004	-0.410	N/A	N/A
323446732	68563	Hypothetical protein	2.333	2.000	0.000	-0.005	-0.026	-0.290	N/A	N/A
323449711	59335	Heat shock protein	0.000	2.333	1.333	-0.080	-0.390	-0.021	0.000	1.750
323449583	54676	Ribosomal protein	0.333	1.000	3.333	-0.010	-0.022	-0.440	0.100	0.300
323455948	70645	Mucin-associated surface protein (MASP)	0.667	0.000	3.333	-0.032	0.000	-0.180	0.200	0.000
323455062	59926	Cytochrome C	2.000	1.000	1.000	-0.200	-0.570	-0.130	2.000	1.000
323450323	29703	Threonyl-tRNA synthetase	1.000	2.000	0.667	-0.440	-0.210	-0.420	1.500	3.000
323446946	68429	Hypothetical protein	1.333	1.667	3.667	-0.094	-0.052	-0.580	0.364	0.455
323455402	21676	Protease	1.000	2.000	1.000	-0.600	-0.350	-0.420	1.000	2.000
323456496	20345	AICARFT/IMPCHase bienzyme, Methylglyoxal synthase-like	1.000	2.000	0.667	-0.440	-0.210	-0.420	1.500	3.000
242620056		30S ribosomal protein S5	0.333	2.000	2.000	-0.086	-0.480	-0.130	0.167	1.000
323450650	65557	Phosphate ABC transporter permease	1.667	0.333	2.000	-0.580	-0.037	-0.053	0.833	0.167
323454389	22992	Translation initiaion factor	0.333	1.333	1.667	-0.140	-0.390	-0.300	0.200	0.800
323448266	33048	Histone	12.667	36.667	41.667	-0.460	-0.010	-0.018	0.304	0.880
323455110	12414	Uroporphyrinogen decarboxylase (URO-D)	2.000	1.333	0.667	-0.110	-0.430	-0.210	3.000	2.000
323455057	22578	Threonine synthase	1.000	2.333	0.667	-0.440	-0.140	-0.330	1.500	3.500

323451149	60167	20S proteasome, A and B subunits	0.667	0.333	2.333	-0.120	-0.019	-0.390	0.286	0.143
323446359	68778	Patched, Sterol-sensing 5TM box	1.667	1.333	0.667	-0.180	-0.430	-0.320	2.500	2.000
323456109	10168	ATPase	2.000	2.000	0.000	-0.011	-0.026	-0.400	N/A	N/A
323453433	53391	Nitrate reducatase	0.000	4.000	0.333	-0.530	-0.005	-0.001	0.000	12.000
323451357	69836	Rab family GTPase	2.000	1.333	0.333	-0.044	-0.250	-0.210	6.000	4.000
323456121	70709	Actin like protein	1.333	2.000	0.333	-0.150	-0.098	-0.570	4.000	6.000
242620053		50S ribosomal protein L5	0.000	2.333	1.000	-0.150	-0.260	-0.021	0.000	2.333
242620100		30S ribosomal protein S6	0.333	2.000	1.667	-0.140	-0.610	-0.130	0.200	1.200
323453700	60020	Elongation factor	0.333	2.000	1.333	-0.230	-0.490	-0.130	0.250	1.500
323448915	32029	Beta ketoacyl ACP synthase	0.333	2.000	1.333	-0.230	-0.490	-0.130	0.250	1.500
323450977	71923	Tubulin, Cell division protein FtsZ	1.333	2.333	0.333	-0.150	-0.060	-0.470	4.000	7.000
323453278	37323	Oxoglutarate dehydrogenase	1.667	1.667	0.333	-0.083	-0.160	-0.430	5.000	5.000
323455128	59919	Hypothetical protein	0.333	1.667	2.000	-0.086	-0.380	-0.200	0.167	0.833
323455320	70771	Amine oxidase	0.667	1.000	1.333	-0.400	-0.400	-0.640	0.500	0.750
323451608	27981	Ribosomal Protein	0.000	1.667	1.333	-0.080	-0.610	-0.064	0.000	1.250
323455983	61076	Flavin containing monooxygenase 5	1.333	1.000	0.000	-0.048	-0.160	-0.340	N/A	N/A
323450621	29090	Ribosomal protein	0.000	1.667	1.667	-0.042	-0.510	-0.064	0.000	1.000
323454199	59942	DnaJ homolog	0.667	1.667	0.667	-0.640	-0.310	-0.370	1.000	2.500
323450083	60218	Ribosomal protein	0.000	1.333	1.667	-0.042	-0.390	-0.110	0.000	0.800
323452263	69799	Peptidase / Proteasome	0.333	1.000	2.000	-0.086	-0.170	-0.440	0.167	0.500
323456325	52346	Phosphatase	0.000	2.000	2.000	-0.022	-0.480	-0.037	0.000	1.000
323450948	28673	Succinyl-CoA synthetase, ATP-citrate lyase/succinyl-CoA ligase, Succinyl-CoA synthetase, ATP-citrate lyase/succinyl-CoA ligase	0.667	0.667	1.667	-0.280	-0.160	-0.560	0.400	0.400
323450133	38247	Heat shock protein	1.000	2.000	0.667	-0.440	-0.210	-0.420	1.500	3.000
323449973	60228	Proteasome	0.000	1.333	1.667	-0.042	-0.390	-0.110	0.000	0.800
323451260	69850	Cobalamin synthesis protein	2.000	1.667	0.000	-0.011	-0.048	-0.300	N/A	N/A
323451909	27356	ATP phosphoribosyltransferase	0.333	2.000	1.667	-0.140	-0.610	-0.130	0.200	1.200
323450497	72023	Serine/threonine-protein phosphatase	1.000	1.667	0.000	-0.100	-0.048	-0.540	N/A	N/A
323452306	26433	RNA binding protein	0.333	1.333	1.000	-0.360	-0.600	-0.300	0.333	1.333
323448914	60302	Malate dehydrogenase	0.667	3.000	0.000	-0.220	-0.004	-0.091	N/A	N/A
323451863	27395	Aspartate/other aminotransferase	0.667	3.000	0.000	-0.220	-0.004	-0.091	N/A	N/A
323451862	27202	H+-transporting two-sector ATPase	1.000	1.667	1.000	-0.600	-0.470	-0.540	1.000	1.667
323457289	59757	Eukaryotic initiation factor 5A hypusine	1.000	1.667	0.667	-0.440	-0.310	-0.540	1.500	2.500
323448128	7478	Peptidyl-prolyl cis-trans isomerase	1.333	1.000	0.667	-0.290	-0.590	-0.340	2.000	1.500
323447945	72648	Phosphofructokinase	0.667	2.000	0.667	-0.640	-0.210	-0.270	1.000	3.000
323449674	69917	Peptidase	0.000	2.000	1.000	-0.150	-0.350	-0.037	0.000	2.000
323457341	70480	Contains pleckstrin-like domain	1.333	2.000	0.333	-0.150	-0.098	-0.570	4.000	6.000
323454473	23252	Iron-dependent fumarate hydratase, Fe-S type hydro-lyases tartrate/fumarate	1.333	1.667	0.000	-0.048	-0.048	-0.580	N/A	N/A
323449899	60237	Ribosomal protein	0.000	1.667	2.000	-0.022	-0.380	-0.064	0.000	0.833
323456455	59830	Ribosomal protein	0.333	0.333	2.333	-0.051	-0.019	-0.670	0.143	0.143
323454954	71078	Calmodulin	0.333	0.333	2.667	-0.030	-0.010	-0.670	0.125	0.125
323451287	28200	Argininosuccinate lyase	1.000	0.667	0.000	-0.100	-0.300	-0.360	N/A	N/A
323454341	9008	Thioredoxin domain 2	0.000	0.667	2.667	-0.006	-0.029	-0.330	0.000	0.250
323448003	67583	Hypothetical protein	0.667	0.000	0.667	-0.640	-0.210	-0.180	1.000	0.000
323450849	7494	Protein of photosystem II	1.000	1.333	1.000	-0.600	-0.600	-0.630	1.000	1.333
323446625	72830	Transcriptional regulatory protein algP	1.333	1.000	1.000	-0.430	-0.570	-0.340	1.333	1.000
323451064	77836	Chloroplast light harvesting protein	0.667	1.333	0.667	-0.640	-0.430	-0.500	1.000	2.000

323456234	61432	NADH-quinone oxidoreductase subunit	1.667	0.667	1.000	-0.300	-0.410	-0.120	1.667	0.667
323455839	61607	Generic methyltransferase	1.667	1.000	0.667	-0.180	-0.590	-0.210	2.500	1.500
323449225	59414	Bifunctional aspartate kinase/homoserine dehydrogenase	1.000	1.667	0.667	-0.440	-0.310	-0.540	1.500	2.500
323453705	37129	Ammonium transporter	0.667	2.333	2.333	-0.080	-0.360	-0.190	0.286	1.000
323446944	72810	Hypothetical protein	0.667	1.000	1.333	-0.400	-0.400	-0.640	0.500	0.750
323446659	72828	ATPase	1.000	1.667	0.333	-0.270	-0.160	-0.540	3.000	5.000
323451333	27870	Ribosomal Protein	0.000	1.333	1.000	-0.150	-0.600	-0.110	0.000	1.333
323456908	70598	Acetyl-coenzyme A synthetase	1.333	0.667	0.333	-0.150	-0.570	-0.210	4.000	2.000
323454832	62132	TPR repeat containing protein	0.000	1.333	1.667	-0.042	-0.390	-0.110	0.000	0.800
323455019	13348	Carbamoylphosphate synthetase 2/aspartate transcarbamylase/dihydroorotase	0.667	2.000	0.333	-0.450	-0.098	-0.270	2.000	6.000
323454055	36910	Ribosomal protein	0.333	0.667	1.667	-0.140	-0.160	-0.610	0.200	0.400
323450361	29693	Triosephosphate isomerase	0.000	2.000	1.333	-0.080	-0.490	-0.037	0.000	1.500
323453878	71352	Aspartyl-tRNA synthetase	0.333	1.000	1.333	-0.230	-0.400	-0.440	0.250	0.750
323451615	71802	Methionyl / Aminoacyl-tRNA synthetase	0.667	2.000	0.000	-0.220	-0.026	-0.270	N/A	N/A
323451627	12112	Na+/H+ antiporter NhaA	0.000	1.333	2.000	-0.022	-0.270	-0.110	0.000	0.667
323446387	68761	KH domain for binding nucleic acids	0.667	2.000	0.667	-0.640	-0.210	-0.270	1.000	3.000
323454189	7695	Ribosomal protein	0.000	1.000	1.667	-0.042	-0.270	-0.190	0.000	0.600
323453547	59995	Prohibitin	2.000	0.667	0.000	-0.011	-0.300	-0.066	N/A	N/A
323454570	71153	Hypothetical protein	0.667	2.667	0.000	-0.220	-0.008	-0.130	N/A	N/A
323453434	37238	Nitrite reductase	0.000	2.333	1.000	-0.150	-0.260	-0.021	0.000	2.333
323456737	70513	Inorganic phosphate transporter	2.333	1.333	0.000	-0.005	-0.089	-0.130	N/A	N/A
323457185	52040	Adaptin	0.000	2.333	1.000	-0.150	-0.260	-0.021	0.000	2.333
323455015	52760	Cycloartenol-C24-methyltransferase	2.333	0.333	0.000	-0.005	-0.550	-0.012	N/A	N/A
323452327	71640	Zn-finger	0.667	1.333	0.000	-0.220	-0.089	-0.500	N/A	N/A
323449390	54723	Exportin	2.333	0.667	0.000	-0.005	-0.300	-0.035	N/A	N/A
323456463	69639	Hypothetical protein	1.000	1.000	1.000	-0.600	-0.570	-0.500	1.000	1.000
323456395	1116	Eukaryotic translation initiation factor	0.667	1.333	0.667	-0.640	-0.430	-0.500	1.000	2.000
323455383	58678	Phenylalanyl-tRNA synthetase	1.667	1.000	0.333	-0.083	-0.380	-0.210	5.000	3.000
323451360	28035	Chorismate synthase	0.667	0.667	1.000	-0.560	-0.410	-0.560	0.667	0.667
323449322	38625	Isopropylmalate synthase	1.667	1.000	0.667	-0.180	-0.590	-0.210	2.500	1.500
323456879	18780	Protease	0.667	0.667	1.667	-0.280	-0.160	-0.560	0.400	0.400
323455013	22474	Ankyrin	0.000	1.333	1.333	-0.080	-0.530	-0.110	0.000	1.000
323451434	28009	Hypothetical protein	1.000	1.333	0.333	-0.270	-0.250	-0.630	3.000	4.000
323450398	3154	Plastidic triose-phosphate/phosphate translocator	1.667	1.000	0.000	-0.023	-0.160	-0.210	N/A	N/A
323447220	68254	Hypothetical protein	0.667	1.667	0.000	-0.220	-0.048	-0.370	N/A	N/A
323446727	34875	Cobalamin-requiring methionine synthase	0.333	2.000	0.333	-0.720	-0.098	-0.130	1.000	6.000
323452805	71598	NADPH protochlorophyllide reductase	1.333	0.333	0.667	-0.290	-0.430	-0.110	2.000	0.500
323453262	71507	Serine/threonine-protein kinase	0.000	1.000	2.000	-0.022	-0.170	-0.190	0.000	0.500
323448712	67109	Thiolase	0.333	0.667	0.667	-0.550	-0.620	-0.610	0.500	1.000
323457297	18821	Myosin	1.667	0.667	0.000	-0.023	-0.300	-0.120	N/A	N/A
323456351	77802	Chloroplast light harvesting protein	1.333	1.667	0.000	-0.048	-0.048	-0.580	N/A	N/A
323449561	38491	Ribosomal protein	0.000	1.333	1.333	-0.080	-0.530	-0.110	0.000	1.000
323454302	23053	Protease	1.667	1.000	0.333	-0.083	-0.380	-0.210	5.000	3.000
323453584	24204	Ribosomal protein	0.000	1.333	0.333	-0.530	-0.250	-0.110	0.000	4.000
323450277	29821	Ribosomal Protein	0.000	1.000	1.333	-0.080	-0.400	-0.190	0.000	0.750
323450718	29089	Photosystem II stability/assembly factor	2.333	0.333	0.333	-0.023	-0.700	-0.012	7.000	1.000

323452552	60080	Proteasome	0.000	0.667	2.000	-0.022	-0.092	-0.330	0.000	0.333
323452930	1689	ABC transporter	1.333	7.000	0.667	-0.016	-0.001	-0.230	2.000	10.500
323449871	54528	HMG-CoA lyase-like, Alpha-isopropylmalate/homocitrate synthase	2.000	0.333	0.000	-0.011	-0.550	-0.026	N/A	N/A
323447741	55500	Nonaspanin	0.000	2.333	0.333	-0.530	-0.060	-0.021	0.000	7.000
242620028		30S ribosomal protein S2	0.000	2.667	0.333	-0.530	-0.036	-0.012	0.000	8.000
323454310	52969	Adenosine kinase	0.000	2.667	0.000	-1.000	-0.008	-0.012	N/A	N/A
323451431	77818	Chloroplast light harvesting protein	0.000	2.000	6.000	-0.110	-0.240	-0.330	0.000	0.333
323453970	60001	Hypothetical protein	1.000	1.333	0.333	-0.270	-0.250	-0.630	3.000	4.000
323451979	78108	Selenoprotein	0.333	1.333	1.000	-0.360	-0.600	-0.300	0.333	1.333
323454125	71117	ABC transporter	1.333	1.000	0.000	-0.048	-0.160	-0.340	N/A	N/A
323448681	32244	KDPG and KHG aldolase	1.000	0.333	1.000	-0.600	-0.250	-0.210	1.000	0.333
323449180	66715	Mannosyltransferase	1.333	0.000	1.333	-0.570	-0.043	-0.032	1.000	0.000
323450841	28553	Electron transfer flavoprotein	1.000	1.000	0.333	-0.270	-0.380	-0.500	3.000	3.000
323456793	18389	Nuclear transport factor 2	0.333	1.333	0.667	-0.550	-0.430	-0.300	0.500	2.000
323449211	38723	PAS	0.000	1.333	1.333	-0.080	-0.530	-0.110	0.000	1.000
323451135	37911	Proteasome	0.000	1.000	1.667	-0.042	-0.270	-0.190	0.000	0.600
323456300	61455	CreA family protein	1.333	0.333	1.000	-0.430	-0.250	-0.110	1.333	0.333
323452724	25961	Hypothetical protein	1.000	1.000	0.667	-0.440	-0.590	-0.500	1.500	1.500
323448268	33034	Aldo/keto reductase	0.667	1.333	0.333	-0.450	-0.250	-0.500	2.000	4.000
323450964	28667	Mannitol phosphate	0.333	1.000	1.000	-0.360	-0.570	-0.440	0.333	1.000
323452169	5924	Hypothetical protein	0.667	2.000	0.000	-0.220	-0.026	-0.270	N/A	N/A
323451897	59068	Nucleolar protein Nop56	0.333	0.333	2.000	-0.086	-0.037	-0.670	0.167	0.167
323448884	55034	Proteasome	0.000	1.000	1.667	-0.042	-0.270	-0.190	0.000	0.600
323454580	70105	Glutathione peroxidase	1.333	1.000	0.000	-0.048	-0.160	-0.340	N/A	N/A
242620059		30S ribosomal protein S13	0.000	1.333	1.333	-0.080	-0.530	-0.110	0.000	1.000
323451363	14994	Phospholipid/glycerol acyltransferase	0.667	2.000	0.000	-0.220	-0.026	-0.270	N/A	N/A
323448448	32655	Nonphototropic hypocotyl	0.000	0.333	2.333	-0.012	-0.019	-0.580	0.000	0.143
242620055		50S ribosomal protein L6	0.000	0.333	2.333	-0.012	-0.019	-0.580	0.000	0.143
323454894	22512	Formylglycineamide ribotide amidotransferase	0.000	2.667	0.000	-1.000	-0.008	-0.012	N/A	N/A
323449382	38538	Glutamate synthase	0.000	1.000	0.000	-1.000	-0.160	-0.190	N/A	N/A
323448821	70378	ATPase, proteasome	1.000	1.000	0.000	-0.100	-0.160	-0.500	N/A	N/A
323450953	28840	Epsilon1-COP	0.667	1.667	0.000	-0.220	-0.048	-0.370	N/A	N/A
323451761	27287	mRNA binding protein	0.667	1.000	0.333	-0.450	-0.380	-0.640	2.000	3.000
323445273	9896	Proteasome	0.000	0.667	1.667	-0.042	-0.160	-0.330	0.000	0.400
323457195	19173	Ribosomal Protein	0.000	0.667	1.667	-0.042	-0.160	-0.330	0.000	0.400
323450275	1254	Lysyl-tRNA synthetase	0.333	1.333	0.667	-0.550	-0.430	-0.300	0.500	2.000
323456994	58606	Glycyl tRNA synthetase	1.000	1.000	0.333	-0.270	-0.380	-0.500	3.000	3.000
323451216	28476	Ribosomal protein	0.000	0.667	1.667	-0.042	-0.160	-0.330	0.000	0.400
323449910	38303	Rhamnose biosynthetic enzyme 1	0.333	0.667	0.000	-0.470	-0.300	-0.610	N/A	N/A
323453288	24967	Glutamyl-tRNA reductase	0.667	0.333	0.333	-0.450	-0.700	-0.390	2.000	1.000
323454888	21939	S-adenosylmethionine-dependent methyltransferase activity	0.333	1.333	0.000	-0.470	-0.089	-0.300	N/A	N/A
323455339	21514	Ribosomal protein	0.000	0.333	1.333	-0.080	-0.140	-0.580	0.000	0.250
323454405	22805	Aminoacyl-tRNA synthetase	0.000	1.333	0.667	-0.280	-0.430	-0.110	0.000	2.000
323449847	72183	Proteasome	0.000	1.000	0.667	-0.280	-0.590	-0.190	0.000	1.500
323457245	19010	Aminoacyl-tRNA synthetase	1.000	1.000	0.000	-0.100	-0.160	-0.500	N/A	N/A
323453077	16	Dynein heavy chain, AAA ATPase	1.000	0.000	0.000	-0.100	-1.000	-0.076	N/A	N/A
323454617	71135	GCN5-related N-acetyltransferase	0.667	0.333	1.000	-0.560	-0.250	-0.390	0.667	0.333
323454603	71137	Prolyl 4-hydroxylase	1.000	1.000	0.000	-0.100	-0.160	-0.500	N/A	N/A
323447558	34011	Glutamine amidotransferase/cyclase	1.000	0.667	0.333	-0.270	-0.570	-0.360	3.000	2.000
323451314	64822	Tnks; tankyrase	1.000	0.667	0.333	-0.270	-0.570	-0.360	3.000	2.000
323455735	70885	Vacuolar-type H+-translocating inorganic pyrophosphatase	0.333	1.000	1.333	-0.140	-0.390	-0.300	0.250	0.750
323451825	2849	Squalene synthase	0.667	0.667	0.667	-0.640	-0.620	-0.560	1.000	1.000
323453323	60042	Elongation factor	0.667	1.000	0.000	-0.220	-0.160	-0.640	N/A	N/A

323451463	59127	SecA-type chloroplast protein transport factor	1.333	0.333	0.000	-0.048	-0.550	-0.110	N/A	N/A
242620084		30S ribosomal protein S14	0.000	0.667	1.000	-0.150	-0.410	-0.330	0.000	0.667
323446340	68788	AMP-dependent synthetase and ligase	1.000	0.667	0.333	-0.270	-0.570	-0.360	3.000	2.000
242620063		30S ribosomal protein S9	0.000	1.000	1.000	-0.150	-0.570	-0.190	0.000	1.000
323450284	4661	Aldose 1-epimerase	0.333	0.667	0.667	-0.550	-0.620	-0.610	0.500	1.000
323456303	52378	Glutaminyl-tRNA synthetase	0.333	1.000	0.333	-0.720	-0.380	-0.440	1.000	3.000
323449383	54714	Ribosomal protein	0.000	1.333	0.667	-0.280	-0.430	-0.110	0.000	2.000
323450814	28676	Ubiquitin-activating enzyme	0.333	1.000	0.000	-0.470	-0.160	-0.440	N/A	N/A
323448551	32534	Prolyl-tRNA synthetase	0.667	0.333	0.333	-0.450	-0.700	-0.390	2.000	1.000
323453669	23934	Sodium dependent transporter	0.333	1.000	0.000	-0.470	-0.160	-0.440	N/A	N/A
323452581	26043	Chaperonin	0.000	1.667	0.000	-1.000	-0.048	-0.064	N/A	N/A
323454658	23725	Cytochrome precurser	2.333	0.000	11.000	0.000	0.000	-0.170	0.212	0.000
323451614	71803	Insulinase-like, Mitochondrial substrate carrier	0.000	0.000	1.333	-0.080	-0.043	-1.000	0.000	0.000
323450997	28593	LMP7-like protein	0.000	0.000	1.333	-0.080	-0.043	-1.000	0.000	0.000
323449787	72138	Hedgehog protein	1.333	0.000	0.000	-0.048	-1.000	-0.032	N/A	N/A
323447426	39368	Isoleucine trna synthetase	0.667	1.000	0.000	-0.220	-0.160	-0.640	N/A	N/A
323449971	30237	Phypo stress protein	0.667	1.000	0.000	-0.220	-0.160	-0.640	N/A	N/A
323449093	3405	Protein kinase	0.333	1.000	0.333	-0.720	-0.380	-0.440	1.000	3.000
323455262	11148	tRNA synthetases	0.333	0.333	1.000	-0.360	-0.250	-0.670	0.333	0.333
323455416	52464	Geranylgeranyl diphosphate synthase	0.667	0.333	0.667	-0.640	-0.430	-0.390	1.000	0.500
323454215	71160	Hypothetical protein	0.333	1.333	0.000	-0.470	-0.089	-0.300	N/A	N/A
323448527	67169	Protein phosphatase, ankyrin	0.333	1.333	0.000	-0.470	-0.089	-0.300	N/A	N/A
323454082	52773	Ribosomal Protein	0.000	1.000	0.667	-0.280	-0.590	-0.190	0.000	1.500
323450170	65948	Hypothetical protein	0.333	0.667	0.667	-0.550	-0.620	-0.610	0.500	1.000
323450794	54097	Ubiquitin-activating enzyme	0.000	1.000	0.333	-0.530	-0.380	-0.190	0.000	3.000
323453528	62976	WW/Rsp5/WWP	0.000	1.000	0.333	-0.530	-0.380	-0.190	0.000	3.000
323448800	70381	ATP-dependent RNA helicase	0.000	1.333	0.000	-1.000	-0.089	-0.110	N/A	N/A
323449569	70314	Coatomer WD associated region	1.000	0.333	0.000	-0.100	-0.550	-0.210	N/A	N/A
323448946	31792	Anthranilate phosphoribosyltransferase	0.667	0.000	0.000	-0.220	-1.000	-0.180	N/A	N/A
323452026	59047	Alcohol dehydrogenase	1.667	0.000	0.000	-0.023	-1.000	-0.014	N/A	N/A
323451541	6384	Ras small GTPase	0.000	1.667	0.000	-1.000	-0.048	-0.064	N/A	N/A
323448259	60333	Mitochondrial carrier protein	1.333	0.333	0.000	-0.048	-0.550	-0.110	N/A	N/A
323457329	19506	Proteasome non-ATPase regulatory subunit	0.000	1.333	0.000	-1.000	-0.089	-0.110	N/A	N/A
323454107	36667	Tyrosine protein kinase	0.000	1.000	0.000	-1.000	-0.160	-0.190	N/A	N/A
323447825	39241	MCM	0.000	1.000	0.000	-1.000	-0.160	-0.190	N/A	N/A
323451030	2169	DEAD/DEAH box helicase domain-containing protein	1.333	0.000	0.000	-0.048	-1.000	-0.032	N/A	N/A
323453797	63307	Chloroplast Chaperonin	1.000	0.000	0.333	-0.270	-0.450	-0.076	3.000	0.000
323452541	78110	Selenoprotein	0.000	0.000	1.333	-0.080	-0.043	-1.000	0.000	0.000
323446199	68863	Cell wall surface anchor protein	0.000	0.000	2.000	-0.190	-0.037	-0.390	0.000	0.000
323450033	54443	Acyl-CoA synthetase	0.333	0.333	0.667	-0.550	-0.430	-0.670	0.500	0.500
323447566	59628	Phosphoglucomutase	1.000	0.333	0.000	-0.100	-0.550	-0.210	N/A	N/A
323455362	21520	Ribose-phosphate pyrophosphokinase	0.333	1.000	0.000	-0.470	-0.160	-0.440	N/A	N/A
323452894	63896	Contain SPX, N-terminal	1.000	0.333	0.000	-0.100	-0.550	-0.210	N/A	N/A
323454860	62184	Predicted membrane protein	0.000	0.333	1.000	-0.150	-0.250	-0.580	0.000	0.333
323450018	72128	Inorganic pyrophosphatase	1.000	0.333	0.000	-0.100	-0.550	-0.210	N/A	N/A
323451609	37770	Alanine transaminase	0.667	0.667	0.000	-0.220	-0.300	-0.560	N/A	N/A
323454420	58861	Phosphoglycerate kinase	1.000	1.000	0.000	-0.100	-0.160	-0.500	N/A	N/A
323456665	70491	RNA binding region	0.000	1.333	0.000	-1.000	-0.089	-0.110	N/A	N/A
323454572	52868	Acyltransferase region, Thioestarase	0.667	0.000	0.333	-0.450	-0.450	-0.180	2.000	0.000
323452696	26083	Methylmalonate-semialdehyde dehydrogenase	0.000	0.667	0.333	-0.530	-0.570	-0.330	0.000	2.000
323447245	34382	Monooxygenase	0.333	0.000	0.667	-0.550	-0.210	-0.420	0.500	0.000
323452117	59057	Delta 1-pyrroline-5-carboxylate reductase (P5CR)	0.000	1.000	0.000	-1.000	-0.160	-0.190	N/A	N/A

323455706	550	AAA ATPase	0.000	1.333	0.667	-0.080	-0.610	-0.064	0.000	2.000
323456297	70759	Aldehyde dehydrogenase	0.000	1.000	0.000	-1.000	-0.160	-0.190	N/A	N/A
323446517	72838	Vacuolar sorting receptor protein	0.000	0.000	1.000	-0.150	-0.094	-1.000	0.000	0.000
323453809	24439	Phosphoglucomutase	0.000	0.000	1.000	-0.150	-0.094	-1.000	0.000	0.000
323446697	60388	3-hydroxyacyl-CoA dehydrogenase	0.000	1.000	0.000	-1.000	-0.160	-0.190	N/A	N/A
323449869	70285	Tryptophanyl-tRNA synthetase	0.000	1.000	0.000	-1.000	-0.160	-0.190	N/A	N/A
323450473	72024	Calcium-binding EF hand	0.667	0.667	0.000	-0.220	-0.300	-0.560	N/A	N/A
323447373	59650	Deoxyxylulose-5-phosphate synthase	0.667	0.000	0.000	-0.220	-1.000	-0.180	N/A	N/A
323447574	67977	Dynein heavy chain, AAA ATPase	0.000	0.667	0.000	-1.000	-0.300	-0.330	N/A	N/A
323456247	58667	Skp-1 component	0.000	0.000	1.000	-0.150	-0.094	-1.000	0.000	0.000
323446558	35012	Ribosomal protein	0.000	0.000	1.333	-0.080	-0.043	-1.000	0.000	0.000
323447255	59665	N-Acetyl-L-glutamate kinase	0.000	1.000	0.000	-1.000	-0.160	-0.190	N/A	N/A
323447748	39278	AAA ATPase	0.000	0.667	0.000	-1.000	-0.300	-0.330	N/A	N/A
323453862	71360	Ubiquitin-protein ligase	0.333	0.667	0.000	-0.470	-0.300	-0.610	N/A	N/A
323450178	65936	Ankyrin	1.000	0.000	0.000	-0.100	-1.000	-0.076	N/A	N/A
323448917	31918	Eukaryotic initiation factor 3	0.333	0.667	0.000	-0.470	-0.300	-0.610	N/A	N/A
323455074	71075	Hypothetical protein	1.000	0.000	0.000	-0.100	-1.000	-0.076	N/A	N/A
323451194	3292	ABC transporter	0.000	0.667	0.333	-0.530	-0.570	-0.330	0.000	2.000
323452072	26912	ATP-dependent RNA helicase DBP3	0.000	0.667	0.333	-0.530	-0.570	-0.330	0.000	2.000
323455685	61839	Pyridoxamine 5'-phosphate oxidase-related	0.333	0.667	0.000	-0.470	-0.300	-0.610	N/A	N/A
323452968	63783	Hypothetical protein	0.000	0.000	1.000	-0.150	-0.094	-1.000	0.000	0.000
323453349	71468	Hypothetical protein	0.000	0.333	0.667	-0.280	-0.430	-0.580	0.000	0.500
323455818	69665	Ras small GTPase	0.000	1.333	0.000	-0.220	-0.048	-0.370	N/A	N/A
323451436	65013	Ubiquitin thioesterase	0.667	0.333	0.000	-0.220	-0.550	-0.390	N/A	N/A
323457189	52028	Vacular sorting protein	0.000	1.000	0.000	-1.000	-0.160	-0.190	N/A	N/A
323456269	70763	Peptidase M, neutral zinc metallopeptidases, zinc-binding site	0.000	0.000	0.667	-0.280	-0.210	-1.000	0.000	0.000
323450302	29630	Acyl-CoA dehydrogenase	0.000	0.667	0.000	-1.000	-0.300	-0.330	N/A	N/A
323457348	35763	S/T protein phosphatase and/or metallophosphoesterase	0.000	0.000	0.667	-0.280	-0.210	-1.000	0.000	0.000
242620052		50S ribosomal protein L24	0.000	0.000	0.667	-0.280	-0.210	-1.000	0.000	0.000
242620048		30S ribosomal protein S3	0.000	0.667	0.000	-1.000	-0.300	-0.330	N/A	N/A
323448907	66948	Ion transport protein	0.000	0.000	0.667	-0.280	-0.210	-1.000	0.000	0.000
323448957	66859	Hypothetical protein	0.667	0.000	0.000	-0.220	-1.000	-0.180	N/A	N/A
323449154	66674	Peptide synthetase	0.667	0.000	0.000	-0.220	-1.000	-0.180	N/A	N/A
323449633	30762	SNF2-related helicase, C-terminal	0.667	0.000	0.000	-0.220	-1.000	-0.180	N/A	N/A
323449944	66042	Mucin-associated surface protein (MASP)	0.000	0.000	0.667	-0.280	-0.210	-1.000	0.000	0.000
323450897	28631	ABC transporter	0.667	0.000	0.000	-0.220	-1.000	-0.180	N/A	N/A
323452907	71551	C2 domain containing protein	0.667	0.000	0.000	-0.220	-1.000	-0.180	N/A	N/A
323453109	37286	Cysteinyl-tRNA synthetase	0.667	0.000	0.000	-0.220	-1.000	-0.180	N/A	N/A
323454275	62732	Hypothetical protein	0.667	0.000	0.000	-0.220	-1.000	-0.180	N/A	N/A
323454523	58835	DNA primase	0.667	0.000	0.000	-0.220	-1.000	-0.180	N/A	N/A

[1]N/A means that the control condition had a value of zero and a fold-change could not be calculated.

Table S2) Proteins separated by cluster. Proteins listed in order of how they appear in Figure 2 from top to bottom.

Cluster	NCBI number	General call
A	323448531	Oxidoreductase
A	242620108	Photosystem I iron-sulfur center subunit VII
A	323449723	Photosystem 1 reaction center subunit
A	323449180	Mannosyltransferase
A	323450650	Phosphate ABC transporter permease
A	323451149	20S proteasome, A and B subunits
A	323452672	Hypothetical protein
A	323447987	Pyridoxal-5'-phosphate-dependent enzyme, beta subunit
A	323446737	Acyl carrier protein
A	323447299	Histone
A	323455795	Hypotheical protein
A	323447058	Hypothetical protein
A	323452673	Hypothetical protein
A	323453613	Chloroplast Ribose 5-phosphate isomerase
A	323454658	Cytochrome precurser
A	323449776	Urease
A	323455948	Mucin-associated surface protein (MASP)
B	242620075	Cytochrome c550
B	323447679	Hypothetical
B	323456455	Ribosomal protein
B	323451614	Insulinase-like, Mitochondrial substrate carrier
B	323450997	LMP7-like protein
B	323451897	Nucleolar protein Nop56
B	323452541	Selenoprotein
B	323446558	Ribosomal protein
B	323449422	Luteovirus ORF6 protein
B	323446199	Cell wall surface anchor protein
B	323454954	Calmodulin
B	323447336	Cyanase
B	323452479	Selenoprotein
B	323455041	Glyceraldehyde-3-phosphate dehydrogenase
B	242620083	photosystem I P700 chlorophyll A apoprotein A2
B	242620069	photosystem II p680 chlorophyll A apoprotein (CP-47)
B	323445392	Mucin-2 precursor
B	323447968	Zn-finger, RING
B	323450079	Cysteine synthase
B	323448543	Enolase (phosphopyruvate dehydratase)
B	242620112	ATP synthase CF1 beta chain
B	323452124	Cytochrome
B	242620086	Ribulose-1,5-bisphosphate carboxylase/oxygenase large subunit [Aureococcus anophagefferens]
B	323447684	Cytochrome c6

B	323456364	Histone
B	323453682	Hypothetical protein
B	323449583	Ribosomal protein
B	323445193	Histone
B	242620087	Ribulose bisphosphate carboxlyase small chain
B	323451650	Chloroplast hydroxymethylbilane synthase
B	323451867	Selenoprotein
B	323451587	Ribosomal Protein
B	323452812	Dihydrolipoamide dehydrogenase
B	323456630	Heparan Sulfate 2-0- sulfotranserase
B	323454341	Thioredoxin domain 2
B	323450925	Ribosomal protein
B	323448060	Ribosomal protein
B	323452552	Proteasome
B	242620051	50S ribosomal protein L14
B	323454406	Armet super family domain
B	323452815	Ribosomal protein L4/L1e
B	323451167	Ribosomal porotein
B	323452189	PT-repeat
B	323449769	Ribosomal protein
B	323449160	Proteasome
B	323445273	Proteasome
B	323457195	Ribosomal Protein
B	323451216	Ribosomal protein
B	323456180	Ribosomal protein L5
B	242620082	photosystem I P700 chlorophyll A apoprotein A1
B	323451387	20S proteasome, A and B subunits
B	323457240	Ammonium transporter
B	323453642	O-acetylhomoserine/O-acetylserine sulfhydrylase
B	323456600	Ribosomal protein L30, L7, Peptidase
B	323447579	Ribosomal protein
B	323448448	Nonphototropic hypocotyl
B	242620055	50S ribosomal protein L6
B	323450867	Acetamidase/Formamidase
C	323453007	Initiation factor
C	242620067	elongation factor Tu
C	323451553	Glutamine synthetase
C	323454637	Chaperonin ATPase
C	323455818	Ras small GTPase
C	323454310	Adenosine kinase
C	323454894	Formylglycineamide ribotide amidotransferase
C	323454033	Triosephosphate isomerase
C	323452581	Chaperonin
C	323451541	Ras small GTPase
D	323451419	Citrate synthase
D	323447741	Nonaspanin
D	242620028	30S ribosomal protein S2

D	323451948	Ribosomal protein
D	323453433	Nitrate reducatase
D	323448256	Nitrate transporter
D	323454388	Splicing factor
D	323453622	Phosphoserine aminotransferase
D	323451767	Hydroxyisobutyrate dehydrogenase
D	242620053	50S ribosomal protein L5
D	323453434	Nitrite reductase
D	323457185	Adaptin
D	323449674	Peptidase
D	323450465	Ribosomal protein L18
D	323455979	ATPase
D	323451117	Ribosomal protein
D	323450214	Ribosomal protein
D	323448815	Ribosomal Protein
D	242620043	50S ribosomal protein L3
D	323448850	Ribosomal protein
D	323453856	Ribosomal protein L6E
D	323452746	Ribosomal protein
D	323456525	ATP synthase
D	242620044	50S ribosomal protein L23
D	323453262	Serine/threonine-protein kinase
D	323450970	Ribosomal protein
D	323454706	Ribonucleoprotein complex subunit
D	323448873	Ribosomal protein
D	323449333	Ribosomal protein
D	323452337	Phosphate ABC transporter
D	323446694	Ribosomal protein
D	323451627	Na+/H+ antiporter NhaA
D	323448266	Histone
D	242620095	30S ribosomal protein S4
D	323447782	Histone
D	323450569	Ribosomal protein
D	323452089	IMP dehydrogenase/GMP reductase
D	323452301	Ribosomal protein
D	242620034	ATP synthase CF1 alpha chain
D	323449640	Ribosomal protein
D	323454360	Ribosomal protein
D	323449038	Peptidase
D	323454189	Ribosomal protein
D	323451135	Proteasome
D	323448884	Proteasome
D	323456545	Ribosomal protein
D	323455169	Ribosomal protein
D	323453239	Proliferating cell nuclear antigen, PCNA
D	323449899	Ribosomal protein
D	323451317	G-protein beta WD-40 repeat (Guanine nucleotide-binding protein)

D	323452787	Ribosomal protein
D	323454110	Ribosomal protein
D	323451373	Ribosomal protein
D	323457181	Ribosomal protein
D	323445949	Ribosomal protein
D	323450083	Ribosomal protein
D	323449973	Proteasome
D	323454832	TPR repeat containing protein
D	323449711	Heat shock protein
D	323455903	Ribosomal protein
D	323450361	Triosephosphate isomerase
D	323454381	Cystathione gamma lyase
D	323447119	Ribosomal protein
D	323449261	Ribosomal protein
D	323448136	Elongation factor
D	323450976	Ribosomal protein
D	323455964	Ribosomal protein
D	323452338	Helicase and restriction enzyme domain
D	323451781	Urea transporter
D	242620045	50S ribosomal protein L2
D	323454820	Chloroplast light harvesting protein
D	323451071	Ribosomal protein
D	323450320	Ribosomal protein
D	323450621	Ribosomal protein
D	323450747	Ribosomal Protein
D	242620066	30S ribosomal protein S7
D	323454039	Translation elongation factor
D	323447664	Protein kinase
D	323455547	Calreticulin precursor, calnexin
D	323456325	Phosphatase
E	323447982	Peptidyl-prolyl cis-trans isomerase
E	323456174	Translational activator
E	323456061	Calcium transporting ATpase
E	323452930	ABC transporter
E	323453726	Chaperonin ATPase
E	323448756	RNA binding protein
E	323452597	AMP-dependent synthetase and ligase
E	323456332	Heat shock protein (Hsp 70)
E	323454696	Tetrahydrofolate dehydrogenase/cyclohydrolase
E	323455687	HMG1/2 (high mobility group) box, Amino acid/polyamine transporter II, Transcription elongation factor S-II, N-terminal
E	323455637	RAN function family member - supported with BLASTp
E	323448025	Tubulin alpha-2 chain
E	323453579	Phosphoglycerate kinase
E	323450901	Actin
E	323453684	H+-transporting two-sector ATPase
E	323456170	Adenosylhomocysteinase

E	323449174	Sulfolipid biosynthesis protein
E	242620037	Hsp70-type chaperone
E	323450445	Co or Mg Chelatase
E	323449760	Glycine cleavage system
E	323457021	Hypothetical
E	323455001	Fructose bisphosphate aldolase
E	323450237	ATP synthase
F	323448914	Malate dehydrogenase
F	323451863	Aspartate/other aminotransferase
F	323452158	Chloroplast light harvesting protein
F	323450616	Pyruvate carboxylase
F	323453694	Glutamate synthase
F	323454769	Nucleoside diphosphate kinase
F	323447110	Triosephosphate isomerase
F	323454246	UDP-glucose 6-dehydrogenase
F	323448027	Chloroplast light harvesting protein
F	323456110	Pyruvate carboxylase
F	323456329	Glutamate-1-semialdehyde aminotransferase
F	323454183	Amino transferase class-I and II
F	323456125	Chloroplast light harvesting protein
F	323448510	S-adenosylmethionine synthetase
F	323455294	ABC transporter
F	323449032	Glyceraldehyde-3-phosphate dehydrogenase
F	323451615	Methionyl / Aminoacyl-tRNA synthetase
F	323452169	Hypothetical protein
F	323451363	Phospholipid/glycerol acyltransferase
F	323450518	Rieske protein (Iron sulfur protein)
F	323455519	Helicase
F	323456379	Carbamoyl-phosphate synthase
F	323450260	Inorganic pyrophosphatase
F	323454570	Hypothetical protein
F	242620089	Conserved hypothetical plastid protein Ycf39
F	323455382	Dynein heavy chain, AAA ATPase
F	323447220	Hypothetical protein
F	323450953	Epsilon1-COP
F	323450958	Peptidase
F	323453338	Acetyl-coenzyme A synthetase
F	323452318	Myosin head, motor region
F	323448097	Chloroplast light harvesting protein
F	323452847	UTP--glucose-1-phosphate uridylyltransferase
F	323456741	Mitochondrial substrate carrier
F	323454181	Zinc-containing alcohol dehydrogenase superfamily
F	323454770	Calreticulin/calnexin
F	323453907	Enolase (phosphopyruvate dehydratase)
F	323454760	Inorganic phosphate transporter
F	323450330	ABC transporter
F	323457264	Nicotinamide nucleotide transhydrogenase

F	323450268	Flavin-containing monooxygenase-like
F	323456208	Synaptobrevin
F	323446732	Hypothetical protein
F	323452005	Chloroplast light harvesting protein
F	323451260	Cobalamin synthesis protein
F	323452273	Hypotheical protein
F	323452383	Ribose-phosphate pyrophosphokinase
F	323457207	Chloroplast light harvesting protein
F	323454417	Beta-ketoacyl ACP synthase
F	323456109	ATPase
F	323455642	5'-nucleotidase
F	323453090	Aconitate hydratase
F	323449755	Amino transferase class-III
F	323450876	Pyruvate kinase
F	323451378	Sterol methyltransferase
F	323452833	CAP protein
F	323448862	Carbamoyl-phosphate synthase, Carboxyl transferase, Biotin carboxylase, Biotin/lipoyl attachment
F	323452848	Phosphoglucomutase
F	323447335	Formate/nitrite transporter
F	323452898	Glutamate dehydrogenase
F	323454682	GDP dissociation protein
F	323450582	Transketolase
F	323454473	Iron-dependent fumarate hydratase, Fe-S type hydro-lyases tartrate/fumarate
F	323456351	Chloroplast light harvesting protein
F	323455486	Clathrin vesicle coat
F	323451977	GDP-mannose 3,5-epimerase
F	323453524	Glutathion transferase
F	323456872	FAD linked oxidase, N-terminal
F	323456684	3-hydroxyacyl-CoA dehydrogenase
F	323448823	Adenylylsulfate kinase
F	323455708	Cell division protein FtsH
F	323448789	GUN4 like domain
F	323454031	Chloroplast light harvesting protein
F	323450235	Ttubulin beta chain
F	323450497	Serine/threonine-protein phosphatase
F	323453325	Phosphoenolpyruvate carboxylase
F	323450177	Ras small GTPase
F	323449109	Low molecular weight phosphotyrosine protein phosphatase
F	323451061	Histidine kinase
F	323453590	ATPase
F	323456607	Aminotransferase
F	323453164	N-ethylmaleimide sensitive fusion protein
F	323450905	Endonuclease/exonuclease/phosphatase
F	323449461	Chloroplast light harvesting protein
F	323457297	Myosin
F	323449672	Chloroplast light harvesting protein

F	323453547	Prohibitin
F	323449390	Exportin
F	323452472	Chloroplast light harvesting protein
F	323451357	Rab family GTPase
F	323449750	Chloroplast light harvesting protein
F	323454677	IspG protein, diphosphate synthetase
F	323456737	Inorganic phosphate transporter
F	323450398	Plastidic triose-phosphate/phosphate translocator
F	323457284	Mucin-associated surface protein
F	323457115	Chloroplast precursor CbxX/CfqX
F	323455682	Phosphoglucose isomerase
F	323456836	Hypothetical protein
F	323454315	Chloroplast light harvesting protein
F	323455675	Chloroplast light harvesting protein
F	323457045	Cobalmin synthesis protein/P47K like
F	323455983	Flavin containing monooxygenase 5
F	323454125	ABC transporter
F	323454580	Glutathione peroxidase
G	323453409	Diaminopimelate epimerase
G	323448492	Chloroplast photosystem II 12 kDa extrinsic protein
G	323455645	Hypothetical protein, no significant BLAST
G	323453799	Pyruvate kinase
G	323450333	Isocitrate dehydrogenase NADP-dependent
G	323454939	Chloroplast light harvesting protein
G	323449474	Semialdehyde dehydrogenase
G	323455998	Alkaline phosphatase
G	323452393	OmpA/MotB domain-containing protein
G	323456271	Chloroplast light harvesting protein
G	323453816	Chloroplast light harvesting protein
G	323448051	Chloroplast light harvesting protein
G	323451463	SecA-type chloroplast protein transport factor
G	323448259	Mitochondrial carrier protein
G	323449871	HMG-CoA lyase-like, Alpha-isopropylmalate/homocitrate synthase
G	323455015	Cycloartenol-C24-methyltransferase
G	242620040	Photosystem II 44 kDa apoprotein (P6)
G	323452748	TB2/DP1/HVA22 related protein
G	242620099	Cytochrome b6
H	323452454	Xanthine dehydrogenase
H	323454481	Sulfate adenylyltransferase
H	323452026	Alcohol dehydrogenase
H	323451404	Tyrosinase, Phytanoyl-CoA dioxygenase
H	323450718	Photosystem II stability/assembly factor
H	323451030	DEAD/DEAH box helicase domain-containing protein
H	323449787	Hedgehog protein

Table S3) Proteins and associated transcript data (SAGE tag counts).

NCBI number	General call	Mean of spectral counts		SAGE tag counts (normalized to library size)		Fold change relaive to control	
		Control	-P	Control	-P	Protein	Transcript
323455041	Glyceraldehyde-3-phosphate dehydrogenase	138.33	61.67	5.62E-05	4.09E-05	-2.24	-1.37
323447300	Histone	52.67	39.67	8.43E-05	4.09E-05	-1.33	-2.06
323453579	Phosphoglycerate kinase	27.00	37.67	5.62E-05	4.09E-05	1.40	-1.37
323456332	Heat shock protein (Hsp 70)	19.67	25.00	5.62E-05	4.09E-05	1.27	-1.37
323454637	Chaperonin ATPase	19.67	19.00	1.15E-03	2.13E-03	-1.04	1.85
323448984	Ferredoxin NADP reductase	22.67	21.67	2.81E-05	4.09E-05	-1.05	1.46
323457021	Hypothetical	16.33	21.00	8.43E-05	8.18E-05	1.29	-1.03
323456989	Fructose bisphosphate aldolase	18.00	16.00	5.34E-04	1.64E-04	-1.13	-3.26
323449461	Chloroplast light harvesting protein	12.00	24.00	3.94E-04	4.91E-04	2.00	1.25
323450901	Actin	10.67	17.67	2.81E-05	8.18E-05	1.66	2.91
323455179	Peptidyl-prolyl cis-trans isomerase	14.00	15.67	2.81E-03	1.64E-03	1.12	-1.72
323455979	ATPase	17.67	5.33	1.12E-04	1.23E-04	-3.31	1.09
323455486	Clathrin vesicle coat	1.00	16.67	4.22E-04	9.41E-04	16.67	2.23
323452189	PT-repeat	17.33	8.33	1.12E-04	4.09E-04	-2.08	3.64
323455687	HMG1/2 (high mobility group) box, Amino acid/polyamine transporter II, Transcription elongation factor S-II, N-terminal	7.00	11.00	3.37E-04	3.27E-04	1.57	-1.03
323447336	Cyanase	18.00	9.67	1.97E-04	4.91E-04	-1.86	2.50
323454769	Nucleoside diphosphate kinase	8.67	13.67	2.81E-04	1.39E-03	1.58	4.95
323454760	Inorganic phosphate transporter	0.33	19.67	3.94E-04	2.25E-03	59.00	5.72
323449723	Photosystem 1 reaction center subunit	14.00	14.00	8.43E-05	8.18E-05	-1.00	-1.03
323448531	Oxidoreductase	13.33	15.33	8.43E-05	4.09E-05	1.15	-2.06
323454939	Chloroplast light harvesting protein	9.33	14.67	8.43E-05	4.09E-04	1.57	4.85
323448051	Chloroplast light harvesting protein	8.00	13.00	2.81E-05	8.18E-05	1.63	2.91
323453090	Aconitate hydratase	5.33	12.67	1.12E-04	4.09E-05	2.38	-2.75
323446473	Expressed protein	13.00	8.67	1.12E-04	4.09E-04	-1.50	3.64
323447782	Histone	9.00	4.33	6.18E-04	8.18E-04	-2.08	1.32
323451957	Rieske protein (Iron sulfur protein), Chloroplast light harvesting protein	7.67	7.33	3.37E-04	6.14E-04	-1.05	1.82
323451317	G-protein beta WD-40 repeat (Guanine nucleotide-binding protein)	15.67	1.33	2.53E-04	8.18E-05	-11.75	-3.09

323453907	Enolase (phosphopyruvate dehydratase)	7.33	10.67	1.97E-04	2.86E-04	1.45	1.46
323453726	Chaperonin ATPase	5.67	8.00	2.81E-05	4.09E-05	1.41	1.46
323455658	Oxygen-evolving enhancer 1	7.00	9.33	2.81E-05	4.09E-05	1.33	1.46
323453500	ADP-ribosylation factor	9.00	7.67	9.56E-04	4.91E-04	-1.17	-1.95
323450172	Peptidase	7.67	6.00	1.97E-04	2.05E-04	-1.28	1.04
323453642	O-acetylhomoserine/O-acetylserine sulfhydrylase	12.67	5.00	5.62E-05	4.09E-05	-2.53	-1.37
323450799	Kringle, PT-repeat, Serine/threonine dehydratase	10.33	6.00	2.81E-05	4.09E-05	-1.72	1.46
323452158	Chloroplast light harvesting protein	4.00	9.33	9.56E-04	4.91E-04	2.33	-1.95
323445392	Mucin-2 precursor	13.33	6.33	4.22E-04	6.55E-04	-2.11	1.55
323454246	UDP-glucose 6-dehydrogenase	2.33	8.33	8.43E-05	1.23E-04	3.57	1.46
323456872	FAD linked oxidase, N-terminal	2.00	10.33	1.69E-04	3.68E-04	5.17	2.18
323454481	Sulfate adenylyltransferase	5.67	13.00	8.43E-05	4.09E-05	2.29	-2.06
323457207	Chloroplast light harvesting protein	5.33	10.00	5.62E-05	3.27E-04	1.88	5.82
323451419	Citrate synthase	7.33	3.33	2.81E-05	4.09E-05	-2.20	1.46
323446545	Chloroplast light harvesting protein	12.33	10.00	1.41E-04	2.05E-04	-1.23	1.46
323447358	Chloroplast light harvesting protein	7.67	5.33	1.41E-04	2.05E-04	-1.44	1.46
323454334	Chloroplast light harvesting protein	6.00	7.67	2.53E-04	2.86E-04	1.28	1.13
323447744	Chloroplast light harvesting protein	6.33	7.67	8.43E-05	1.23E-04	1.21	1.46
323450268	Flavin-containing monooxygenase-like	0.33	12.33	5.90E-04	1.84E-03	37.00	3.12
323455568	Chloroplast light harvesting protein	6.33	8.00	3.09E-04	4.91E-04	1.26	1.59
323455382	Dynein heavy chain, AAA ATPase	4.33	7.33	1.41E-04	2.86E-04	1.69	2.04
323454019	Chloroplast light harvesting protein	5.33	6.33	2.53E-04	1.10E-03	1.19	4.37
323453856	Ribosomal protein L6E	10.00	1.67	1.69E-04	4.09E-05	-6.00	-4.12
323456180	Ribosomal protein L5	14.00	2.33	4.22E-04	4.91E-04	-6.00	1.16
323453541	Pyruvate kinase	5.67	6.33	2.81E-05	1.23E-04	1.12	4.37
323452454	Xanthine dehydrogenase	5.67	11.00	8.43E-05	4.09E-05	1.94	-2.06
323450616	Pyruvate carboxylase	2.67	7.67	5.62E-05	4.09E-05	2.87	-1.37
323450905	Endonuclease/exonuclease/phosphatase	2.67	11.00	5.62E-05	4.09E-05	4.12	-1.37
323452472	Chloroplast light harvesting protein	4.00	10.33	5.62E-05	3.68E-04	2.58	6.55
323454267	Inositol phosphatase	5.33	7.33	5.62E-05	4.09E-05	1.38	-1.37
323456271	Chloroplast light harvesting protein	4.00	10.00	1.12E-04	1.23E-04	2.50	1.09
323449755	Amino transferase class-III	0.33	10.00	1.69E-04	5.32E-04	30.00	3.15

323454635	Chloroplast 3-oxoacyl-[acyl-carrier protein] reductase orecursor	7.33	4.67	8.43E-05	4.09E-05	-1.57	-2.06
323449750	Chloroplast light harvesting protein	4.67	8.33	1.41E-04	2.45E-04	1.79	1.75
323454622	Ubiquitin	8.33	4.33	2.25E-04	8.18E-05	-1.92	-2.75
323452479	Selenoprotein	8.33	5.33	8.43E-04	1.19E-03	-1.56	1.41
323453956	Chloroplast light harvesting protein	4.67	6.00	1.35E-03	1.55E-03	1.29	1.15
323451749	Calcium-binding EF-hand, Pleckstrin-like, LMBR1-like conserved region	6.00	6.33	2.81E-05	4.09E-05	1.06	1.46
323450447	Chloroplast light harvesting protein	5.33	6.33	5.62E-05	8.18E-05	1.19	1.46
323455169	Ribosomal protein	9.33	0.67	1.43E-03	6.14E-04	-14.00	-2.34
323450465	Ribosomal protein L18	7.00	1.67	8.43E-05	1.23E-04	-4.20	1.46
323457181	Ribosomal protein	9.67	0.33	3.09E-04	2.45E-04	-29.00	-1.26
323450876	Pyruvate kinase	1.00	7.67	5.62E-05	8.18E-05	7.67	1.46
323451948	Ribosomal protein	5.67	3.00	2.81E-05	8.18E-05	-1.89	2.91
323454655	Chloroplast light harvesting protein	4.00	6.00	1.12E-04	2.05E-04	1.50	1.82
323454039	Translation elongation factor	6.67	2.67	9.56E-04	4.09E-04	-2.50	-2.34
323450925	Ribosomal protein	8.33	1.00	1.41E-03	8.59E-04	-8.33	-1.64
323450518	Rieske protein (Iron sulfur protein)	2.33	6.00	3.65E-04	1.64E-04	2.57	-2.23
323451117	Ribosomal protein	6.00	2.00	1.88E-03	1.02E-03	-3.00	-1.84
323447987	Pyridoxal-5'-phosphate-dependent enzyme, beta subunit	6.67	4.67	2.81E-05	8.18E-05	-1.43	2.91
323453146	Chloroplast light harvesting protein	5.67	5.33	2.81E-05	1.23E-04	-1.06	4.37
323456741	Mitochondrial substrate carrier	0.67	6.00	1.69E-04	2.86E-04	9.00	1.70
323455317	Inorganic pyrophosphatase	4.33	5.33	1.12E-04	4.09E-05	1.23	-2.75
323449640	Ribosomal protein	6.33	1.00	3.09E-04	2.45E-04	-6.33	-1.26
323456110	Pyruvate carboxylase	1.67	4.33	2.81E-05	4.09E-05	2.60	1.46
323455642	5'-nucleotidase	0.33	6.00	3.65E-04	2.41E-03	18.00	6.61
323453007	Initiation factor	3.33	2.33	1.41E-04	4.09E-05	-1.43	-3.43
323453325	Phosphoenolpyruvate carboxylase	0.67	5.33	5.62E-05	4.09E-05	8.00	-1.37
323450330	ABC transporter	0.33	7.00	1.97E-04	2.45E-04	21.00	1.25
323456061	Calcium transporting ATpase	1.67	2.67	5.34E-04	9.00E-04	1.60	1.69
323455294	ABC transporter	1.00	4.00	1.12E-04	6.96E-04	4.00	6.19
323448025	Tubulin alpha-2 chain	1.00	3.67	1.97E-04	1.23E-04	3.67	-1.60
323455059	Dihydrolipoamide S-acetyltransferase	3.33	4.33	1.41E-04	4.09E-05	1.30	-3.43
323447119	Ribosomal protein	5.33	0.33	5.62E-04	4.50E-04	-16.00	-1.25
323447711	Heat shock protein Hsp90	3.33	4.00	2.81E-04	8.18E-05	1.20	-3.43
323454985	Histidinol dehydrogenase	4.33	2.33	2.25E-04	8.18E-05	-1.86	-2.75

323450867	Acetamidase/Formamidase	5.67	2.00	1.97E-04	4.09E-05	-2.83	-4.81
323457045	Cobalmin synthesis protein/P47K like	1.33	4.67	5.90E-04	5.73E-04	3.50	-1.03
323451977	GDP-mannose 3,5-epimerase	0.33	4.33	3.37E-04	6.96E-04	13.00	2.06
323452597	AMP-dependent synthetase and ligase	2.00	3.00	5.62E-05	4.09E-05	1.50	-1.37
323450333	Isocitrate dehydrogenase NADP-dependent	1.33	7.00	3.94E-04	2.45E-04	5.25	-1.60
323452437	Dihydrolipoamide dehydrogenase	3.67	3.00	3.94E-04	6.14E-04	-1.22	1.56
323448256	Nitrate transporter	1.33	0.33	3.37E-04	4.09E-05	-4.00	-8.24
323455645	Hypothetical protein, no significant BLAST	2.33	5.67	2.25E-04	3.68E-04	2.43	1.64
323454364	Serine hydroxymethyltransferase	1.67	3.00	1.41E-04	8.18E-05	1.80	-1.72
323453341	Tryptophan synthase	2.33	3.00	5.62E-05	4.09E-05	1.29	-1.37
323448626	Elongation factor	2.33	2.67	6.18E-04	6.14E-04	1.14	-1.01
323456516	Enoyl-acyl carrier	2.00	3.33	1.97E-04	4.09E-05	1.67	-4.81
323449254	Carbamoyl-phosphate synthase	1.67	2.00	2.81E-05	1.23E-04	1.20	4.37
323448815	Ribosomal Protein	7.00	0.33	8.43E-05	8.18E-05	-21.00	-1.03
323451587	Ribosomal Protein	6.67	0.33	3.37E-04	1.64E-04	-20.00	-2.06
323446694	Ribosomal protein	3.67	1.00	5.90E-04	3.68E-04	-3.67	-1.60
323455547	Calreticulin precursor, calnexin	4.00	1.00	2.81E-05	1.23E-04	-4.00	4.37
323450079	Cysteine synthase	4.67	1.67	2.25E-04	1.23E-04	-2.80	-1.83
323454033	Triosephosphate isomerase	1.33	1.33	8.43E-05	4.09E-05	1.00	-2.06
323451116	Aliphatic amidase	3.67	2.33	6.18E-04	4.50E-04	-1.57	-1.37
323453409	Diaminopimelate epimerase	1.00	4.67	3.37E-04	2.05E-04	4.67	-1.65
323453165	Ras GTPase	1.33	3.00	1.69E-04	1.23E-04	2.25	-1.37
323451373	Ribosomal protein	3.67	0.67	3.37E-04	8.18E-05	-5.50	-4.12
323454382	20S proteasome	2.67	1.67	6.46E-04	5.32E-04	-1.60	-1.22
323450585	Phosphoglycerate/bisphospho glycerate mutase	2.33	2.67	1.69E-04	1.23E-04	1.14	-1.37
323456684	3-hydroxyacyl-CoA dehydrogenase	0.33	3.00	1.12E-04	4.09E-05	9.00	-2.75
323455682	Phosphoglucose isomerase	0.33	3.67	5.62E-05	1.23E-04	11.00	2.18
323446737	Acyl carrier protein	4.00	2.00	5.62E-05	4.09E-05	-2.00	-1.37
323457240	Ammonium transporter	4.00	1.00	5.62E-05	4.09E-05	-4.00	-1.37
323454160	Peptidase	2.00	1.33	5.59E-03	9.21E-03	-1.50	1.65
323452383	Ribose-phosphate pyrophosphokinase	0.33	3.67	1.12E-04	8.18E-05	11.00	-1.37
323448438	RNA binding protein	3.00	1.33	8.71E-04	3.27E-04	-2.25	-2.66
323454510	Proteasome	3.00	2.67	7.59E-04	4.91E-04	-1.12	-1.55
323452898	Glutamate dehydrogenase	0.33	3.00	1.69E-04	4.09E-05	9.00	-4.12
323451071	Ribosomal protein	3.33	0.33	2.81E-05	8.18E-05	-10.00	2.91
323450177	Ras small GTPase	0.33	2.67	3.37E-04	2.45E-04	8.00	-1.37
323449160	Proteasome	5.00	0.33	7.87E-04	8.59E-04	-15.00	1.09

323454354	Ormate nitrite transporter	2.33	2.00	3.09E-04	4.91E-04	-1.17	1.59
323450131	Xanthine/uracil/vitamin C permease	1.67	2.33	2.81E-05	4.09E-05	1.40	1.46
323452963	Light inducinble protein	1.33	2.33	6.18E-04	5.32E-04	1.75	-1.16
323449422	Luteovirus ORF6 protein	3.33	1.33	5.62E-05	1.23E-04	-2.50	2.18
323455449	Ribosomal protein	2.67	1.00	2.53E-04	2.86E-04	-2.67	1.13
323451675	Hypothetical protein	1.67	2.00	8.43E-05	4.09E-05	1.20	-2.06
323452748	TB2/DP1/HVA22 related protein	1.00	3.00	7.03E-04	3.27E-04	3.00	-2.15
323453524	Glutathion transferase	0.33	2.33	1.41E-04	1.23E-04	7.00	-1.14
323454682	GDP dissociation protein	0.33	2.33	8.43E-05	8.18E-05	7.00	-1.03
323453963	Chloroplast light harvesting protein	1.67	2.00	2.81E-05	4.09E-05	1.20	1.46
323452943	Ribosomal protein	2.67	0.67	2.08E-03	1.02E-03	-4.00	-2.03
323455143	Ribosomal protein	3.00	0.67	5.62E-05	4.09E-05	-4.50	-1.37
323452812	Dihydrolipoamide dehydrogenase	5.00	0.33	1.12E-04	1.23E-04	-15.00	1.09
323448587	Adenylosuccinate synthetase	2.67	1.00	1.69E-04	2.45E-04	-2.67	1.46
323456068	Heat shock protein	1.67	1.00	8.43E-05	4.09E-05	-1.67	-2.06
323448447	Endopeptidase Clp activity	2.00	2.00	5.34E-04	3.68E-04	1.00	-1.45
323447335	Formate/nitrite transporter	0.33	2.00	4.78E-04	6.55E-04	6.00	1.37
323450320	Ribosomal protein	3.00	0.33	8.43E-05	1.64E-04	-9.00	1.94
323453003	Vesicle coat complex	1.67	1.67	5.62E-04	4.50E-04	1.00	-1.25
323453823	Brix domain	1.00	2.33	2.81E-05	4.09E-05	2.33	1.46
323453684	H+-transporting two-sector ATPase	0.67	1.67	7.59E-04	4.50E-04	2.50	-1.69
323448789	GUN4 like domain	0.33	2.33	2.25E-04	8.18E-05	7.00	-2.75
323453085	Calcium-binding EF-hand	1.00	1.00	2.81E-05	4.09E-05	1.00	1.46
323455637	RAN function family member - supported with BLASTp	0.33	1.33	3.09E-04	1.64E-04	4.00	-1.89
323454406	Armet super family domain	2.67	0.33	3.94E-04	3.27E-04	-8.00	-1.20
323454381	Cystathione gamma lyase	2.00	0.33	2.81E-05	1.64E-04	-6.00	5.82
323451378	Sterol methyltransferase	0.33	2.33	1.41E-04	1.23E-04	7.00	-1.14
323453289	BLASTp putative protein with GPS domain	1.33	0.67	2.81E-04	4.91E-04	-2.00	1.75
323450531	Calcium ATPase	1.33	1.33	2.81E-05	4.09E-05	1.00	1.46
323449845	Hypothetical protein	0.67	1.67	1.41E-04	1.64E-04	2.50	1.16
323450569	Ribosomal protein	3.00	0.33	2.53E-04	3.68E-04	-9.00	1.46
323452077	Ribosomal protein	2.33	0.33	5.90E-04	4.09E-04	-7.00	-1.44
323452089	IMP dehydrogenase/GMP reductase	3.00	0.33	2.81E-05	4.09E-05	-9.00	1.46
323452833	CAP protein	0.33	2.33	2.81E-04	2.45E-04	7.00	-1.14
323456017	CTP synthase	1.00	1.00	5.62E-05	4.09E-05	1.00	-1.37
323452600	Inorganic phosphate transporter	0.33	1.33	2.81E-05	4.09E-05	4.00	1.46
323447291	Phosphoglycerate mutase	0.67	2.00	1.97E-04	4.09E-05	3.00	-4.81
323447671	Ribosomal protein	2.33	0.67	3.09E-04	2.05E-04	-3.50	-1.51

323449776	Urease	2.33	1.33	5.62E-05	8.18E-05	-1.75	1.46
323453239	Proliferating cell nuclear antigen, PCNA	2.33	0.33	1.97E-04	4.09E-05	-7.00	-4.81
323452338	Helicase and restriction enzyme domain	1.67	0.33	8.43E-05	1.23E-04	-5.00	1.46
323455998	Alkaline phosphatase	0.33	4.33	3.37E-04	9.82E-04	13.00	2.91
323455705	Serine hydroxymethyltransferase	0.67	1.00	2.81E-05	1.23E-04	1.50	4.37
323456188	Heat shock protein	0.67	0.67	2.81E-05	8.18E-05	1.00	2.91
323456208	Synaptobrevin	0.33	2.33	1.97E-04	6.55E-04	7.00	3.33
323452846	Argininosuccinate synthase	0.67	1.33	1.12E-04	4.09E-05	2.00	-2.75
323449583	Ribosomal protein	3.33	0.33	1.97E-04	8.18E-05	-10.00	-2.40
323456496	AICARFT/IMPCHase bienzyme, Methylglyoxal synthase-like	0.67	1.00	1.97E-04	8.18E-05	1.50	-2.40
323454389	Translation initiaion factor	1.67	0.33	3.09E-04	8.18E-05	-5.00	-3.78
323455110	Uroporphyrinogen decarboxylase (URO-D)	0.67	2.00	1.12E-04	1.23E-04	3.00	1.09
323456121	Actin like protein	0.33	1.33	2.81E-04	2.05E-04	4.00	-1.37
323453700	Elongation factor	1.33	0.33	8.43E-05	4.09E-05	-4.00	-2.06
323453278	Oxoglutarate dehydrogenase	0.33	1.67	8.43E-05	1.64E-04	5.00	1.94
323454199	DnaJ homolog	0.67	0.67	8.43E-05	1.23E-04	1.00	1.46
323450083	Ribosomal protein	1.67	0.33	6.18E-04	2.86E-04	-5.00	-2.16
323452263	Peptidase / Proteasome	2.00	0.33	2.25E-04	4.09E-04	-6.00	1.82
323450948	Succinyl-CoA synthetase, ATP-citrate lyase/succinyl-CoA ligase, Succinyl-CoA synthetase, ATP-citrate lyase/succinyl-CoA ligase	1.67	0.67	2.81E-05	1.23E-04	-2.50	4.37
323451260	Cobalamin synthesis protein	0.33	2.00	2.81E-05	8.18E-05	6.00	2.91
323451909	ATP phosphoribosyltransferase	1.67	0.33	1.97E-04	8.18E-05	-5.00	-2.40
323448914	Malate dehydrogenase	0.33	0.67	1.38E-03	1.47E-03	2.00	1.07
323457289	Eukaryotic initiation factor 5A hypusine	0.67	1.00	7.03E-04	1.23E-04	1.50	-5.72
323448128	Peptidyl-prolyl cis-trans isomerase	0.67	1.33	1.12E-04	4.09E-05	2.00	-2.75
323447945	Phosphofructokinase	0.67	0.67	1.04E-03	9.00E-04	1.00	-1.16
323449674	Peptidase	1.00	0.33	2.25E-04	1.23E-04	-3.00	-1.83
323454473	Iron-dependent fumarate hydratase, Fe-S type hydro-lyases tartrate/fumarate	0.33	1.33	2.81E-05	1.23E-04	4.00	4.37
323449899	Ribosomal protein	2.00	0.33	8.43E-05	1.23E-04	-6.00	1.46
323456455	Ribosomal protein	2.33	0.33	1.97E-04	1.23E-04	-7.00	-1.60
323451287	Argininosuccinate lyase	0.33	1.00	5.62E-05	4.09E-05	3.00	-1.37
323453705	Ammonium transporter	2.33	0.67	5.62E-05	4.09E-05	-3.50	-1.37
323446944	Hypothetical protein	1.33	0.67	5.62E-04	2.45E-04	-2.00	-2.29
323454055	Ribosomal protein	1.67	0.33	2.25E-04	4.09E-05	-5.00	-5.50
323450361	Triosephosphate isomerase	1.33	0.33	8.43E-05	4.09E-05	-4.00	-2.06

323453878	Aspartyl-tRNA synthetase	1.33	0.33	5.62E-05	8.18E-05	-4.00	1.46
323454189	Ribosomal protein	1.67	0.33	5.06E-04	4.91E-04	-5.00	-1.03
323453434	Nitrite reductase	1.00	0.33	3.94E-04	4.09E-05	-3.00	-9.62
323455015	Cycloartenol-C24-methyltransferase	0.33	2.33	2.25E-04	1.64E-04	7.00	-1.37
323452327	Zn-finger	0.33	0.67	2.81E-05	8.18E-05	2.00	2.91
323449390	Exportin	0.33	2.33	8.43E-05	4.09E-05	7.00	-2.06
323455383	Phenylalanyl-tRNA synthetase	0.33	1.67	5.62E-05	4.09E-05	5.00	-1.37
323451434	Hypothetical protein	0.33	1.00	5.62E-05	8.18E-05	3.00	1.46
323452805	NADPH protochlorophyllide reductase	0.67	1.33	2.81E-05	8.18E-05	2.00	2.91
323448712	Thiolase	0.67	0.33	5.62E-05	8.18E-05	-2.00	1.46
323449561	Ribosomal protein	1.33	0.33	5.62E-05	1.64E-04	-4.00	2.91
323450277	Ribosomal Protein	1.33	0.33	1.41E-04	8.18E-05	-4.00	-1.72
323447741	Nonaspanin	0.33	0.33	8.43E-05	4.09E-05	1.00	-2.06
323451431	Chloroplast light harvesting protein	6.00	0.33	8.43E-04	4.05E-03	-18.00	4.80
323456793	Nuclear transport factor 2	0.67	0.33	3.94E-04	8.18E-05	-2.00	-4.81
323451135	Proteasome	1.67	0.33	6.75E-04	5.73E-04	-5.00	-1.18
323448268	Aldo/keto reductase	0.33	0.67	2.81E-05	4.09E-05	2.00	1.46
323452169	Hypothetical protein	0.33	0.67	4.22E-04	3.27E-04	2.00	-1.29
323448884	Proteasome	1.67	0.33	8.43E-05	4.09E-05	-5.00	-2.06
323454580	Glutathione peroxidase	0.33	1.33	2.81E-05	4.09E-05	4.00	1.46
323448448	Nonphototropic hypocotyl	2.33	0.33	2.81E-05	4.09E-05	-7.00	1.46
323454894	Formylglycineamide ribotide amidotransferase	0.33	0.33	2.81E-05	4.09E-05	1.00	1.46
323448821	ATPase, proteasome	0.33	1.00	3.37E-04	6.14E-04	3.00	1.82
323450953	Epsilon1-COP	0.33	0.67	2.25E-04	2.45E-04	2.00	1.09
323454888	S-adenosylmethionine-dependent methyltransferase activity	0.33	0.33	5.62E-05	4.09E-05	1.00	-1.37
323449847	Proteasome	0.67	0.33	2.81E-04	1.23E-04	-2.00	-2.29
323454603	Prolyl 4-hydroxylase	0.33	1.00	2.81E-05	1.64E-04	3.00	5.82
323447558	Glutamine amidotransferase/cyclase	0.33	1.00	8.43E-05	4.09E-05	3.00	-2.06
323453323	Elongation factor	0.33	0.67	8.43E-05	4.09E-05	2.00	-2.06
323448551	Prolyl-tRNA synthetase	0.33	0.67	2.81E-05	4.09E-05	2.00	1.46
323449787	Hedgehog protein	0.33	1.33	8.43E-05	2.05E-04	4.00	2.43
323447426	Isoleucine trna synthetase	0.33	0.67	4.78E-04	3.27E-04	2.00	-1.46
323449971	Phypo stress protein	0.33	0.67	1.12E-04	2.05E-04	2.00	1.82
323455262	tRNA synthetases	1.00	0.33	5.62E-05	4.09E-05	-3.00	-1.37
323455416	Geranylgeranyl diphosphate synthase	0.67	0.67	1.69E-04	8.18E-05	1.00	-2.06
323450170	Hypothetical protein	0.67	0.33	8.43E-05	4.09E-05	-2.00	-2.06
323449569	Coatomer WD associated region	0.33	1.00	8.71E-04	2.45E-04	3.00	-3.55
323451541	Ras small GTPase	0.33	0.33	2.25E-04	1.23E-04	1.00	-1.83

323448259	Mitochondrial carrier protein	0.33	1.33	1.41E-04	1.64E-04	4.00	1.16
323457329	Proteasome non-ATPase regulatory subunit	0.33	0.33	1.12E-04	8.18E-05	1.00	-1.37
323453797	Chloroplast Chaperonin	0.33	1.00	8.43E-05	1.23E-04	3.00	1.46
323450033	Acyl-CoA synthetase	0.67	0.33	1.12E-04	1.23E-04	-2.00	1.09
323451609	Alanine transaminase	0.33	0.67	2.81E-05	4.09E-05	2.00	1.46
323454572	Acyltransferase region, Thioestarase	0.33	0.67	1.69E-04	2.05E-04	2.00	1.21
323452117	Delta 1-pyrroline-5-carboxylate reductase (P5CR)	0.33	0.33	1.12E-04	4.09E-05	1.00	-2.75
323446697	3-hydroxyacyl-CoA dehydrogenase	0.33	0.33	5.62E-05	1.23E-04	1.00	2.18
323449869	Tryptophanyl-tRNA synthetase	0.33	0.33	8.43E-05	2.45E-04	1.00	2.91
323447574	Dynein heavy chain, AAA ATPase	0.33	0.33	8.43E-05	1.64E-04	1.00	1.94
323446558	Ribosomal protein	1.33	0.33	3.65E-03	2.41E-03	-4.00	-1.51
323447748	AAA ATPase	0.33	0.33	4.22E-04	1.23E-04	1.00	-3.43
323451194	ABC transporter	0.33	0.33	5.62E-05	4.09E-05	1.00	-1.37
323452072	ATP-dependent RNA helicase DBP3	0.33	0.33	2.81E-05	8.18E-05	1.00	2.91
323455685	Pyridoxamine 5'-phosphate oxidase-related	0.33	0.33	5.62E-05	8.18E-05	1.00	1.46
323456269	Peptidase M, neutral zinc metallopeptidases, zinc-binding site	0.67	0.33	1.69E-04	2.86E-04	-2.00	1.70
323450302	Acyl-CoA dehydrogenase	0.33	0.33	2.25E-04	4.50E-04	1.00	2.00

CHAPTER FOUR

Targeted gene expression in cultures and field populations of *Aureococcus anophagefferens*: Patterns in nitrogen and phosphorus metabolism.

Louie L. Wurch[a]

Elyse A. Walker [c]

Christopher J. Gobler[c]

Sonya T. Dyhrman[b,d]

[a]MIT-WHOI Joint Program in Oceanography/Applied Ocean Science and Engineering, Cambridge, MA 02139

[b]Woods Hole Oceanographic Institution Biology Department

Woods Hole, MA 02543

[c]Stony Brook University, School of Marine and Atmospheric Sciences

Stony Brook, NY 11794

[d]Corresponding author: sdyhrman@whoi.eduFax: (508) 457-2134

Abstract:

Aureococcus anophagefferens, the harmful alga responsible for brown tides, has adversely affected coastal ecosystems in the Eastern U.S. Past research efforts have focused on the factors leading to bloom initiation and decline such as nutrient preference and supply. However, these field studies have relied on community level approaches such as bulk uptake rates and elemental composition. Gene expression offers a promising metric for examining species-specific nutrition in natural populations of *A. anophagefferens*. In this study, quantitative gene expression assays were developed to examine nitrogen (N) and phosphorus (P) deficiency in axenic cultures of *A. anophagefferens*. Results demonstrate that a phosphate transporter (PTA3) is up-regulated over 500-fold in cells experiencing P-deficiency relative to a P-replete environment. This expression signal degrades upon P re-addition in a matter of hours. Furthermore, PTA3 expression was not regulated by N deficiency, but was up-regulated about 40-fold when cells were exponentially growing on ammonium. Four genes involved in N metabolism were examined as a potential marker of N deficiency including a xanthine/uracil/vitamin C transporter (XUV), a formate/nitrite transporter (NAR1.3), a urea transporter (DUR2), and a formamidase/acetamidase enzyme (FMD2). Expression patterns demonstrate all N metabolism genes tested show differential expression in response to N supply. The most promising candidate for assaying N deficiency was the XUV gene, which was up-regulated ~50-fold when nitrate grown cells experience N deficiency and ~35-fold when ammonium grown cells experience N deficiency. XUV expression rapidly

declined after two hours. Further, XUV expression was not governed by P supply. The expression of XUV and PTA3 was analyzed in samples from a natural brown tide bloom. Results suggest that as the bloom is growing toward peak cell densities, *A. anophagefferens* is not experiencing N or P deficiency and may be growing on ammonium.

Introduction:

Brown tides caused by the pelagophyte *Aureococcus anophagefferens* have adverse effects on the coastal environment and caused substantial losses to commercially important shellfish where these events occur (see reviews by Gobler et. al. 2005, Sunda et al. 2006). As a result, *A. anophagefferens* blooms are classified as ecosystem destructive algal blooms, a term prescribed to harmful algal blooms (HABs) that can modify or degrade ecosystems (Sunda et al. 2006). The ability of *A. anophagefferens* to dominate its environment under certain conditions, and the severe consequences of its presence in coastal ecosystems, has led to *A. anophagefferens* becoming a widely studied HAB species.

Substantial effort has been invested into defining the environmental conditions that allow *A. anophagefferens* blooms to initiate, persist and eventually decline. Field studies have shown that nutrient supply and nutrient type may be important in this aspect (as reviewed Gobler et al. 2005). Natural assemblages of phytoplankton during brown tide events can assimilate reduced N (e.g. ammonia) and DON (e.g. urea and amino acids) and have a higher affinity for these compounds compared to nitrate (Lomas et al.

1996, Berg et al. 1997; 2003, Mulholland et al. 2002; 2004). Low nitrate inputs have been positively correlated to brown tides around Long Island (LaRoche et al. 1997) while mesocosm experiments during a bloom pointed to an inverse correlation between DIN enrichment and *A. anophagefferens* cell densities (Keller and Rice, 1989). Experiments with DIN enrichment led to a decrease in the relative abundance of *A. anophagefferens* within the phytoplankton community (Gobler and Sañudo-Wilhelmy 2001, Gobler et al. 2002; 2004, Kana et al. 2004) signifying that *A. anophagefferens* is outcompeted when DIN is high. These results suggest that *A. anophagefferens* may not be experiencing N deficiency during peak bloom periods.

Although not as well studied, phosphorus (P) may be playing a significant role in controlling *A. anophagefferens* blooms. Culture work has demonstrated that *A. anophagefferens* can utilize some dissolved organic phosphorus (DOP) compounds such as glycerol-phosphate and adenosine monophosphate (Dzurica et al. 1989, Wurch et al. 2011). As with DIN, *A. anophagefferens* blooms tend to correlate with relatively low dissolved inorganic phosphorus (DIP) concentrations (Gobler et al. 2005). Further, during peak *A. anophagefferens* cell densities there is a significant reduction of DOP (Gobler et al. 2004). If *A. anophagefferens* is not experiencing N deficiency at peak cell densities, it is possible that P deficiency might be constraining these blooms.

Past studies of both N and P have provided valuable insight into how N and P availability may influence blooms. However, one of the fundamental challenges in definitively linking N and P supply to bloom dynamics is that there is a disconnect between single species responses and nutrient chemistry. Nutrient concentrations are not

equal to nutrient fluxes, so it is difficult to correlate *in situ* nutrient measurements with N or P deficiency. Elemental ratios (e.g particulate C:N:P) and nutrient uptake rates are community level approaches (Dyhrman 2008). In the case of brown tides, it is important to know the physiology of *A. anophagefferens* specifically. A potential way to bridge this gap is through the use of molecular techniques such as targeted gene expression. This approach offers a means in which the nutritional physiology of individual species living in complex mixed assemblages can be examined at the cellular level (Dyhrman 2008). However, this approach hinges on the ability to accurately comprehend both the organism's physiological potential encoded within its genome and how that genome is expressed under distinct environmental conditions.

Due to its importance, *A. anophagefferens* was the first HAB species to have its genome sequenced (Gobler et al. 2011). Insights gained from the genome sequence have provided a framework for understanding the potential niche of *A. anophagefferens* and how it responds to changes in its environment. For example, *A. anophagefferens* possesses genes for the uptake and/or metabolism of a variety of both inorganic and organic nitrogen (N) compounds including nitrate, formate/nitrite, ammonia, nitriles, urea, amino acids and peptides, and others (Gobler et al. 2011). These data are supported by culture studies demonstrating the ability of *A. anophagefferens* to utilize these compounds as a sole N source (Berg et al. 2002, Mulholland et al. 2002, MacIntyre et al. 2004, Pustizzi et al. 2004, Berg et al. 2008). However, it is the ordered expression of the genome that determines an organism's ability to occupy a given environmental niche (as opposed to its potential niche). A global transcriptome profiling study revealed that *A.*

anophagefferens up-regulates genes involved in reduced and organic N metabolism when nitrate is unavailable including a xanthine/uracil/vitamin C permease (XUV) and acetamidase/formamidase (FMD2) (Wurch et al. 2011). Another study identified that *A. anophagefferens* also up-regulates a urea transporter (DUR2) and nitrite transporter (NAR1.3) under N deficiency. *A. anophagefferens* also contains genes for the uptake and/or metabolism of inorganic and organic phosphorus (P) compounds including esters, diesters and nucleotides (Gobler et al. 2011) and these genes are induced during P deficiency (Wurch et al. 2011). A phosphate transporter (PTA3) in *A. anophagefferens* was shown to be particularly responsive to P supply (Wurch et al. 2011, and Chapter 3). These results suggest that gene expression may be a good approach for assaying N and P deficiency in *A. anophagefferens*.

In this study, the expression patterns of the gene targets described above were examined through detailed time-course culture experiments as *A. anophagefferens* transitioned from a nutrient replete to N- or P-deficient environment. Expression patterns were also examined as *A. anophagefferens* transitioned back into a nutrient replete environment. Quantitative assays were developed for tracking the expression patterns of these gene targets in natural field populations. This work serves as a critical step in linking culture experiments with natural populations of *A. anophagefferens* and provides a platform for tracking N and P deficiency in *A. anophagefferens* populations over the course a brown tide bloom.

Materials and Methods:

Phosphorus experiment

Axenic *A. anophagefferens* strain CCMP 1984 was obtained from the Provasoli-Guillard Center for the Culture of Marine Phytoplankton and used for all culture experiments. Control cultures were grown in triplicate, while low P cultures were grown in quadruplicate. Locally collected Vineyard Sound seawater was filtered (0.2 μm) twice and used to make modified L1 media (see below) with no silica (Guillard and Hargraves 1993). Vitamins (thiamine, biotin, and B_{12} were sterile filtered (0.2 μm) and added to the media after autoclaving. For the P experiment, P concentrations in L1 media were modified as follows: L1 replete (+P control; 36 μM PO_4^{3-}) and low phosphate (low P; 2 μM PO_4^{3-}) (Table 1). Cells were grown at 18°C on a 14:10 hour light:dark cycle (140 μmol quanta m^{-2} s^{-1}) and growth was monitored daily by cell counting on a hemacytometer and tracking fluorescence on a Turner Designs fluorometer. Nutrient samples were collected by filtering out cells through acid washed 0.2 μm polycarbonate filters and into acid washed tubes. Nutrient samples were sent to the Woods Hole Oceanographic Institution Nutrient Analytical Facility for analysis of ammonium, silicate, phosphate, nitrate + nitrite concentrations. Control cells were harvested on day 6 (Figure 1). Starting on day 4, cells were harvested daily for the low P treatment. On day 7 of the experiment, low P cells were pooled and redistributed into 4 flasks at equal volume. Two of the flasks were refed 36 μM phosphate (low P/+P) while the other two flasks were not changed (low P/-P). In both cases, cells were harvested at T=2, 4, 6, 24 and 48 hours after redistribution (Table 1). Approximately 5 to 10 x 10^7 cells were

harvested by filtration onto a 0.2 μm polycarbonate filter and immediately placed in 1 mL CTAB extraction solution (Teknova, Hollister CA) amended with 1% m/v polyvinylpyrrolidone, incubated at 50°C for 20 minutes, and snap frozen in liquid nitrogen. Samples were stored at -80°C until further processing.

Nitrogen experiment

Strain and media preparation methods were identical to those described above except for the nutrient conditions. N concentrations in L1 media were modified as follows: L1 replete control (+N control; 883 μM NO_3^-), nitrate grown (low NO_3^-; 50 μM NO_3^-), ammonium grown (low NH_4^+; 50 μM NH_4^+) and a no N added negative control (no N added) (Table 1). Growth was monitored and nutrient samples were collected as described above. Photosynthetic efficiency of photosystem II was determined daily for the nitrogen experiment in all treatments by the F_v/F_m method (Parkhill et al. 2001). In brief, 10 mL aliquots of cells were dark adapted for 30 minutes and initial fluorescence (F_0) was determined on a Turner Designs Fluorometer. Then, 50 μL of 3 mM 3'-(3,4 dichlorophenyl)-1',1'-dimethyl urea (DCMU) in 100% ethanol was added to each aliquot and maximal fluorescence (F_m) was determined after 30 seconds. F_v/F_m was calculated by: $F_v/F_m = (F_m-F_0)/F_m$. Between 5 and 10 $x10^7$ cells were harvested daily starting on day 5 of the low NO_3^- condition. On day 7, low NO_3^- cells were pooled and re-distributed into 4 flasks. Two of the flasks were not changed (low NO_3^-/-NO_3^-). In the other two flasks, nitrate was added to a concentration of 883 μM (low NO_3^-/+NO_3^-). In both the low NO_3^-/-NO_3^- and low NO_3^-/+NO_3^- conditions, cells were harvested at T=2, 4, 6, 24,

and 48 hours after redistribution (5 to 10 x 10^7 cells). On day 9, low NH_4^+ cells were pooled and re-distributed into 4 flasks. Two of the flasks were not changed (low NH_4^+/-NH_4^+). In the other two flasks, ammonium was added to a concentration of only 50 μM (low NH_4^+/+NH_4^+) due to toxicity of ammonium at high concentrations. In both the low NH_4^+/-NH_4^+ and low NH_4^+/+NH_4^+ conditions, cells were harvested at T=2, 4, 6, 24, and 48 hours after redistribution (5 to 10 x 10^7).

Culture RNA isolation

Approximately 1.0-4.0 μg of RNA was isolated from each sample using the UltraClean® Plant RNA Isolation Kit (MO BIO Laboratories, Inc., Carlsbad CA) with modified manufacturer's instructions. Samples were removed from -80°C and incubated at 65°C for 10 minutes. Then, the samples were centrifuged at 10,000 x *g* to separate cell lysate from the filter and 650 μL of supernatant was transferred to a fresh 1.5 mL tube. Second, 300 μL of PMR1 was added to each sample and vortexed, followed by the addition of 800 μL of PMR4 to each sample and again vortexed. Last, samples were loaded onto the columns and RNA extraction continued according to manufacturer's instructions. Isolated RNA was then treated with TURBO™ DNase (Ambion, Austin TX) to remove potential genomic DNA contamination. The RNA was quantified spectrophotometrically for yield and purity. For each sample, 100 ng of RNA was primed with oligo dT primers and reverse transcribed into cDNA using the iScript Select cDNA Synthesis kit (Bio-Rad, Hercules CA). A second reaction containing no reverse transcriptase served as a control for genomic DNA contamination. Subsequent qRT-PCR

analysis using reference and target genes showed no amplification (C_T values = N/A) in these controls suggesting all samples were free of genomic DNA contamination.

qRT-PCR assay

Species-specific primers were designed from genomic sequences for the following genes using MacVector (MacVector, Inc., Cary NC) or Primer3 (Rozen and Skaletsky 2000): Xanthine/Uracil/Vitamin C transporter (XUV; JGI protein ID: 52593), acetamidase/formamidase (FMD2; JGI protein ID: 37987), urea transporter (DUR2; JGI protein ID: 71789) and phosphate transporter (PTA3; JGI protein ID: 22152). Primers from a previous study (Berg et al. 2008) were also used for a formate/nitrite transporter (NAR1.3) and the constitutively expressed ubiquitin-conjugating enzyme (UbE2). UbE2 was demonstrated to be a good reference gene for *A. anophagefferens* because of its constitutive expression patterns over a range of physiological conditions (Berg et al. 2008). In this study, the C_T values of UbE2 across treatments were fairly stable, with the majority of samples falling between 29-31. Amplicons for all primer sets were screened for secondary structure using Mfold software (Zuker 2003) to confirm the primers were qRT-PCR compatible. A qRT-PCR assay was designed to optimize primer efficiency between 90-110 % and examine relative abundance of cDNA transcripts across treatments using the comparative C_T ($2^{-\Delta\Delta Ct}$) method (Livak and Schmittgen 2001). The ΔC_T (C_T target – C_T reference) was examined over a range of cDNA concentrations (1 – 0.001 ng) to determine which concentrations produced near equal amplification efficiencies between target and reference amplicons. A plot of the log cDNA dilution

versus ΔC_T was constructed to ensure the absolute value of the slope did not differ significantly from zero. All qRT-PCR reactions were run in triplicate using Brilliant® II Fast SYBR® Green qRT-PCR Master Mix (Agilent Technologies, Santa Clara CA) and analyzed on a Bio-Rad iCycleriQ® qRT-PCR detection system (Bio-Rad. Hercules CA) with the following cycling parameters: 1x 95°C 5 minutes, 45x: 95°C for 10 seconds, 62°C for 30 seconds. A dissociation curve was performed to check for non-specific amplification by holding PCR reactions at 95°C for 1 minute and lowering the temperature by 0.5°C every 10 seconds to 55°C. A list of all primer sequences, concentration, and efficiencies can be found in Table 2.

Fold-changes of target genes among conditions were determined using the Relative Expression Software Tool (REST) located at http://www.gene-quantification.de/download.html. REST accounts for differences in efficiency between primer sets. The *P*-values for each biological replicate were determined by a pair-wise fixed reallocation randomization analysis (Pfaffl et al. 2002). The fold-changes of the target genes were then averaged from two biological replicates for each condition. Differences between conditions were determined using a one-way analysis of variance (ANOVA) with a Tukey post test (significantly different if P-value < 0.05 between conditions). Statistical *P*-values, average fold-changes, and standard deviations for each gene target on every biological sample are listed in Tables 4-9.

Expression of XUV and PTA3 from natural populations

Natural samples during a brown tide bloom in Quantuck Bay (Suffolk County, Long Island, NY) were collected throughout the summer season in 2007. *A. anophagefferens* cell counts were determined according to the methods described in Stauffer et al. 2008. For RNA samples, approximately 25 mL of natural sea water was filtered onto 0.2 μm polycarbonate filters and stored at -80°C. CTAB buffer (Teknova, Hollister CA) amended by the addition of 1% mass/volume polyvinylpyrrolidone was subsequently added for further processing. Samples were incubated at 65°C for 10 minutes, centrifuged for 2 minutes at 10,000 x *g* and 750 μL was transferred to a fresh tube. Then, 750 μL of chloroform: isoamyl alcohol (24:1) was added and samples were vortexed for 5 minutes. Samples were then centrifuged for 15 minutes and the supernatant was transferred to a fresh tube. The addition of chloroform: isoamyl alcohol (24:1) was then repeated and samples were vortexed and centrifuged as described above. Again, supernatant was transferred to a fresh tube and 300 μL of 5M NaCl and 600 100% μL Isopropyl alcohol was added to each sample and stored at -20°C for at least 90 minutes. Samples were then centrifuged at 10,000 x *g* for 15 minutes and the supernatant was carefully removed from the RNA pellet. The RNA pelletes were washed by the addition of 100 μL of 100% ethanol. Molecular grade water was then added to the RNA pellets. RNA was then treated with TURBO™ DNase (Ambion, Austin TX) to remove potential genomic DNA contamination. The RNA was quantified spectrophotometrically for yield and purity. For each sample, 100 ng of RNA was primed with oligo dT primers and reverse transcribed into cDNA using the iScript Select

cDNA Synthesis kit (Bio-Rad, Hercules CA). A second reaction containing no reverse transcriptase served as a control for genomic DNA contamination. Subsequent qRT-PCR analysis using reference and target genes showed no amplification (C_T values = N/A) in these controls suggesting all samples were free of genomic DNA contamination. A qRT-PCR assay was designed for the XUV and PTA3 genes as described above. New efficiencies were calculated from dilutions of cDNA generated from two field samples tested: 6-25-07 and 7-2-07.

Results:

Phosphorus experiment:

To examine phosphate transporter (PTA3) expression as a function of phosphate availability, *A. anophagefferens* cells were grown in batch cultures under phosphate replete (+P control) and low P conditions (Figure 1). A comparison of +P control and low P growth data show that by day 6, low P cell concentrations and fluorescence were slightly lower than in the +P control, suggesting that day 6 represents the onset of stationary phase of growth (Figure 1). By day 7, external phosphate concentrations were below detection limit (50 nM) while nitrate concentrations remained high and *A. anophagefferens* cell densities had not increased from the previous day (Figure 1, Table 2).

Expression of PTA3 was examined in low P cells on days 4-7 and compared to expression in the +P control to calculate a fold change. On day 4, low P cell growth resembled the +P control (Figure 1). Expression of PTA3 in low P cells on this day was

not detected (Figure 2A, Table 3). On day 5, expression of PTA3 was roughly 500-fold higher in low P cells relative to the +P control (Figure 2A, Table 3) corresponding with low external phosphate concentrations (Figure 1, Table 2). On day 6, PTA3 expression peaked at approximately 2000-fold higher than the +P control (Figure 2A). This peak expression coincided with onset of stationary growth due to P deficiency and phosphate concentrations below the detection limit. Finally, on day 7, expression of PTA3 was still over 500-fold greater than the +P control (Figure 2A, Table 3).

To examine how quickly phosphate re-addition would repress PTA3 expression, a re-feed experiment was conducted on low P cells. As growth had become stationary on day 7 and external phosphate concentrations were below detection, this time was chosen to examine phosphate addition. Phosphate was spiked into two low P cultures (low P/+P), while two were left unchanged (low P/-P). After 24 hours, low P/+P cells resumed growth while low P/-P cells remained in stationary phase (Figure 1).

Expression of PTA3 was examined at 2, 4, 6, 24, and 48 hours after phosphate addition (low P/+P) or no phosphate addition (low P/-P) and compared to expression at T_0, where PTA3 expression was over 500-fold higher than in the +P control. In the low P/-P cells, there was no significant difference in expression of PTA3 over the course of the 48 hours relative to T_0 (Figure 2B, Table 4). After only 2 hours of phosphate addition, PTA3 was down-regulated almost 100-fold in low P/+P cells relative to T_0 (Figure 2B, Table 4). By 4 hours, PTA3 was down-regulated approximately 600-fold (Figure 2B, Table 4). After 6 hours, PTA3 was undetectable in one of the biological replicates. At 6 hours, the PTA3 transcript from one biological replicate was not detected,

while the other replicate was down-regulated 200-fold. By 24 hours, the expression of PTA3 was undetectable in all biological replicates and remained undetectable after 48 hours (Figure 2B, Table 4).

Nitrogen experiment

A. anophagefferens cells were grown on N replete (+N), low nitrate (low NO_3^-), and low ammonium (low NH_4^+) to examine how the expression patterns of the following four genes are influenced by both N source and N supply: xanthine/uracil/vitamin C transporter (XUV), formate/nitrite transporter (NAR1.3), urea transporter (DUR2), and acetamidase/formamidase (FMD2). *A. anophagefferens* cells were also grown in a no N added control to ensure that growth in the other conditions was due to added N compounds and not residual N from the seawater base (Figure 3A-C). The fluorescence of cells in the low NO_3^- condition was identical to cells in the +N condition until day 6, where the low NO_3^- cells reached a peak fluorescence of approximately 30 relative fluorescence units (Figure 3A). Continuing into day 7, cell concentrations continued to increase, but fluorescence remained steady in the low NO_3^- condition (Figure 3A,B). This transition between day 6 and day 7 coincided with a rapid drop in F_v/F_m (Figure 3C).

A. anophagefferens cells in the low NH_4^+ condition stayed in the lag phase of growth for a longer period of time, and did not reach onset of stationary phase growth until day 9 (Figure 4A-C). As with the low NO_3^- condition, the transition into stationary phase coincided with a rapid decline in F_v/F_m (Figure 3C). There was no noticeable growth in the no N added control and F_v/F_m steadily decreased throughout the experiment

in this condition (Figure 3A-C). As such, cell counts and F_v/F_m measurements were stopped after day 7 and fluorescence measurements were stopped after day 8 for this condition.

Exponentially growing *A. anophagefferens* cells from day 7 in the low NH_4^+ condition were used as the reference condition for examining the expression of N metabolism genes as a function of N source and supply (Figure 4). The expression of XUV was roughly 3-fold higher on day 5, 24-fold higher on day 6, and 50-fold higher on day 7 of the low NO_3^- condition relative to the reference condition (Figure 5A, Table 5). In the NH_4^+ condition, expression of XUV was not significantly different from the control condition on day 8, but was about 35-fold higher on day 9 (Figure 5B). In both cases, expression of XUV increased as N supply decreased (Figures 3-5, Table 3). The NAR1.3 gene displayed a similar expression pattern as XUV. In the low NO_3^+ condition, NAR1.3 expression was approximately 4-fold higher on day 5, 46-fold higher on day 6, and 30-fold higher on day 7 (Figure 5B, Table 6). NAR1.3 expression was also over 8-fold higher on day 8 and over 17-fold higher on day 9 in the NH_4^+ condition (Figure 5B, Table 6). For DUR2, expression patterns were similar to XUV and NAR1.3, but the fold-changes were lower, reaching a maximum expression of about 10-fold higher than the reference condition on day 7 of the low NO_3^- condition (Figure 5C, Table 6). The FMD2 gene was expressed almost 18-fold higher on day 5 of the low NO_3^- condition in one biological replicate, but was not detected in the other biological replicate (Figure 5D, Table 6). Expression of FMD2 appeared to steadily decrease as cells reached stationary phase in the low NO_3^- condition. The XUV, NAR1.3, and DUR2 gene expression

patterns were similar in the low NH_4^+ conditions, but the absolute fold-changes were lower (Figure 5A-C). The FMD2 gene was not differentially expressed in the low NH_4^+ condition (Figure 5D).

A re-feed experiment was conducted to examine how quickly N re-addition would influence expression patterns of these N metabolism genes. Nitrate was spiked into two low NO_3^- cultures on day 7 (low NO_3^-/+NO_3^-), while two were left unchanged (low NO_3^-/-NO_3^-). Similarly, ammonium was spiked into two low NH_4^+ cultures (low NH_4^+/+NH_4^+) while two were left unchanged (NH_4^+/-NH_4^+). After 24 hours, fluorescence and cell concentrations increased in both the low NO_3^-/+NO_3^- and low NH_4^+/+NH_4^+ conditions (Figure 3, 4). Further, F_v/F_m recovered in the low NO_3^-/+NO_3^- condition, but continued to decline low NO_3^-/-NO_3^- cells (Figure 3C). In the low NH_4^+ condition, cells were refed ammonium at the point where F_v/F_m was beginning to decline (Figure 4). Therefore, the addition of NH_4^+ delayed the decline in F_v/F_m by 24 hours rather than recovering it as seen in the case of the low NO_3^-/+NO_3^- condition (Figure 5).

Expression of XUV, NAR1.3, DUR2, and FMD2 was examined at T=2, 4, 6, 24, and 48 hours after N re-addition and compared to a T_0: low NO_3^- cells on day 7 for the low NO_3^-/-NO_3^- and low NO_3^-/+NO_3^- conditions low NH_4^+ cells on day 9 for the low NH_4^+/-NH_4^+ and low NH_4^+/-NH_4^+ conditions (Figure 6, 7). In the low NO_3^-/+NO_3^- condition, expression of XUV continued to increase for 4 hours where it reached maximum levels of about 4-fold higher than the reference condition (Figure 6A, Table 8). After only 2 hours of nitrate re-addition, expression of XUV decreased over 70-fold compared to the reference condition (Figure 6A, Table 8). The expression of XUV

remained down-regulated relative to the reference condition over the course of the re-feed until T=48 hours where it was no longer detectable (Figure 6A, Table 8). The expression patterns of NAR1.3 and DUR2 were similar to that of XUV in both the low NO_3^-/-NO_3^- and low NO_3^-/+NO_3^- conditions, but the magnitudes of the fold-changes were less (Figure 6B, C, Table 8). The C_T values for the FMD2 gene were outside the acceptable range for the low NO_3^-/+NO_3^- condition at T=2 and 24 hours. However, at T=4, 6, and 48 hours, the expression of FMD2 was significantly less than the control condition (Figure 6D, Table 8).

In the ammonium re-addition experiment, XUV, NAR1.3, DUR2, and FMD2 were all significantly down-regulated at T=2 hours in the low NH_4^+/+NH_4^+ condition (Figure 7, Table 9). XUV was down-regulated over 120-fold in one biological replicate, and undetectable in the second biological replicate at T=2 hours in the low NH_4^+/+NH_4^+ condition (Figure 7A, Table 9). After 4 hours, XUV expression was undetectable in both biological replicates. Continuing into T=6, 24, and 48 hours, XUV expression increased in the low NH_4^+/+NH_4^+ condition, but was still significantly less than the reference condition (Figure 7A, Table 9). In the low NH_4^+/-NH_4^+ condition, expression of XUV showed little difference to the reference condition until T=48 when expression was over 10-fold lower than the reference condition (Figure 7A, Table 9). Expression of NAR1.3 followed a similar pattern to XUV in the low NH_4^+/+NH_4^+ condition (Figure 7B, Table 9). At T=2 hours, expression of NAR1.3 in the low NH_4^+/+NH_4^+ condition was over 40-fold less than the reference condition in one biological replicate and not detected in the second biological replicate (Figure 7B, Table 9). At T=4 and 6 hours, expression of

NAR1.3 in the low NH_4^+/+NH_4^+ condition was still significantly less than the reference condition, but the fold-changes were less different (Figure 7B, Table 9). After 24 and 48 hours, expression of NAR1.3 in the low NH_4^+/+NH_4^+ condition was not statistically different from the reference condition (Figure 7B, Table 9). No significant difference in expression of NAR1.3 was detected in the low NH_4^+/-NH_4^+ condition at any time point (Figure 7B, Table 9). Expression of DUR2 was significantly less in the low NH_4^+/+NH_4^+ condition relative to the reference condition throughout the experiment, but again, the largest fold-changes were earlier in the experiment (Figure 7C, Table 9). Similar to XUV, in the low NH_4^+/-NH_4^+ condition DUR2 expression was significantly less at T=24 and 48 hours relative to the reference condition (Figure 7C, Table 9). Finally, expression of FMD2 in the low NH_4^+/+NH_4^+ condition was about 35-fold less than the reference condition in one biological replicate and undetectable in the second biological replicate (Figure 7D, Table 9). It remained undetectable in the low NH_4^+/+NH_4^+ condition for the rest of the time course (Figure 7D, Table 9). Conversely, in the low NH_4^+/-NH_4^+ condition, expression of FMD2 was not significantly different than the reference condition over the time course (Figure 7D, Table 9).

Expression of XUV was tested on low P conditions to ensure that expression patterns are indicative of N deficiency only. Expression was compared to exponentially growing *A. anophagefferens* cells from day 7 in the low NH_4^+ condition. No significant differences in expression of XUV were observed on any low P sample tested relative to the reference condition. Expression of PTA3 was also tested on low NO_3^- and low NH_4^+ conditions to ensure that expression patterns are indicative of P deficiency only.

Exponentially growing +P control cells were used as the reference condition. Expression of PTA3 was undetectable in all low NO_3^- samples tested. However, expression of PTA3 was up-regulated about 40-fold on low NH_4^+ day 7 (exponentially growing cells on ammonium). This expression decreased to only 4-fold higher than the reference condition as cells in the low NH_4^+ condition entered stationary phase. Upon ammonium re-addition, PTA3 expression increased to a maximum of 60-fold higher on low NH_4^+/+NH_4^+ T=6 hours.

Expression of XUV and PTA3 from natural populations

Two samples from different stages of a natural brown tide bloom in Quantuck Bay, (Suffolk County, Long Island, NY) were analyzed for XUV and PTA3 expression (Figure 8). Exponentially growing cells on ammonium (N replete: low NH_4^+ day 7) were used as the reference condition for XUV expression and exponentially growing P replete cells (+P control day 6) were used as the reference condition for PTA3 expression. Expression of XUV was ~2-fold higher in both field samples tested relative to the reference condition (Figure 8). Expression of XUV during N-deficient conditions (low NO_3^- day 7) is plotted for comparison. The expression of PTA3 was tested on only one field sample (6-25-07) due to problems with obtaining a near 100% amplification efficiency over a range of cDNA dilutions on the field sample from 7-2-07. Analysis of the sample from 6-25-07 demonstrated that PTA3 expression was approximately 80-fold higher than the reference condition. For comparison, expression of PTA3 from P replete

exponentially growing cells on ammonium (low NH_4^+ day 7) and stationary phase P-deficient cells (low P day 7) is shown for comparison (Figure 8).

Discussion:

The aim of this research was to explore nutritional strategies of *A. anophagefferens* by analyzing the expression patterns of genes involved in P and N acquisition over time as *A. anophagefferens* transitioned into and out of a nutrient-deficient environment. Furthermore, these data were used to establish a species-specific indicator of P or N deficiency in natural populations of *A. anophagefferens*.

Assaying P deficiency

In a transcriptome profiling study, a phosphate transporter (PTA3) was shown to be up-regulated under P-deficient conditions (Wurch et al. 2011). Additionally, the protein for this gene also increases under P-deficiency (Chapter 3). Here, PTA3 expression was examined daily in batch cultures as *A. anophagefferens* approached P deficiency. PTA3 expression was first induced on day 5, before a noticeable effect was observed on cell growth (Figure 2A). In the first biological replicate, external phosphate concentrations were below the detection limit of the assay (<50 nM) on day 5 and expression of the PTA3 was over 600 fold higher relative to the +P control. In the second biological replicate, phosphate concentrations were approximately 156 nM and expression of PTA3 was about 360-fold higher relative to the +P control. These results hint at a correlation between external phosphate concentrations and PTA3 expression.

The highest expression levels of PTA3 correlated with the onset of stationary phase, when external phosphate concentrations were below the detection limit.

It is clear that PTA3 is induced under P deficiency, but in order to use it as a physiological marker it is important to determine how quickly the signal degrades upon alleviation of P deficiency. The re-feed experiment demonstrated that PTA3 expression is significantly down-regulated after 2 hours of P resupply (Figure 2B). This was the first time point examined, so it is difficult to determine exactly how quickly *A. anophagefferens* adjusts its expression of PTA3 when moving from a P-deficient to P replete environment. However, these results suggest that expression of PTA3 may be linked to P supply. If P is abundant, the PTA3 transcript is rapidly lost. If P becomes deficient, *A. anophagefferens* induces PTA3. A possible explanation for this induction is that *A. anophagefferens* is simply increasing the number of phosphate transporters, or switching to a more efficient one, when phosphate becomes low. This strategy has been seen in other eukaryotic phytoplankton (Chung et al. 2003, Dyhrman et al. 2006).

A recent proteomics study in *Ostreococcus tauri* revealed that proteins involved in phosphate transport were up-regulated under low nitrogen conditions (Le Bihan et al. 2011), therefore it was important to explore how PTA3 expression was influenced by N supply. In this study, the expression of PTA3 was not affected by N deficiency. When *A. anophagefferens* cells were growing on nitrate as their sole N source, and P was abundant, PTA3 expression was undetectable regardless of growth phase. This suggests that PTA3 expression is specific to P supply, an important consideration when interpreting expression patterns from field samples. However, PTA3 expression was

about 40-fold higher when cells were actively growing on ammonium as their sole N source. This result is consistent with a previous study in which this same gene (labeled PHO) was up-regulated ~68 times higher when cells were grown on ammonium relative to cells nitrate (Berg et al. 2008). The fact that PTA3 was not induced under N deficiency indicates that although PTA3 might be regulated by N source, it is not influenced by N deficiency. Given the magnitude of fold-changes of PTA3 under P-deficient conditions, it should be possible to resolve whether or not the expression of PTA3 is being influenced by growth on ammonium or general P deficiency. However, more work needs to be done to examine is PTA3 expression is influenced by other N sources other than ammonium and nitrate.

Assaying N deficiency

Four genes were considered for potential markers of N deficiency in *A. anophagefferens*. The xanthine/uracil/vitamin C permease is putatively involved with transport of nucleobases (purines and pyrimidines). It is unknown whether *A. anophagefferens* can utilize these compounds as a sole N source, however other algae, like the coccolithophore *Emiliania huxleyi* have been shown to utilize hypoxanthine, among other purine derivatives, as its sole N source (Palenik and Henson 1997). Furthermore, it was previously shown that *A. anophagefferens* induces this XUV during N deficiency, suggesting that purines/pyrimidines could be a potential N source (Wurch et al. 2011). In this study, as *A. anophagefferens* transitioned into an N-deficient state, XUV expression increased. The highest XUV expression levels corresponded to a rapid

decline in F_v/F_m. When ammonium or nitrate were re-supplied to the cells, the transcript signal was rapidly lost. The magnitude of the fold changes and the rapid loss of signal upon N re-addition suggests XUV is a good marker for assaying N deficiency in *A. anophagefferens*. This gene could potentially be used as a marker of N deficiency in other phytoplankton groups as well because it was demonstrated to be up-regulated under N deficiency in the diatom *Thalassiosira pseudonana* using a tiling array experiment (Mock et al. 2008).

The NAR1.3 and DUR2 genes also increased expression levels as cells approached N deficiency, however the fold changes were not nearly as high as seen in a previous study, which examined the expression of these genes under acute N deficiency (Berg et al. 2008). However, it is difficult to cross compare because of differences in seawater base (natural seawater versus artificial seawater) and reference conditions. In Berg et al. 2008, N replete cells grown on acetamide were used as the reference conditions. Nonetheless, the observation here that these genes are up-regulated under N deficiency is consistent with the overall patterns from the previous study. Little is known about whether *A. anophagefferens* can utilize nitrite as an N source. Furthermore, it is difficult to distinguish whether this transporter is transporting nitrite or formate. Formate is a compound that does not contain N, and therefore would not be a potential N source. Urea, however, has been suggested to play an important role in *A. anophagefferens* growth (see review by Gobler et al. 2005). The expression of the urea transporter (DUR2) indicates that *A. anophagefferens* may be actively taking up urea. DUR2 was also induced as *A. anophagefferens* transitioned into N deficiency. This result

supports the hypothesized importance of urea an N source when inorganic sources are unavailable.

Finally, expression of FMD2 was analyzed. FMD2 putatively hydrolyzes amides such as formamide or acetamide. In *E. huxleyi*, both formamide and acetamide were shown to be excellent N sources for growth (Palenik and Henson 1997). Acetamide has also been shown to support the growth of *A. anophagefferens* (Berg et al. 2008). Here, the expression of FMD2 was highest when cells were exponentially growing on nitrate. This is intriguing because the reference condition was exponentially growing cells on ammonium. As cells growing on nitrate transitioned into stationary phase, FMD2 expression started to decline. At first, these patterns suggest that FMD2 regulation is sensitive to the presence of nitrate and may be indicative of growth on nitrate. However, this result is confounded by the fact that when N-deficient cells were re-supplied with nitrate, or re-supplied with ammonium, FMD2 expression declined.

In the ammonium re-addition experiment, all 4 genes tested were initially down-regulated. However, after 48 hours the expression patterns trended toward T_0 (N-deficient conditions). This is most likely due to the fact that only 50 μM ammonium was re-supplied (compared to 883 μM nitrate), which was not enough to keep the cultures from N deficiency over 48 hours. The F_v/F_m rapidly declined between days 10 and 11 (corresponding to T=24 and 48 hours after ammonium re-supply) suggesting that cells were actually experiencing N deficiency during that time. This would explain the expression patterns trending back toward T_0 over the 48 hour period when ammonium was re-supplied, but not when the much more concentrated nitrate was re-supplied.

Expression of XUV and PTA3 from natural populations

The expression patterns of XUV and PTA3 were examined in field populations on June 25, 2007 during brown tide bloom. This point marked the beginning of a rapid increase in growth as *A. anophagefferens* cell densities increased from ~6.48x10^6 cells/mL to 8.82x10^6 cells/mL in a 24 hour period. Expression of XUV was about two-fold higher than the reference condition (exponentially growing cells on ammonium). Given the magnitude of XUV up-regulation when cells are N-deficient, a 2-fold change would indicate that the cells were probably not experiencing N deficiency. The ~60-fold up-regulation of the PTA3 gene, however, is suggestive that these cells were growing on ammonium. A second sample was tested for XUV expression later in the bloom when cell concentrations were decreasing. Again, XUV was only up-regulated ~2-fold, suggesting that even when the bloom was declining, cells were not in a period of N deficiency.

One caveat to this interpretation is the fact that during acute N deficiency, when *A.anophagefferens* cells were initially grown on ammonium and in stationary phase for 48 hours, expression of XUV started to decline (Figure 7A). Therefore, it may be that the cells are so N-deficient that they can no longer express XUV. Analysis of other ancillary data such as nutrient concentration or particulate C:N:P ratios may help discern which scenario is actually occurring.

Summary

The results of this research provide a method for assaying N and P deficiency in natural populations of the harmful alga *A. anophagefferens*. As *A. anophagefferens* transitions from a nutrient replete to N-deficient state, the XUV gene is induced. After only two hours of re-supplying N, the XUV signal rapidly degrades. Thus XUV is tightly linked with N supply. This is also the case for the PTA3 gene. As *A. anophagefferens* enters a P-deficient state, PTA3 is highly expressed, and the signal is rapidly degraded upon P re-supply. PTA3 is also induced, albeit at much lower levels, when cells are actively growing on ammonium. Therefore, PTA3 can potentially be used to assay both P deficiency as well as growth on ammonium. Application to natural bloom samples demonstrate that this method has strong potential for tracking the nutritional physiology of *A. anophagefferens* in its natural environment. More field samples need to be tested at different stages of the bloom and compared between years to distinguish the nutritional controls of *A. anophagefferens* blooms.

Table 1) Culture conditions in this study.

Notation:	Description:
+P	Cells grown in L1 replete media at 36 μM PO_4^{3-}
low P	Cells grown in modified L1 media at 2 μM PO_4^{3-}
+N	Cells grown in L1 replete media at 883 μM NO_3^-
low NO_3^-	Cells grown in modified L1 media at 50 μM NO_3^-
low NO_3^-/-NO_3^-	Stationary phase, low NO_3^- cells with no NO_3^- addition
low NO_3^-/+NO_3^-	Stationary phase, low NO_3^- cells with 883 μM NO_3^- addition
low NH_4^+	Cells grown in modified L1 media at 50 μM NH_4^+
low NH_4^+/-NH_4^+	Stationary phase, low NH_4^+ cells with no NH_4^+ addition
low NH_4^+/+NH_4^+	Stationary phase, low NH_4^+ cells with 50 μM NH_4^+ addition
no N added	Cells grown in L1 replete media with no nitrogen added

Table 2) List of primers used in this study.

Gene target:	Gene symbol:	Accession:	Sequence:	Efficiency:	CT Range:	Concentration:	Amplicon size:
Xanthine/Uracil/VitaminC permease	XUV	JGI: 52593	F: GTTCATGACGGCCATCTTCT R: TCGTCGATCTTCGGGTAGAG	105.0	25-33	260 nM	245 nt
Formamidase	FMD2	JGI: 37987	F: CCAGATCAAGAACGACGACA R: GTAGTGGTCCGTGAGGAAGC	111.4	27-34	400 nM	208 nt
Formate/Nitrite transporter	NAR1.3	NCBI: EH058542	F: GAACTGGTTCGTCTGCTGG R: CAGAAGTCGCCGTTGAAGTC	99.6	28-34	400 nM	201 nt
Urea transporter	DUR2	JGI: 71789	F: CCACTACACCTTCCTCTTCTTCGG R: CGTCTTCTTGAGCATCTCCCAG	92.1	25-33	400 nM	292 nt
Phosphate transporter	PTA3	JGI: 22152	F: CATCCTCTACGGCATCACCAAG R: ATCCAGAAGACGGAGTTGACGC	104.9	22-36	300 nM	141 nt
Ubiquitin-conjugating enzyme	UbE2	NCBI: EH058515	F: GCGAGCTCCAGGACTTTATG R: CGGGGTCGAGGAAGTAGAC	102.7	28-35	400 nM	192 nt

Table 3. Nutrient concentrations from the phosphorus and nitrogen experiments. Numbers are reported as the average ± standard deviation of 2 or 3 measurements from a single biological sample.

Sample (biological replicate):	Day(s) after inoculation:	µM NH_4^+:		µM Silicate:		µM PO_4^{3-}:		µM NO_2^-+NO_3^-:	
low P 4-27 (1)	1 (Figure 1)	0.931	±0.100	58.099	±0.578	1.382	±0.025	958.176	±17.598
low P 4-27 (2)	1 (Figure 1)	0.583	±0.024	87.298	±2.666	1.408	±0.139	951.954	±0.000
low P 4-29 (1)	3 (Figure 1)	0.691	±0.043	55.114	±0.178	1.310	±0.060	909.735	±6.912
low P 4-29 (2)	3 (Figure 1)	0.304	±0.024	84.614	±0.180	1.275	±0.026	1316.925	±8.447
low P 5-1 (1)	5 (Figure 1)	1.157	±0.010	56.559	±0.267	<0.050*		899.180	±4.241
low P 5-1 (2)	5 (Figure 1)	<0.050*		86.960	±0.886	0.156	±0.216	1328.579	±8.820
low P 5-2 (1)	6 (Figure 1)	2.248	±0.240	54.108	±2.577	<0.050*		887.291	±3.456
low P 5-2 (2)	6 (Figure 1)	0.603	±0.052	84.470	±1.333	<0.050*		927.066	±8.799
low P 5-3 (1)	7 (Figure 1)	1.719	±0.030	54.580	±0.755	<0.050*		886.624	±4.400
low P 5-3 (2)	7 (Figure 1)	<0.050*		87.095	±3.658	<0.050*		1233.886	±7.899
low NO_3^- 5-7 (1)	2 (Figure 2)	1.442	±0.212	58.162	±1.733	20.433	±1.785	52.637	±1.408
low NO_3^- 5-7 (2)	2 (Figure 2)	1.161	±0.174	48.672	±2.444	21.740	±1.092	54.566	±0.616
low NO_3^- 5-9 (1)	4 (Figure 2)	<0.050*		80.642	±0.525	22.907	±1.184	32.198	±0.220
low NO_3^- 5-9 (2)	4 (Figure 2)	<0.050*		74.192	±1.362	21.912	±0.503	30.239	±3.784
low NO_3^- 5-10 (1)	5 (Figure 2)	<0.050*		77.298	±0.889	26.698	±0.334	18.417	±0.352
low NO_3^- 5-10 (2)	5 (Figure 2)	<0.050*		56.654	±1.200	22.855	±0.478	18.821	±0.044
low NO_3^- 5-11 (1)	6 (Figure 2)	<0.050*		72.584	±0.444	23.717	±0.045	0.063	
low NO_3^- 5-11 (2)	6 (Figure 2)	<0.050*		54.171	±0.622	24.631	±0.919	0.063	±0.002
low NO_3^- 5-12 (1)	7 (Figure 2)	0.217	±0.010	71.642	±1.777	17.998	±0.417	<0.050*	
low NO_3^- 5-12 (2)	7 (Figure 2)	0.662	±0.221	52.600	±1.333	20.833	±0.084	<0.050*	
low NH_4^+ 5-7 (1)	2 (Figure 3)	77.794	±0.566	81.383	±0.444	24.640	±1.575	2.878	±0.189
low NH_4^+ 5-7 (2)	2 (Figure 3)	68.485	±0.694	50.338	±0.355	15.004	±0.622	2.206	±0.761
low NH_4^+ 5-9 (1)	4 (Figure 3)	63.894	±0.708	74.156	±1.777	22.897	±0.722	2.207	±0.003
low NH_4^+ 5-9 (2)	4 (Figure 3)	60.494	±0.424	73.103	±1.244	27.466	±0.251	2.455	±0.251
low NH_4^+ 5-11 (1)	6 (Figure 3)	50.326	±0.495	79.812	±7.999	21.555	±1.413	1.969	±0.136
low NH_4^+ 5-11 (2)	6 (Figure 3)	49.236	±0.226	52.066	±0.133	20.617	±0.505	2.845	±0.276
low NH_4^+ 5-13 (1)	8 (Figure 3)	7.709	±0.976	76.669	±1.777	23.647	±0.723	2.728	±0.216
low NH_4^+ 5-13 (2)	8 (Figure 3)	6.638	±0.455	49.269	±1.066	32.250	±0.418	2.106	±0.216
low NH_4^+ 5-14 (1)	9 (Figure 3)	0.958	±0.150	79.497	±3.111	20.466	±0.352	<0.050*	
low NH_4^+ 5-14 (2)	9 (Figure 3)	0.158	±0.029	51.831	±1.116	24.633	±0.462	<0.050*	

* Detection limit of the assay

Table 4. Expression data for phosphate transporter (PTA3). A value under "Regulation" shows the fold change of that sample relative to the reference condition (+P control day 6: exponentially growing cells on replete phosphate; Figure 1). Bold indicates statistically signicant (*P*-value<0.05) fold-changes using a pair-wise fixed reallocation randomization analysis based on triplicate wells. The high and low range represent the range of fold-changes calculated from the standard error of the mean (- and + error) for fold-changes.

Gene:	Sample (biological replicate):	Regulation:	Low range:	High range:	(-) error:	(+) error:	*P*-value:	Reference:
PTA3	low P day 4 (1)	ND[1]	-	-	-	-	-	+P control day 6
PTA3	low P day 4 (2)	ND	-	-	-	-	-	+P control day 6
PTA3	low P day 5 (1)	**636.326**	446.596	1044.638	189.730	408.312	0.000	+P control day 6
PTA3	low P day 5 (2)	**376.755**	274.893	467.175	101.862	90.420	0.000	+P control day 6
PTA3	low P day 6 (1)	**2148.111**	1463.828	2966.989	684.283	818.878	0.000	+P control day 6
PTA3	low P day 6 (2)	**1675.419**	1201.020	2127.074	474.399	451.655	0.000	+P control day 6
PTA3	low P day 7 (1)	**548.219**	378.044	843.319	170.175	295.100	0.000	+P control day 6
PTA3	low P day 7 (2)	**597.947**	456.954	776.513	140.993	178.566	0.021	+P control day 6

[1]ND: Not detected, meaning the C_T values were higher than the effective efficiency range for the primers or no amplification occurred at all.

Table 5. Expression data for phosphate transporter (PTA3). A value under "Regulation" shows the fold change of that sample relative to the reference condition (low P day 7: stationary phase P-deficient cells; Figure 1). Bold indicates statistically signicant (*P*-value<0.05) fold-changes using a pair-wise fixed reallocation randomization analysis based on triplicate wells. The high and low range represent the range of fold-changes calculated from the standard error of the mean (- and + error) for fold-changes.

Gene:	Sample (biological replicate):	Regulation:	Low range:	High range:	(-) error:	(+) error:	*P*-value:	Reference:
PTA3	low P/-P T=2h (1)	-1.499	0.000	-1.302	N/A	0.197	0.336	low P day 7 (1)
PTA3	low P/-P T=2h (2)	2.257	1.305	4.240	0.952	2.935	0.170	low P day 7 (2)
PTA3	low P/+P T=2h (1)	**-66.667**	-76.923	-55.556	10.256	11.111	0.000	low P day 7 (1)
PTA3	low P/+P T=2h (2)	**-125.000**	-166.667	-71.429	41.667	53.571	0.000	low P day 7 (2)
PTA3	low P/-P T=4h (1)	2.268	1.704	2.843	0.564	0.575	0.165	low P day 7 (1)
PTA3	low P/-P T=4h (2)	1.052	0.707	1.769	0.345	0.717	0.903	low P day 7 (2)
PTA3	low P/+P T=4h (1)	**-1000.000**	-1000.000	-500.000	0.000	500.000	0.000	low P day 7 (1)
PTA3	low P/+P T=4h (2)	**-250.000**	-1000.000	-66.667	750.000	183.333	0.000	low P day 7 (2)
PTA3	low P/-P T=6h (1)	1.217	0.628	3.467	0.589	2.250	0.907	low P day 7 (1)
PTA3	low P/-P T=6h (2)	**4.470**	2.579	6.707	1.891	2.237	0.033	low P day 7 (2)
PTA3	low P/+P T=6h (1)	ND[1]	-	-	-	-	-	low P day 7 (1)
PTA3	low P/+P T=6h (2)	**-200.000**	-333.333	-111.111	133.333	88.889	0.000	low P day 7 (2)
PTA3	low P/-P T=24h (1)	-7.246	-28.571	-1.647	21.325	5.599	0.106	low P day 7 (1)
PTA3	low P/-P T=24h (2)	**2.372**	1.337	3.379	1.035	1.007	0.000	low P day 7 (2)
PTA3	low P/+P T=24h (1)	ND	-	-	-	-	-	low P day 7 (1)
PTA3	low P/+P T=24h (2)	ND	-	-	-	-	-	low P day 7 (2)
PTA3	low P/-P T=48h (1)	-1.143	-1.276	-1.019	0.133	0.123	0.490	low P day 7 (1)
PTA3	low P/-P T=48h (2)	1.073	0.634	2.094	0.439	1.021	0.830	low P day 7 (2)
PTA3	low P/+P T=48h (1)	ND	-	-	-	-	-	low P day 7 (1)
PTA3	low P/+P T=48h (2)	ND	-	-	-	-	-	low P day 7 (2)

[1]ND: Not detected, meaning the C_T values were higher than the effective efficiency range for the primers or no amplification occurred at all.

Table 6. Expression data for xanthine/uracil/vitamin C permease (XUV), acetamidase/formamidase (FMD2), urea transporter (DUR2), and formate/nitirte transporter (NAR1.3). A value under "Regulation" shows the fold change of that sample relative to the reference condition (low NH_4^+ day 7: exponentially growing cells on ammonium; Figure 4). Bold indicates statistically signicant (P-value<0.05) fold-changes using a pair-wise fixed reallocation randomization analysis based on triplicate wells. The high and low range represent the range of fold-changes calculated from the standard error of the mean (- and + error) for fold-changes.

Gene:	Sample (biological replicate):	Regulation:	Low range:	High range:	(-) error:	(+) error:	*P*-value:	Reference:
XUV	low NO_3 day 5 (1)	2.237	1.059	5.769	1.178	3.532	0.202	low NH_4^+ day 7
XUV	low NO_3 day 5 (2)	**5.885**	4.485	7.956	1.400	3.471	0.000	low NH_4^+ day 7
XUV	low NO_3 day 6 (1)	**16.445**	9.953	32.485	6.492	16.040	0.000	low NH_4^+ day 7
XUV	low NO_3 day 6 (2)	**33.032**	25.440	39.022	7.592	13.582	0.000	low NH_4^+ day 7
XUV	low NO_3 day 7 (1)	**54.988**	26.762	94.600	28.226	39.612	0.000	low NH_4^+ day 7
XUV	low NO_3 day 7 (2)	**44.185**	36.290	54.694	7.895	18.404	0.036	low NH_4^+ day 7
NAR1.3	low NO_3 day 5 (1)	**1.918**	1.080	2.783	0.838	0.865	0.020	low NH_4^+ day 7
NAR1.3	low NO_3 day 5 (2)	**6.104**	1.712	36.083	4.392	29.979	0.000	low NH_4^+ day 7
NAR1.3	low NO_3 day 6 (1)	**36.046**	23.850	48.814	12.196	12.768	0.008	low NH_4^+ day 7
NAR1.3	low NO_3 day 6 (2)	**56.269**	35.176	94.147	21.093	37.878	0.000	low NH_4^+ day 7
NAR1.3	low NO_3 day 7 (1)	**47.553**	34.430	61.293	13.123	13.740	0.010	low NH_4^+ day 7
NAR1.3	low NO_3 day 7 (2)	**12.855**	7.717	22.141	5.138	9.286	0.000	low NH_4^+ day 7
DUR2	low NO_3 day 5 (1)	-2.037	-4.132	-1.170	2.096	0.867	0.127	low NH_4^+ day 7
DUR2	low NO_3 day 5 (2)	5.295	3.631	6.983	1.664	1.688	0.053	low NH_4^+ day 7
DUR2	low NO_3 day 6 (1)	**5.505**	4.303	8.139	1.202	2.634	0.033	low NH_4^+ day 7
DUR2	low NO_3 day 6 (2)	**10.653**	9.064	13.572	1.589	2.919	0.000	low NH_4^+ day 7
DUR2	low NO_3 day 7 (1)	**12.628**	10.008	19.039	2.620	6.411	0.000	low NH_4^+ day 7
DUR2	low NO_3 day 7 (2)	**9.848**	8.756	11.840	1.092	1.992	0.000	low NH_4^+ day 7
FMD2	low NO_3 day 5 (1)	ND[1]	-	-	-	-	-	low NH_4^+ day 7
FMD2	low NO_3 day 5 (2)	**18.157**	8.258	36.106	9.899	17.949	0.030	low NH_4^+ day 7
FMD2	low NO_3 day 6 (1)	**9.942**	4.457	17.529	5.485	7.587	0.019	low NH_4^+ day 7
FMD2	low NO_3 day 6 (2)	**12.484**	6.089	26.068	6.395	13.584	0.000	low NH_4^+ day 7
FMD2	low NO_3 day 7 (1)	**8.536**	4.249	16.339	4.287	7.803	0.000	low NH_4^+ day 7
FMD2	low NO_3 day 7 (2)	3.558	1.76	7.204	1.798	3.646	0.141	low NH_4^+ day 7

[1]ND: Not detected, meaning the C_T values were higher than the effective efficiency range for the primers or no amplification occurred at all.

Table 7. Expression data for xanthine/uracil/vitamin C permease (XUV), acetamidase/formamidase (FMD2), urea transporter (DUR2), and formate/nitirte transporter (NAR1.3). A value under "Regulation" shows the fold change of that sample relative to the reference condition (low NH_4^+ day 7: exponentially growing cells on ammonium; Figure 3). Bold indicates statistically signicant (*P*-value<0.05) fold-changes using a pair-wise fixed reallocation randomization analysis based on triplicate wells. The high and low range represent the range of fold-changes calculated from the standard error of the mean (- and + error) for fold-changes.

Gene:	Sample (biological replicate):	Regulation:	Low range:	High range:	(-) error:	(+) error:	*P*-value:	Reference:
XUV	NH_4^+ day 8 (1)	1.737	0.915	3.543	0.822	1.806	0.193	low NH_4^+ day 7
XUV	NH_4^+ day 8 (2)	1.015	0.797	1.267	0.218	0.252	0.868	low NH_4^+ day 7
XUV	NH_4^+ day 9 (1)	**21.247**	9.948	44.746	11.299	23.499	0.008	low NH_4^+ day 7
XUV	NH_4^+ day 9 (2)	**50.050**	42.978	60.215	7.072	10.165	0.012	low NH_4^+ day 7
NAR1.3	NH_4^+ day 8 (1)	-1.037	-2.525	-0.467	1.488	0.571	0.894	low NH_4^+ day 7
NAR1.3	NH_4^+ day 8 (2)	**15.979**	7.890	28.455	8.089	12.476	0.000	low NH_4^+ day 7
NAR1.3	NH_4^+ day 9 (1)	**10.792**	7.169	17.334	3.623	6.542	0.000	low NH_4^+ day 7
NAR1.3	NH_4^+ day 9 (2)	**10.452**	5.910	20.984	4.542	10.532	0.000	low NH_4^+ day 7
DUR2	NH_4^+ day 8 (1)	**1.833**	1.482	2.130	0.351	0.297	0.035	low NH_4^+ day 7
DUR2	NH_4^+ day 8 (2)	**2.908**	1.723	4.628	1.185	1.720	0.000	low NH_4^+ day 7
DUR2	NH_4^+ day 9 (1)	**7.160**	6.294	9.045	0.866	1.885	0.036	low NH_4^+ day 7
DUR2	NH_4^+ day 9 (2)	**4.738**	2.906	7.360	1.832	2.622	0.000	low NH_4^+ day 7
FMD2	NH_4^+ day 8 (1)	1.399	0.603	3.309	0.796	1.910	0.593	low NH_4^+ day 7
FMD2	NH_4^+ day 8 (2)	-1.018	-2.632	-0.406	1.613	0.612	0.900	low NH_4^+ day 7
FMD2	NH_4^+ day 9 (1)	3.073	1.465	7.724	1.608	4.651	0.099	low NH_4^+ day 7
FMD2	NH_4^+ day 9 (2)	**4.507**	2.280	9.451	2.227	4.944	0.000	low NH_4^+ day 7

Table 8. Expression data for xanthine/uracil/vitamin C permease (XUV), acetamidase/formamidase (FMD2), urea transporter (DUR2), and formate/nitirte transporter (NAR1.3). A value under "Regulation" shows the fold change of that sample relative to the reference condition (low NO_3^- day 7: stationary phase N-deficient cells grown on nitrate; Figure 3). Bold indicates statistically signicant (*P*-value<0.05) fold-changes using a pair-wise fixed reallocation randomization analysis based on triplicate wells. The high and low range represent the range of fold-changes calculated from the standard error of the mean (- and + error) for fold-changes.

Gene:	Sample (biological replicate):	Regulation:	Low range:	High range:	(-) error:	(+) error:	*P*-value:	Reference:
XUV	low NO_3^-/-NO_3^- T=2h (1)	**2.374**	1.541	3.833	0.833	1.459	0.000	low NO_3^- day 7 (2)
XUV	low NO_3^-/-NO_3^- T=2h (2)	2.700	1.460	4.264	-	-	0.094	low NO_3^- day 7 (2)
XUV	low NO_3^-/+NO_3^- T=2h (1)	**-100.000**	-125.000	-55.556	25.000	44.444	0.037	low NO_3 day 7 (2)
XUV	low NO_3^-/+NO_3^- T=2h (2)	**-47.619**	-62.500	-34.483	14.881	13.136	0.034	low NO_3 day 7 (2)
XUV	low NO_3^-/-NO_3^- T=4h (1)	**5.627**	3.834	9.505	1.793	3.878	0.000	low NO_3 day 7 (2)
XUV	low NO_3^-/-NO_3^- T=4h (2)	**2.290**	1.809	2.804	0.481	0.514	0.000	low NO_3 day 7 (2)
XUV	low NO_3^-/+NO_3^- T=4h (1)	**-41.667**	-111.111	-19.231	69.444	22.436	0.033	low NO_3 day 7 (2)
XUV	low NO_3^-/+NO_3^- T=4h (2)	**-18.519**	-22.727	-14.706	4.209	3.813	0.000	low NO_3 day 7 (2)
XUV	low NO_3^-/-NO_3^- T=6h (1)	-1.274	-4.587	-0.447	3.313	0.827	0.766	low NO_3 day 7 (2)
XUV	low NO_3^-/-NO_3^- T=6h (2)	3.336	3.021	3.962	0.315	0.626	0.058	low NO_3 day 7 (2)
XUV	low NO_3^-/+NO_3^- T=6h (1)	**-90.909**	-333.333	-21.277	242.424	69.632	0.010	low NO_3 day 7 (2)
XUV	low NO_3^-/+NO_3^- T=6h (2)	**-50.000**	-62.500	-35.714	12.500	14.286	0.000	low NO_3 day 7 (2)
XUV	low NO_3^-/-NO_3^- T=24h (1)	**-3.311**	-6.711	-1.493	3.400	1.819	0.000	low NO_3 day 7 (2)
XUV	low NO_3^-/-NO_3^- T=24h (2)	N/A	-	-	-	-	-	low NO_3 day 7 (2)
XUV	low NO_3^-/+NO_3^- T=24h (1)	ND[1]	-	-	-	-	-	low NO_3 day 7 (2)
XUV	low NO_3^-/+NO_3^- T=24h (2)	**-52.632**	-90.909	-23.810	38.278	28.822	0.030	low NO_3 day 7 (2)
XUV	low NO_3^-/-NO_3^- T=48h (1)	-1.570	-5.650	-0.389	4.080	1.181	0.648	low NO_3 day 7 (2)
XUV	low NO_3^-/-NO_3^- T=48h (2)	-1.045	-3.861	-0.251	2.816	0.794	1.000	low NO_3 day 7 (2)
XUV	low NO_3^-/+NO_3^- T=48h (1)	ND	-	-	-	-	-	low NO_3 day 7 (2)
XUV	low NO_3^-/+NO_3^- T=48h (2)	ND	-	-	-	-	-	low NO_3 day 7 (2)
NAR1.3	low NO_3^-/-NO_3^- T=2h (1)	1.885	0.948	3.024	0.937	1.139	0.290	low NO_3^- day 7 (1)
NAR1.3	low NO_3^-/-NO_3^- T=2h (2)	3.379	1.581	5.808	1.798	2.429	0.102	low NO_3^- day 7 (2)
NAR1.3	low NO_3^-/+NO_3^- T=2h (1)	**-4.016**	-7.143	-2.381	3.127	1.635	0.000	low NO_3 day 7 (1)
NAR1.3	low NO_3^-/+NO_3^- T=2h (2)	**-1.131**	-1.212	-1.029	0.081	0.102	0.018	low NO_3 day 7 (2)
NAR1.3	low NO_3^-/-NO_3^- T=4h (1)	**-1.883**	-2.899	-1.152	1.015	0.731	0.023	low NO_3 day 7 (1)
NAR1.3	low NO_3^-/-NO_3^- T=4h (2)	**-1.567**	-2.062	-1.079	0.494	0.489	0.050	low NO_3 day 7 (2)
NAR1.3	low NO_3^-/+NO_3^- T=4h (1)	**-10.101**	-16.949	-6.452	6.848	3.649	0.000	low NO_3 day 7 (1)
NAR1.3	low NO_3^-/+NO_3^- T=4h (2)	**-4.274**	-8.264	-2.833	3.991	1.441	0.000	low NO_3 day 7 (2)
NAR1.3	low NO_3^-/-NO_3^- T=6h (1)	1.178	0.911	1.718	0.267	0.540	0.477	low NO_3 day 7 (1)
NAR1.3	low NO_3^-/-NO_3^- T=6h (2)	1.751	1.042	2.539	0.709	0.788	0.085	low NO_3 day 7 (2)
NAR1.3	low NO_3^-/+NO_3^- T=6h (1)	**-17.241**	-27.027	-12.048	9.786	5.193	0.001	low NO_3 day 7 (1)
NAR1.3	low NO_3^-/+NO_3^- T=6h (2)	**-7.813**	-16.949	-4.673	9.137	3.140	0.000	low NO_3 day 7 (2)
NAR1.3	low NO_3^-/-NO_3^- T=24h (1)	-1.088	-1.661	-0.623	0.573	0.465	0.681	low NO_3 day 7 (1)
NAR1.3	low NO_3^-/-NO_3^- T=24h (2)	N/A	-	-	-	-	-	low NO_3 day 7 (2)
NAR1.3	low NO_3^-/+NO_3^- T=24h (1)	N/A	-	-	-	-	-	low NO_3 day 7 (1)
NAR1.3	low NO_3^-/+NO_3^- T=24h (2)	**-5.348**	-7.937	-4.115	2.589	1.232	0.000	low NO_3 day 7 (2)
NAR1.3	low NO_3^-/-NO_3^- T=48h (1)	**-1.689**	-2.375	-1.163	0.686	0.526	0.039	low NO_3 day 7 (1)
NAR1.3	low NO_3^-/-NO_3^- T=48h (2)	1.401	0.687	3.567	0.714	2.166	0.704	low NO_3 day 7 (2)
NAR1.3	low NO_3^-/+NO_3^- T=48h (1)	**-9.434**	-15.152	-6.494	5.718	2.940	0.000	low NO_3 day 7 (1)
NAR1.3	low NO_3^-/+NO_3^- T=48h (2)	**-4.405**	-7.042	-3.115	2.637	1.290	0.000	low NO_3 day 7 (2)
DUR2	low NO_3^-/-NO_3^- T=2h (1)	-1.330	-2.625	-0.925	1.295	0.405	0.683	low NO_3 day 7 (1)
DUR2	low NO_3^-/-NO_3^- T=2h (2)	3.023	1.232	7.108	1.791	4.085	0.164	low NO_3 day 7 (2)
DUR2	low NO_3^-/+NO_3^- T=2h (1)	**-10.309**	-11.905	-9.174	1.595	1.135	0.040	low NO_3 day 7 (1)
DUR2	low NO_3^-/+NO_3^- T=2h (2)	**-5.263**	-6.135	-4.255	0.872	1.008	0.000	low NO_3 day 7 (2)
DUR2	low NO_3^-/-NO_3^- T=4h (1)	-1.992	-3.067	-0.924	1.075	1.068	0.109	low NO_3 day 7 (1)
DUR2	low NO_3^-/-NO_3^- T=4h (2)	1.000	0.638	1.741	0.362	0.741	0.986	low NO_3 day 7 (2)

DUR2	low NO_3^-/+NO_3^- T=4h (1)	**-12.346**	-20.833	-5.952	8.488	6.393	0.003	low NO_3 day 7 (1)
DUR2	low NO_3^-/+NO_3^- T=4h (2)	**-2.770**	-4.425	-1.761	1.655	1.010	0.025	low NO_3 day 7 (2)
DUR2	low NO_3^-/-NO_3^- T=6h (1)	1.083	0.674	1.614	0.409	0.531	0.830	low NO_3 day 7 (1)
DUR2	low NO_3^-/-NO_3^- T=6h (2)	**2.307**	1.333	3.561	0.974	1.254	0.041	low NO_3 day 7 (2)
DUR2	low NO_3^-/+NO_3^- T=6h (1)	**-8.264**	-12.658	-5.587	4.394	2.678	0.001	low NO_3 day 7 (1)
DUR2	low NO_3^-/+NO_3^- T=6h (2)	**-2.924**	-4.587	-1.821	1.663	1.102	0.036	low NO_3 day 7 (2)
DUR2	low NO_3^-/-NO_3^- T=24h (1)	**-3.175**	-4.950	-1.757	1.776	1.417	0.000	low NO_3 day 7 (1)
DUR2	low NO_3^-/-NO_3^- T=24h (2)	N/A	-	-	-	-	-	low NO_3 day 7 (2)
DUR2	low NO_3^-/+NO_3^- T=24h (1)	N/A	-	-	-	-	-	low NO_3 day 7 (1)
DUR2	low NO_3^-/+NO_3^- T=24h (2)	**-6.849**	-7.576	-5.714	0.726	1.135	0.000	low NO_3 day 7 (2)
DUR2	low NO_3^-/-NO_3^- T=48h (1)	**-2.538**	-3.802	-1.859	1.264	0.679	0.000	low NO_3 day 7 (1)
DUR2	low NO_3^-/-NO_3^- T=48h (2)	1.154	0.555	2.093	0.599	0.939	0.760	low NO_3 day 7 (2)
DUR2	low NO_3^-/+NO_3^- T=48h (1)	**-50.000**	-71.429	-34.483	21.429	15.517	0.001	low NO_3 day 7 (1)
DUR2	low NO_3^-/+NO_3^- T=48h (2)	**-10.989**	-18.182	-6.211	7.193	4.778	0.000	low NO_3 day 7 (2)
FMD2	low NO_3^-/-NO_3^- T=2h (1)	-1.429	-2.618	-0.739	1.189	0.689	0.473	low NO_3 day 7 (1)
FMD2	low NO_3^-/-NO_3^- T=2h (2)	ND	-	-	-	-	-	low NO_3 day 7 (2)
FMD2	low NO_3^-/+NO_3^- T=2h (1)	ND	-	-	-	-	-	low NO_3 day 7 (1)
FMD2	low NO_3^-/+NO_3^- T=2h (2)	ND	-	-	-	-	-	low NO_3 day 7 (2)
FMD2	low NO_3^-/-NO_3^- T=4h (1)	**-2.740**	-4.444	-1.656	1.705	1.084	0.019	low NO_3 day 7 (1)
FMD2	low NO_3^-/-NO_3^- T=4h (2)	1.322	0.930	2.077	0.392	0.755	0.342	low NO_3 day 7 (2)
FMD2	low NO_3^-/+NO_3^- T=4h (1)	ND	-	-	-	-	-	low NO_3 day 7 (1)
FMD2	low NO_3^-/+NO_3^- T=4h (2)	**-3.906**	-7.407	-2.119	3.501	1.788	0.018	low NO_3 day 7 (2)
FMD2	low NO_3^-/-NO_3^- T=6h (1)	1.072	0.548	2.028	0.524	0.956	0.907	low NO_3 day 7 (1)
FMD2	low NO_3^-/-NO_3^- T=6h (2)	**3.806**	1.953	9.010	1.853	5.204	0.002	low NO_3 day 7 (2)
FMD2	low NO_3^-/+NO_3^- T=6h (1)	**-21.277**	-34.483	-11.628	13.206	9.649	0.002	low NO_3 day 7 (1)
FMD2	low NO_3^-/+NO_3^- T=6h (2)	-3.534	-6.494	-1.866	2.960	1.668	0.061	low NO_3 day 7 (2)
FMD2	low NO_3^-/-NO_3^- T=24h (1)	-2.358	-11.765	-0.689	9.406	1.669	0.496	low NO_3 day 7 (1)
FMD2	low NO_3^-/-NO_3^- T=24h (2)	N/A	-	-	-	-	-	low NO_3 day 7 (2)
FMD2	low NO_3^-/+NO_3^- T=24h (1)	N/A	-	-	-	-	-	low NO_3 day 7 (1)
FMD2	low NO_3^-/+NO_3^- T=24h (2)	ND	-	-	-	-	-	low NO_3 day 7 (2)
FMD2	low NO_3^-/-NO_3^- T=48h (1)	-1.669	-3.731	-0.723	2.062	0.947	0.375	low NO_3 day 7 (1)
FMD2	low NO_3^-/-NO_3^- T=48h (2)	**7.696**	4.412	15.657	3.284	7.961	0.002	low NO_3 day 7 (2)
FMD2	low NO_3^-/+NO_3^- T=48h (1)	**-21.277**	-37.037	-10.101	15.760	11.176	0.003	low NO_3 day 7 (1)
FMD2	low NO_3^-/+NO_3^- T=48h (2)	-2.262	-5.587	-0.976	3.324	1.287	0.236	low NO_3 day 7 (2)

[1]ND: Not detected, meaning the C_T values were higher than the effective efficiency range for the primers or no amplification occurred at all.

Table 9. Expression data for xanthine/uracil/vitamin C Permease (XUV), acetamidase/formamidase (FMD2), urea transporter (DUR2), and formate/nitirte transporter (NAR1.3). A value under "Regulation" shows the fold change of that sample relative to the reference condition (low NH_4^+ day 9: stationary phase N-deficient cells grown on ammonium; Figure 4). Bold indicates statistically signicant (*P*-value<0.05) fold-changes using a pair-wise fixed reallocation randomization analysis based on triplicate wells. The high and low range represent the range of fold-changes calculated from the standard error of the mean (- and + error) for fold-changes.

Gene:	Sample (biological replicate):	Regulation:	Low Range:	High Range:	(-) error:	(+) error:	*P*-value:	Reference:
XUV	low NH_4^+/-NH_4^+ T=2 h (1)	1.222	0.713	1.779	0.509	0.557	0.323	low NH_4^+ day 9 (1)
XUV	low NH_4^+/-NH_4^+ T=2 h (2)	-1.410	-3.115	-0.548	1.705	0.862	0.581	low NH_4^+ day 9 (2)
XUV	low NH_4^+/+NH_4^+ T=2 h (1)	ND[1]	-	-	-	-	-	low NH_4^+ day 9 (1)
XUV	low NH_4^+/+NH_4^+ T=2 h (2)	**-125.000**	-142.857	-111.111	17.857	13.889	0.000	low NH_4^+ day 9 (2)
XUV	low NH_4^+/-NH_4^+ T=4 h (1)	1.210	0.717	2.031	0.493	0.821	0.561	low NH_4^+ day 9 (1)
XUV	low NH_4^+/-NH_4^+ T=4 h (2)	**-4.348**	-8.850	-2.688	4.502	1.660	0.000	low NH_4^+ day 9 (2)
XUV	low NH_4^+/+NH_4^+ T=4 h (1)	ND	-	-	-	-	-	low NH_4^+ day 9 (1)
XUV	low NH_4^+/+NH_4^+ T=4 h (2)	ND	-	-	-	-	-	low NH_4^+ day 9 (2)
XUV	low NH_4^+/-NH_4^+ T=6 h (1)	1.593	1.115	2.960	0.478	1.367	0.088	low NH_4^+ day 9 (1)
XUV	low NH_4^+/-NH_4^+ T=6 h (2)	-1.439	-3.289	-0.848	1.851	0.591	0.804	low NH_4^+ day 9 (2)
XUV	low NH_4^+/+NH_4^+ T=6 h (1)	**-50.000**	-125.000	-15.385	75.000	34.615	0.024	low NH_4^+ day 9 (1)
XUV	low NH_4^+/+NH_4^+ T=6 h (2)	ND	-	-	-	-	-	low NH_4^+ day 9 (2)
XUV	low NH_4^+/-NH_4^+ T=24 h (1)	**-3.205**	-5.495	-2.141	2.289	1.064	0.030	low NH_4^+ day 9 (1)
XUV	low NH_4^+/-NH_4^+ T=24 h (2)	-3.155	-5.495	-1.718	2.340	1.436	0.181	low NH_4^+ day 9 (2)
XUV	low NH_4^+/+NH_4^+ T=24 h (1)	**-9.615**	-16.129	-6.173	6.514	3.443	0.000	low NH_4^+ day 9 (1)
XUV	low NH_4^+/+NH_4^+ T=24 h (2)	**-15.625**	-28.571	-10.204	12.946	5.421	0.000	low NH_4^+ day 9 (2)
XUV	low NH_4^+/-NH_4^+ T=48 h (2)	**-22.222**	-25.000	-20.000	2.778	2.222	0.000	low NH_4^+ day 9 (1)
XUV	low NH_4^+/+NH_4^+ T=48 h (2)	-13.699	-33.333	-5.587	19.635	8.112	0.176	low NH_4^+ day 9 (2)
NAR1.3	low NH_4^+/-NH_4^+ T=2 h (1)	2.657	1.816	3.633	0.841	0.976	0.100	low NH_4^+ day 9 (1)
NAR1.3	low NH_4^+/-NH_4^+ T=2 h (2)	1.541	1.267	1.892	0.274	0.351	0.106	low NH_4^+ day 9 (2)
NAR1.3	low NH_4^+/+NH_4^+ T=2 h (1)	ND	-	-	-	-	-	low NH_4^+ day 9 (1)
NAR1.3	low NH_4^+/+NH_4^+ T=2 h (2)	**-45.455**	-76.923	-26.316	31.469	19.139	0.023	low NH_4^+ day 9 (2)
NAR1.3	low NH_4^+/-NH_4^+ T=4 h (1)	1.768	1.396	2.719	0.372	0.951	0.104	low NH_4^+ day 9 (1)
NAR1.3	low NH_4^+/-NH_4^+ T=4 h (2)	**-2.342**	-2.959	-1.709	0.617	0.633	0.000	low NH_4^+ day 9 (2)
NAR1.3	low NH_4^+/+NH_4^+ T=4 h (1)	**-9.434**	-10.638	-8.130	1.204	1.304	0.000	low NH_4^+ day 9 (1)
NAR1.3	low NH_4^+/+NH_4^+ T=4 h (2)	**-11.111**	-20.833	-4.608	9.722	6.503	0.000	low NH_4^+ day 9 (2)
NAR1.3	low NH_4^+/-NH_4^+ T=6 h (1)	-1.312	-2.137	-0.901	0.824	0.411	0.451	low NH_4^+ day 9 (1)
NAR1.3	low NH_4^+/-NH_4^+ T=6 h (2)	-2.358	-3.135	-1.818	0.776	0.540	0.103	low NH_4^+ day 9 (2)
NAR1.3	low NH_4^+/+NH_4^+ T=6 h (1)	**-18.182**	-20.000	-15.873	1.818	2.309	0.011	low NH_4^+ day 9 (1)
NAR1.3	low NH_4^+/+NH_4^+ T=6 h (2)	**-6.410**	-10.753	-3.344	4.342	3.066	0.000	low NH_4^+ day 9 (2)
NAR1.3	low NH_4^+/-NH_4^+ T=24 h (1)	-1.486	-3.704	-0.611	2.218	0.875	0.550	low NH_4^+ day 9 (1)
NAR1.3	low NH_4^+/-NH_4^+ T=24 h (2)	-1.376	-3.378	-0.333	2.003	1.042	0.709	low NH_4^+ day 9 (2)
NAR1.3	low NH_4^+/+NH_4^+ T=24 h (1)	-1.159	-2.151	-0.752	0.992	0.406	0.698	low NH_4^+ day 9 (1)
NAR1.3	low NH_4^+/+NH_4^+ T=24 h (2)	-1.362	-2.347	-0.619	0.985	0.743	0.585	low NH_4^+ day 9 (2)
NAR1.3	low NH_4^+/-NH_4^+ T=48 h (1)	-1.309	-2.137	-0.894	0.828	0.415	0.392	low NH_4^+ day 9 (1)
NAR1.3	low NH_4^+/-NH_4^+ T=48 h (2)	1.274	0.866	1.919	0.408	0.645	0.346	low NH_4^+ day 9 (2)
NAR1.3	low NH_4^+/+NH_4^+ T=48 h (1)	1.052	0.927	1.227	0.125	0.175	0.424	low NH_4^+ day 9 (1)
NAR1.3	low NH_4^+/+NH_4^+ T=48 h (2)	-1.558	-2.967	-0.655	1.410	0.902	0.375	low NH_4^+ day 9 (2)
DUR2	low NH_4^+/-NH_4^+ T=2 h (1)	1.136	0.783	1.770	0.353	0.634	0.654	low NH_4^+ day 9 (1)
DUR2	low NH_4^+/-NH_4^+ T=2 h (2)	2.090	1.403	2.952	0.687	0.862	0.106	low NH_4^+ day 9 (2)
DUR2	low NH_4^+/+NH_4^+ T=2 h (1)	**-5.882**	-8.264	-3.155	2.382	2.728	0.000	low NH_4^+ day 9 (1)
DUR2	low NH_4^+/+NH_4^+ T=2 h (2)	**-12.048**	-17.544	-9.091	5.496	2.957	0.016	low NH_4^+ day 9 (2)
DUR2	low NH_4^+/-NH_4^+ T=4 h (1)	1.190	0.752	1.681	0.438	0.491	0.430	low NH_4^+ day 9 (1)
DUR2	low NH_4^+/-NH_4^+ T=4 h (2)	**1.113**	0.732	1.879	0.381	0.766	0.000	low NH_4^+ day 9 (2)
DUR2	low NH_4^+/+NH_4^+ T=4 h (1)	**-8.772**	-11.765	-7.299	2.993	1.473	0.000	low NH_4^+ day 9 (1)
DUR2	low NH_4^+/+NH_4^+ T=4 h (2)	**-26.316**	-40.000	-18.519	13.684	7.797	0.000	low NH_4^+ day 9 (2)
DUR2	low NH_4^+/-NH_4^+ T=6 h (1)	-1.522	-2.020	-1.302	0.498	0.220	0.069	low NH_4^+ day 9 (1)
DUR2	low NH_4^+/-NH_4^+ T=6 h (2)	-1.357	-2.793	-0.531	1.436	0.826	0.544	low NH_4^+ day 9 (2)
DUR2	low NH_4^+/+NH_4^+ T=6 h (1)	**-4.566**	-7.576	-3.205	3.010	1.361	0.000	low NH_4^+ day 9 (1)

DUR2	low NH_4^+/+NH_4^+ T=6 h (2)	**-22.222**	-34.483	-16.393	12.261	5.829	0.000	low NH_4^+ day 9 (2)
DUR2	low NH_4^+/-NH_4^+ T=24 h (1)	**-2.336**	-3.534	-1.531	1.197	0.805	0.000	low NH_4^+ day 9 (1)
DUR2	low NH_4^+/-NH_4^+ T=24 h (2)	-2.817	-8.000	-1.021	5.183	1.795	0.232	low NH_4^+ day 9 (2)
DUR2	low NH_4^+/+NH_4^+ T=24 h (1)	**-2.088**	-4.149	-1.110	2.062	0.978	0.000	low NH_4^+ day 9 (1)
DUR2	low NH_4^+/+NH_4^+ T=24 h (2)	**-8.850**	-13.158	-5.587	4.308	3.263	0.007	low NH_4^+ day 9 (2)
DUR2	low NH_4^+/-NH_4^+ T=48 h (1)	**-2.717**	-3.448	-1.855	0.731	0.862	0.000	low NH_4^+ day 9 (1)
DUR2	low NH_4^+/-NH_4^+ T=48 h (2)	-2.128	-8.130	-0.770	6.002	1.358	0.123	low NH_4^+ day 9 (2)
DUR2	low NH_4^+/+NH_4^+ T=48 h (1)	-2.525	-3.636	-1.502	1.111	1.024	0.071	low NH_4^+ day 9 (1)
DUR2	low NH_4^+/+NH_4^+ T=48 h (2)	**-6.173**	-11.111	-3.584	4.938	2.589	0.000	low NH_4^+ day 9 (2)
FMD2	low NH_4^+/-NH_4^+ T=2 h (1)	**2.086**	1.236	3.545	0.850	1.459	0.000	low NH_4^+ day 9 (1)
FMD2	low NH_4^+/-NH_4^+ T=2 h (2)	-1.175	-1.859	-0.668	0.684	0.508	0.704	low NH_4^+ day 9 (2)
FMD2	low NH_4^+/+NH_4^+ T=2 h (1)	ND	-	-	-	-	-	low NH_4^+ day 9 (1)
FMD2	low NH_4^+/+NH_4^+ T=2 h (2)	**-35.714**	-55.556	-20.833	19.841	14.881	0.000	low NH_4^+ day 9 (2)
FMD2	low NH_4^+/-NH_4^+ T=4 h (1)	**3.816**	2.585	6.546	1.231	2.730	0.040	low NH_4^+ day 9 (1)
FMD2	low NH_4^+/-NH_4^+ T=4 h (2)	1.792	1.051	3.337	0.741	1.545	0.195	low NH_4^+ day 9 (2)
FMD2	low NH_4^+/+NH_4^+ T=4 h (1)	ND	-	-	-	-	-	low NH_4^+ day 9 (1)
FMD2	low NH_4^+/+NH_4^+ T=4 h (2)	ND	-	-	-	-	-	low NH_4^+ day 9 (2)
FMD2	low NH_4^+/-NH_4^+ T=6 h (1)	-1.508	-2.364	-0.935	0.856	0.574	0.340	low NH_4^+ day 9 (1)
FMD2	low NH_4^+/-NH_4^+ T=6 h (2)	-2.584	-5.495	-1.297	2.911	1.287	0.128	low NH_4^+ day 9 (2)
FMD2	low NH_4^+/+NH_4^+ T=6 h (1)	**-7.937**	-18.868	-3.378	10.931	4.558	0.000	low NH_4^+ day 9 (1)
FMD2	low NH_4^+/+NH_4^+ T=6 h (2)	ND	-	-	-	-	-	low NH_4^+ day 9 (2)
FMD2	low NH_4^+/-NH_4^+ T=24 h (1)	ND	-	-	-	-	-	low NH_4^+ day 9 (1)
FMD2	low NH_4^+/-NH_4^+ T=24 h (2)	-1.282	-10.101	-0.163	8.819	1.119	0.839	low NH_4^+ day 9 (2)
FMD2	low NH_4^+/+NH_4^+ T=24 h (1)	ND	-	-	-	-	-	low NH_4^+ day 9 (1)
FMD2	low NH_4^+/+NH_4^+ T=24 h (2)	ND	-	-	-	-	-	low NH_4^+ day 9 (2)
FMD2	low NH_4^+/-NH_4^+ T=48 h (1)	1.926	1.040	2.719	0.886	0.793	0.148	low NH_4^+ day 9 (1)
FMD2	low NH_4^+/-NH_4^+ T=48 h (2)	1.152	0.607	2.582	0.545	1.430	0.684	low NH_4^+ day 9 (2)
FMD2	low NH_4^+/+NH_4^+ T=48 h (1)	ND	-	-	-	-	-	low NH_4^+ day 9 (1)
FMD2	low NH_4^+/+NH_4^+ T=48 h (2)	ND	-	-	-	-	-	low NH_4^+ day 9 (2)

[1]ND: Not detected, meaning the C_T values were higher than the effective efficiency range for the primers or no amplification occurred at all.

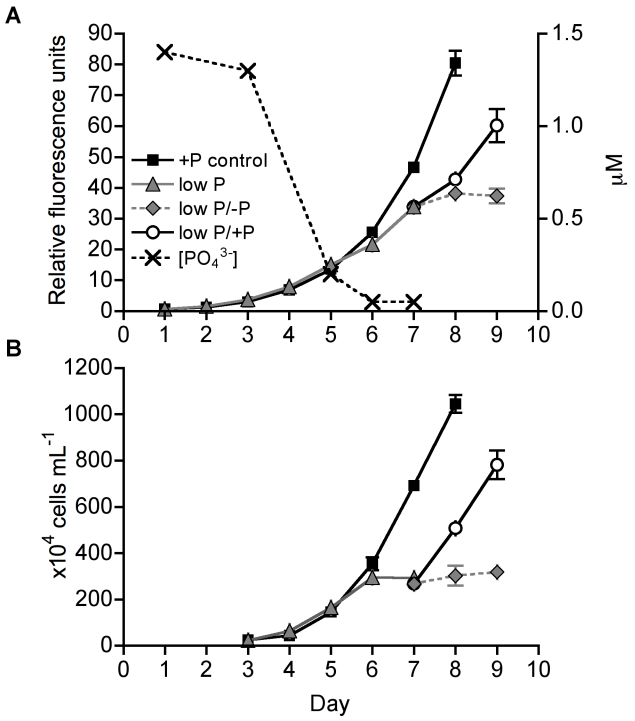

Figure 1. Growth of *A. anophagefferens* in phosphorus replete (+P control) and low phosphorus (low P) conditions tracked by (A) fluorescence and (B) cell concentration. On day 7, low P cells were pooled and redistributed. Phosphorus was re-supplied to two cultures (low P/+P) while two were left unchanged (low P/-P). Error bars represent standard error of the mean of 3 biological replicates for the +P control, 4 biological replicates for the low P, and 2 biological replicates for both low P/-P and low P/+P. External phosphate concentrations are also plotted in panel (A) with error bars representing standard error of the mean of two biological replicates.

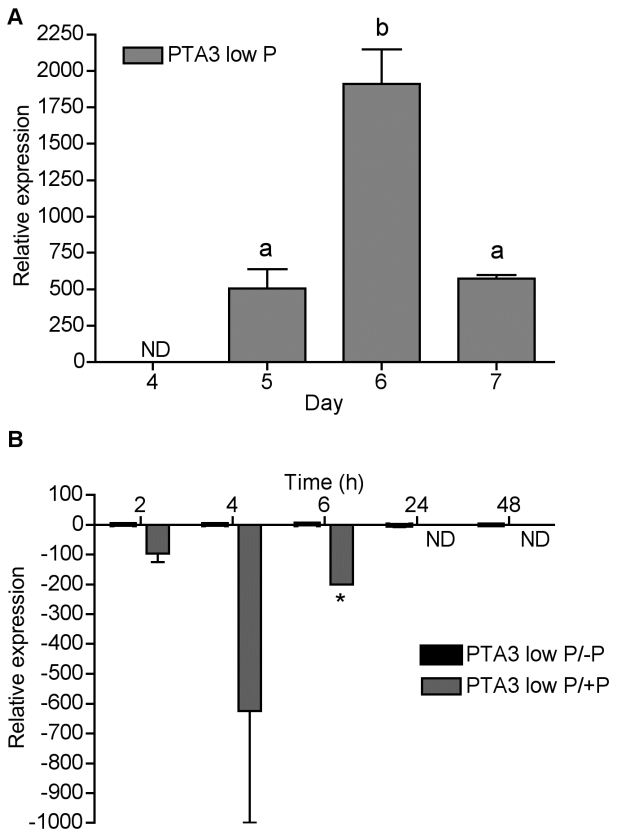

Figure 2. Bar graph comparing the expression of a phosphate transporter (PTA3) over the course of the (A) low P and (B) P re-addition experiments: top low P/-P and bottom low P/+P. Transcript data are plotted as average fold-change relative to a reference condition using the comparative C_T method for qRT-PCR with a reference gene that encodes a ubiquitin-conjugating enzyme. Error bars specify standard error of the average fold change of duplicate biological samples between the sample conditions and the reference condition. Letters indicate statistical difference (*P*-value < 0.05) based upon a one-way ANOVA Tukey post test (e.g "a" is different than "b"). The reference condition for the low P condition was exponentially growing P replete cells (+P control). The reference condition for the P re-addition conditions was T_0 (low P cells day 7). An asterisk (*) indicates that the transcript was only detected in one biological replicate. ND means the transcript was not detected. In graph (B), the data were not significantly different from each other, so no letters are shown.

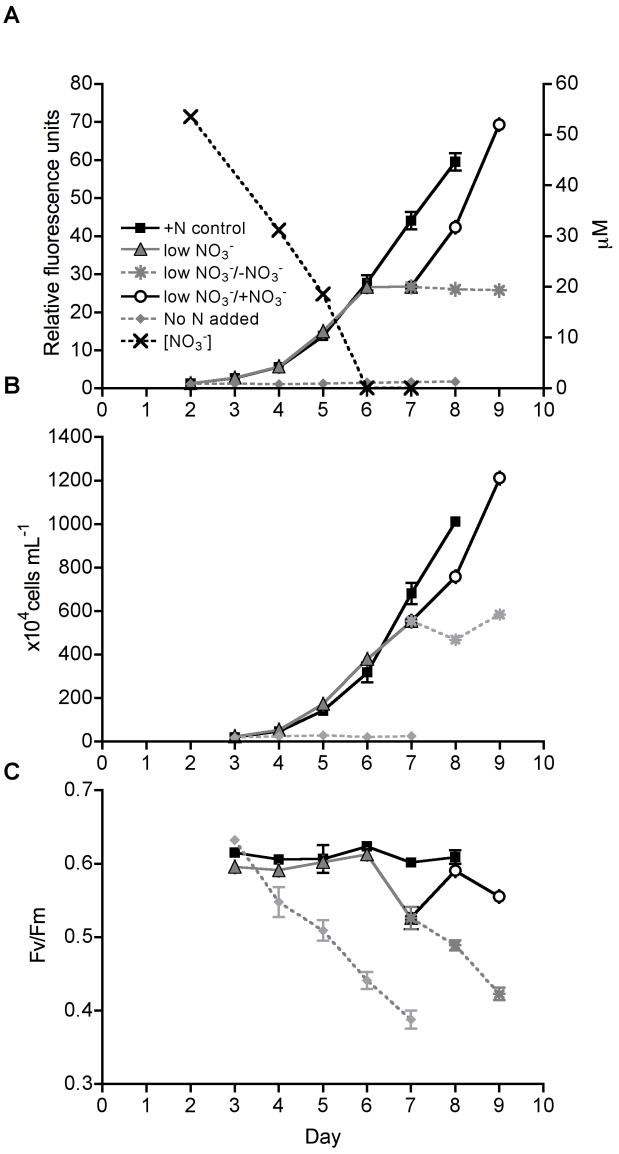

Figure 3. Growth of *A. anophagefferens* under nitrate replete (+N control), low nitrate (low NO_3^-), and no nitrogen added (no N added) conditions tracked by (A) fluorescence and (B) cell concentration. The F_v/F_m ratio was also tracked in all conditions (C). On day 7, low NO_3^- cells were pooled and redistributed. Nitrate was re-supplied to two cultures (low NO_3^-/+NO_3^-) while two were left unchanged (low NO_3^-/-NO_3^-). Error bars represent standard error of the mean of 3 biological replicates for the +N control, low NO_3^-, and no N added conditions and 2 biological replicates for both low NO_3^-/-NO_3^- and low NO_3^-/+NO_3^- conditions. External nitrate concentrations are also plotted in panel (A) with error bars representing standard error of the mean of two biological replicates.

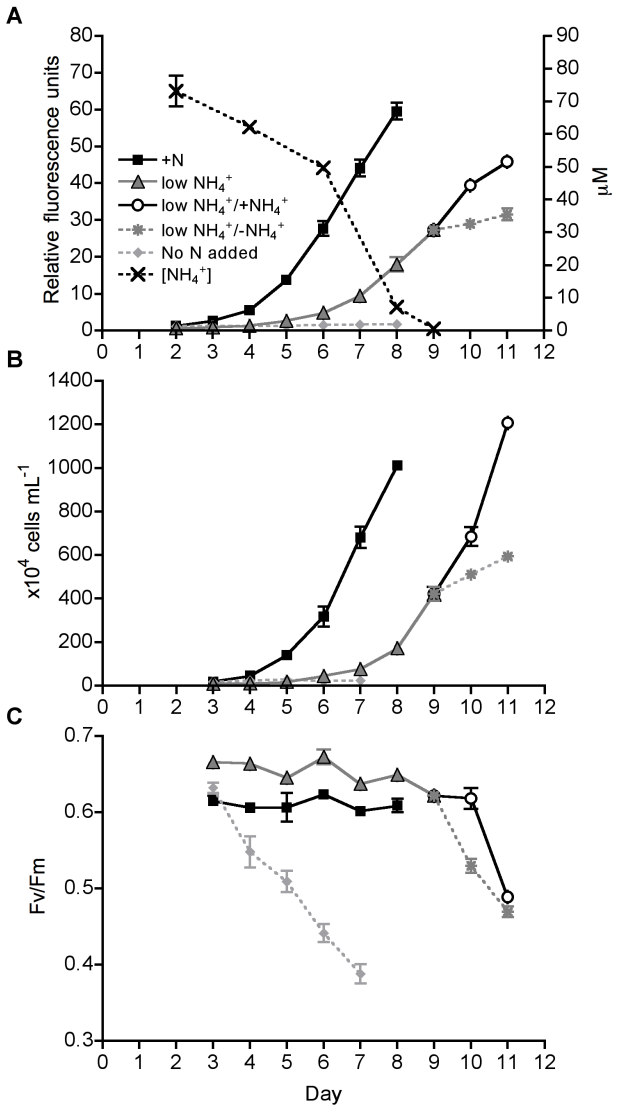

Figure 4. Growth of *A. anophagefferens* under nitrogen replete (+N control), low ammonium (low NH_4^+), and no nitrogen added (no N added) conditions tracked by (A) fluorescence and (B) cell concentration. The F_v/F_m ratio was also tracked in all conditions (C). On day 9, low NH_4^+ cells were pooled and redistributed. Ammonium was re-supplied to two cultures (low NH_4^+/+NH_4^+) while two were left unchanged (low NH_4^+ /-NH_4^+). Error bars represent standard error of the mean of 3 biological replicates for the +N control, low NH_4^+, and no N added conditions and 2 biological replicates for both low NH_4^+/-NH_4^+ and low NH_4^+/+NH_4^+ conditions. External ammonium concentrations are also plotted in panel (A) with error bars representing standard error of the mean of two biological replicates.

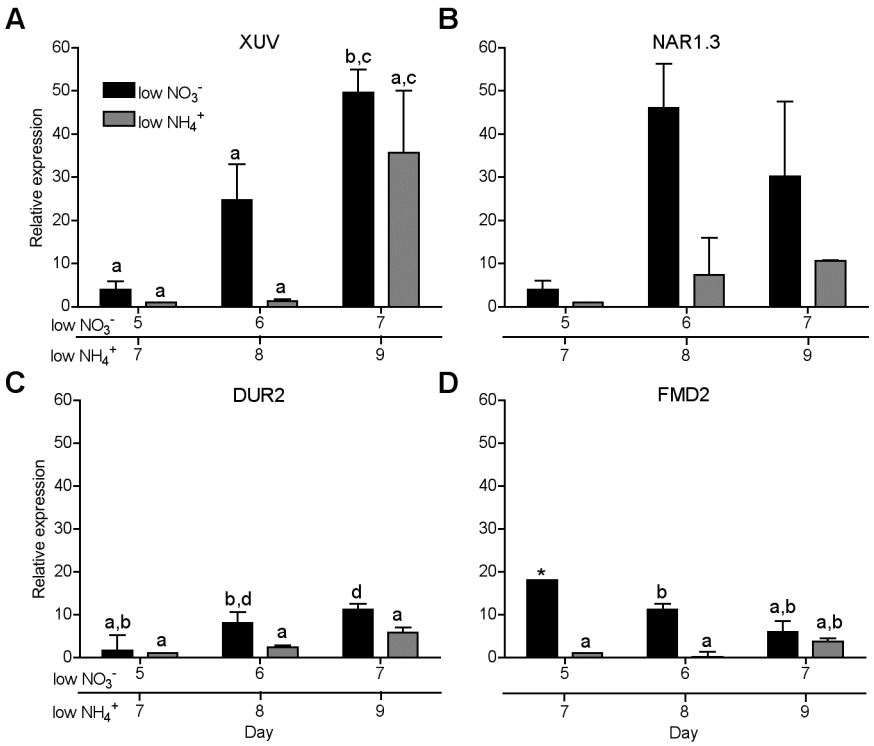

Figure 5. Bar graph comparing the expression of (A) xanthine/uracil/vitamin C permease (XUV), (B) Formate/nitrite transporter (NAR1.3), (C) urea transporter (DUR2), and an acetamidase/formamidase (FMD2) over the course of the low NO_3^- and low NH_4^+ experiments. Transcript data are plotted as average fold-change relative to a reference condition using the comparative C_T method for qRT-PCR with a reference gene that encodes a ubiquitin-conjugating enzyme. Error bars specify standard error of the average fold change of duplicate biological samples between the sample conditions and the reference condition. Letters indicate statistical difference (*P*-value < 0.05) based upon a one-way ANOVA Tukey post test (e.g. "a" is different than "b"). The reference condition for all samples was exponentially growing cells on ammonium (low NH_4^+ day 7). An asterisk (*) indicates that the transcript was only detected in one biological replicate. In graph (B), the data were not significantly different than each other, so no letters are shown.

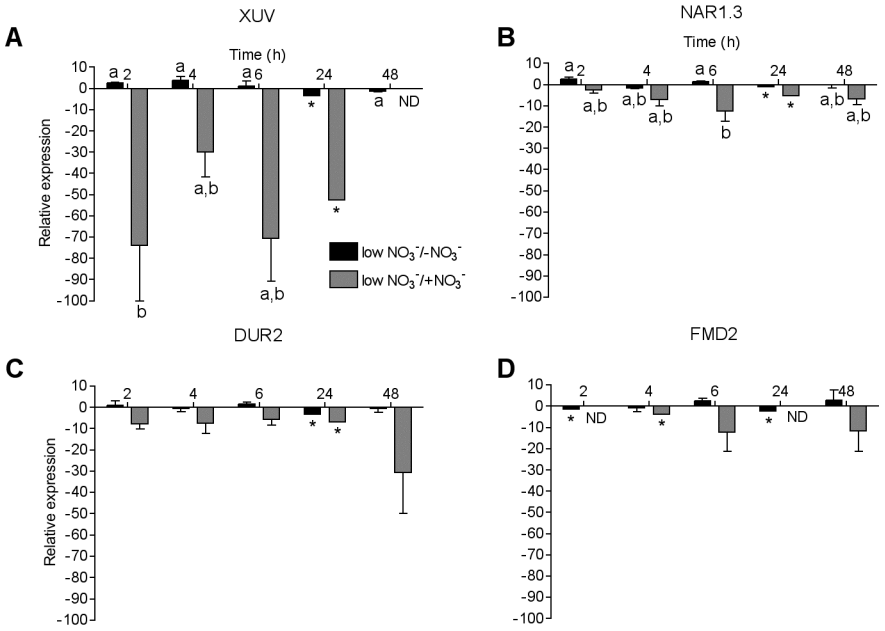

Figure 6. Bar graph comparing the expression of (A) xanthine/uracil/vitamin C permease (XUV), (B) Formate/nitrite transporter (NAR1.3), (C) urea transporter (DUR2), and an acetamidase/formamidase (FMD2) over the course of the nitrate re-addition experiment. Black bars indicate cells that were not refed nitrate while gray bars indicate cells that were re-supplied with nitrate. Transcript data are plotted as average fold-change relative to a reference condition using the comparative C_T method for qRT-PCR with a reference gene that encodes a ubiquitin-conjugating enzyme. Error bars specify standard error of the average fold change of duplicate biological samples between the sample conditions and the reference condition. Letters indicate statistical difference (P-value < 0.05) based upon a one-way ANOVA Tukey post test (e.g. "a" is different than "b"). The reference condition for all samples was N-deficient cells grown on nitrate at T_0 (low NO_3^- day 7). An asterisk (*) indicates that the transcript was only detected in one biological replicate. ND means the transcript was not detected. In graphs (C) and (D), the data were not significantly different from each other, so no letters are shown.

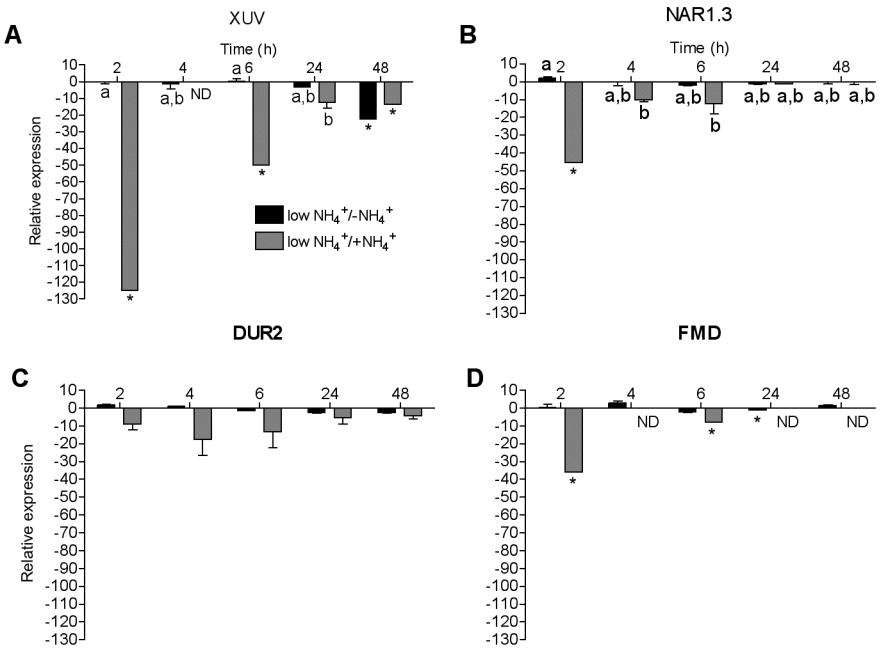

Figure 7. Bar graph comparing the expression of (A) xanthine/uracil/vitamin C permease (XUV), (B) Formate/nitrite transporter (NAR1.3), (C) urea transporter (DUR2), and an acetamidase/formamidase (FMD2) over the course of the ammonium re-addition experiment. Black bars indicate cells that were not refed ammonium while gray bars indicate cells that were re-supplied with ammonium. Transcript data are plotted as average fold-change relative to a reference condition using the comparative C_T method for qRT-PCR with a reference gene that encodes a ubiquitin-conjugating enzyme. Error bars specify standard error of the average fold change of duplicate biological samples between the sample conditions and the reference condition. Letters indicate statistical difference (*P*-value < 0.05) based upon a one-way ANOVA Tukey post test (e.g. "a" is different than "b"). The reference condition for all samples was N-deficient cells grown on ammonium at T_0 (low $NH4^+$ day 7). An asterisk (*) indicates that the transcript was only detected in one biological replicate. ND means the transcript was not detected. In graphs (B) and (D), the data were not significantly different from each other, so no letters are shown.

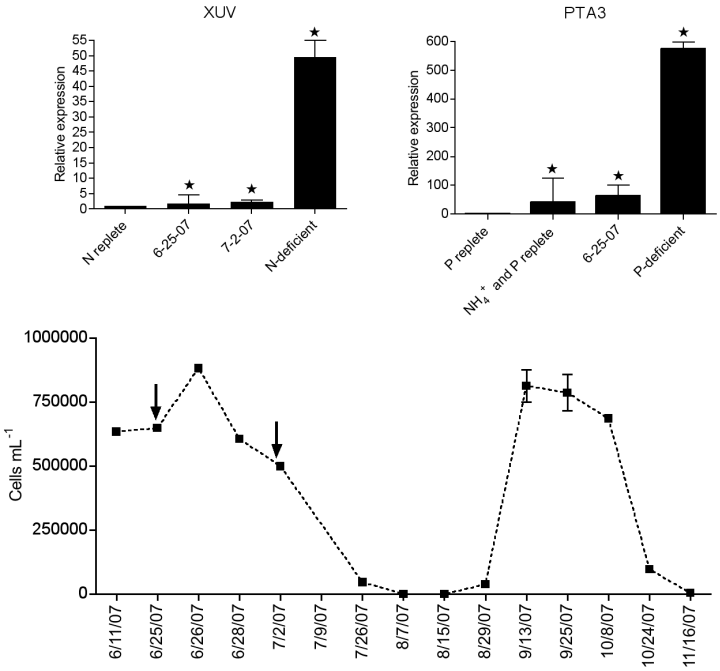

Figure 8. Bar graph comparing the expression of xanthine/uracil/vitamin C permease (XUV: upper left panel) and phosphate transporter (PTA3: upper right panel) from field samples taken during a 2007 brown tide bloom in Quantuck Bay (Suffolk County, NY). For comparison, XUV expression from N-replete and N-deficient conditions are plotted. PTA3 expression in P replete, ammonium grown P replete, and P-deficient conditions are plotted for comparison as well. Transcript data are plotted as average fold-change relative to a reference condition using the comparative C_T method for qRT-PCR with a reference gene that encodes a ubiquitin-conjugating enzyme. Error bars specify standard error of the average fold change of duplicate biological samples between the sample conditions and the reference condition. The reference condition for all samples was N-deficient cells grown on ammonium at T_0 (low $NH4^+$ day 7). A star (★) indicates that the fold change was significantly higher than the reference condition (*P*-value of less than 0.05) based upon a pair-wise fixed reallocation randomization analysis. *A. anophagefferens* cell densities over the course of the bloom are shown on the bottom panel. Arrows indicate the dates that were sampled for expression.

References:

Berg, G. M., Glibert, P.M., Lomas, M.W., and Burford, M.A. (1997) Organic nitrogen uptake and growth by the chrysophyte *Aureococcus anophagefferens* during a brown tide event. *Mar. Biol.* **129**: 377-387.

Berg, G.M., Repeta, D.J., and LaRoche, J. (2002) Dissolved organic nitrogen hydrolysis rates in axenic cultures of *Aureococcus anophagefferens* (Pelagophyceae): comparison with heterotrophic bacteria. *Appl. Environ. Microbiol.* **68**: 401-404.

Berg, G.M., Repeta, D.J., and LaRoche, J. (2003) The role of the picoeukaryote *Aureococcus anophagefferens i*n cycling of marine high-molecular weight dissolved organic nitrogen. *Limnol. Oceanogr.* **48**: 1825-1830.

Berg, G.M., Shrager, J., Glockner, G., Arrigo, K.R., and Grossman, A.R. (2008) Understanding nitrogen limitation in *Aureococcus anophagefferens* (Pelagophyceae) through cDNA and qRT-PCR analysis. *J. Phycol.* **44**: 1235-1249.

Chung CC, Hwang SPL, Chang J (2003) Identification of a high affinity phosphate transporter gene in a prasinophyte alga, Tetraselmis chui, and its expression under nutrient limitation. *Appl. Environ. Microbiol.* **69**: 754-759.

Dyhrman ST, Haley ST, Birkeland SR, Wurch LL, Cipriano MJ et al. (2006) Long Serial Analysis of Gene Expression for gene discovery and transcriptome profiling in the widespread marine coccolithophore Emiliania huxleyi. *Appl. Environ. Microbiol.* **72:** 252-260.

Dyhrman, S.T. (2008) Molecular approaches to diagnosing nutritional physiology in harmful algae: Implications for studying the effects of eutrophication. *Harmful Algae* **8**: 167-174.

Dzurica, S., Lee, C., Cosper, E.M., and Carpenter, E.J. (1989) Role of environmental variables, specifically organic compounds and nutrients, in the growth of the chrysophyte *Aureococcus anophagefferens*. p. 229-252. *In* E.M. Cosper, V.M. Bricelj, and E.J. Carpenter (eds.), Novel Phytoplankton Blooms: Causes and Impacts of Recurrent Brown Tides and Other Unusual Blooms, Volume 35. Springer, New York.

Gobler, C.J., and Sañudo-Wilhelmy, S.A. (2001) Effects of organic carbon, organic nitrogen, inorganic nutrients, and iron additions on the growth of phytoplankton and bacteria during a brown tide bloom. *Mar. Ecol. Prog. Ser.* **209**: 19-34.

Gobler, C. J., Renaghan, M.J., and Buck, N.J. (2002) Impacts of nutrients and grazing mortality on the abundance of *Aureococcus anophagefferens* during a New York brown tide bloom. *Limnol. Oceanogr.* **47**: 129-141.

Gobler, C. J., Boneillo, G.E., Debenham, C., and Caron, D.A. (2004) Nutrient limitation, organic matter cycling, and plankton dynamics during an *Aureococcus anophagefferens* bloom in Great South Bay, N.Y. *Aquat. Microb. Ecol.* **35**: 31-43.

Gobler, C. J., Lonsdale, D.J., and Boyer, G.L. (2005) A review of the causes, effects, and potential management of harmful brown tide blooms caused by *Aureococcus anophagefferens* (Hargraves et Sieburth). *Estuaries* **28**: 726-749.

Gobler, C.J., Berry, D.L., Dyhrman, S.T., Wilhelm, S.W., Salamov, A. et al. (2011) Niche of harmful algal *Aureococcus anophagefferens* revealed through ecogenomics. **108:** 4352-4357.

Guillard R.R.L. and Hargraves P.E. (1993) *Stichochrysis immobilis* is a diatom, not a chrysophyte. Phycologia 32: 234-236.

LaRoche, J., Nuzzi, R., Waters, R., Wyman, K., Falkowski, P.G., and Wallace, D.W.R. (1997) Brown tide blooms in Long Island's coastal waters linked to variability in groundwater flow. *Glob. Change Biol.* **3**: 397–410.

Le Bihan, T., Martin, S.F., Chirnside, E.S., van Ooijen, G., Barrios-Llerena, M.E. et al. (2011) Shotgun proteomics analysis of the unicellular alga *Ostreococcus tauri. J. Prot.* doi:10.1016/j.jprot.2011.05.028

Lomas, M.W., Glibert, P.M., and Berg, G.M. (1996) Characterization of nitrogen uptake by natural populations of *Aureococcus anophagefferens* (Chrysophyceae) as a function of incubation duration, substrate concentration, light, and temperature. *J. Phycol.* **32**: 907-916.

MacIntyre, H.L., Lomas, M.W., Cornwell, J.C., Suggett, D., Gobler, C.J., Koch, E., and Kana, T.M. (2004) Mediation of benthic-pelagic coupling by microphytobenthos: an energy and nutrient based model for initiation of blooms of *Aureococcus anophagefferens. Harmful Algae* **3**: 403-437.

Mock T., Samanta M.P., Iverson V., Berthiaume C., Robison M., Holtermann K., et al. (2008) Whole genome expression profiling of the marine diatom *Thalassiosira pseudonana* identifies genes involved in silicon bioprocesses. *Proc. Nat. Acad. Sci.* U.S.A. 105:1579–1584.

Mulholland, M.R., Gobler, C.J., and Lee, C. (2002) Peptide hydrolysis, amino acid oxidation and N uptake in communities seasonally dominated by *Aureococcus anophagefferens*. *Limnol. Oceanogr.* **47**: 1094-1108.

Mulholland, M.R., Boneillo, G., and Minor E.C. (2004) A comparison of N and C uptake during brown tide (*Aureococcus anophagefferens*) blooms from two coastal bays on the east coast of the USA. *Harmful Algae.* **3**: 361-376.

Palenik, B., and Henson S.E. (1997) The use of amides and other organic nitrogen sources by the phytoplankton *Emiliania huxleyi. Limnol. Oceanogr.* **42:** 1544-1551.

Parkhill J., Maillet, G., and Cullen, J.J. (2001) Fluorescence-based maximal quantum yield for PSII as a diagnostic of nutrient stress. *J. Phycol.* **37:** 517–529.

Pustizzi, F., MacIntyre, H.L., Warner, M.E., and Hutchins, D.A. (2004) Interaction of nitrogen source and light intensity on the growth and photosynthesis of the brown tide alga *Aureococcus anophagefferens*. *Harmful Algae* **3**: 343-360.

Stauffer, B.A., Schaffner R.A., Wazniak, C. and Caron, D.A. (2008) Immunofluorescence flow cytometry technique for enumeration of the brown-tide alga, *Aureococcus anophagefferens. Appl. Environ. Microbiol.* **74**: 6931-6940.

Sunda, W.G., Graneli, E., and Gobler, C.J. (2006) Positive feedback and the development and persistence of ecosystem disruptive algal blooms. *J. Phycol.* **42**: 963-974.

Wurch L.L., Haley S.T., Orchard E.D., Gobler C.J., and Dyhrman S.T. (2011) Nutrient-regulated transcriptional responses in the brown tide forming algal Aureococcus anophagefferens. *Environ. Microbiol.* 13: 468-481.

CHAPTER 5

Summary and Future Directions

Summary

Phytoplankton in the world's oceans form the base of the marine food web and play a significant role in climate regulation and nutrient cycling. Therefore, studying the controls on phytoplankton growth and distribution remains a critical area of research in biological oceanography. A component of this research entails how different species of phytoplankton partition themselves into distinct niches that allow them to co-exist, or in some cases, how one phytoplankton species can gain a competitive advantage over all co-occurring phytoplankton leading to a monospecific or near monospecific bloom.

Aureococcus anophagefferens is a species of phytoplankton that has the capability of completely dominating the coastal systems where it occurs, often to the complete exclusion of other phytoplankton species (Gobler et al. 2005, Sunda et al. 2006). Therefore, *A. anophagefferens* serves as an excellent model for studying nutrient acquisition strategies that allow it to gain a competitive advantage. Due to the harmful nature of *A. anophagefferens* blooms, it is also imperative to determine the nutritional controls on *A. anophagefferens* growth in its natural setting. However, it is difficult to link nutrient supply to the growth of an individual species within a mixed assemblage of microorganisms as traditional metrics of phytoplankton nutrition rely upon community level assays such as bulk uptake rates and elemental composition (Dyhrman 2008). Molecular techniques offer the ability to target the physiology on an individual species,

even in the presence of other microorganisms. In this thesis, I utilized a range of techniques to study the molecular underpinnings of nutrient acquisition in *A. anophagefferens* and develop a method for assaying nitrogen (N) and phosphorus (P) controls on *A. anophagefferens* growth *in situ*.

In the first data chapter (Chapter 2), I profiled the global transcriptional patterns of *A. anophagefferens* under nitrogen (N) and phosphorus (P) deficiency. The goal was to understand how *A. anophagefferens* adjusts the expression of its genome when inorganic N and P are unavailable. Results demonstrated that *A. anophagefferens* exhibits a broad transcriptional response to both N and P deficiency. When N is deficient, *A. anophagefferens* up-regulates genes involved in reduced and organic N metabolism such as an ammonium transporter, a xanthine/uracil/vitamin C permease, an acetamidase/formamidase, and two peptidases. These results are consistent with culture and field studies suggesting the importance of reduced and organic N in fueling *A. anophagefferens* blooms (reviewed in Gobler et al. 2005). When P is deficient, *A. anophagefferens* up-regulates a phosphate transporter, a 5'-nucleotidase, and an alkaline phosphatase. This suggests that *A. anophagefferens* may increase phosphate uptake capacity and utilize P from organic compounds such as nucleotides and esters. An additional experiment confirmed that *A. anophagefferens* could utilize adenosine monophosphate as its sole P source in culture.

A logical next step was to examine whether or not these changes in the transcriptome were manifested at the protein level. In the second data chapter (Chapter 3), shotgun mass spectrometry was used to detect proteins and monitor their abundance in nutrient replete, low P, and P-refed conditions. Results demonstrated that *A.*

anophagefferens increases the abundance of proteins involved in P scavenging, including a phosphate transporter, 5'-nucleotidase, and alkaline phosphatase. These results were consistent with results from Chapter 2 in which these same three genes were up-regulated at the transcriptional level. Additionally, the abundance of a sulfolipid biosynthesis protein increased during low P conditions. In the ocean, it has been demonstrated that some phytoplankton are able to reduce their P requirement by substituting P lipids with sulfolipids (Van Mooy et al. 2009). An analysis of lipids in *A. anophagefferens* revealed that under low P conditions, the sulfolipid sulphoquinovosyldiacylglycerol (SQDG) was nearly 1.5-fold greater while cellular phospholipids were about 8-fold less. Therefore, *A. anophagefferens* may be able to reduce its P quota or scavenge P from phospholipids under P deficiency. Comparison of protein abundances between the –P and P-refed conditions identified variations in the timing of protein degradation and turnover. These results suggest that knowledge of protein turnover is critical in interpreting protein presence from metaproteomic datasets, which are often snapshot views of community protein levels.

In the final data chapter (Chapter 3), the goal was to develop a quantitative gene expression method for assaying N and P deficiency in natural populations of *A. anophagefferens* and apply this method to identify nutrient controls on natural blooms. Candidate genes were chosen based upon their expression patterns from Chapter 2 or from a previous study (Berg et al. 2008). A detailed time course culture experiment was performed to examine how expression patterns of these candidate genes changed as *A. anophagefferens* transitioned from a nutrient replete to N- or P-deficient conditions. Then, N or P was re-supplied to examine how quickly the N- and P-deficient signals

degraded. Results from this work illustrate that a xanthine/uracil/vitamin C permease (XUV) is significantly up-regulated as *A. anophagefferens* experiences N deficiency and the signal degrades within 2 hours after N re-supply. This gene is not regulated by P deficiency. Therefore, XUV is a good candidate for assaying N deficiency in natural populations. A phosphate transporter (PTA3) was significantly up-regulated under P deficiency and the signal degraded within 2 hours of P re-supply. This gene was not regulated by N deficiency. However, this gene was up-regulated when cells were actively growing on ammonium, although the fold-changes were far less than under P deficiency (~40-fold higher on ammonium, ~500-fold higher under P deficiency). Therefore, this gene is a good candidate for assaying P deficiency, and may also be a good candidate for tracking growth on ammonium. The expression patterns of XUV were tested on two samples from a 2007 *A. anophagefferens* bloom. Expression patterns showed that *A. anophagefferens* was not N-deficient during peak cell densities. Results from PTA3 expression show that *A. anophagefferens* may be utilizing ammonium as cell densities increase toward peak levels. This work represents a critical step in linking nutrient supply to *A. anophagefferens* bloom ecology.

Implications

A great deal of expression data was generated from this thesis. Although impossible to discuss every gene in detail, there were a few genes that were of particular interest that genes were discussed throughout the data chapters and are summarized in Table 1. An inorganic phosphate transporter is transcriptionally induced when *A. anophagefferens* experiences P deficiency. Subsequently, the protein for this gene

becomes more abundant. Thus *A. anophagefferens* is either utilizing a higher affinity phosphate transporter, or increasing the number of phosphate transporters, to cope with low P. Upon P re-supply, the transcript for this gene is rapidly lost, while the protein remains abundant, suggesting that once this protein is made *A. anophagefferens* does not immediately degrade it when P is available. This could be due to the fact that it is a membrane protein and is not as accessible to degradation. Alternatively, *A. anophagefferens* may keep this protein available to deal with variable P supply.

A 5'-nucleotidase and alkaline phosphatase were both transcriptionally up-regulated under P deficiency, with a concomitant increase in protein levels (Table 1). These enzymes scavenge P from organic sources. The 5'-nucleotidase cleaves phosphate from nucleotides and a signal peptide suggests that this enzyme is secreted. Therefore, exogenous nucleotides may be important for *A. anophagefferens* to meet its P demand. Alkaline phosphatases are also often associated with cell surfaces, again suggesting that exogenous esters may be a P source for *A. anophagefferens*. These results imply that exogenous organic P compounds may be fueling *A. anophagefferens* growth when inorganic forms are low or not available.

A variety of genes were transcriptionally regulated by N supply, many of which are involved with transport or metabolism of organic N compounds: nucleobases (purines/pyrmidines), amides, urea, formamide (Table 1). Another group is examining the protein responses as a function of N supply, so those data are unavailable at this time. However, insights from differential transcript abundance show that a xanthine/uracil/vitamin C permease, urea transporter, and acetamidase/formamidase are sensitive to N supply. As *A. anophagefferens* transitions into N deficiency, these genes

are up-regulated, although the degree of regulation is variable among genes. As nitrate or ammonium is re-supplied to N-deficient cells, these transcripts are repressed. These results imply that organic compounds, particularly urea, purines/pyrmidines, amides, and formamide are important sources of N when nitrate and ammonium are unavailable. It would require further investigation to determine if these expression patterns are also sensitive to nutrient type (e.g. growth on ammonium versus growth on urea). Nonetheless, these data support field studies that suggest an importance of organic compounds in fueling *A. anophagefferens* growth.

Due to the severe harm caused by *A. anophagefferens*, it is critical to devise potential mitigation and prevention strategies. From a pure N and P standpoint, it is clear that organic compounds serve as an important nutritional source for *A. anophagefferens*. This complicates the issue because the sources of these organic compounds are not well understood. For example, and increase in nitrate levels from groundwater could lead to increased biomass from other algae. This can, in turn, lead to an increase in organic compounds. Previous studies have shown that *A. anophagefferens* does not appear to be experiencing N deficiency over the course of a bloom, but the algal community as a whole could be (Gobler et al. 2005). Thus, trying to reduce N inputs into the system may inadvertently facilitate *A. anophagefferens* by hurting its competitors. More work needs to be done to understand whether P is ever limiting to *A. anophagefferens*, as this could be a more promising approach for mitigating or even preventing brown tides from occurring.

Future Directions

Not surprisingly, this thesis raises additional questions and provides a platform for exciting future directions. First, advances in technology are facilitating deeper sequencing efforts. In Chapter 2, the transcriptional changes observed represent only the most highly expressed genes. Deeper sequencing during N and P deficiency would allow a higher resolution analysis of the global transcriptional responses. Additionally, transcriptome analysis over time would eliminate the problem of a snapshot view. For example, Chapter 3 illustrates how the proteome of *A. anophagefferens* changes in response to P deficiency and release from P deficiency, thus identifying differences in protein turnover/degradation. It would be valuable to determine how the transcriptome changes over time as *A. anophagefferens* transitions in and out of nutrient deficient conditions.

In Chapter 3, an unexpected result was the increased abundance of a sulfolipid biosynthesis protein under P deficiency. Oddly, this protein was even more abundant 24 hours after P-deficient cells were re-supplied with phosphate. Obtaining lipid data from a 24 hour re-feed would identify whether sulfolipids continued to increase and give a better idea of how quickly *A. anophagefferens* can adjust its cellular lipids to meet its P demands.

Gene expression assays for N and P deficiency were developed in Chapter 4. Due to time constraints, only a few samples from a natural bloom in 2007 were analyzed. Thanks to the efforts of Dr. Christopher Gobler's group at SUNY Stony Brook, samples have been collected throughout the bloom cycle over multiple years. Screening these samples for N and P deficiency and comparing between years would provide tremendous

insight into the nutrient controls on brown tide blooms in Long Island. My future plans are to screen samples from a 2009 bloom in Quantuck Bay (Suffolk County, Long Island, NY). Additionally, these gene targets are good indicators of N and P deficiency, but it may be possible to find other gene targets whose expression patterns are indicative of growth on a particular compound (e.g. urea). This would provide a new and useful approach for studying *A. anophagefferens* bloom ecology.

Table 1. List of main genes discussed throughout multiple data chapters of this thesis, which chapters they are discussed in, and a summary of their behavior with respect to nitrogen (N) and phosphorus (P) supply.

Name	Gene Symbol	Chapters	Function	Insights
Inorganic phosphate transporter	PTA3	2,3,4	Transports phosphate	Under P deficiency, this gene is up-regulated at both the transcript and protein level. The transcript is quickly lost upon P re-supply, while the protein remains abundant for at least 24 hours.
5'-nucleotidase	NTD	2,3,4	Cleaves phosphate from nucleotides	Under P-deficiency, this gene is up-regulated at the transcript and protein level. After P-resupply, the protein remains abundant for at least 24 hours.
Alkaline phosphatase	AP	2,3,4	Cleaves phosphate from esters	Under P-deficiency, this gene is up-regulated at the transcript and protein level. After P-resupply, the protein is lost or degraded within 24 hours.
Xanthine/Uracil/Vitamin C permease	XUV	2,4	Transports nucleobases (purines and pyrmidines)	Under N deficiency, this gene is up-regulated at the transcript level. The transcript is rapidly lost upon re-supply of both nitrate and ammonium.
Formate/Nitrite transporter	NAR1.3	2,4	Transports formate/nitrite	Under N deficiency, this gene is up-regulated at the transcript level. The transcript is rapidly lost upon re-supply of both nitrate and ammonium.
Urea Transporter	DUR2	2,3,4	Transports urea	Under N deficiency, this gene is up-regulated at the transcript level. The transcript is rapidly lost upon re-supply of both nitrate and ammonium. The protein for this gene is less abundant under P deficiency.
Acetamidase/ Formamidase	FMD2	2,3,4	Hydrolyzes amides	Although this gene appears induced under N deficiency, the changes in expression are smaller compared to the other genes. The transcript is lost upon re-supply of both nitrate and ammonium, with ammonium causing the largest reducstion, The protein for this gene is less abundant under P deficiency.

References:

Berg, G.M., Shrager, J., Glockner, G., Arrigo, K.R., and Grossman, A.R. (2008) Understanding nitrogen limitation in *Aureococcus anophagefferens* (Pelagophyceae) through cDNA and qRT-PCR analysis. *J. Phycol.* **44**: 1235-1249.

Dyhrman, S.T. (2008) Molecular approaches to diagnosing nutritional physiology in harmful algae: Implications for studying the effects of eutrophication. *Harmful Algae* **8**: 167-174.

Gobler, C. J., Lonsdale, D.J., and Boyer, G.L. (2005) A review of the causes, effects, and potential management of harmful brown tide blooms caused by *Aureococcus anophagefferens* (Hargraves et Sieburth). *Estuaries* **28**: 726-749.

Sunda, W.G., Graneli, E., and Gobler, C.J. (2006) Positive feedback and the development and persistence of ecosystem disruptive algal blooms. *J. Phycol.* **42**: 963-974.

Van Mooy B.A.S., Fredricks H.F., Pedler B.E., Dyhrman S.T., Karl D.M. et al. (2009) Phytoplankton in the ocean use non-phosphorus lipids in response to phosphorus scarcity. *Nature* **458**: 69-72.